Th-Pos1

SPECIFIC ASSOCIATION BETWEEN $Kv\beta_{1b}$ AND THE POTASSIUM CHANNEL Kv1.3. ((**S. Ghanshani**, G.. A. Gutman*, K. G. Chandy)) Depts. of Physiology and Biophysics, and of Microbiology and Molecular Genetics*, University of California, Irvine CA 92697.

Potassium (K^+) channel alpha subunits have been shown to associate with accessory beta subunits. Site-specific mutagenesis studies on Kv1.5 suggest that the N-terminal tetramerization domain of Kv channels interacts with β-subunits, although other parts of the protein may also be involved. More recently, the expression of $Kv\beta_1$ and $Kv\beta_2$ has been shown to be inducible in stimulated lymphocytes, coincident with a similar increase in the levels of functional Kv1.3 channels. To study the potential interaction between Kvβ1 and Kv1.3, the highly conserved core-domain of human $Kv\beta_{1b}$ and the N-terminal domain of Kv1.3 were overexpressed in *E. coli*. The C-terminal 329 amino acids of $Kv\beta_{1b}$ were attached in-frame to the C-terminal end of maltose binding protein (MBP) in the pMALc2 expression vector through a poly-asparagine linker containing a hydroxylamine cleavage site (N/G). An $MRGSH_6$ epitope was attached to the C-terminal end of human Kvb_{1b} to allow its immunological detection and purification by nickel chelate-chromatography. Elution of the fusion protein with maltose from an amylose column, hydroxylamine cleavage, and nickel chelate chromatography yielded ~2mg/L of human Kvb_{1b} protein. The N-terminal tetramerization domain (residues 50-177) of Kv1.3 (containing a C-terminal FLAG epitope [DYKDDDDK] and a poly-His sequence) was cloned into the pET-22b vector, expressed along with the chaperonin genes, GroEL and GroES, and the protein purified using nickel chelate chromatography and gel filtration. A modified version of the α-β binding assay utilized by Yu et al. (*Neuron* 16:441-453, 1996) was employed to study the interaction between $Kv\beta_{1b}$ and Kv1.3. Purified Kv1.3 N-terminal protein was bound to an anti-FLAG immunoadsorbent column, over which a mixture of hydroxylamine-cleaved MBP and human $Kv\beta_{1b}$ proteins was passed. MBP did not bind, and was detected in the flow-through along with some human $Kv\beta_{1b}$. Following extensive washing, a high salt elution buffer was used to release Kv1.3-bound $Kv\beta_{1b}$, and Kv1.3 protein was subsequently eluted with an excess of FLAG peptide. In parallel experiments, we loaded the MBP/$Kv\beta_{1b}$ protein mixture onto the Kv1.3-bearing column, and eluted the $Kv\beta_{1b}$-Kv1.3 complex with the FLAG peptide. In the absence of Kv1.3 on the column, $Kv\beta_{1b}$ did not bind and was found in the flow-through. These preliminary studies suggest that Kv1.3 interacts with human $Kv\beta_{1b}$ in a specific manner. By making site-directed mutations of $Kv\beta_{1b}$ and generating chimeras of $Kv\beta_{1b}$ and a related superfamily protein, aldose reductase, we hope to identify key regions in $Kv\beta_{1b}$ that are involved in the α–β interaction. (Supported by USPHS grant AI24783)

Th-Pos2

MULTIMERIC ASSEMBLY OF Kvβ SUBUNITS WITH Kv1.2 POTASSIUM CHANNEL A-SUBUNITS PRODUCES FUNCTIONALLY DISTINCT SINGLE CHANNELS. ((**EA Accili***, J Kiehn, Q Yang, Z Wang, AM Brown and BA Wible**)). Rammelkamp Center, MetroHealth Campus and the *Departments of Physiology and Biophysics, and **Biochemistry, School of Medicine, CWRU, Cleveland, Ohio, 44109.

Biochemical data have shown that voltage-gated K^+ channels (Kv) consist of integral membrane α-subunits complexed with cytoplasmic β subunits in a 1:1 stoichiometry. Multiple Kvβ subunits have been cloned and variably affect the kinetic properties of coexpressed Kvα subunits. Taken together, this suggests that the multimeric assembly of functionally distinct Kvβ subunits with Kvα tetramers should generate phenotypically distinct single channels. Here we show that Kvβ1.2 produces partial inactivation of Kv1.2 currents and increases surface expression of coexpressed Kv1.2 α-subunits. Coexpression of Kv1.2 with Kvβ1.2 in Xenopus oocytes results in single channels with shorter open times and a reduced open probability compared to those resulting from coexpression of Kv1.2 with Kvβ1.2-NΔ20, a mutant which lacks the first 20 amino acids of the N-terminus and does not confer inactivation upon Kv1.2 currents. The properties of single channels expressed upon injection of Kv1.2 alone or together with Kvβ1.2-NΔ20 do not differ. However, single channels with intermediate properties predominate after coexpression of Kv1.2 with equal amounts of both Kvβ1.2 and Kvβ1.2-NΔ20 indicating multimeric assembly of Kvα and Kvβ subunits. From analysis of whole-oocyte currents, a Hill factor of about four was determined from a plot of increasing amounts of Kvβ1.2 versus steady-state current block. The results suggest four Kvβ1.2 subunits assemble with a Kv1.2 tetramer to produce inactivation and increase surface expression of the channel complex. (Supported by HL 36930 and the AHA/Northeast Ohio Affiliate)

Th-Pos3

SEPARATION OF FUNCTIONAL DOMAINS WITHIN THE hKvß1.3 K+ CHANNEL BETA SUBUNIT. ((**V.N. Uebele**, S.K. England, D.J. Snyders, P.B. Bennett and M.M. Tamkun)) Depts. of Pharmacol. and Mol. Physiol. and Biophys., Vanderbilt University, School of Medicine, Nashville, TN 37232.

We have previously reported that, when coexpressed with hKv1.5 in *Xenopus* oocytes, hKvß1.3 induces 1) a voltage dependent, partial inactivation (53.1±1.1% at +70 mV), 2) a 12.9±0.5 mV hyperpolarizing shift in the activation midpoint and 3) an increased deactivation time constant at -50 mV (10.2±0.4 vs. 23.6±1.46 ms). We hypothesized that these effects involved different domains of the ß subunit. Removal of 10 to 68 amino acids from the N-terminus of hKvß1.3 prevented inactivation, but still shifted the activation midpoint (-8.6±1.0 mV shift for Kvß1.3(Δ37N)) and altered the deactivation time constant at -50 mV (15.1±1.84 ms). Deletion of 91 N-terminal amino acids (leaving only the conserved C-terminal domain of hKvß1.3), prevented all three effects. To determine if a complete inactivation "ball" was contained within the amino terminus of the ß subunit, two different tandem constructs were made which contained either the first 19 or 87 amino acids of hKvß1.3 linked to the N-terminus of hKv1.5. Expression of the 19 amino acid tandem resulted in currents nearly identical to hKv1.5. This result, combined with the deletion data, indicates that the first 10 amino acids are required, but insufficient, for inactivation. Expression of the 87 amino acid tandem resulted in currents that displayed a voltage dependent, partial inactivation, similar to that observed with wild-type coexpression studies. Thus, the incomplete inactivation induced by wild-type hKvß1.3 is not due to non-stoichiometric assembly. The activation midpoint and deactivation time constant were not shifted. These results suggest that separate domains of hKvß1.3 induce inactivation and shift the activation midpoint. The effects on deactivation may be a direct result of the shift in activation midpoint.

Th-Pos4

SIALIDATION MODIFIES THE FUNCTION OF KV1.1 POTASSIUM CHANNELS. ((**W.B. Thornhill** and J.F. Margiotta)), Dept. Physiology and Biophysics, Mount Sinai School of Medicine, New York, NY 10029.

Sialidase sensitivity of brain Kv1.1 potassium (K) channels suggests that the tetramer contains 150-200 negatively-charged sialic acids, some of which are in an unusual tandem-linked structure. To examine the role of sialidation in K channel function, CHO cells deficient in glycosylation (Lec mutants) were transfected with rat brain Kv1.1 cDNA. Patch-clamping techniques determined that functional Kv1.1 channels were expressed in all cell lines but the voltage dependence of activation ($V_{1/2}$) was shifted to more positive voltages (up to 23mV) and the activation kinetics were slower in the Lec mutants compared with controls. A similar shift in $V_{1/2}$ to positive voltages was recorded in control cells expressing Kv1.1 following treatment with sialidase or by raising extracellular calcium. In contrast, these treatments had little or no effect on the Lec mutants, indicating that channel sialic acids appear to be the negative charges sensitive to screening by calcium. The data suggest that sialic acid addition modifies Kv1.1 function, possibly by influencing the local electric field detected by its voltage-sensor, but that these carbohydrates are not required for cell surface expression. Supported by NIH grants to WB Thornhill and JF Margiotta.

Th-Pos5

DECREASED EXPRESSION OF Kv4 SUBFAMILY CHANNEL mRNAs IN RENAL HYPERTENSIVE RAT HEARTS. ((**K. Takimoto**, D. Li, K.M. Hershman, P. Li*, E.K. Jackson* and E.S. Levitan)) Depts. of Pharmacology and Clinical Pharmacology*, Univ. of Pittsburgh, Pittsburgh, PA15261

Cardiac hypertrophy is associated with changes in electrical properties of myocytes, typically prolongation of action potential. To investigate underlying molecular mechanisms, expression of voltage-gated K^+ channel mRNAs was measured. While generating a Kv4.3 probe, we discovered a previously unreported 19-a.a. insertion at the C-terminal intracellular region. RNase protection assays suggest that this longer isoform of Kv4.3 is predominant in rat heart. We then examined effects of cardiac hypertrophy produced by renal hypertension in rats. Levels of Kv4.2 and Kv4.3 mRNAs dramatically decreased in 2 kidney-1 clip rat ventricles. The decrease in the two channel transcripts was prevented by giving the angiotensin-converting enzyme (ACE) inhibitor captopril in drinking water. No significant change in LQT1 mRNA expression was obtained by renal artery stenosis or by administration of the ACE inhibitor. Thus, renal hypertension causes specific reduction of Kv4.2 and Kv4.3 mRNAs. Our results suggest that the decrease in expression of Kv4 subfamily channels, which is proposed to encode *Ito* in cardiac myocytes, is at least in part responsible for the action potential prolongation seen in hypertrophied myocytes. Supported by NIH (HL55312). ESL is an established investigator of A.H.A..

Th-Pos6

SUPPRESSION OF NEURONAL AND CARDIAC TRANSIENT OUTWARD CURRENTS BY VIRAL GENE TRANSFER OF A DOMINANT NEGATIVE Kv4.2 CONSTRUCT ((**David C. Johns**, H. Bradley Nuss, Eduardo Marban)) The Johns Hopkins University, Baltimore MD

To probe the molecular identity of A-type currents, we expressed a truncated version of Kv4.2 in heart cells and in neurons. The rat Kv4.2 coding sequence was truncated at a position just past the first transmembrane segment (S1) and subcloned into an adenovirus shuttle vector downstream of a CMV promoter (pKv4.2st). We hypothesized that this construct would act as a dominant-negative suppressor of currents encoded by the Kv4 family, by analogy to Kv1 channels. Cotransfection of wild-type Kv4.2 with a ß-galactosidase (ß-gal) expression vector in CHO cells produced robust transient outward currents at two days (14.0 pA/pF at 50mV, n=5). Cotransfection with pKv4.2st markedly suppressed the currents (0.8 pA/pF, n=6, $P<0.02$; cDNA ratio of 2:1 Kv4.2 st:wt), but, in parallel experiments, did not alter the density of coexpressed Kv1.5 channels. We then engineered an adenovirus (AdKv4.2st) designed to overexpress Kv4.2st in infected cells. A-type currents in rat cerebellar granule cells were decreased two days after AdKv4.2st infection as compared to those infected by a ß-gal reporter virus (98.8 pA/pF vs. 258.2 pA/pF in Ad ß-gal cells, n=4+4, $p<0.02$). Likewise, the transient outward current in adult rat ventricular myocytes was suppressed by AdKv4.2st but not by Ad ß-gal (8.8 pA/pF vs. 21.4 pA/pF in ß-gal cells, n=6+6, $p<0.05$). We conclude that the Kv4 family encodes the A-type currents in cerebellar granule cells and in rat ventricle. Overexpression of dominant negative constructs may be of general utility in dissecting the contributions of various genes to excitability.

Th-Pos7

HIGH-LEVEL EXPRESSION OF *Shaker* K^+ CHANNELS IN COS CELLS: USE OF A NON-RECOMBINANT ADENOVIRUS EXPRESSION SYSTEM. ((Cuello, L.G. and Perozo, E.)) Dept. of Molecular Physiology and Biological Physics. University of Virginia. Charlottesville. VA 22908.

Structural studies in membrane proteins require a steady supply of relatively large amounts of pure, functional protein. Here, we describe the biochemical characterization and heterologous expression of Shaker K^+ channels in COS cells, using an efficient and flexible expression system based on a stable adenovirus-polylysin-DNA complex. The method takes advantage of the receptor-mediated uptake of adenovirus coated sequentially with: polylysin, a Shaker expression vector, and polylysin again. Simple overlay of this complex on non-confluent COS cells is enough to generate transfectants with very high efficiencies. Channel expression was monitored by toxin binding assay using a recombinant Agitoxin I labeled with ^{3}H-NEM. Expression levels reach at least 10 pmol/plate, or about 6 $x10^6$ channels per cell after 72 h. Three expression vectors were compared in terms of expression levels, and the following expression potencies were found: pMT3>>pcDNA3>pGW1. Channels were solubilized in a number of non-ionic detergents and the stability of the solubilized channel in each detergent studied by its ability to bind toxin. We found that the channel is fairly stable in CHAPS (more than 50% of binding sites preserved after 24 h @ RT). However, stability was critically dependent upon addition of extra lipids at the time of solubilization. One key advantage of this expression strategy is that, by not requiring the use of recombinant virus, it allows easy expression of a large number of mutants with minimum additional work. This is particularly useful when using structural methods based on the site-directed placement of reporter groups (EPR, Fluorescence)

(Supported by NIH grant GM54690)

Th-Pos8

ELECTRO-MECHANICAL COUPLING OF CELL MEMBRANES DETECTED BY ATOMIC FORCE MICROSCOPY.

(J. Mosbacher*, F. Sachs+, and J.K.H. Hoerber*) *cell biophysics, EMBL, Heidelberg, Germany and +Biophysics, SUNY, Buffalo, NY.

The anticipated movement of the voltage-sensing element in voltage-gated ion channels is well within the range of height detection of Scanning Force Microscopes (SFMs). Simultaneous gating of a cluster of channels in the contact area between the cell membrane and the SFM tip (about 100 nm in diameter) should move the cantilever by about 0.5 nm (French et al., *Neuron* 16: p. 407-13, 1996). We tried to directly measure this movement in whole cell voltage clamp by overexpressing a non-inactivating *Shaker* K^+-channels in HEK293 cells and measuring height changes of the cell membrane during changes in voltage. To improve detection, we modulated the step potentials with a sinusoidal carrier with p-p amplitudes of 10-60 mV and frequencies of 60- 2500 Hz.

The SFM signal spectrum showed that depolarization produced outward movements with amplitudes ranging from 0.2-15 nm depending, almost linearly, on the carrier amplitude with a slight decrease at higher frequencies. Leaky cells showed less movement, but there was not much correlation of movement with V_{hold}. The phase shift between SFM signals and voltage was nearly 90 degrees at frequencies up to 400 Hz suggesting a capacitive origin. Surprisingly, untransfected control cells showed similar signals! Tests for artifacts used sealed and open pipettes at different ionic conditions showing no movement except when the bath solution was replaced with H_2O.

The SFM signal did not arise from channel gating movements because they were 1) too large, 2) too weakly voltage-dependent, and 3) independent of transfection. Electrostatic double layer effects are unlikely (Butt, *Biophys. J.* 60:777-85, 1991) as are inverse flexo-electrical effects of the lipid bilayer. Rotation of membrane bound dipolar molecules may account for these movements. The motions, however, must be heavily damped to avoid showing saturation with the biasing potential. Since the motion appears nearly linear with voltage, its contribution to cell capacitance would be invisible in most gating current experiments. The presence of these rather large motions raises the possibility of voltage modulation of many membrane bound structures.

JM acknowledges an EMBO fellowship LTF599/1994; FS supported by USARO and MDA.

Th-Pos9

IRREVERSIBLE DISAPPEARANCE OF K CHANNELS CAUSED BY TEA IN THE ABSENCE OF EXTRACELLULAR POTASSIUM IONS. *((Kamran Khodakhah, Alexey I Melishchuk, and Clay M Armstrong))* Department of Physiology, University of Pennsylvania, Philadelphia, PA 19104. (Spon. Zhe Lu)

Tetraethylammonium (TEA) is a potassium channel blocker widely used for reversible blockade of potassium channels in many preparations. Much to our surprise, it was noticed that after intracellular perfusion of voltage clamped squid giant axons with TEA in the absence of external K^+, we were unable to recover all the potassium current (I_K) after washout of TEA. In axons clamped at a holding potential of -110 mV, following 5 minutes perfusion of 20 mM intracellular TEA <5% of the I_K recovered upon complete washout. Similar results were obtained with different batches of TEA synthesized by various manufacturers, in addition to TEA freshly recrystallized in the laboratory, ruling out the possibility of chemical degradation or contamination. The irreversible disappearance of K channels by TEA could be prevented by addition of >10 mM K^+ to the extracellular medium. The rate of disappearance of K channels was reduced with lowering the TEA concentration. Further, there is some evidence suggesting that at a holding potential of -110 mV the rate of disappearance of K channels caused by 1 mM TEA could be increased by applying depolarizing voltage steps which repeatedly opened the channels. It has been reported that removal of K^+ from both the inside and outside of squid giant axons results in the disappearance of the K channels. It is possible that the irreversible action of TEA in the absence of external K^+ is through a similar process of dekalification.

Th-Pos10

THE HUMAN ALDOSE REDUCTASE ACCELERATES INACTIVATION OF rKv1.4 CHANNELS SIMILARLY TO hKvβ2 SUBUNITS.

((**Nannette Marr**, R. Schönherr, and S.H. Heinemann)) Max-Planck-Gesellschaft, AG Molekulare & zelluläre Biophysik, D-07747 Jena, Germany.

mRNA coding for the A-type channels rKv1.4 was injected into *Xenopus* oocytes and currents were measured with a two-electrode voltage clamp. The inactivation time course was assayed at +50 mV. Upon coexpression of the human aldose reductase (EC 1.1.1.21; kindly provided by M. Petrash) which only shares 20% homology with hKvβ subunits, the inactivation was accelerated by a factor of 2-3. A similar effect was obtained by coexpression of hKvβ2. A point mutantion in the aldose reductase which was shown to impair its enzyme activity (Y48F, Tarle et al., 1993. JBC, 268:25687) did not affect the efficacy to alter the inactivation of rKv1.4 indicating that the enzyme activity is not a requirement for the modulation of K^+ channels. A homologous mutation in hKvβ2 (Y90F) did not alter the effects of hKvβ2 either. The aldose reductase did not induce inactivation when coexpressed with the delayed rectifer channels hKv1.5 and rKv1.1. However, when the N-terminal domain of hKvβ1 was spliced to the N-terminus of the aldose reductase it was enabled to induce inactivation: e.g., after a 1-s pulse to +50 mV, current of rKv1.1 was reduced to 94±1% (n=15), upon coexpressed of aldose reductase to 37±9% (n=12). These results suggest that the aldose reductase interacts with K^+ channels similarly to hKvβ subunits. As the aldose reductases are members of a large gene family it is expected that a very large variety of proteins is able to interact with K^+ channels in a similar way. Since the 3D-structures of several aldose reductases are known, they provide interesting options for biophysical studies of interactions between aldose reductase and K^+ channels.

Th-Pos11

DIFFERENTIAL EXPRESSION OF KV1.5 AND KV2.1 K CHANNELS IN PLASMA MEMBRANE VERSUS RECYCLING VESICLES ((**William F. Wonderlin**)) Dept. Pharmacol. & Toxicol., West Virginia Univ., Robert C. Byrd Health Sciences Ctr., Morgantown, WV 26505

We examined the subcellular distribution of Kv1.5 and Kv2.1 channels in N1E-115 neuroblastoma cells. Vesicles that deliver proteins to the cell surface were released from saponin-permeabilized cells in the presence of ATP and separated on a Ficoll velocity gradient into three peaks: rapidly-sedimenting (RS) vesicles that deliver newly-synthesized proteins, slowly-sedimenting (SS) vesicles that deliver recycled proteins and non-sedimenting (NS) material including detergent and proteins solubilized from the plasma membrane. Kv1.5 and Kv2.1 channels in the RS, SS and NS peaks were assayed by SDS-PAGE and immuno-probing with channel-specific antibodies (gift of J. Trimmer). Virtually all of the Kv2.1 immunoreactivity was detected in the NS fractions, indicating that Kv2.1 channels were expressed in the plasma membrane, but were rare in RS or SS vesicles. In contrast, Kv1.5 immunoreactivity was strongest in a subpopulation of small (35-45 nm) SS vesicles, weaker in the NS peak and barely detectable in RS vesicles. We previously identified two subpopulations of SS vesicles, including larger SS vesicles of the receptor-mediated cell-surface recycling system and smaller SS vesicles whose formation was inhibited by Brefeldin A (BFA) and some of which carried synaptobrevin II (SBII), a synaptic vesicle protein. Kv1.5 immunoreactivity was clearly colocalized in the gradient with the smaller SS vesicles, but Kv1.5 immunoreactivity was not affected by pretreatment with BFA (10 μg/ml) for 90 min. The distribution of Kv1.5 channels was also not affected by depolarization with 50 mM extracellular K for 90 min or 18 hours, suggesting that the distribution of Kv1.5 channels between SS vesicles and the plasma membrane is not simply regulated by membrane potential. The presence of Kv1.5, but not Kv2.1, channels in recycling vesicles suggests that fundamentally different mechanisms might regulate the cell surface expression of these K channels. Supported by NSF grant IBN-9319496.

Th-Pos12

CLONING AND EXPRESSION IN MAMMALIAN CELLS OF Kv1.5 CHANNELS OF RABBIT PORTAL VEIN VASCULAR SMOOTH MUSCLE ((**O. Clément-Chomienne**, K. Ishii*, M.P. Walsh and W.C. Cole)) The Smooth Muscle Research Group, University of Calgary, Calgary, Alberta, Canada and *Department of Pharmacology, Yamagata University School of Medicine, Yamagata, Japan.

Delayed rectifier K^+ current (I_{KDR}) is a dominant K^+ conductance of rabbit portal vein (RPV) and is enhanced by protein kinase A and inhibited by protein kinase C (Aiello et al., Am. J. Physiol. 268: H296, Am. J. Physiol. 271: H109; Clément-Chomienne et al., J. Physiol. 495: 689). The presence of voltage-gated Kv1.5 channels in rabbit portal vein smooth muscle was shown using an affinity-purified antibody raised against the C-terminus of Kv1.5: freshly dispersed portal vein myocytes permeabilized with Triton X-100 (0.1% for 4 min) exhibited positive staining with anti-Kv1.5 and TRITC-labelled anti-rabbit IgG. cDNA encoding Kv1.5 was isolated from rabbit portal vein mRNA by RT-PCR using oligonucleotides synthesized according to the sequence of rabbit heart Kv1.5 (Sasaki et al., FEBS Lett. 372: 20 (1995)). When expressed in mouse L cells, macroscopic currents due to RPV Kv1.5 exhibited kinetic and voltage-dependent properties comparable to those of native 4-aminopyridine-sensitive I_{KDR}. The figure shows representative families of macroscopic currents of an untransfected L cell and an L cell transfected with rabbit portal vein Kv1.5. Supported by MRC, HSFA and AHFMR.

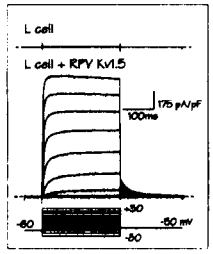

Th-Pos13

COMPLEX HETEROTETRAMERIC SUBUNIT ASSEMBLY OF VOLTAGE-GATED K^+ CHANNELS: BASIS FOR HIGH-AFFINITY TOXIN INTERACTION AND PHARMACOLOGY

((**R.O.Koch**[1], S.G.Wanner[1], A.Koschak[1], M.Trieb[1] M.Hanner[2], G.J.Kaczorowski[2], R.S.Slaughter[2], M.L. Garcia[2] & H.-G.Knaus[1])) [1]Inst. Bioch.Pharmacology, A-6020 Innsbruck, Austria, [2]Merck Research Laboratories, Rahway, NJ 07065.

Neurons require a specific pattern of K^+ channel subunit expression, as well as precise regulation of subunit coassembly into heterotetrameric channels, for proper integration and transmission of electrical signals. *In vivo* subunit coassembly was investigated by studying the pharmacological profile, distribution, and subunit composition of voltage-gated *Shaker* (K_v1) K^+ channels in rat cerebellum as labeled by [^{125}I]margatoxin ([^{125}I]MgTX; K_d=0.04 pM). High-resolution receptor autoradiography showed spatial receptor expression mainly in basket cell terminals (52% of all cerebellar sites) and the molecular layer (39% of sites). Sequence-directed antibodies indicated overlapping expression of $K_v1.1$ and $K_v1.2$ protein in basket cell terminals, while the molecular layer expressed $K_v1.1$, $K_v1.2$, $K_v1.3$ and $K_v1.6$ subunits. Immunoprecipitation experiments revealed that all [^{125}I]MgTX receptors contain at least one $K_v1.2$ subunit with 83% being heterotetramers of $K_v1.1$ and $K_v1.2$ subunits. Moreover, 33% of these $K_v1.1$/$K_v1.2$ channels contain either an additional $K_v1.3$ or $K_v1.6$ subunit. Only a minority (< 20%) are homotetrameric $K_v1.2$ channels. Heterologous coexpression of $K_v1.1$/$K_v1.2$ subunits in COS-1 cells combined the pharmacological profile of both parent channels and reconstituted the native MgTX receptor phenotype. Subunit assembly provides the structural basis for toxin binding pharmacology and can lead to the association of as many as three distinct K^+ channel subunits to form functional channels *in vivo*.

Th-Pos14

EVIDENCE THAT DROSOPHILA SHAKER AND EAG K^+ CHANNEL SUBUNITS DO NOT CO-ASSEMBLE IN XENOPUS OOCYTES

((**C.-Y. Tang**, C.T. Schulteis, R.M. Jiménez, and D.M. Papazian)) Department of Physiology, UCLA School of Medicine, Los Angeles, CA 90095-1751.

The Shaker and ether-a-go-go (eag) K^+ channels of *Drosophila* both belong to the superfamily of voltage-gated ion channels, but are members of two distinct K^+ channel subfamilies. Previous *in vitro* studies in *Xenopus* oocytes have demonstrated that heteromultimers are not formed among different subfamilies of K^+ channels (Covarrubias et al., *Neuron* 7:763,1991). Nevertheless, functional and genetic analyses in *Drosophila* suggested a possible association between Shaker and eag proteins (Zhong and Wu, *Science* 252:1562, 1991). We therefore examined this possibility in *Xenopus* oocytes using both electrophysiological and biochemical approaches. Shaker and eag cRNA were co-injected into oocytes in a 1:1 molar ratio. In two-electrode-voltage clamp experiments, we found no significant difference in the time course of Shaker inactivation upon expression of Shaker in the absence or presence of eag. This result contrasts with a recent report using a similar approach (Chen et al., *Neuron* 17:535, 1996). For biochemical studies, the Shaker and eag proteins were co-expressed and metabolically labeled in oocytes. After solubilization under conditions that maintain Shaker subunit associations, proteins were immunoprecipitated with a Shaker-specific antibody and subjected to SDS-PAGE analysis. Only Shaker but not eag protein was precipitated. In conclusion, both our functional and biochemical data indicate that Shaker and eag do not co-assemble in *Xenopus* oocytes. (Supported by the NIH (GM43459), the Keck Foundation, and the Pew Charitable Trusts. C.T.S. is a predoctoral fellow of the Howard Hughes Medical Institute)

Th-Pos15

LOCALIZATION AND MOBILITY OF GFP-K+ CHANNEL FUSION PROTEINS.

((**N. Veyna-Burke, D. Li, K. Takimoto, K. Hoyt, S. Watkins, and E.S. Levitan**)) **Dept. of Pharmacology, University of Pittsburgh, Pittsburgh, PA 15261. (Spon. W. Han)**

Little is known about targeting and movement of K+ channels. To facilitate tracking of channels, we have fused GFP (Green Fluorescent Protein) to the Kv1.4 and Kv1.5 voltage-gated K+ channels and to the Kir3.1G-protein activated K+ channel. In each case GFP was added near the N-terminus of the channel alpha subunits. Constructs were then transiently transfected into HEK 293 cells and visualized using FITC fluorescent optics. Channel fusion proteins preferentially localized to the plasma membrane (PM). Also, in some cells a strong perinuclear signal was evident likely reflecting the presence of subunits in the ER. Whole cell and cell attached patch clamp recordings indicate that the GFP-Kv1.4 subunits efficiently produce active channels. However, N-type inactivation was lost probably because some of the N-terminal channel sequence was replaced with GFP. Whole cell recordings revealed that photobleaching the GFP moiety did not affect channel gating. Thus, damage produced by bleaching may be local and limited. Using a laser confocal microscope, we have conducted FRAP experiments. These show that a fraction of GFP-Kv1.4 channels are mobile in the PM and in the ER. Cotransfection with PSD95 reduced this fraction and slowed diffusion of mobile channels in the PM. Further experiments will be aimed at determining (1) mobility differences between the Kv and Kir channels, (2) mobility in the ER and PM, and (3) channel domains that affect movement and targeting. Supported by the NIH. ESL is an AHA Established Investigator.

Th-Pos16

TRANSLATION OF THE CARDIAC POTASSIUM CHANNEL, Kv1.4, BY INTERNAL RIBOSOME ENTRY.

((**D. Laidlaw-Negulescu**, L. E.-C. Leong*, K.G. Chandy, B.L. Semler*, and G.A. Gutman*)) Depts. of Physiology and Biophysics, and *Microbiology and Molecular Genetics, Univ. of California, Irvine, CA 92697.

The voltage-gated potassium channel Kv1.4 is expressed in heart, brain and skeletal muscle. We have recently mapped two transcripts found in heart and brain (3.5 and 4.5 kb), and shown them to differ only in their 3' non-coding regions (NCR), the result of alternative use of two polyadenylation sites (Wymore et al., 1996). The typical 5' NCR of vertebrate genes is ~70 nt in length and contains few if any AUG codons upstream of the authentic translational start site. By contrast, the 5' NCRs of these Kv1.4 transcripts are 1.2 kb long, and contain 18 abortive AUG codons. These features, which are shared with some other Kv channel transcripts, are thought to inhibit conventional cap-dependent scanning by the 40S ribosomal subunit. These unusual properties led us to investigate the possibility that translation initiation of these transcripts may be mediated by an internal ribosome entry segment (IRES), a mechanism common in some viruses (notably picornaviruses) but so far known in only one vertebrate gene, the immunoglobulin heavy-chain binding protein BiP. IRES activity was measured by transfecting NIH-3T3 or COS-1 cells with a bicistronic vector containing the Kv1.4 5' NCR inserted between an upstream chloramphenicol acetyl transferase (CAT) gene and a downstream luciferase (LUC) gene . The CAT gene is translated in a cap-dependent manner, but the LUC gene is translated only if an IRES is contained within the intercistronic spacer. Our results show high levels of expression of LUC following transfection with such constructs, indicating that the 5' NCR of Kv1.4 is capable of directing translation initiation by internal ribosome entry. Deletion analysis has localized the IRES activity within the 3' proximal half of the 5' NCR. Efforts are underway to define the secondary structure and RNA binding proteins required for IRES activity. Such IRES elements may play important roles in the regulation of expression of Kv1.4 and related channel genes. (Supported by USPHS grant AI24783)

K CHANNELS: MISCELLANEOUS

Th-Pos17

FUNCTIONAL CHARACTERIZATION OF THE CLONED CAT MINK CURRENT EXPRESSED IN *XENOPUS* OOCYTE.

((**C.F. Lo**, M. Cuddy, Y. Qu, L.-S. Chen, R. Numann and T.J. Colatsky)) Division of Cardiovascular and Metabolic Diseases, Wyeth-Ayerst Research, Princeton, NJ 08543-8000.

We have recently isolated a cardiac cDNA clone encoding cat minK (cminK). It has >72% amino acid sequence homology to the rat, mouse, rabbit, guinea pig, and human minK. Expression of cminK in *Xenopus* oocytes elicited a slowly activating outward K^+ current with a monovalent cation selectivity of K^+>Rb^+>Cs^+>>Na^+>Li^+. CminK current was blocked by azimilide, a class III antiarrhythmic drug, with an IC_{50} of approximately 4 μM. CminK current activation failed to reach steady-state even after 15 s depolarization to +50 mV, and the time course of activation could be reasonably well described by a sum of two exponentials plus an initial delay. The voltage dependency of activation ($V_{1/2}$) of cminK was similar to that of human minK, but more positive than the $V_{1/2}$ of rat, mouse, and guinea pig minK. Deactivation of cminK current followed a bi-exponential time course, which was voltage- and temperature-dependent. Comparing to human minK, cminK current has a slower time course of deactivation (at -60 mV τ_1 was slower by ~25%, τ_2 was slower by ~50%; n=13-17). CminK was modulated by Ca^{2+} and phosphorylation. Ionomycin increased current amplitude and prolonged the deactivation time constants of cminK. Conversely, current amplitude decreased in the absence of extracellular Ca^{2+}. Chelating intracellular Ca^{2+} by injecting EGTA into oocytes attenuated the cminK current. Interestingly, thapsigargin had a bi-phasic effect on cminK: it initially decreased the current amplitude, followed by an increase of current that was dependent on extracellular Ca^{2+}. Protein kinase A activation, induced by 8-bromo-cAMP or forskolin plus IBMX, increased the amplitude of cminK and shifted the voltage of half activation to a negative direction. Human minK current was regulated in a similar manner by Ca^{2+} and protein kinase A. In summary, cminK has similar but not identical properties to that seen in human and other mammalian minK clones.

Th-Pos18

The transmembrane domain in minK K^+ channel subunits is extended.

((**Kwok-Keung Tai**, and Steve A. N. Goldstein)) Departments of Pediatrics and Cellular and Molecular Physiology, Boyer Center for Molecular Medicine, Yale University School of Medicine, New Haven, CT. 06536-0812.

MinK has just 130 amino acids with 23 central residues (45-67) that are hydrophobic, bounded by charged residues and predicted to cross the membrane in α-helical conformation. While epitopes at positions 22 and 103 confirm these sites are external and intracellular, respectively, the disposition of residues across the membrane is undetermined. To gain further insight into the secondary structure of the pore-forming transmembrane domain of minK we used Cd^{2+} to probe the side-chain exposure of cysteine-substituted mutants. Wild-type minK channels expressed in Xenopus oocytes and studied by two-electrode voltage clamp are insensitive to exposure to 0.1 mM Cd^{2+} from the bath solution. When minK residues 42 to 60 are changed individually to cysteine, mutation of position 55 is found to create a channel sensitive to reversible block by Cd^{2+}. The effect of Cd^{2+} on F55C-minK channels is reversible and dose-dependent. That block does not alter gating kinetics suggests it proceeds by a direct pore occlusion mechanism. That block shows almost no voltage-dependence argues the binding site for Cd^{2+} is superficial to the transmembrane electric field ($\delta = 0.05 \pm 0.01$, n = 5 oocytes). Previously, we showed that cysteines in positions 44, 45 and 47 rendered channels sensitive to modification by a negatively-charged methanethiosulfonate derivative and thus argued these sites were exposed to the external aqueous solution as well as the channels' 'filter' against anions. The current findings argue that minK residues as far into the hydrophobic stretch as position 55 are in ready contact with the extracellular solution and suggests that minK has an extended transmembrane conformation like that in the pore-forming regions of K^+ channel subunits bearing P domains.

Th-Pos19

Counting the subunits in a two P domain K^+ channel

((**Ke-Wei Wang** and Steve A. N. Goldstein)) Departments of Pediatrics and Cellular and Molecular Physiology, Boyer Center for Molecular Medicine, Yale University School of Medicine, New Haven, Connecticut 06536-0812.

Tok1 is an outward rectifier K^+ channel from *S. cerevisiae* and the founding member of a new superfamily of K^+ channels with two P domains in each subunit. Because subunits with a single P domain aggregate as tetramers to form functional K^+ channels, we expect Tok1 subunits to associate as dimers. To test this hypothesis, Tok1 is expressed in Xenopus oocytes where channel currents are studied by two-electrode voltage clamp and subunit surface expression measured by fluorescence microscopy. Subunit stoichiometry is evaluated as follows. Point mutations are made in either the first P domain (P_1) or the second (P_2) and mutations that ablate channel function but leave surface expression unaltered are identified. Subunit surface expression is studied by confocal microscopy using Tok1 subunits carrying a green fluorescent protein (GFP) derivative on their carboxy termini. When wild-type subunits are co-expressed with P domain mutants, whole cell channel currents decrease. This suggests that the subunits are interacting to form non-functional channel complexes and, thus, that at least two subunits are associating. The decrease in current is fit by a simple binomial distribution to calculate subunit stoichiometry. That mutations in either P_1 or P_2 can produce electrically silent channels (whose subunits are found on the cell surface) argues that both domains on each Tok1 subunit contribute to pore formation and are required for function. Preliminary results favor a model in which the channel pore is formed from four P domains (P_1-P_2 + P_1-P_2) contributed by two Tok1 subunits.

Th-Pos20

FUNCTIONAL EXPRESSION OF COCHLEAR SLO POTASSIUM CHANNELS IN HEK293 CELLS and XENOPUS OOCYTES

((**T. Michael**, K. Ramanathan, E.M.C. Jones, J.J.Art, R. Fettiplace & P.A. Fuchs)) Depts. Otolaryngology-HNS and Biomedical Engineering, The Johns Hopkins School of Medicine, Baltimore, MD 21205, Dept. Neurophysiology, U. Wisconsin, Madison, WI 53706.

Large conductance, calcium-activated (BK) potassium channels are central to the excitability of mechanosensory hair cells of vertebrates. BK channels are encoded by alternatively-spliced transcripts of the slo gene in mammalian brain. Here we show that chick cochlear homologues of the slo gene (cslo1 and cslo2) encode BK channels when expressed in heterologous cells. Cslo clones were identified by homology screening of a chick cochlear cDNA library (Jiang et al., 1995, Soc. Neurosci. 25:524). A full- length clone, cslo1, was expressed in HEK293 cells by transient transfection. Whole-cell and 'macro' patch currents were voltage and calcium-dependent and were blocked by charybdotoxin. The channels were half-activated at 0 mV in 16 μM calcium. A hybrid clone containing the alternative carboxy terminus found in a partial clone, cslo2, produced very similar currents. Single channel recordings were made in excised patches from Xenopus oocytes injected with cslo cRNA. Unitary conductance (300 pS) and half-activating calcium concentration at 0 mV (10 μM) were similar for both cslo1 and the hybrid cslo2. The deactivation time constant was voltage-dependent and at -50 mV was 2.3 ±0.6 ms for cslo1 and 2.4 ±0.2 ms for hybrid cslo2. Thus in these experiments the alternative carboxy tails found in cslo1 and cslo2 did not result in functionally distinct BK channels. The properties of cslo (1 and 2) resemble one kinetic class of BK channels found in turtle cochlear hair cells.

Th-Pos21

LARGE CONDUCTANCE K_{Ca} CHANNELS FROM RAT CEREBELLUM INCORPORATED INTO LIPID BILAYERS

((*Ottolia, M., Gazzotti, P., *Possani, L.D., *Prestipino, G.)) *Inst. of Cybernetics and Biophysics, CNR, Genoa, Italy. * Inst. of Biotech./UNAM, Cuernavaca 62271, Mexico. * Inst. of Bioch. III, ETH-Zentrum, CH-8092 Zurich

Membrane vesicles from rat cerebellum were isolated and reconstituted into lipid bilayers. Incorporation of membrane vesicles mainly led to the activity of two different potassium channels: 1) a voltage dependent potassium channel with a conductance of about 50 pS (250/5 mM KCl) and insensitive to internal Ca^{2+} and 2) a large-conductance calcium and voltage activated potassium channel (K_{Ca}). K_{Ca} channels from rat cerebellum had a conductance of 298 pS in symmetrical potassium (250 mM KCl). They were activated by depolarizing membrane potentials. Single channel voltage activation curve gave an effective valence of about 2. Increasing the internal Ca^{2+} concentration reversibly shifted the voltage activation curve toward more negative potentials. Reconstituted K_{Ca} channels were sensitive to micromolar concentrations of external TEA. The fitted dose response curve gave a K_d of 142 μM at 20 mV and a Hill coefficient of 1. K_{Ca} channels were blocked by nanomolar concentrations of external charybdotoxin but they were insensitive to nanomolar concentrations of external Noxiustoxin. Finally, K_{Ca} channels from rat cerebellum reconstituted into lipid bilayers also respond to the addition of the *Androctonus australis hector* venom. This venom was active only from the external side of the channel and was able to block K_{Ca} channels but not the 50 pS voltage activated potassium channel. Toxins from this venom will be purified and tested on the reconstituted potassium channels.

Th-Pos22

FUNCTIONAL CO-LOCALIZATION OF CALCIUM-ACTIVATED POTASSIUM CHANNELS AND CALCIUM CHANNELS IN RABBIT CORONARY ARTERY MYOCYTES.

((**A. Guia** and N. Leblanc)) Montreal Heart Institute, 5000 Bélanger St., Montreal, Quebec, Canada H1T 1C8.

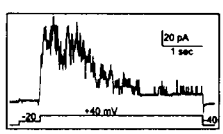

The activity of Ca^{2+}-activated K^+ channels (K_{Ca}) is known to be increased by sarcolemmal Ca^{2+} entry. Further, there are indications that K_{Ca} may be co-localized with sarcolemmal Ca^{2+} channels, although this has not been proven. The goal of this study was to assess whether K_{Ca} may be activated by adjacent Ca^{2+} channels in vascular smooth muscle. We demonstrate that the transient activation of K_{Ca} elicited by activation of Ca^{2+} channels is dissociated from the rise in cytosolic Ca^{2+} concentration (in whole-cell voltage-clamped cells loaded with Indo-1). Single-channel studies from cell-attached patches were performed with the cells bathed in Ca^{2+}-free depolarizing media. Physiological Ca^{2+}-containing pipette solution elicited, in two of six cells, a transient activation of K_{Ca} which decayed in two to five seconds. This transient activation was itself temporary during repeated stimulation. The proportion of cells displaying a transient increased to 8 of 10 cells when the pipette also contained Bay-K 8644, a Ca^{2+} channel activator (sample trace shown). No transient activation of K_{Ca} was observed with Ca^{2+}-free pipette solution, both in the presence or in the absence of Bay-K 8644. The open probability of K_{Ca} was increased in the presence of Ca^{2+} and further by the addition of BAY-K 8644 in the pipette tip. These results suggest a functional proximity of K_{Ca} and Ca^{2+} channels which may play an important role in the regulation of resting membrane potential, Ca^{2+} entry and tone.

Th-Pos23

VISUALIZATION AND FUNCTIONAL ANALYSIS OF A CLONED MAXI K^+ CHANNEL (m*Slo*) FUSED TO GREEN FLUORESCENT PROTEIN (GFP)

((**Michael P. Myers**, Jay Yang, and Per Stampe)) Depts. of Pharm. and Physiol., and Anesthesiology, University of Rochester School of Medicine and Dentistry, Rochester, New York 14642.

Recent advances in the study of the structure and function of ion channels has been limited by the problems of expression, identification, and isolation of cloned channels. We previously reported that a GFP probe could be used as a reporter gene to optimize expression of a recombinant, large conductance, calcium-activated potassium channel (Maxi K^+). Recently, we have refined this probe by constructing a fusion protein between m*Slo* (cloned from a complex mouse gene), and the jellyfish green fluorescent protein (GFP). When m*Slo*-GFP is expressed in COS-7 cells, confocal laser scanning and conventional optical fluorescent (pictured at right) microscopy reveals robust fluorescence localized to the cell membrane. Fluorescing cells that are patch clamped exhibit whole cell currents with a direction consistent with potassium currents, while non-fluorescing cells show no significant whole cell currents. Whole cell currents activate at voltages above -50 mV, and any further hyperpolerizations result in no currents. Excised inside out patches reveal single channel currents of about 16 pA (2.8 mM KCl and 100 μM Ca^{2+} in the bath, 140 mM KCl and 1 mM Ca^{2+} in the pipet, with a holding potential of +40 mV), and calculated conductances in the range of those expected for the Maxi K^+. The functional integrity of this construct will be confirmed by a full kinetic and pharmacological profile obtained from channels reconstituted into lipid bilayers. Among the growing pool of GFP fusion constructs, this new chimera represents a tagged potassium channel and makes it possible to label Maxi K^+ channels in living mammalian tissue-culture cells. As newly constructed GFP chimeras emerge for the study of physiological processes in living organisms, this work provides another area of insight illuminated by GFP.

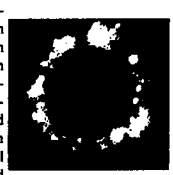

Th-Pos24

MOLECULAR CONSTITUENTS OF MAXI K_{Ca} CHANNELS IN HUMAN CORONARY SMOOTH MUSCLE CELLS.

((**Y. Tanaka**, P. Meera and L. Toro)) Dept. of Anesthesiology, UCLA School of Medicine, Los Angeles, CA 90095-1778.

Large conductance voltage-activated and calcium-sensitive potassium (Maxi K_{Ca}) channels are involved in the regulation of vascular smooth muscle cell excitability and vascular tone. At the molecular level, the Maxi K_{Ca} channel is composed of at least two subunits, the pore-forming α subunit and the modulatory membrane bound β subunit. The functional coupling of α and β subunits, as reflected by an increase in the channel Ca^{2+} sensitivity, requires μM $[Ca^{2+}]_i$ (Meera *et al.*, *FEBS Letters* **382**:84-88, 1996). In the present study, the presence of α and β subunits of the Maxi K_{Ca} channel was examined in freshly dissociated human coronary smooth muscle cells. The results were compared with those from oocytes expressing the human α (*hslo*) and β (hK$_{V,Ca}$β) subunits. Maxi K_{Ca} channels were abundant in human coronary cells. In patches with unitary currents, the majority of the channels were activated at low threshold potentials (Vh ≤ -65 mV, $[Ca^{2+}]_i$ = 18 μM). These values were close to the results from oocytes expressing both *hslo* and hK$_{V,Ca}$β. Macroscopic currents (Vh ≈ -80 mV) from human coronary smooth muscle cells and from oocytes expressing *hslo* and hK$_{V,Ca}$β were increased by dehydrosoyasaponin I (DHS-I) (250 nM). As previously shown for *mslo* (McManus *et al.*, *Neuron* **14**:645-650, 1995), DHS-I did not increase the currents from oocytes expressing *hslo* alone. These results strongly suggest that most of the Maxi K_{Ca} channels in human coronary artery consist of α and β subunits. We propose that the coupling of α and β subunits in coronary smooth muscle cells makes the Maxi K_{Ca} channels respond efficiently to increases in the local $[Ca^{2+}]_i$, and thus serve as a major factor in controlling coronary tone.

L.T. is an AHA-Established Investigator. Supported by NIH grant HL47382.

Th-Pos25

CA^{2+} CHANNEL SUB-TYPES INVOLVED IN BK CURRENT ACTIVATION IN RAT CHROMAFFIN CELLS. ((**M. Prakriya** and C. J. Lingle)) Dept. Of Anesthesiology, Washington University School Of Med. St. Louis MO 63110 (sponsored by J. M. Nerbonne)

BK channels are activated in response to elevations of submembrane $[Ca^{2+}]_i$ during action potential activity, and in some cells, play a role in fast repolarization during action potentials. Here, we examine the role of the various types of Ca^{2+} channels found in rat chromaffin cells in driving BK current activation. Whole-cell BK current was activated by brief Ca^{2+} influx steps (5 ms steps to -9 mV). Current through Ca^{2+} channels was measured using 10 mM Ba^{2+} as the charge carrier. The effects of Ca^{2+} channel blockers on either Ca^{2+} or BK current activation were determined, whenever possible in the same cells. The L-type Ca^{2+} channel antagonist, nifedipine (5 μM) blocked ~31% of the Ca^{2+} current, but reduced the BK current activated by Ca^{2+} influx by ~75%. The N-type blocker ω-Conotoxin GVIA (CgTx) (2 μM) blocked ~24% of the Ca^{2+} current, and ~28% of the BK current activated by Ca^{2+} influx. CgTx had both irreversible and reversible effects on the Ca^{2+} current in most cells. The P-type Ca^{2+} current inhibitor, ω-Agatoxin IVA (AgaTx) (150 nM) blocked ~12% of the Ca^{2+} current and about 17% of the BK current activated with influx. Bay K 8644 (1 μM) enhanced the Ba^{2+} current to ~140% of control, but resulted in a 220% increase in the BK current elicited with Ca^{2+} influx. None of the Ca^{2+} channel blockers tested affected BK current directly. These data suggest that L-type channels are more strongly coupled to BK current activation than either the CgTx- or the AgaTx-sensitive Ca^{2+} channels in rat chromaffin cells.

Th-Pos26

THE β-SUBUNIT OF HIGH CONDUCTANCE CALCIUM-ACTIVATED POTASSIUM CHANNELS CONTRIBUTES TO THE FORMATION OF THE TOXIN-BINDING SITE. ((M. **Hanner**[1], W.A. Schmalhofer[1],H.-G. Knaus[2], G.J. Kaczorowski[1] and M.L Garcia[1])) [1]Merck Research Laboratories, Rahway, NJ 07065, [2]Institute for Biochemical Pharmacology, Innsbruck, A-6020 Austria.

Mammalian high conductance, calcium-activated potassium (maxi-K) channels are composed of two subunits. Channels from oocytes injected with cDNAs encoding both α and β subunits are more sensitive to activation by voltage and calcium than channels composed of the α subunit alone. To examine the functional role of the β subunit, binding of ^{125}I-charybdotoxin (^{125}I-ChTX) was performed to membranes derived from COS-1 cells transfected with α or α + β subunits. Under low ionic strength conditions, the equilibrium dissociation constant (K_d) for ^{125}I-ChTX to either α or α + β membranes was 45.1 pM and 0.84 pM, respectively. The dissociation rate constant (k_{-1}) for the α subunit was 0.1735 min^{-1} compared to 0.0238 min^{-1} for the α/β heteromultimer. There is a 7.3 fold stabilization of the toxin bound state produced by the β subunit. The association rate constant (k_{+1}) for α and α/β was 0.0033 pM^{-1} min^{-1} and 0.0153 pM^{-1} min^{-1}, respectively. Expression of the β subunit resulted in a 4.7 fold increase in the on-rate kinetics, suggesting that significant electrostatic interactions between toxin and negative charges at the β subunit occured. Mutation of the negatively charged amino acids to neutral in the extracellular loop of the β subunit confirmed that amino acids E62, E64, E65, E67 and E94 determine the on-rate kinetics. The dissociation rate constants of these mutations were unchanged compare to wild-type α + β subunits, except for mutation E94A that caused a 4-fold increase in the off-rate kinetics. These results demonstrate that the auxiliarly β subunit contributes to the toxin-binding site of the pore forming α subunit.

Th-Pos27

PAXILLINE INHIBITION OF THE ALPHA-SUBUNIT OF THE HIGH-CONDUCTANCE CALCIUM-ACTIVATED POTASSIUM CHANNEL. ((M. Sanchez, D. Wunderler, A. Kamassah, and **O.B. McManus**)) Dept. of Membrane Biochemistry and Biophysics, Merck Research Labs, P.O. Box 2000, Rahway, NJ , 07065

High conductance calcium-activated (maxi-K) channels are potently blocked by a family of indole diterpenes that includes paxilline. Paxilline stimulates binding of charybdotoxin (ChTX) to maxi-K channels in vascular smooth muscle and blocks these channels in electrophysiological experiments (Knaus *et al.*, 1994). These results suggested that paxilline blocked maxi-K channels at a site distinct from the ChTX binding site located near the external entrance to the pore. Here we have examined block of the cloned alpha subunit (slo) of the maxi-K channel in excised membrane patches after internal application of paxilline. Paxilline caused a reversible inhibition of channel currents with slow washout kinetics. In the presence of 10 μM intracellular calcium, paxilline blocked currents elicited by brief voltage pulses with a K_i of 1.9 nM and a Hill coefficient near one. Changing the internal calcium by ten fold caused a two to three fold change in the K_i for paxilline block, with less block occurring at high calcium concentrations. Paxilline reduced the maximum of the conductance-voltage relation in a calcium-sensitive manner with less block occurring at high calcium concentrations, and caused a 20 mV depolarizing shift in the midpoint for channel opening. The time-course of relief of paxilline block by elevated calcium was more rapid than washout of paxilline suggesting an allosteric interaction between calcium and paxilline.

Th-Pos28

EFFECTS OF CALCIUM ON SINGLE SK CHANNELS EXPRESSED IN XENOPUS OOCYTES. ((**BH Hirschberg**, J Maylie and JP Adelman)) Oregon Health Sciences University, Vollum Institute, Portland, Oregon

Several members of a family of small conductance calcium-activated potassium channels (SK channels) have recently been cloned (Köhler, 1996). The cloned SK channels fall into two classes with respect to their sensitivity to apamin. The apamin-sensitive subtypes (K_i = 60 pM) are expressed in brain regions where slow afterhyperpolarizations (sAHPs) are blocked by apamin, and the apamin-insensitive channels (not blocked by 100 nM) are expressed where the sAHPs are apamin-insensitive. Expression of the cloned SK channels in *Xenopus* oocytes results in currents which are voltage-independent and calcium-dependent, with a K_D of 0.6 μM and a Hill coefficient close to 4. Single channels have a unit conductance of 9-10 pS in symmetrical 120 mM K. Taken together, these results strongly suggest that the cloned SK channels represent the channels which underlie the sAHP in central neurons and other excitable cell types. We are presently investigating the mechanism by which calcium affects the channels by examining single channel behavior in membrane patches excised from *Xenopus* oocytes. Specifically, we are determining the open- and closed-time distributions, and the open probability as a function of intracellular calcium concentration. Although the open probability varies significantly among patches, it generally reflects the calcium-dependence seen in macropatches: the open probability increases over a range of [Ca] from 0.2 - 1 μM. In a representative single channel patch with an open probability greater than 0.9 at 1 μM calcium, the closed duration histogram showed one major component of ~ 1 ms. Lowering intracellular calcium to 0.4 μM resulted in the appearance of at least one additional long closed time. So far, our data are consistent with a model in which at least one calcium-dependent transition is followed by a calcium-independent transition.

Th-Pos29

IS HIGH CONDUCTANCE Ca^{2+}-DEPENDENT K CHANNEL A GOOD Ca^{2+} INDICATOR? ((Alvaro Muñoz, Lucía García and **Agustín Guerrero**)) Dept of Biochemistry, CINVESTAV-IPN, Mexico city.

Activity of high conductance, Ca^{2+} dependent K^+ channels (maxi K) has been used as an indicator of internal Ca^{2+} concentrations near the plasma membrane. However, Ca^{2+} sensitivity of maxi K channels has been obtained in *in vitro* studies in excised patches or by incorporating these channels in planar bilayers. We have combined microfluorometry of Fura-2 and patch clamp in the cell attached mode to study the relationship between $[Ca^{2+}]_i$ and the activity of maxi K channels in single urinary bladder smooth muscle cells. $[Ca^{2+}]_i$ was transitorily increased by the application of ionomycin and this change measured with Fura-2 was correlated with the activity of maxi K channels recorded at a membrane potential of 0 mV. We have found that the channel activity achieved 10% at 0.7 ± 0.1 μM and 90% at 1.3 ± 0.12 μM of free $[Ca^{2+}]_i$ in agreement with Hill numbers of 8 ± 3 been required to fit this relationship. This Hill number obtained in intact cells is much higher than previously described in excised patches. We have also observed that the channel activity could drop at elevated $[Ca^{2+}]_i$. A variable relationship between $[Ca^{2+}]_i$ and the activity of the maxi K channel and a very high Hill number when the channel is recorded *in situ* make maxi K channels an unreliable indicator of Ca^{2+} changes near the plasma membrane.

Th-Pos30

Ca^{2+} AND K^+ CHANNELS IN HUMAN ESOPHAGEAL SMOOTH MUSCLE. ((**Gregory R. Wade, Harold G. Preiksaitis and Stephen M. Sims**)) Dept. of Physiology, Univ. of Western Ontario, London, Canada (Sponsored by M. Sherebrin)

Ion channel diversity may contribute to the distinct patterns of excitation and contraction in different smooth muscles. A goal of our studies is to characterise the various ion channel types in human esophagus. For this study, cells were dissociated from disease free segments of longitudinal esophageal body retrieved during surgery. Whole-cell currents were recorded using the nystatin perforated-patch configuration. Freshly dissociated cells were initially relaxed and exhibited voltage-activated inward and outward currents. When patch pipettes contained Cs^+ (to block K^+ channels), depolarization to potentials more positive than -40 mV evoked a transient inward current with peak amplitude at +10 mV. This was identified as L-type Ca^{2+} current based upon its activation and inactivation characteristics, and pharmacological sensitivity to nifedipine and BAY K 8644. With K^+ in the electrode, depolarization elicited outward current with transient and persistent components. The persistent current was blocked by TEA (5 mM), charybdotoxin (100 nM) and iberiotoxin (50 nM), suggesting a Ca^{2+}-dependent K^+ current. Single-channel recordings confirmed the presence of the maxi-K^+ channel (γ = 224±4 pS). The transient outward current activated with a delay, peaked within 100 ms, decayed over the course of several seconds, and was blocked by 4-AP (5 mM). Therefore, the delayed rectifier of human esophagus has characteristics consistent with Kv1.2 and/or Kv1.5 K^+ channel(s). In conclusion, the longitudinal body of human esophageal smooth muscle exhibits L-type Ca^{2+} channels, maxi K^+ channels and delayed rectifier K^+ channels. Supported by the Medical Research Council of Canada and The Ontario Thoracic Society.

Th-Pos31

MICROVASCULAR ENDOTHELIAL CELLS LACK INWARD RECTIFIER K^+ CURRENT. ((**H.M. Himmel**, N. Murawski*, U. Rauen*, U. Ravens))
Inst. für Pharmakologie & *Physiol. Chemie, Universität Essen, Germany.

NO-generation in endothelial cells (EC) depends on transmembrane Ca^{2+}-influx along the electrochemical gradient. This gradient is big in macrovascular EC due to their negative membrane potential which is related to a prominent inward rectifier K^+-current (I_{K1}). Since local blood flow is controlled by microvascular EC, we were interested in I_{K1} function in these cells. EC from rat liver (RLEC) and human omentum (HOEC) were used as models for microvascular EC; macrovascular EC from bovine aorta (BAEC) and human arteria iliaca (HAIEC) served as controls. Voltage ramps (range -120 to +60 mV; V_H -40 mV; 0.2 Hz; 24°C) in microvascular EC resulted in an almost linear IV-relation with small current densities (pA/pF at -110 mV: -2.9±0.3, n=55, RLEC; -0.6±0.1, n=13, HOEC), outward rectification positive to +10 mV, and reversal potentials (E_{rev}) of -32±3 mV (RLEC) and -26 ±4 mV (HOEC). Current at -110 mV was increased by both zero and 140 mM $[K^+]_o$, E_{rev} was shifted towards 0 mV. Such properties are not consistent with I_{K1}. In contrast, voltage ramps in macrovascular EC showed an inwardly rectifying current (pA/pF at -110 mV: -7.8±0.5, n=47, BAEC; -2.2± 0.3, n=5, HAIEC) which reversed close to the K^+ equilibrium potential (-84 mV). This current was abolished by zero $[K^+]_o$ or Ba^{2+} (1 mM), and increased by 140 mM $[K^+]_o$ with E_{rev} shifted towards 0 mV, and thus is considered as I_{K1}. The absence of I_{K1} in microvascular EC suggests large regional differences in the regulation of endothelial cell function.

Th-Pos32

K^+ CHANNEL HOMOLOGUES IN THE *METHANOCOCCUS JANNASCHII* GENOME, EVIDENCE FOR INTRAGENIC DUPLICATION IN THE EVOLUTION OF THE TANDEM-PORE K^+ CHANNEL GENE FAMILY. ((**K.A. Ketchum**, H.-P. Klenk, O. White, and J.C. Venter)) The Institute for Genomic Research, 9712 Medical Center Drive, Rockville, Maryland, 20850.

K^+-selective ion channels are a diverse group of proteins with a complex evolutionary history. All members of this gene family encode a structural motif (M1-P-M2) consisting of a highly conserved pore-region bordered by two membrane-spanning helices. Sub-families are distinguished by the presence of additional membrane segments (inward-rectifier vs. *Shaker* channels), multiple M1-P-M2 motifs (tandem-pore channels), or associated regulatory domains (cyclic nucleotide-gated channels). These differences indicate that both intragenic duplication and domain fusion have played a role in the evolution of K^+ channel genes. Sequences from the Archaeon *Methanococcus jannaschii* provide examples of these evolutionary steps and new insights into the origin of channel proteins. Three open reading frames (ORFs MJ0138.1, MJ0139, and MJ1357) were identified with peptide segments similar to the P-region of K^+-selective channels. In each ORF the P-like sequence was positioned between hydrophobic tracks consistent with the structure of a M1-P-M2 motif. MJ0138.1 and MJ1357 have a predicted membrane topology similar to IRK1/ROMK1 inward-rectifier channels with only two transmembrane segments. By contrast, MJ0139 is analogous to *Shaker* K^+ channels with 5 hydrophobic regions and a positively charged S4-like segment. Interestingly, MJ0139 is immediately followed by MJ0138.1 on the *M. jannaschii* chromosome (MJ1357 is 500 kb from these two genes). The ORFs are translated in the same reading frame and separated by the three nucleotides that comprise the stop codon for MJ0139. Their M1-P-M2 sequences display 65% identity (85% similarity) suggesting that the adjacent pore motifs originated from an incomplete, intragenic duplication. The fusion of these two ORFs would result in a protein with striking similarity to the tandem-pore channels found in eukaryotes. Hence, these Archaeon sequences may represent an intermediate stage in K^+ channel evolution.

Th-Pos33

ELECTROPHYSIOLOGICAL AND MOLECULAR CHARACTERIZATION OF A K^+ CHANNEL IN PHOTORECEPTORS OF THE HORSESHOE CRAB, *LIMULUS POLYPHEMUS*. ((**Chaves, D.**[1], Jeziorski, M.C.[2], Battelle, B.-A.[2], Renninger, G.H.[1])).
[1]Department of Physics, University of Guelph, Guelph, Canada, N1G 2W1. [2]Whitney Laboratory, University of Florida, St. Augustine, FL 32086.

Light depolarizes the photoreceptor cells of the horseshoe crab, *Limulus polyphemus*. Voltage-gated ion channels shape this electrical response. Ion channels found by patch-clamp recordings of photoreceptor cells dissociated from the compound eye include voltage-dependent native K^+ channels. One K^+ channel has an excised patch conductance of about 20 pS. The other K^+ channel which is a slow inactivating channel has an excised patch conductance of about 85 pS. Solution exchange experiments performed on inside-out excised patches confirmed that these are K^+ channels.

Using RT-PCR with degenerate primers designed against the Shaker family of K^+ channels, we isolated a 1 kb fragment from ventral eye RNA. Subsequent cloning strategies were used to isolate the 5′ and 3′ fragments of the corresponding cDNA, which encodes a homolog of the Kv1 subgroup of Shaker channels. Preliminary studies suggest this sequence is also represented in the lateral eye.

The channel was expressed in *Xenopus laevis* oocytes and two-electrode voltage-clamp recordings of whole cell currents were made. The channel is slow inactivating. Using the patch-clamp technique, we hope to compare the functional properties of the cloned K^+ channel to the native K^+ channels. Characterization of this ion channel in the *Limulus* photoreceptors will contribute to a complete understanding of phototransduction and the physiological role of ion channels in the visual circadian rhythm in *Limulus*.
Research sponsored in part by NSERC Canada, and by U.S. funding agencies: NIMH (MH10625) and NSF (IBN9211327).

Th-Pos34

THREE TYPES OF OUTWARD K^+ CURRENTS IN RAT MESENTERIC ARTERY SMOOTH MUSCLE CELLS. ((**V.P. Mokh**))
Institute of Experimental Cardiology, Moscow, 121552, Russia.
(Spon. By S. Zakharov)

Three types of outward K^+ currents were recorded in single smooth muscle cells (SMC) from rat mesenteric artery using patch-clamp technique (whole-cell configuration). SMC resting potential was about - 45mV. The first component of the current was a typical delayed rectifier (K^+_{dr}) current, and was found in about 90% of SMC. It was voltage- and time-dependent, activated at -40 mV and showed only partial inactivation even after 5 seconds of depolarisation. 10 mM 4-aminopyridine (4-AP) inhibited K^+_{dr} current almost completely, while 1 mM TEA had no effect. Application of 4-AP caused SMC depolarisation of 35 mV. Second component, present in all SMC, was a typical calcium- and voltage- dependent (K^+_{Ca}) current : this current was noisy, voltage- and time-dependent, activated at positive potentials, and was less pronounced when pipettes contained no Ca^{2+} and 5 mM EGTA. It was effectively blocked by TEA, but was resistant to 4-AP. Inhibition of K^+_{Ca} current by TEA caused no significant changes in SMC resting potential. Third component was ATP-regulated (K^+_{ATP}) current. It was present only in 25% of SMC. When pipettes contained 5 mM ATP this current was not observed. K^+_{ATP} current was weakly potential-dependent and was inhibited by glibenclamide which induced SMC depolarization of about 20 mV. Thus, three types of outward current could be physiologically and pharmacologically distinguished in SMC from rat mesenteric artery. Our data strongly suggest that K^+_{dr} channels play the main role in regulation of SMC resting potential in normal resistance arteries.

Th-Pos35

NOVEL POTASSIUM CONDUCTANCE IN ANDROGEN-SENSITIVE PROSTATE CANCER CELL LINE, LNCaP: INVOLVEMENT IN CELL PROLIFERATION ((**R. Skryma§**, N. Prevarskaya§, L. Dufy-Barbe* and Bernard Dufy*)) §Laboratory of Cells Physiology, University of Lille 1 and *Laboratory of Neurophysiology,CNRS UMR 5543,University of Bordeaux II, France.

Membrane ion channels are known to play important roles in the regulation of cell processes, including proliferation, apoptosis, differentiation and tumorization. However, nothing is known about the expression of ion channels in prostate cells (both normal and malignant), and their possible role in physiological and pathological functions. We therefore studied ion conductances and their role in the proliferation of LNCaP cells, an androgen-sensitive human prostate cancer cell line, derived from a lymph node of a subject with metastatic carcinoma of the prostate. We applied patch-clamp recording techniques for electrophysiological studies and ^{3}H-thymidine incorporation, MTT and protein synthesis assays for cell growth studies. Only one type of ion channel, a potassium K^+ channel with a unitary conductance of 70-80 pS was identified. This channel, which was depressed by a rise in intracellular Ca^{2+}, had a high sensitivity to tetraethylammonium (with half-block of 150 µM) and was also inhibited by 2 nM α-dendrotoxin, 20 nM mast cell degranulating peptide and 20 µM verapamil. K^+ channel inhibitors decreased the number of metabolically active cells, [^{3}H]thymidine incorporation and protein synthesis, in a dose-dependent fashion, indicating that K^+ channels are involved in cell growth. We conclude from our findings that the human cancer prostate cell line LNCaP has a new type of K^+ channel, likely to play an essential role in the physiology of these cells and, more specifically, in cell proliferation.

Th-Pos36

CLONED LARGE-CONDUCTANCE CALCIUM-ACTIVATED POTASSIUM CHANNELS FROM PREGNANT RAT MYOMETRIUM
((**K.M. Lawrence**, C.J. Fenech, H. Zhang, T.B. Bolton)) Department of Pharmacology and Clinical Pharmacology, St George's Hospital Medical School, Cranmer Terrace, London SW17 ORE. U.K. (Spon. by I. Greenwood).

We have cloned using a combination of rapid amplification of cDNA ends (RACE) and high fidelity long polymerase chain reactions (PCR), two full length α subunit isoforms of a large-conductance calcium-activated potassium channel (rm1 and rm2) from (day 12) pregnant rat myometrial smooth muscle. Both isoforms exhibit no additional exons at any of the previously reported splice junctions and were highly homologous with other mammalian clones within their core region. One of our isoforms, rm1, possessed an additional 30 unique amino acids at its 3' end. cRNA encoding rm1 microinjected into *Xenopus* oocytes produced a large outward whole cell current which was blocked by tetraethylammonium (TEA, IC_{50} 0.4mM) and charybdotoxin (ChTx, IC_{50} between 100 and 500nM) and was doubled in size by NS1619 (100µM). In inside-out patches (120mM KCl in bath solution, 2mM KCl in pipette) single channels were sensitive to internal calcium and had a conductance of 100pS; current reversed at -104mV. Thus expressed rm1 was approximately an order of magnitude less sensitive to TEA and ChTx than endogenous channels and some cloned α subunits alone. These discrepancies in pharmacology may be due to the unique 3' terminus of rm1. Alternatively this isoform may require the presence of β regulatory subunits.

Th-Pos37

ELECTROPHYSIOLOGICAL CHARACTERIZATION OF RAT BLADDER SMOOTH MUSCLE CELLS. ((C. Siemer and S. Grissmer)) Dept. Applied Physiology, University Ulm, D-89081 Ulm, Germany (spon. by A. Herrmann-Frank).

For characterization of ion channels in detrusor smooth muscle cells, we isolated single cells from rat bladder similar to the isolation procedure reported by Klöckner & Isenberg *(Pflügers Arch.* 405:329-339, 1985). Female WAG rats (~200 g) were killed by cervical dislocation. The bladder was dissected, cut open and rinsed with physiological solution (in mM: NaCl 100, KCl 10, KH_2PO_4 1.2, $MgCl_2$ 5, glucose 20, taurine 50, MOPS 5, adjusted to pH 6.9 with NaOH). After removement of the urothelium the detrusor muscle was cut into small pieces (1 mm x 5 mm) which were digested in a collagenase containing solution (in mM: KOH 130, taurine 20, pyruvate 5, creatine 5, HEPES 10, adjusted to pH 7.4 with methanesulfonic acid, and complemented with 1 mg/ml collagenase (Sigma C2139), 0.2 mg/ml pronase E (Serva) and 1 mg/ml fatty acid free albumin) for 40 minutes. Single cells were obtained by trituration of the muscle pieces through a Pasteur pipette in Na-Glu solution (in mM: Na glutamate 80, NaCl 55, KCl 6, $MgCl_2$ 2, glucose 11, HEPES 10, adjusted to pH 7.4 with NaOH and complemented with 1 mg/ml fatty acid free albumin). The cells were stored on ice until use. For measurements the cells were superfused with mammalian Na Ringer (in mM: NaCl 160, KCl 4.5, $CaCl_2$ 2, $MgCl_2$ 1, HEPES 5, adjusted to pH 7.4 with NaOH). The patch pipettes were filled with a KF solution (in mM: KF 145, $MgCl_2$ 2, $CaCl_2$ 1, EGTA 10, HEPES 10, adjusted to pH 7.2 with KOH). In the experiment shown in the figure a family of voltage pulses from -50 to 0 mV was applied to the cell in whole cell recording mode (holding potential -80 mV). Two current components can easily be detected. A fast activating, rapidly inactivating current can be observed at potentials more positive than -40 mV. A slower activating current with little inactivation during 200 ms pulses can be elicited at more depolarized potentials, i.e. ~20 mV. Both current components could contribute to the resting potential of those cells, thereby influencing muscle tone. Supported by a grant from Pfizer Ltd., Sandwich, England.

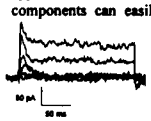

Th-Pos38

AT LEAST THREE K^+ CURRENTS ARE INVOLVED IN RESONANCE IN FROG SACCULAR HAIR CELLS. ((C.E. Armstrong and W.M. Roberts)) Inst. of Neuroscience, Univ. of Oregon, Eugene, OR 97403.

Electrical resonance found in many types of auditory and vestibular hair cells is thought to contribute to frequency selectivity in these sensory systems. In response to injected current steps, the membrane potential of resonant hair cells undergoes damped sinusoidal oscillations, the frequency of which is thought to be equal to the cells characteristic frequency. The ionic basis for electrical resonance has been well characterized in enzymatically dissociated hair cells from the sacculus of *Rana pipiens*. In these cells physiological and modeling studies show that resonant frequencies around 200Hz can be attributed to two major currents: a voltage gated Ca^{2+} current and a Ca^{2+}-dependent K^+ current. In the intact saccular epithelium, however, we find that in addition to the Ca^{2+} current at least three potassium currents are involved in the generation of resonant frequencies between 30-110 Hz . Whole-cell current clamp and voltage clamp recordings from a semi-intact preparation reveal the presence of a Ca^{2+} current and three K^+ currents: a K_{Ca} current, a voltage-dependent K^+ current (K_V), and an inward rectifier K^+ current (K_{IR}). Application of extracellular blockers for each of these currents affects the cells resonance. Resonance was altered or eliminated by blocking the K_{Ca} current with 100nM iberiotoxin (Ibtx), by blocking K_{IR} current with 5mM Cs^+, or by using concentrations of 4-AP (1mM) that block the majority of K_V while sparing the K_{Ca} current. Our results using enzymatically dissociated hair cells were consistent with previous findings: 100 nM Ibtx or 6 mM TEA eliminated nearly all of the outward current and abolished resonance, whereas 1 mM 4-AP had no effect on resonance. These results indicate that at least three, rather than a single, K^+ current is involved in generation of resonance in frog saccular hair cells.

Th-Pos39

EVIDENCE FOR TWO COMPONENTS OF DELAYED RECTIFIER K^+ CURRENT IN SMOOTH MUSCLE CELLS OF SMALL MESENTERIC RESISTANCE ARTERIES FROM RATS. ((**G.J. Waldron**, K.A. Loutzenhiser, C.R. Triggle and W.C. Cole)) The Smooth Muscle Research Group, University of Calgary, Calgary, Canada.

Small diameter arteries contribute to control of peripheral vascular resistance. Voltage-gated, delayed rectifier K^+ current (I_{KDR}) participates in regulating arterial diameter, however, the properties of this conductance in myocytes from small arteries are poorly characterized. Myocytes (26 ± 1 pF) were isolated from rat mesenteric arteries (<300 µm) with collagenase and studied by standard whole-cell patch clamp technique (with 5 mM EGTA in the pipette). Depolarizing steps to >-40 mV from -60 mV elicited I_{KDR} which inactivated slowly (complete within 8-10 sec) and was inhibited by 4-aminopyridine (0.01-10 mM). The density of I_{KDR} at +30 mV was 10.2 ± 1 pA/pF (n = 8). The voltage-dependence of inactivation was investigated using 10 sec conditioning pulses to between -110 and +20mV followed by 250 msec steps to +30mV. The steady-state inactivation curve was biphasic and best fit as the sum of two Boltzmann functions (see figure). This indicates that I_{KDR} of mesenteric resistance arteries consists of two components with distinct inactivation properties. Support: CHS/MRC (GJW) and MRC (CRT & WCC).

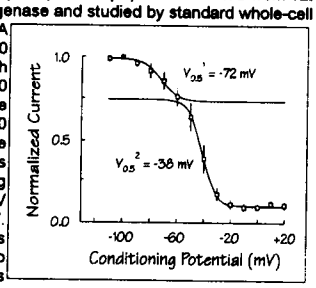

Th-Pos40

DELAYED RECTIFIER CURRENT IN HEALTHY PRIMATE CARDIAC MYOCYTES. ((**Siân A. Rees**, Anthony Wright and Trevor Powell)) University Laboratory of Physiology, Parks Road, Oxford, OX1 3PT.

It is extremely difficult to obtain healthy human cardiac tissue which may be used to investigate ion channel function at the cellular level. We have isolated ventricular myocytes from a species of non-human primate, *Callithrix jacchus*, the common marmoset, in an attempt to aid extrapolation of data from the commonly used rodent to human. Action potentials (AP) were recorded using perforated patch technique; delayed rectifier (I_K) and inward rectifier current (I_{K1}) by whole-cell voltage clamp (33-35°C). At 1 Hz, AP duration was 198±25 ms and the resting potential was -74±3 mV (n=6). Values at 3 Hz were 144±23 ms and -76±5 mV, respectively (n=4). I_K was measured using the envelope of tails test which can be used to aid dissection of I_K subtypes; cells were depolarised from -40 mV to +40 mV for durations 50 ms-2.9 s (18 durations; n=8). Current measured during the pulse and tail current were both relatively small, similar to rapid I_K (I_{Kr}) in guinea pig; I_{Kpulse} was 24±4, 33±8 ad 48±10 pA and I_{Ktail} was 115±13, 108±12 and 96±10 pA, at 100 ms, 0.4 s and 2.9 s, respectively. Analysis of the ratio I_{Ktail}/I_{Kpulse} indicated that there was only one I_K subtype, similar to I_{Kr}. When a protocol was employed which maximally activates I_{Kr} (-40 to -10 mV, 250 ms), a current sensitive to the I_{Kr} blocker, dofetilide, was activated (ED_{50}=30 nM). I_{K1} was measured using 200 ms steps between 0 and -120 mV (holding potential -40 mV). From the resulting I-V curve E_{rev} was -75 mV. Current at -120 mV was -10.9±1.7 nA compared with 0.36±0.05 nA at -40 mV (n=7). In conclusion, marmoset ventricular cells express functional I_{Kr} and I_{K1}, but no discernable I_{Ks}.

CALCIUM CHANNELS III

Th-Pos41

THE INHIBITORY EFFECT OF PROPOFOL ON L-TYPE Ca^{2+} CHANNELS IN ISOLATED SMOOTH MUSCLE CELLS LEADS TO RELAXATION IN MAMMARY ARTERY RINGS OF HUMAN.

((**J.F. Desaphy#**, E. Le Pelley*, F. Le Brun*, J. Fusciardi* and M. Joffre#)) # Lab. Physiologie Animale, CNRS URA 1869, Faculté des Sciences; * Dept. Anesthésie, CHU La Milétrie, Faculté de Médecine, 86000 Poitiers, France. (Spon. by E. Gallucci)

Propofol (2,6-diisopropylphenol) is an useful short-acting intravenous anesthetic. It was reported to induce peripheral vasodilatation increasing systemic arterial pressure by about 30 %. We investigated the effect of propofol on human vascular smooth muscle cells *in vitro*. Human internal mammary arteries were obtained during coronary bypass surgery with approval of patients and of our hospital ethical advisory committee. The anesthetic was tested on contractile properties of artery rings and on L-type calcium channels of isolated smooth muscle cells.

Whole-cell L-type currents were observed by the patch-clamp method with barium ions as charge carriers and in the presence of 1 µM Bay K-8644. In these conditions, 10^{-5} M propofol (a therapeutical concentration) reduces current amplitude by about 50 %. At 5.10^{-4} M, amplitude is reduced by about 66 %. Activation threshold and peak potential are not modified by the anesthetic. Currents are not affected by the solvent Intralipid at 1 %. Propofol was also tested on the contractile properties of vascular rings obtained from the same arteries. Incubation with 10^{-3} M propofol completely prevents the contraction induced by 40 mM KCl. At concentrations superior to 10^{-5} M, the anesthetic induces relaxation of vascular rings precontracted by 40 mM KCl. These effects are independent of the presence of endothelium.

In conclusion, we postulate that the hypotension clinically observed in response to propofol may be due, at least in part, to an inhibitory effect of the anesthetic on L-type calcium channels of vascular smooth muscle cells.

Th-Pos42

"LEAK" CALCIUM CHANNELS IN A7R5 VASCULAR SMOOTH MUSCLE CELLS. ((**C. Obejero-Paz**, S.W. Jones and A. Scarpa)) Dept. of Physiology and Biophysics, Case Western Reserve University. Cleveland OH 44106.

We have previously characterized the presence of two leak calcium channels in A7r5 cells using the cell attached configuration of the patch clamp technique and continuous recordings at negative membrane potentials. We have extended these studies using voltage ramps between -90 mV and +90 mV in order to investigate their current-voltage relationship. We used 110 mM Ba^{2+} as current carrier. Possible L-type calcium channel activity was excluded based on the conductance and gating properties of these channels.The most frequent leak channels observed showed slope conductances of 6.0 ± 0.3 pS (n=7) and 16 ± 3 pS (n=11) (See Figure). 16 pS channels had an almost linear current voltage relationship whereas 6 pS channel did not show outward currents. The reversal potentials were 40 ± 13 mV (6pS, extrapolated) and 9 ± 9 mV (16 pS, measured). This suggest that 6 pS channels are at least 9 times more permeable for Ba^{2+} than K^+ whereas 16 pS channels do not discriminate between the two cations. In a single patch we observed possible third type of channel with a slope conductance of 15 pS but no outward current. These results suggest that calcium entry at resting potentials in A7r5 cells can be explained by at least two different channels with distinct selectivity. Supported by NIH HL41618.

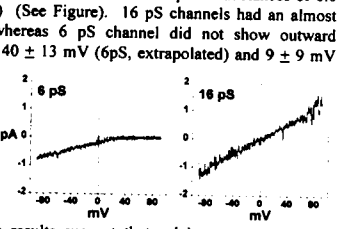

Th-Pos43

ALUMINUM FLUORIDE (ALF_3) DECREASES THE NUMBER OF FUNCTIONAL L-TYPE CALCIUM CHANNELS IN A7R5 VASCULAR SMOOTH MUSCLE DERIVED CELLS. ((**J. R. Serrano**. C. Obejero-Paz and A. Scarpa)) Dept. of Physiology and Biophysics, Case Western Reserve University. Cleveland OH 44106 (Spon. by D. Orosz)

The role of heterotrimeric G (HG) proteins in the control of calcium channel activity in vascular smooth muscle cells is not well understood. In order to investigate the kinetic mechanisms involved in the regulation of L-type calcium channels by G proteins we performed single channel experiments using the cell attached configuration of the patch clamp technique and 110 mM Ba^{2+} as current carrier. The cell membrane potential was zeroed with a high potassium solution. HG proteins were activated with a depolarizing solution containing 10 mM NaF plus 10 μM $AlCl_3$. 10 mM NaF was used as control. In four out of four experiments AlF_3 decreased channel activity (measured as NPo) by 64 ± 16 % during the first 4 min of exposure to the activating solution. This effect was only partially reversible. The decrease in channel activity was accounted by a decrease in the number of available channels. This was determined using ensemble analysis of multichannel patches (see figure) or by counting the number of null sweeps. The single channel current, the mean open time distribution and the first latency distribution were not affected. NaF on the other hand had no effect on channel activity. These results suggest that activation of HG proteins decrease the number of active calcium channels with no effect on the fast gating mechanisms. Supported by NIH HL41618.

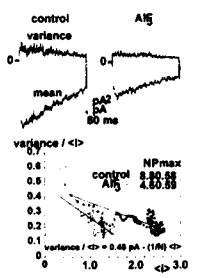

Th-Pos44

T-TYPE AND L-TYPE Ca^{2+} CURRENTS IN CANINE BRONCHIAL SMOOTH MUSCLE CELLS ((**L. Janssen**)) Asthma Research Group, McMaster University, Hamilton, Ontario, Canada L9H 5E1 (Spon. by J. Huizinga)

Ca^{2+} currents in airway smooth muscle of the human, guinea-pig, horse, pig, cow and rat have been found to be exclusively L-type in nature. We examined the voltage-dependent Ca^{2+} currents in freshly dissociated smooth muscle cells obtained from canine bronchi (3^{rd}-5^{th} order). When cells were depolarized from -40 mV, we observed an inward current which: (1) exhibited threshold and peak activation at ≈-35 mV and +10 mV respectively; (2) inactivated slowly with half-inactivation at -20 mV; (3) deactivated rapidly (τ<1 ms) upon repolarization; and (4) was abolished by nifedipine and suppressed by cholinergic agonist. These characteristics are typical of L-type Ca^{2+} current. During depolarization from -70 or -80 mV, however, many cells exhibited a second inward current superimposed upon the L-type Ca^{2+} current. Activation of this other current was first noted at -60 mV, was maximal at ≈-20 mV, and very rapid (reaching a peak within 10 ms). Inactivation of the other current was also rapid (τ≈3ms) and half-maximal at ≈-70 mV. There was a persistent "window" current over the physiologically-relevant range of potentials (*i.e.*, -60 to -30 mV). This current was also sensitive to nifedipine (though less so than the L-type current) and to Ni^{2+}. In contrast to the L-current, this second current was not suppressed by cholinergic stimulation. Finally, the tail currents evoked upon repolarization to the holding potential decayed ≈10 times more slowly than did L-type tail currents. These characteristics are all typical of T-type Ca^{2+} current. We conclude that there is a prominent T-type Ca^{2+} current in canine bronchial smooth muscle; this current may play a central role in excitation-contraction coupling, refilling of the internal Ca^{2+} pool, and in electrical slow waves. Since airflow resistance is determined primarily by the smaller airways and not the trachea, these findings may be significant with respect to airway physiology and the mechanisms underlying airway hyperreactivity and asthma.

Th-Pos45

EFFECT OF PROSTAGLANDIN E_2 ON CALCIUM CURRENT OF CANINE COLONIC CIRCULAR SMOOTH MUSLE CELLS. ((S.I. Cho and K.M. Sanders)) Department of Physiology and Cell Biology, University of Nevada, Reno NV, 89557 USA

Prostaglandins are known to affect the electrical and mechanical activity of smooth muscles, and in gastrointestinal muscles there are varying effects of these compounds depending upon the anatomical source of the muscle. For example, PGE_2 relaxes circular muscle, but contracts longitudinal muscle. We evaluated the effects of PGE_2 on Ca^{2+} currents in enzymatically dispersed colonic smooth muscle cells, using the whole cell patch-clamp technique at 33°C. PGE_2 (10^{-9} to $3x10^{-6}$ M) increased dihydropyridine-sensitive Ca^{2+} current in a concentration-dependent manner in dialyzed cells and in cells with amphotericin perforated patches. The peak increase in Ca^{2+} current was 25 ± 7% (mean ± SD) at 10^{-7} M PGE_2. The effect of PGE_2 on Ca^{2+} current was slow to develop and completely reversible. There was little run-down in the current during exposure to PGE_2. PGE_2 increases cAMP production in smooth muscles, and previous studies have noted similar effects on Ca^{2+} current with other agents that enhance cAMP. In the present study, however, we saw further enhancement in Ca^{2+} current after pre-treatment with forskolin (10^{-6} M). This suggests that, in addition to cAMP-mediated effects, there may be additional mechanisms by which PGE_2 enhances Ca^{2+} current in visceral myocytes. (Supported by DK41315)

Th-Pos46

INTRACELLULAR Ca^{2+} INHIBITS SMOOTH MUSCLE L-TYPE Ca^{2+} CHANNELS BY INTERACTION WTH A SINGLE MEMBRANE ASSOCIATED SITE AND BY ACTIVATION OF A CYCLOSPORIN A SENSITIVE PATHWAY.
((**K. Groschner** and K. Schuhmann)) Dept. of Pharmacol. & Toxicol., Univ. of Graz, Austria.

Modulation of L-type Ca^{2+} channels by tonic elevation of cytoplasmic Ca^{2+} was studied in human umbilical vein smooth muscle. Single L-type channels were recorded both in cell-free patches and intact cells using Ba^{2+} as charge carrier. Ca^{2+} channel activity in cell-free, inside-out patches was stabilized with calpastatin plus ATP, and the channels were exposed to varying Ca^{2+} concentrations at the cytoplasmic side. Ca^{2+}-dependent inhibition of Ca^{2+} channel activity in cell-free patches was characterized by an IC_{50} of 2 μM and a Hill coefficient close to unity. Ca^{2+} suppressed channel activity in cell-free patches mainly due to a reduction of open probability, whereas availability was barely affected. In intact cells, intracellular Ca^{2+} was raised by increasing extracellular Ca^{2+} in the presence of the ionophore A23187. The level of intracelluar Ca^{2+} was determined in parallel by measurement of fura-2 fluorescence and the activity of large conductance Ca^{2+}-activated K^+ channels. Inhibition of L-type Ca^{2+} channels in intact cells was characterized by an IC_{50} of 150 nM, a Hill coefficient close to 4, and was based on a reduction of both open probability and availability. Ca^{2+}-dependent inhibition of Ca^{2+} channel activity in intact smooth muscle cells was not mediated by changes in intracellular pH and remained unaffected in the presence of the protein kinase inhibitor H-7 (10 μM) or the cytoskeleton disruptive agent cytochalasin B (20 μM). However, the calcineurin (protein phosphatase type 2B) inhibitor cyclosporin A (1 μg/ml) completely and reversibly prevented Ca^{2+}-dependent inhibition in intact cells. Our results suggest that L type Ca^{2+} channels of smooth muscle are controlled by two distinct mechanisms of negative feedback regulation. These mechanisms are based on the interaction of intracellular Ca^{2+} with i) a membrane associated target which may reside on the channel protein itself, and ii) a cyclosporin A-sensitive target, most likely protein phosphatase 2B.
Supported by the Austrian Research Funds (S6605)

Th-Pos47

NEUROKININ A CHANGES VOLTAGE DEPENDENT CHARACTERISTICS OF L-TYPE CALCIUM CHANNELS IN TAENIA COLI SMOOTH MUSCLE CELLS. ((**A.E.Belevich**, A.V.Zima and M.F.Shuba)) Nerve-muscle physiology dept., Bogomoletz Inst. of Physiology, Kiev, Ukraine.

The effect of neurokinin A (NKA) on L-type calcium channel current (Ica) in smooth muscle cells (SMC) isolated from taenia coli of guinea pig has been investigated using perforated patch technique with amphotericin B. NKA in a dose-dependent manner inhibited Ica with IC50 of 24nM, maximal inhibition of 45 % for 5μM and threshold concentration causing inhibition of 5pM. The action of NKA was only partially reversible. NKA (5μM) shifted maximum of current-voltage relationship from 10mV to 0mV. Inactivation of control I Ca,0mV was best described as the sum of two exponentials: τ1=27.8 ms and τ2=184.8 ms . Application of NKA (5μM) significantly decreased the second exponential time constant of Ica decay to 129.3 ms, while first exponential time constant of Ica decay remained unaffected (τ1=28.5ms). In addition, 5μM of NKA changed voltage dependence of steady-state inactivation of Ica: shifted potential of half inactivation from -35.5 mV to -40.6 mV and decreased fraction of noninactivating channels from 0.06 to 0.008. It is proposed that NKA provide negative feedback to its exitatory action on SMC by inhibition of Ica and that this inhibitory action can be partially attributed to the changes in voltage dependent characteristics of L-type calcium channels.

Th-Pos48

CLONING AND FUNCTIONAL EXPRESSION OF A VOLTAGE-GATED CALCIUM CHANNEL α_1 SUBUNIT FROM THE JELLYFISH *CYANEA CAPILLATA*. ((**Michael C. Jeziorski**, Robert M. Greenberg, and Peter A. V. Anderson)) The Whitney Laboratory, University of Florida, St. Augustine, FL 32086. (Spon. by M. S. Kilberg)

Jellyfish and other cnidarians represent the earliest existing metazoans and the simplest organisms in which differentiation of neurons and muscle cells is evident. While previous electrophysiological studies have established the presence of voltage-gated calcium currents in excitable cells of cnidarians, the structural similarity between cnidarian calcium channels and their vertebrate counterparts is not yet known. We have used homology-based cloning techniques to isolate from *Cyanea* RNA a full-length cDNA encoding a homologue of the α_1 subunit of mammalian voltage-gated calcium channels. A probe derived from this product detects a single 8.5 kb band in *Cyanea* RNA. The inferred sequence of the protein, 1911 amino acids in length, exhibits 47-53% identity to vertebrate L-type α_1 subunits and 42-43% identity to vertebrate non-L-type channels. Expression of the *Cyanea* α_1 subunit cDNA in *Xenopus* oocytes produces a rapidly activating, slowly inactivating voltage-sensitive current that is carried by Ca^{2+} ions. This expression does not require co-expression of a *Cyanea* calcium channel β subunit, which we have also cloned. The channel is permeable to Sr^{2+} and Ba^{2+} ions, although the current carried by Ba^{2+} is no greater than that produced by Ca^{2+}. The Ca^{2+} current is sensitive to block by nifedipine (IC_{50}=100 μM), as well as to block by Ni^{2+}, Cd^{2+}, and Co^{2+}, but is insensitive to ω-conotoxin GVIA (10 μM) and ω-conotoxin MVIIC (5 μM), suggesting that the *Cyanea* channel is representative of the L-type subgroup of calcium channels. These data establish that homologues of mammalian voltage-gated calcium channels are represented in the earliest neuromuscular systems. (Supported by NRSA grant MH 10625 to MCJ.)

Th-Pos49

PERMEATION DIFFERENCES IN RAT AND RABBIT L-TYPE CARDIAC Ca CHANNELS, BASED ON DIVALENT ION BLOCK

((W. **Yuan**, K.S. Ginsburg, L. Li & D.M. Bers)) Department of Physiology, Loyola University Chicago, Maywood, IL 60153

In a previous study comparing L-type Ca channel current in rat and rabbit ventricular myocytes (*J. Physiol.*493:733, 1996) we found differences in channel gating properties and in the reversal potential (E_{rev}) for the nonselective monovalent cation current through the Ca channels (I_{NS}, i.e. in the complete absence of divalent cations). This implied a larger permeability ratio (P_{Na}/P_{Ca}) in rabbit than rat ventricular myocytes. Here we confirmed the higher P_{Na}/P_{Ca} ratio in rabbit *vs* rat by studying shifts of E_{rev} with various solutions (e.g. with $[Na]_i$=10 mM increasing $[Na]_o$ from 10 to 40 mM gave P_{Na}/P_{Cs}= 2.698 vs 1.996, p=0.002). We also studied divalent cation block of I_{NS} and I_{Ca}. Rabbit I_{Ca} was more sensitive to block by both Cd (K_i = 6.4 μM *vs* 10.5 μM) and Mg (K_i = 6.9 mM *vs* 12.5 mM, see Fig). Rabbit I_{NS} was also more sensitive to Mg block (K_i = 18.8 μM *vs* 35.6 μM), but similar to rat for Ca block (K_i = 163 nM *vs* 131 nM). Since the putative pore regions of the α_1-subunits have the same amino acid sequence in rabbit and rat, differences in permeation properties are not expected. The small differences in P_{Na}/P_{Cs} and divalent cation block we observed could reflect subtle differences in the permeation pathway due to parts of the channel molecule outside the pore region or to other features of the channel's environment in the membrane.

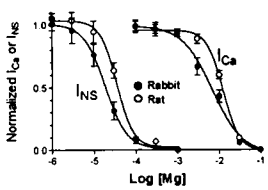

Th-Pos50

CHARACTERIZATION L-TYPE CALCIUM CHANNELS IN FROG SYMPATHETIC NEURONS. ((**Hye Kyung Lee** & Keith S. Elmslie)) Department of Physiology, Tulane University Medical School, New Orleans, LA, 70112.

When measured by the whole-cell patch clamp technique, L-current in frog sympathetic neurons comprises ~5% of the total calcium current. However, we have encountered L-channels in a surprisingly large number of cell-attached patches (~33%) and have begun to study their properties.

We have examined L-channel activity in 36 patches exposed to 1 μM BayK-8644. The slope conductance ranged from 19 to 32 pS (mean 24 pS) and the single channel current amplitude at 0 mV ranged from -1.0 to -1.6 pA (mean -1.3 pA). This broad range could be due to multiple L-channel types. However, a histogram of current amplitude at 0 mV showed a monophasic distribution with a peak at -1.3 pA (0.1 pA bin width). A similar histogram of single channel conductance was also monophasic (peak = 22 pS), but the distribution was skewed to the right. We are currently examining P_o and τ_o to determine if kinetics can help differentiate multiple L-channel types. However, it is possible that the observed variability results from a single L-channel type which allows a large range of single channel conductances.

The high frequency of L-channel patches in this study is counter to our expectations from whole-cell data. Perforated patch recordings, which retain cytoplasmic constituents like the cell-attached patch configuration, may resolve the discrepancy between whole-cell and single-channel data.

Supported by grants from LEQSF and NIH

Th-Pos51

DETECTION OF L-TYPE CALCIUM CHANNELS AND THEIR RELATIONSHIP TO GLUCAGON RELEASE IN INR1G9 CELLS. ((**B.H. Reiss**, †R. Leonard, ‡E. Hayes, †R. Parmar, †J. Schaeffer, *H.C. Fehmann, & †J. Arena)) *Dept. of Pharmacology & Physiology, UMDNJ, Newark,NJ 07107, *Univ. of Marburg, Marburg, Germany, & †Merck Research Labs., Rahway, NJ 07065

A pharmacological approach was used to analyze Ca^{2+} currents(I_{Ca}) and their role in K^+ stimulated glucagon release in a hamster glucagonoma cell line (INR1G9). Calcium currents were recorded by whole-cell patch clamp, with the pipette solution containing in mM: 110 CsCl, 3 $MgCl_2$, 5 TEA Cl, 25 HEPES, 11 EGTA, 2.5 ATP, 0.2 GTP, and 0.1 Leupetin. The bath solution contained in mM: 100 NaCl, 20 TEA Cl, 10 HEPES, 1.0 $MgCl_2$, 20 $BaCl_2$, and 16 Dextrose, with 3 μM of TTX, pH 7.35. Inward currents were elicited by depolarizing voltage steps between -70 and +60 mV in 10 mV increments from holding potentials (V_H) of -90 and -50 mV. In control bath solution with V_H = -90 mV, inward currents activated at -50 mV, peaked between 0 and 20 mV, and reversed near 60 mV. Currents did not inactivate significantly during 40 ms test pulses from either holding potential. Current amplitudes could be enhanced by addition of 1 uM BAY-K8644. Nifedipine added to the bath solution caused a dose- and voltage-dependent block of inward currents recorded at 0 mV. Nifedipine also inhibited K^+-stimulated

[Nifedipine], nM	Ratio of I_{Ca} for $V_{H=-50}/V_{H=-90}$
0	0.75 ± 0.14
10	0.47 ± 0.04
50	0.41 ± 0.05
200	0.31 ± 0.06

glucagon secretion, by radio-immunoassay: 10 nM nifedipine produced 88% ± 8% block of release. The decrease in secretion and I_{Ca} with low concentrations of nifedipine, plus the voltage-dependence of nifedipine block, and the enhancement of I_{Ca} with Bay-K8644 all point to a component of the Ca^{2+} channel current being carried by L-type Ca^{2+} channels. These findings implicate L-type Ca^{2+} channels in controlling glucagon secretion.

Th-Pos52

DIHYDROPYRIDINE RECEPTORS AND A-TYPE POTASSIUM CHANNELS IN VESICLES DERIVED FROM SKELETAL MUSCLE PLASMA MEMBRANES. ((**J. Camacho** and J. A. Sánchez)) Departament of Pharmacology. CINVESTAV, I.P.N., A. P.14- 740 México, D. F. 07000.

Dihydropyridines receptors (DHPr) play a crucial role in excitation - contraction coupling of skeletal muscle (SM). Nevertheless, electrophysiological experiments are complicated because of their localization in the transverse tubular system membranes (TTS) and their tight relation to sarcoplasmic reticulum. Vesicles derived from SM plasma membranes are an alternative preparation to study electrical properties of SM in a relative isolated manner. In the present experiments we demonstrate that these vesicles have DHPr and A-type potassium channels.

Methods. Vesicles derived from SM plasma membrane of *Rana montezumae* were obtained as described (Standen, B. *et al., Proc. Roy. Soc. Lond.* B, **221**, 455, 1984), except that no protease was used. Collagenase was applied at a concentration of 50 U/ml for 90 minutes. Currents were recorded with the patch-clamp technique in the "whole-cell" configuration. Ba^{2+} (30 mM) in the bath or K^+ (120 mM) in the pipette were used to record Ba^{2+} (I_{Ba}+) and K^+ (I_K+) currents respectively. I_{Ba}+ was blocked with nifedipine (1 μM), thereafter flash photolysis (150 watts, 1 s with a Hg-Xe lamp (Orel Co.)) was used to unblock DHPr.

Results I_{Ba}+ through L-type calcium channels were recorded. Partially blocked I_{Ba}+ reached a maximum amplitude of -140 pA at +40 mV; time to peak was 163 ms and the inactivation time constant (τ_i) had a value of 260 ms. Flash photolysis increased I_{Ba}+ up to 70% with no changes either in time to peak or τ_i. I_K+ resembling those through A-type K^+ channels were also recorded. The limiting value of τ_i of these transient currents was 26 ms; half - voltage of steady-state inactivation was -66 mV and the current was completely blocked in the presence of 4-aminopyridine (5 mM).

Conclusions. Our experiments : 1.- Demonstrate that DHPr and A-type K+ channels are present in the vesicles. 2.- Show that DHPr are functional since currents activate and inactivate as in cells. 3.- Suggest that the vesicles arise from the TTS.

Th-Pos53

MEMBRANE TOPOLOGY OF THE TRP CALCIUM CHANNEL FAMILY. ((**K. Machaca**, and H. C. Hartzell)). Emory University. Atlanta, GA 30322.

PLC linked signaling pathways result in the production of IP3 and the release of Ca from intracellular pools. Depletion of Ca stores opens store-operated Ca channels (SOCCs) on the plasma membrane to allow replenishment of Ca pools. SOCC regulation is poorly understood. The *Drosophila* trp channel is thought to function as a SOCC, as are two human homologues. Understanding the topology of the trp family will help provide clues about the regulation of these channels. Here we present data indicating that both the hydrophilic N- and C-termini of this protein family are cytoplasmic. We used an *in vitro* coupled transcription-translation system, in the presence or absence of microsomal membranes, to assay for the glycosylation status of the trp homologues. We show that neither htrp1, htrp3 or dtrp appear to be glycosylated in this assay. Furthermore, dtrp in *Drosophila* eye also appears to be unglycosylated. This suggests that both the N- and C-termini are cytoplasmic, since both contain several consensus glycosylation sites in the different homologues. In addition we have tested the topology of the C-terminus of htrp1 directly using anti-C-terminus antibodies in an epitope protection assay. These results confirm the cytoplasmic location of the C-terminus. We are presently in the process of expanding on these results by constructing trp-prolactin fusion proteins that span each transmembrane domain. We will then use anti-prolactin antibodies in the epitope protection assay to test the topology of the prolactin epitope in the epitope protection assay.

Th-Pos54

EXOGENOUS SPHINGOSINE INHIBITS I_{CRAC}.

((**Chris Mathes** and Reinhold Penner)) Max-Planck-Institute for Biophysical Chemistry, 37077 Göttingen, Germany.

Generally, agonists which stimulate phospholipase C (PLC) and elevate intracellular IP_3 levels activate a Ca current which is important for refilling depleted internal stores. PLC activation, however, does not function in isolation from other intracellular signaling processes. The sphingomyelin pathway, for example, cross-talks with the PLC pathway. Sphingosine is an important intermediate involved in sphingomyelin metabolism. Therefore we tested the effects of exogenously applied sphingosine on the store-operated calcium current (SOCC), I_{CRAC}, in rat basophilic leukemia cells (RBL-2H3). Using the whole-cell patch clamp method, we observe that sphingosine blocks I_{CRAC} in the micromolar range. When 5 μM sphingosine is applied before activation of I_{CRAC} (with 20 μM IP_3 and 10 EGTA) nearly complete block is achieved. When sphingosine is applied 50 seconds after acquiring the whole-cell configuration (near the peak of I_{CRAC}) there is a delay of 10-20 s before the onset of inhibition. Concentrations between 5 and 30 μM block ~100% of the current within ~100 seconds. Lower concentrations lead to block which proceeds more slowly. For example, 1 μM sphingosine blocks approximately 70% of I_{CRAC} in 400 seconds. Concentrations between 100 nM and 30 μM were tested and a dose-response curve was constructed by measuring the percentage of inhibition at 50 s after applying sphingosine. The apparent IC_{50} is 5 μM. At this concentration, block proceeds with a time constant of 46 ± 5 s (mean ± SEM; n=4). Because exogenous shingosine may accumulate in the membrane, we cannot rule out non-specific effects. Alternatively, however, these results suggest that sphingosine, or one of its metabolites in the sphingomyelin pathway, is important for regulation of SOCC.

Th-Pos55

ULTRAVIOLET LIGHT ACTIVATES A CALCIUM-PERMEABLE NON-SELECTIVE CATION CURRENT. ((**F. Mendez** and R. Penner)) Max-Planck-Institute for Biophysical Chemistry, 37077 Göttingen, Germany.

Excess ultraviolet light causes cell damage. We studied the effects of UVA on the cell membrane using the patch-clamp technique. Monochromatic light between 340 and 380 nm activated a sustained cationic current in RBL-1 cells depending on wavelength and light intensity. Its current to noise relationship and its inhibition by micromolar concentrations of trivalents suggested an ionic conductance rather than an unspecific leak, so we termed the current I_{LINC} (*L*ight induced *N*on-selective *C*ationic current). A similar current could be activated by applying peroxidants, while antioxidants significantly impeded its activation. We were also able to record single-channel-like current fluctuations in both outside-out patch-clamp experiments and in artificial bilayers under the same conditions. Since I_{LINC} could be activated in every cell type we studied it may be the major mechanism by which Ca^{2+} can enter the cell leading to cell death after membrane damage due to oxidative stress, especially during sunburn.

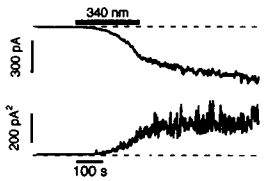

Mean current and noise at -40 mV after ultraviolet light treatment in RBL-1 cells.

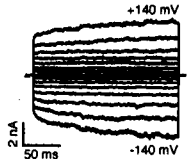

Voltage dependence measured by 200 ms rectangular voltage pulses.

Th-Pos56

NUMERICAL STUDY OF ELECTRODIFFUSION AND THE EFFECTS OF MOBILE BUFFERS IN THE VICINITY OF AN ION CHANNEL ((**W. Baumgartner**[1], F.J. Sigworth[2])) [1]University of Linz, A-4040 Linz and [2]Yale University, New Haven CT 06510

A numerical algorithm was set up to calculate the dynamic concentration behavior of charged particles in the vicinity of a membrane pore. It takes into account alteration of the electric potential due to the charge of the transported ions. Additionally the finite on- and off-kinetics of mobile buffers such as EGTA or BAPTA can be added to the simulation. The calculations were carried out using a modified Crank-Nicolson algorithm to solve the partial differential equations describing the problem. These are the Nernst-Plank equations of the different particle species, the Poisson equation and the law of mass conservation.

It was found, that the electrostatic effect on the concentration of permeating ions is negligible in the presence of physiological salt concentrations. Nevertheless there are electrostatic effects on other ion species near the channel mouth. We present studies on the effect of a Ba^{++}-current through a Ca^{++}-channel onto the Ca^{++}-concentration in the bath, and on the amplification of the Ca^{++}-effect on the Ca^{++}-activated K^+-channel due to the K^+-current. Additionally the effect of mobile buffers was simulated and the numerical results are compared with some common analytically obtained approximations.

(Supported by FWF-project S6607-MED)

Th-Pos57

RYANODINE RECEPTOR FROM LOBSTER SKELETAL MUSCLE IS ACTIVATED BY SUB-MICROMOLAR CYTOSOLIC FREE-CALCIUM. ((**Kerry E. Quinn and Barbara E. Ehrlich**)) **Department of Physiology, University of Connecticut, Farmington, CT 06030.**

Vertebrate and invertebrate muscle differ in the arrangement of ryanodine receptors (RyR) (Loesser, J. Musc. Res. Cell Motil.13:161, 1992) and calcium (Ca)-dependence of Ca release from intracellular membranes (Seok, J. Biol. Chem. 267:15893, 1992). To examine invertebrate RyR regulation by cytosolic compounds at the single channel level, sarcoplasmic reticular (SR) vesicles from lobster tail muscle were incorporated into lipid bilayers. The presence of RyRs was confirmed by modification of channel currents with ryanodine. The Ca-dependence of single channel activity was described by a bell-shaped curve, with a peak at pCa 6.3. In comparison, the Ca-dependence of mammalian RyR has a peak at pCa 5.5. The current to voltage relationship of the lobster RyR demonstrated a slope conductance approximately half of that observed in RyRs isolated from mammalian skeletal muscle (49 pS vs 102 pS). The response to caffeine and ATP were similar in both the mammalian and lobster RyR. These findings suggest differences in Ca activation of intracellular signaling between invertebrate and vertebrate species.

Supported by NIH Grant GM51480 and The Grass Foundation

Th-Pos58

FACTORS INFLUENCING CA^{2+} RELEASE CHANNEL STABILITY ((**Dolores H. Needleman** and Susan L. Hamilton)) Department of Molecular Physiology and Biophysics, Baylor College of Medicine, Houston, TX 77030

Optimal [^{3}H]ryanodine binding to the skeletal muscle Ca^{2+} release channel (ryanodine receptor) is dependent upon a number of factors. It is stimulated by Ca^{2+}, ATP (or ATP analogs), and high ionic strength. However, loss of binding can occur over time making it difficult to define equilibrium conditions. This loss can be prevented by the addition of BSA or CHAPS. The dissociation of bound [^{3}H]ryanodine from SR membranes is characterized by a fast and a slow component. The presence of CHAPS or BSA slows dissociation by converting this to a single exponential dissociation with only the slower component observable. Examination of the association of [^{3}H]ryanodine as a function of time reveals an overshoot in the binding curve. The presence of CHAPS or BSA prevents the decrease in binding which occurs with time. Addition of CHAPS or BSA after the decrease in binding has occurred only partially reverses the inhibition. Pretreatment of membranes with CHAPS does not prevent the loss of binding. These effects do not correlate with a proteolytic event. One possible mechanism for the ability of CHAPS and BSA to stabilize [^{3}H]ryanodine binding is that these reagents prevent Ca^{2+} release channel denaturation.

Th-Pos59

IDENTIFICATION AND FUNCTIONAL RECONSTITUTION OF THE TYPE-2 INOSITOL 1,4,5-TRIPHOSPHATE RECEPTOR FROM VENTRICULAR CARDIAC MYOCYTES. ((Pablo J. Perez, J. Ramos-Franco*, M. Fill, and **G.A. Mignery**)), *Instituto Nacional de Cardiología, Mexico City, México, and Loyola University Chicago, Maywood. IL 60153.

The inositol 1,4,5-triphosphate receptor ($InsP_3R$) is an intracellular Ca^{2+} release channel that mediates the rise in cytoplasmic Ca^{2+} in response to receptor activated production of $InsP_3$. It has been suggested that heart contains the type-1 $InsP_3R$ (Moschella & Marks, 1993) and that it is concentrated in the Purkinje cells (Gorza et al., 1993 & 1995). The identity of the $InsP_3R$ isoform in isolated cardiac myocytes was determined by immunoblotting, $InsP_3$ binding, mRNA screening by PCR, DNA sequencing and by function analysis in planar lipid bilayers. Acutely dissociated ventricular myocytes from ferret and rat hearts expressed significant levels of $InsP_3R$ as determined by immunoblotting with a consensus $InsP_3R$ antibody. $InsP_3$ binding experiments indicate the $InsP_3R$ in the myocytes bound $InsP_3$ with high affinity (K_D=23.6 nM & B_{MAX}=0.46 pmol/mg) suggesting the type-2 isoform was the predominate species present. PCR analysis and subsequent DNA sequencing established that the receptor was indeed type-2. The type-2 $InsP_3R$ from ferret heart was then incorporated into planar lipid bilayers (PE/PC; 7:3; 50 mg/ml). Using Cs^+ as the main ion carrier (220/20 mM gradient) with 200 nM free Ca^{2+}, single channel currents displaying multiple conductance states (388 & 274 pS) were observed. These channels were Ca^{2+} selective and activated by $InsP_3$. Addition of 60 nM $InsP_3$ to the cytoplasmic side, increased Po from about 0.02 to 0.23 with an apparent affinity higher than that reported for type-1 $InsP_3R$ (K_D's 58 vs. 160 nM; Watras et al.,1991). The channel was heparin sensitive (1.5 mg/ml) and was not affected by ryanodine (7 μM). These data indicate that the type-2 $InsP_3$ receptor is the predominant, if not exclusive, $InsP_3R$ isoform expressed in cardiac myocytes.

Supported AHA Grants (GAM + MF) and a NIH grant NS-29640 (MF).

Th-Pos60

EVIDENCE FOR MULTIPLE TYPES OF VOLTAGE-GATED Ca^{++} CHANNELS IN RABBIT CAROTID BODY TYPE 1 CELLS. ((**J.L. Overholt** and N.R. Prabhakar)) Case Western Reserve University, Cleveland, OH 44106.

Carotid bodies (CB) are sensory organs that detect changes in arterial oxygen. Type 1 (T1) cells are presumed to be the initial sites for sensory transduction, and Ca^{++}-dependent neurotransmitter release from T1 cells is believed to be an obligatory step in this response. Relatively little is known about the types of Ca^{++} channels present in these cells. We tested the effect of specific Ca^{++} channel blockers on current recorded from freshly dissociated, adult rabbit CB T1 cells using whole-cell patch clamp. Macroscopic Ba^{++} current elicited from a holding potential of -80 mV activated at a V_m of ≈-30 mV, peaked between 0 and +10 mV, and did not inactivate substantially during 25 ms steps to positive test potentials. There was no evidence for T-type channels. On steps to 0 mV, 6 mM Co^{++} decreased peak inward current by 97±1%. 2 μM nisoldipine, 1 μM ω-conotoxin GVIA and 100 nM ω-agatoxin IVa each blocked a portion of the macroscopic Ca^{++} current (23±7, 33±6 and 19±3% after rundown correction, respectively). Simultaneous application of these blockers failed to block all of the macroscopic Ca^{++} current (66±5%). Individual block was not additive to combined block. This may be due to ω-conotoxin GVIA block of the α_{1D} subunit found in some L-type channels. These results suggest that Ca^{++} current in rabbit T1 cells is conducted by L, N, P and an as yet unidentified channel type. Hypoxia-induced neurotransmitter release from T1 cells may involve one or more of these channels. Supported by NIH HL-07288, HL-2580 and HL-02599.

Th-Pos61

VOLTAGE-SENSITIVE Ca^{2+} CHANNELS (L, N AND P/Q-TYPES) EXPRESSED IN OVARIAN CARCINOMA. ((**M. A. Sciamanna**, M. Oguro-Okano, J. Black*, G. E. Griesmann, and V. A. Lennon)) Depts. of Immunology, Neurology, *Psychiatry, and Laboratory Medicine/Pathology, Mayo Clinic, Rochester, MN 55905.

Paraneoplastic neurologic autoimmune disorders are a manifestation of immune responses to tumor-expressed proteins. These responses appear to limit tumor growth and metastasis. Serum autoantibodies in 50% of these patients bind to neuronal Ca^{2+} channels of N or P/Q-type. In some cases IgG is the effector of neurologic dysfunction (N Engl J Med 332:1467, 1995). We investigated Ca^{2+} channel expression in ovarian carcinoma cell lines established from patients with cerebellar autoimmunity (OV-5, -18, -19 and -20), peripheral nervous system autoimmunity (OV-16 and -208), and no neurologic dysfunction (OV-4). RT-PCR and Southern hybridization revealed that all lines expressed N-type (α_{1B}, 488 bp) Ca^{2+} channel transcripts, all except OV-5 and OV-19 expressed L-type (α_{1D}, 845 bp) transcripts, and only OV-18 and OV-16 expressed P/Q-type (α_{1A}, 844 bp) Ca^{2+} channel transcripts. GK-5, a B lymphoma cell line, served as a negative control; it did not express $\alpha_{1A,B \text{ or } D}$ transcripts. Assays of depolarization-dependent $^{45}Ca^{2+}$ influx revealed voltage-sensitive Ca^{2+} channel activity in all lines except OV-19. The L-type channel antagonist, nifedipine, blocked this activity in a dose-dependent manner in all lines expressing α_{1D}. The diversity of Ca^{2+} channels expressed in ovarian carcinoma cells complements the diversity of neurological signs observed with the paraneoplastic syndromes related to this tumor. These channels merit investigating as potential targets for ovarian cancer therapy. *Supported by NCI Grant CA-37343.*

Th-Pos62

GENETIC DISSECTION OF CALCIUM CURRENTS IN DROSOPHILA LARVAL MUSCLE. ((**H. Xu**, M. Chopra, D. Ren, D.F. Eberl and L.M. Hall)) Department of Biochemical Pharmacology, State University of New York, Buffalo, NY 14260-1200.

There are two pharmacologically distinct calcium currents in Drosophila larval muscle. One, designated the D current, is blocked by diltiazem and dihydropyridines; the other, designated the A current, is blocked by amiloride. Using two electrode voltage-clamping of larval muscle, we have identified the α1 subunit gene responsible for the D current. A premature stop codon in this gene leads to embryonic lethality, while missense mutations allow survival to the adult stage, albeit at reduced viability. A missense mutation in the highly conserved IS1 domain of this subunit drastically reduces the dihydropyridine-sensitive D current but is without effect on the amiloride-sensitive A current. These results demonstrate that the different calcium currents in the larval muscle are encoded by distinct gene products. Kinetic analysis suggests that there is significant increase in the activation time constant of this calcium channel in the missense mutant compared with wild type. Thus, a point mutation in Drosophila has identified a conserved region in the α1 subunit which affects channel activation rate when mutated.

Th-Pos63

NONSELECTIVE CATION AND L-TYPE Ca^{2+} CHANNELS ARE ACTIVE AT SUBTHRESHOLD VOLTAGES IN RINm5F INSULIN-SECRETING CELLS. ((**E.S. Levitan**)) Dept. of Pharmacology, University of Pittsburgh, Pittsburgh, PA 15261

Perforated patch current clamp recordings revealed small spontaneous depolarizations in RINm5F insulinoma cells that can sometimes trigger a burst of action potentials. Two channels appear responsible for this activity. The first is a ~42 pS channel that is easily detected in whole cell mode. Current through this channel is inward between -100 and -45 mV and does not reverse at E_{Cl}. Conductance is halved when both Na^+ is replaced with NMG, but is unaffected by substitution of pipette K^+ with Cs^+. Bursts of channel activity produce increases in $[Ca^{2+}]i$ measured by INDO-1 microfluorimetry. Gating is not affected by changes in voltage and $[Ca^{2+}]_i$. Thus, this channel is a nonselective cation channel that appears similar to a recently described pineal channel (Nature 382:165). The other channel produces a negative slope conductance region in voltage ramps. Depolarization from -60 mV to potentials $\geq$-50 mV increases $[Ca^{2+}]i$ and this effect is inhibited by nimodipine. Thus, this channel appears to be an L-type voltage-gated Ca^{2+} channel. Interupting action potential activity by voltage clamping at threshold (i.e. -40 <V< -35 mV) or -60 mV indicates that Ca^{2+} influx through L channels inbetween action potentials accounts for a significant fraction of the increase in $[Ca^{2+}]_i$ produced by electrical activity. These results suggest that nonselective cation and L channel currents may subserve two functions. First, they produce depolarizing drive to trigger and maintain action potential bursts. Second, Ca^{2+} influx through these channels may facilitate secretion. Supported by the NIH. ESL is an AHA Established Investigator.

Th-Pos64

CALCIUM SIGNALING IN RAT MEDULLARY THYROID CARCINOMA (6.23) CELLS. ((**K. L. Crowley** and D.S. Krafte)) Immunological Diseases, Boehringer Ingelheim Pharmaceuticals, Inc. Ridgefield, CT 06877.

Rat Medullary Thyroid Carcinoma (rMTC) cells express a variety of voltage-dependent calcium channels (VDCC) which contribute to calcium signaling in this cell line (Biagi and Enyeart, Am. J. Physiol. 260 (Cell Physio.29):C1263-C1263, 1991). In this study we have investigated VDCC activity using patch-clamp and fluorescent dye techniques at the single cell and cell population level. In patch clamp experiments peak amplitudes of -106 ± 18 pA (n=15) were observed during test depolarization from -80 mV to +10-+20 mV. The current-voltage curve was biphasic with the suggestion of multiple channel types as previously reported. At the single cell level, Ca transients induced by 60 mM KCl addition showed a rapidly decaying component (τ = 7 sec) and a maintained plateau. This rapid component most likely reflects a contribution from T-type Ca channels and a rapidly inactivating phase of L-type current. Extending the Ca measurements to a cuvette-based system illustrated that Ca levels decayed slowly in the cell population with a τ value of 148 ± 15 s. The rapidly inactivating component of the signal was lost in the population studies. Pharmacological characterization of VDCC activity in the cuvette-based system demonstrated that verapamil blocked Ca transients with an IC_{50} values of approximately 4 μM. Nifedipine also inhibited transients but blockade was more evident at later times. To determine whether one could extend this type of study to a microtiter plate-based assay, we investigated endpoint fluorescence measurements on an SLT platereader using the same KCl-induced depolarization to activate VDCCs. Calibration of the fluo-3 signal in this system gave a K_d for the dye of 1.58 μM. Kinetics of the Ca transient were comparable to those in the cuvette-based system (τ = 166 ± 31 s) with IC_{50} values for verapamil and diltiazem of 11 ± 2 μM (n=50) and 35 ± 13 μM (n=7), respectively. From our studies we can conclude that cuvette and microtiter-based fluorescent systems can be utilized for pharmacological assessment of VDCC blockers. However, since rapid kinetic events are lost and certain types of quantitative pharmacological assessments are more difficult, single cell systems may be necessary when detailed analysis is required.

Th-Pos65

ESTROGEN RECEPTOR DISRUPTION INCREASES EXPRESSION OF THE CARDIAC L-TYPE CALCIUM CHANNEL IN A TRANSGENIC MOUSE ((**B.D. Johnson**†, W. Zheng§, K. Kauser§, A.D. Freay§, K.S. Korach‡, T. Scheuer†, W.A. Catterall†, G.M. Rubanyi§)) †Dept. of Pharmacology, University of Washington, Seattle, WA 98195-7280, §Berlex Biosciences, Richmond, CA 94804, ‡Receptor Biology Section, NIEHS, Research Triangle Park, NC 27709 (Spon. by T. Hinds†)

A role for estrogen in protecting against cardiovascular diseases has been well documented by studies in animals and in women undergoing estrogen replacement therapy (ERT) after menopause. Although some of the positive effects of ERT are likely mediated by changes in lipid metabolism, there may be direct effects on smooth and cardiac muscle function. To address whether estrogen altered the activity of the L-type Ca^{2+} channel, a critical element in cardiac contractility, we examined cardiac myocytes from male mice in which the α isoform of the estrogen receptor had been disrupted (ERKO mice). Binding of dihydropyridine Ca^{2+} channel antagonist PN200-110 was increased 45.6% in cardiac membranes from the ERKO mice compared to controls, suggesting that a lack of estrogen receptors in the heart increased the number of Ca^{2+} channels. Whole-cell patch clamp of acutely isolated adult cardiac ventricular myocytes indicated that Ca^{2+} channel current (carried by either Ca^{2+} or Ba^{2+}) was increased by 34%. Ca^{2+} channel voltage-dependence and kinetic properties were not altered. Examination of electrocardiogram parameters in ERKO mice showed a 38% increase in the heart-rate-corrected QT interval (QTc) without changes in QRS or PQ intervals. Taking this system as a model for decreased estrogen activity, these results suggest that decreased estrogen may lead to an increase in the number of cardiac L-type Ca^{2+} channels and abnormalities in cardiac contractility.

(Supported by NIH Grant P01 HL44948 and the MDA)

Th-Pos66

SILENT CALCIUM CHANNELS IN INVERTEBRATE SKELETAL MUSCLE FIBERS ((**J. Monterrubio**, L. Lizardi and C. Zuazaga)) Inst. of Neurobiology, U. of Puerto Rico Med. Sci. Campus, San Juan, PR 00901.

In sharp contrast to other crustacean skeletal muscles, the superficial flexors of *Atya lanipes* do not generate Ca^{2+} action potentials and have no detectable inward Ca^{2+} current (Lizardi *et al.* J. Membr. Biol. 129: 167, 1992). We reinvestigated Ca channel permeation and block in intact fibers using Ba^{2+} and Sr^{2+} as charge carriers. Current clamp experiments show that Ba^{2+} and Sr^{2+} action potentials could be elicited in Ca^{2+} -free, EGTA (5 mM)-containing solutions. The maximum rate of rise, $\dot{V}_{max}$, tends to saturate as Ba^{2+} or Sr^{2+} concentration was increased. The $\dot{V}_{max}$, and K_m values were 5.16 V/sec and 13.5 mM for Sr^{2+} and 4.45 V/sec and 23.2 mM for Ba^{2+}. Even at high (138 mM) divalent cation concentration, Ba^{2+} action potentials were graded in amplitude depending upon the strength of the depolarizing stimuli; Sr^{2+} action potentials were all-or-none. Three-microelectrode voltage clamp experiments show that the peak inward current decreased about 5-fold when Sr^{2+} was replaced by Ba^{2+}. When Sr^{2+} was the charge carrier, $[Ca^{2+}]_o$ blocked the Ca channels with a half-blockage concentration of *ca.* 400 μM. We conclude that in the absence of Ca^{2+}, these invertebrate Ca channels become permeable to other divalents ($Sr^{2+} > Ba^{2+}$) and that in physiological solution the permeation of Ca^{2+} is blocked by Ca^{2+} *per se*. (Supported by NIH NS-07464, RR-03051, GM08224).

Th-Pos67

DIFFERENTIAL BLOCK OF TWO TYPES OF SODIUM CHANNELS BY ANTICONVULSANTS CAN BE EXPLAINED BY STEADY-STATE INACTIVATION. ((J.-H. Song, K. Nagata, C.-S. Huang, J.Z. Yeh and **T. Narahashi**)) Dept. Mol. Pharmacol. and Biol. Chem., Northwestern Univ. Med. Sch., Chicago, IL 60611.

The differential effects of the anticonvulsants phenytoin (DPH) and carbamazepine (CBZ) on tetrodotoxin-sensitive (TTX-S) and tetrodotoxin-resistant (TTX-R) sodium channels of rat dorsal root ganglion neurons were studied using the patch clamp technique. The action potentials from TTX-S cells were more sensitive to DPH and CBZ than those from TTX-R cells. The steady-state inactivation curve of TTX-S sodium channels was located at potentials more negative than that of TTX-R sodium channels by as much as 20-25 mV. Furthermore DPH and CBZ shifted the TTX-S inactivation curve in the hyperpolarizing direction more than TTX-R inactivation curve. The differences between the two types of sodium channels in these two parameters account for the more potent block of TTX-S than TTX-R channels at resting membrane potential. This study clearly demonstrates that differential block of TTX-S and TTX-R channels by anticonvulsants can be explained solely by the differences in inactivation kinetics which may or may not be due to different amino acid components. Supported by NIH Grant NS14144.

Th-Pos68

ROLE OF SELECTIVITY FILTER REGION OF THE SODIUM CHANNEL IN LOCAL ANESTHETIC BLOCK. ((**A. Sunami**, S.C. Dudley, G. Lipkind, H.A. Fozzard)) University of Chicago, Chicago, IL 60637.

The local anesthetic binding site is thought to be on the cytoplasmic side of Na^+ channel, and several residues in transmembrane segment 6 of domain IV have been shown to be important for the action of local anesthetics. The selectivity filter region forms a narrow ring in the outer vestibule and projects deeply into the membrane. Therefore, the selectivity filter residues may influence access and binding of local anesthetics. We tested this idea by mutagenesis of the adult rat skeletal muscle Na^+ channel (μ1) expressed in *Xenopus* oocytes. Mutating a positively charged residue to a negative one in the putative selectivity filter of domain III (K1237E) increased resting block (tonic block from -120 mV) by lidocaine (K_d=154 μM) compared to wild type (K_d=572 μM). An intermediate effect of resting block resulted from neutralization of the positive charge (K1237S, K_d=281 μM). Phenol, an analog of the hydrophobic part of lidocaine showed no difference in resting block between wild type (K_d=6.5 mM) and K1237E (K_d=5.6 mM). Replacement of a neutral residue in domain IV by a negatively charged residue (A1529D) and neutralizing the negative charge in domain II (E755A) had little effect on the resting block of lidocaine. However, when a permanently charged quaternary derivative of lidocaine, QX-222 was externally applied, the wild type channel showed no block, but A1529D and E755A exhibited 29.0±2.8 and 38.2±2.5% block (500 μM QX222, 0.05 Hz). Neither K1237E nor K1237S allowed block of external QX222. When another quaternary derivative, QX314 was intracellularly applied, complete recovery from use-dependent block by QX314 was observed in A1529D (τ=4 min), whereas wild type showed nearly no recovery within 15 min. In A1529D, recovery from block by extracellular QX314 had the same time course as that of block by intracellular QX314. We conclude that the selectivity filter limits extracellular access and intracellular escape of local anesthetics, and may be close to the local anesthetic receptor site.

Th-Pos69

ION SELECTIVITY IN SODIUM CHANNELS: MOLECULAR MECHANICS STUDIES ON THE SOLVATED MODEL FOR THE PORE REGION OF THE VOLTAGE-GATED SODIUM CHANNEL.((**R. Sankararamakrishnan**, Shankar Subramaniam and Eric Jakobsson)) National Center for Supercomputer Applications, Beckman Institute, University of Illinois, Urbana, IL-61801.

The putative model for the sodium pore has been proposed by Guy and Durell (1). The P segments are modeled as helix-turn-helix (HTH) motif. These segments from each homologous repeat come together to form a vestibule. The residues involved in the ion selectivity are located in the turn in the HTH motif and form a narrow selectivity filter. In order to investigate the molecular basis for ion selectivity, molecular mechanics calculations were carried out on the solvated model of sodium pore region. The ion was placed in a succession of positions along the channel axis, at 0.5 A intervals. The energy was minimized at each position and the energy profiles were calculated for three ionic species viz. sodium, potassium and chloride. The energy profiles clearly demonstrate that the proposed model discriminates between anions and cations, with anions having to encounter a large energy barrier upon entry into the channel.This seems to be the result of the interactions of the negatively charged residues with the ions. Analysis of sidechain conformations for the energy minimized structures reveal that the Lys-85 residue at the narrow selectivity filter undergoes significant conformational changes when the ion moves from one side of the selectivity filter to the other side. Changes in the conformation of Lys-85 side chain lead to changes in the minimum pore radius. Variation in the minimum pore radius for the energy minimized structures is up to 1A. Potential of mean force calculations via molecular dynamics simulations to determine the specificity of sodium ions in the sodium channels are currently in progress.

(1) Guy, H.R. & S.R. Durell, (1995) in Ion channels and *Genetic Diseases (D.*C. Dawson & R.A. Frizell, Eds.) Rockefeller University Press.

Th-Pos70

INHIBITION BY ELIPRODIL (SL82.0715) OF VOLTAGE-GATED Na^+ CHANNELS IN RAT CULTURED CORTICAL NEURONS.

((**Bruno Biton**, Patrick Granger, Henri Depoortere and Patrick Avenet))
Synthélabo Recherche, CNS Department, 31 Ave. P. Vaillant Couturier, 92220 Bagneux, France. (Spon. by J. Kupper)

The inhibitory properties of the neuroprotective compound eliprodil (SL82.0715) on voltage-gated Na^+ currents have been investigated in cultured cortical neurons of rat. The voltage-dependence of eliprodil inhibition was studied by eliciting Na^+ currents from a holding voltage of -60 or -80 mV. At a holding voltage of -80 mV, eliprodil maximally blocked about 25% of the Na^+ current with an IC_{50}>100 μM. In contrast, depolarizing the holding voltage to -60 mV increased by 60% the maximal effect of eliprodil and decreased the IC_{50} to 3.1 ±1 μM. Veratridine, applied at 30 μM at a holding voltage of -60 mV, induced a sustained inward current which was dose-dependently inhibited by eliprodil. The concentration-response curve of this inhibition was very similar to that obtained for voltage-activated currents, suggesting that eliprodil blocks Na^+ channels by stabilizing the inactivated state. In favor of this hypothesis, eliprodil at 1 μM shifted the steady-state inactivation of the Na^+ current by 10 mV toward negative potentials. The delay of recovery from inactivation was also lengthened. These results demonstrate that, in addition to its antagonism of NMDA receptors and high-voltage activated Ca^{2+} channels, eliprodil is a potent voltage-dependent blocker of Na^+ channels, a property which is likely to play a part in its neuroprotective activity.

Th-Pos71

COCAINE INHIBITION OF HUMAN HEART SODIUM CHANNELS EXPRESSED IN *XENOPUS* OOCYTES. M.E. O'Leary and A.P. Thomas, Department of Pathology, Anatomy and Cell Biology, Jefferson Medical College, Philadelphia, PA. 19104.

The time course of cocaine inhibition of human heart Na channels (hH1) expressed in *Xenopus* oocytes was measured using a two pulse protocol consisting of a variable duration prepulse (1 ms to 60 s) to -10 mV to inactivate channels and promote cocaine binding, a rest pulse (-100 mV /150 ms) during which non-modified channels recover, followed by a -10 mV test pulse. With 100 μM cocaine the observed inhibition is biphasic. A small rapid component (τ_f=3 ms) is co-incident with the times that channels are open and may reflect cocaine block of channels. The majority of the inhibition (94%) occurs at a slower rate (τ_s=505 ms). This slow inhibition develops long after channels have undergone fast inactivation (τ_f=3 ms) but well before the onset of slow inactivation (τ_{SI}=7 sec). The slow component of cocaine inhibition is likely to reflect drug binding to fast inactivated channels. Plots of the apparent inhibition rate ($1/\tau_s$) versus [Coc] is consistent with a first order binding reaction yielding an estimate of cocaine affinity for inactivated channels of 2 μM. The effects of cocaine on inactivation-deficient (Q^3) mutant channels was also examined. In two-pulse experiments the onset of cocaine inhibition of the Q^3 mutant was found to be mono-exponential (τ=11 ms, 100 μM) and more rapid than WT. Moreover, cocaine produces a time-dependent block of Q^3 Na currents (τ= 12.5 ms) that is potentiated by reducing $[Na]_{out}$. The rapid onset and antagonism by external permeant cations are consistent with a blocking mechanism with an apparent affinity of 103 μM. Resting Q^3 channels are relatively insensitive to cocaine (K_D>1 mM). Cocaine both stabilizes hH1 Na channels in an inactivated state and blocks channels at physiologically relevant concentrations. Both mechanisms are likely to play a role in producing the cardiotoxic effects frequently associated with cocaine abuse.

Th-Pos72

USE-DEPENDENT BLOCK OF SKELETAL MUSCLE SODIUM CURRENT BY CHIRAL DERIVATIVES OF MEXILETINE AND TOCAINIDE AND ANTIMYOTONIC ACTIVITY ON ADR MOUSE. ((**A. De Luca**, F. Natuzzi, S. Piemo, H. Jockusch*, A. Duranti°, G. Lentini°, C. Franchini°, V. Tortorella° and D. Conte Camerino)). Dept. of Pharmacobiology and °Dept. of Medicinal Chemistry, Univ. of Bari, Italy and *Developmental Biol. Unit, Univ. of Bielefeld, Germany.

To search for more potent antimyotonic agents, chiral analogs of mexiletine (Mex) and tocainide (Toc) were synthetized and tested *in vitro* on sodium currents of frog muscle fibers by means of vaseline gap voltage clamp method. Test pulses from the holding potential of -100mV to -20mV were both infrequently and repetitively applied (at 10Hz) to evaluate tonic and use-dependent block, respectively. The compouds showed different degree of stereoselectivity, the R enantiomers being more potent than the S ones. The elongation of the alkyl chain of mexiletine as in [R-3-(2,6-dimethylphenoxy)-2-methylpropanamine] (Me2) led to a reduction of the tonic block with respect to R-(-) Mex (IC_{50}=108μM *vs.* 55μM) but to a strong use-dependent behaviour with a tenfold decrease of IC_{50}. An increase of lipophylicity as in [RS-2-(4-chloro-2-methylphenoxy)-1-benzen-ethanamine] led to a potent sodium channel blocker (IC_{50}=30μM) with a spare use-dependent behaviour. [R-2,6-valinoxylidide], a Toc analog with an increased hindrance on the chiral carbon atom, was twofold (IC_{50}=209μM) and tenfold (IC_{50}=27μM) more potent than Toc in tonic and use-dependent block, respectively. All of the above compounds left-shifted the steady-state inactivation curves. Cyclic tocainide derivatives (pyrrolo-imidazolonic) did not produce tonic block up to 500μM but slowly developed an use-dependent block upon prolonged stimulation, suggesting an open-channel block. A higher use-dependent behaviour may increase the antimyotonic activity. Thus, the effects of Mex and Me2 were tested *in vitro* by current clamp method, on muscle fibers of myotonic ADR mouse. Mex and Me2 selectively suppressed spontaneous myotonic hyperexcitability at lower concentrations than those effective on the action potentials evoked by depolarizing stimuli, being Me2 twice as potent as Mex. (Telethon-Italy, project # 579).

Th-Pos73

μ-CONOTOXIN BINDING TO THE VOLTAGE-GATED Na⁺ CHANNEL: STRUCTURAL IMPLICATIONS FOR THE OUTER VESTIBULE. ((**N.S. Chang***, S. Dudley, Jr.*, G. Lipkind*, R.J. French†, and H. Fozzard*)) *University of Chicago, Chicago, IL 60637 and †University of Calgary, T2N 4N1.

The structure of the voltage-gated Na⁺ channel can not currently be studied using direct methods. Our laboratory has modeled the outer vestibule by inferring the complementary binding surface for the specific, high affinity toxins, tetrodotoxin (TTX) and saxitoxin (STX) (Biophys. J. 66:1, 1994). Using our model and available data on residues important for binding, we predicted a binding conformation for μ-conotoxin (μ-CTX) (Biophys. J. 69:1657, 1995), a marine toxin with nanomolar IC_{50}'s for certain Na⁺ channel isoforms. Similar to TTX and STX, a guanidinium group located at arginine-13 (R13) of μ-CTX is critical for binding. Using mutant and wild-type adult rat skeletal muscle Na⁺ channels (μ1) heterologously expressed in *Xenopus* oocytes, we determined IC_{50}'s for blockade of sodium current by wild-type μ-CTX and by R13 mutants of the toxin. μ1 residues E403, E755, E758, and D1532, all critical for TTX and STX binding, were selected for mutation. Double mutant cycle analysis was performed to determine the coefficients of interaction (Ω) between channel mutants and R13 toxin mutants (table). As predicted, we found a strong interaction between R13 and glutamate 758 (E758) of the channel. Ω values for R13K (lysine for arginine) were all insignificant with the exception of those with E758, and even these were quite diminished compared to the other R13 mutants with E758. Therefore, the R13 interactions found here appear to be primarily electrostatic except with E758, where there is a significant non-electrostatic contribution as well. As we had predicted, R13 does not interact with D1532. However, the interaction with E755, a member of the putative selectivity filter, is weaker than predicted. These data suggest that μ-CTX may bind to the outer edge of the vestibule.

Ω values	E403Q	E755A	E758Q	E758K	D1532N
R13A	8.2	6.4	113.6	80.5	4.2
R13D	5.0	1.5	53.7	921.1	3.5
R13K	1.6	1.4	8.7	4.5	1.4
R13Q	18.2	6.2	59.4	70.2	NT

NT= not tested

Th-Pos74

CHARACTERIZATION OF μ-CONOTOXIN BINDING SITE ON VOLTAGE-GATED NACHS: CHIMERIC AND SINGLE POINT MUTATION ANALYSIS. ((**M. Chahine**, C.Sato, P. Marcotte, L.-Q. Chen and R.G. Kallen)) Laval Hospital, Research Center, Laval University Ste-Foy, Québec, Canada G1V 4G5, electrotechnical laboratory, Supermolecular Science Division,Tsukuba City, Japan and Dept. of Biochem. and Biophys., University of Pennsylvania School of Medicine, Philadelphia, PA 19104-6059.

Voltage-gated sodium channels (NaChs) from rat skeletal muscle (rSkM1) and from human heart (hH1) present different sensitivities to the small inhibitor peptide μ-conotoxin (μ-CTX), rSkM1 being sensitive and hH1 being relatively resistant. In order to identify which of the structural variations between rSkM1 and hH1 are responsible for this affinity difference and to localize the binding site of μ-CTX, we tested the effects of μ-CTX on both chimeric channels between rSkM1 and hH1 and single point mutant channels expressed in *Xenopus laevis* oocytes under voltage-clamp conditions. In a previous study we showed that both D1 and D2 possess important determinants for μ-conotoxin binding. In order to obtain data at the amino acid level, μ-CTX was tested on many single point mutant channels made in D1 and D2. In this study we describe a mutation in D2 rSkM1 Ala728Leu. That affects significantly the binding of μ-CTX (IC_{50}=817.4±72.5nM), this mutation increases slightly the affinity of tetrodotoxin. Analogs of μ-CTX were also tested on this mutant channel in order to identify which amino acid(s) interact(s) with the alanine at position 728 on rSkM1. The decrease in affinity of μ-CTX for rSkM1(Ala728Leu) is additional to that caused by the previously reported, μ-CTX mutation rSkM1(Tyr401Cys). Finally, we propose a model of the binding site of μ-CTX on D2 from NaCh.

Th-Pos75

PHRIXOTOXINS, NOVEL Na^+ CHANNEL BLOCKERS FROM TARANTULA VENOM. ((Ray A. Caldwell and Clive M. Baumgarten))
Dept. of Physiology, Medical College of Virginia, VCU, Richmond, VA 23298.

Natural toxins are important tools for studying ion channels. Here we report on phrixotoxins (PrTx), a family of Na^+ channel blockers from *Phrixotrichus spetulatus* and *P. auratus*, South American spiders. Whole-cell I_{Na} was measured in freshly dissociated rabbit ventricular myocytes at 22-23°C. The bath contained (in mM): 10 NaCl, 130 CsCl, 0.5 $CaCl_2$, 3 $MgCl_2$, 0.01 $CdCl_2$, 10 HEPES, 10 glucose (pH 7.4), and the pipette contained: 2.5 Na_2ATP, 120 CsAsp, 20 CsCl, 2.5 $MgCl_2$, 0.062 $CaCl_2$, 5 Cs_2EGTA, 5 HEPES (pH 7.1). *P.s.* venom initially was assessed by 20-ms pulses to -17 mV at 0.125 Hz from -137 mV. Venom fully and reversibly inhibited I_{Na} with an ID_{50} of 1.57 × 10^{-5} U (~1:63,700 dilution; 1 U = pure venom). *P.s.* venom was equipotent. Both onset and washout were well fit by single exponentials, but $\tau_{washout}$ for *P.s.*, 69.6 ± 4.6 s, was significantly slower than for *P.a.*, 42.9 ± 5.3 s, indicating the toxins differ. Whereas PrTx did not alter the h_∞ curve, the $V_{1/2}$ for activation appeared to reversibly shift positive by 8.7 mV and its slope factor appeared to reversibly increase by 2.6 mV. Similar reductions of I_{Na} by inactivation did not affect either activation parameter. Activation appeared to shift only because PrTx block was voltage-dependent and decreased on depolarization. Assuming PrTx only reduced $\bar{g}_{Na}$, the voltage-dependence of block for both *P.s.* and *P.a.* between -57 and +48 mV was well-described by a Woodhull model with the binding site for PrTx at an electrical distance ($z\delta$) of 0.6 from the outside. Because $z\delta$ is greater than δ for the selectivity filter, the effective valence of PrTx is likely to be ≥ +2. Unblock on depolarization extended over a much wider voltage range than activation and was unaffected by increasing $[Na^+]_i$ 3-fold. Thus unblock appears to be primarily voltage rather than state or current-dependent. PrTx may be useful as a probe of the pore of Na^+ channels. (Supported by NIH HL46764.)

Th-Pos76

MOLECULAR MODELING OF BINDING OF TTX, STX, AND μCTX BY Na^+ CHANNELS. ((**G. Lipkind** and H.A. Fozzard)) Cardiac Electrophysiology Labs, The University of Chicago, Chicago, IL 60637.

Mutational studies have identified a region of the S5-S6 loops of voltage-gated Na^+ channels (P region) responsible for tetrodotoxin (TTX), saxitoxin (STX), and μ-conotoxin (μCTX) block. We previously modeled this region as four β-hairpins with C strands from each domain forming the outer funnel for toxin binding (Lipkind & Fozzard, Biophys J 66:1,1994).This model requires revision in light of new mutational studies. The monotonic change in electrical distances for Cd^{2+} block of Cys mutations in the C strands (Chiamvimonvat *et al*, Neuron 16:1037,1996) confirm a β-hairpin model, with extended conformations of both strands. The amino acid residues on the ends of the modeled P regions determine the external border of the funnel, and the side chains of D400, E755, K1237, and A1529 (skeletal isoform) form the narrow selectivity ring at the bottom. Both TTX and STX block by binding directly to the selectivity filter. TTX is located closer to domain I and participates in strong hydrophobic interactions with Y401, but STX is closer to domains II and IV, forming salt bridges with E755 and D1532. Such shift leads to different effects of sulfhydryl reagents on block by TTX and STX (Kirsch *et al*, Biophys J 67:2305,1994).The external borders of the funnel do not allow the bulky μCTX to move deeply into the pore; rather, it occludes the pore entrance. The side chain of R13, crucial for binding by this toxin, is located only in the force field of the outer ring of negatively charged residues (E403, E758, D1241, D1532), interacting stronger with E758 (Dudley *et al*, Biophys J 69:1657,1995).

Th-Pos77

A MUTATION IN THE OUTER VESTIBULE SUGGESTING DIFFERENCES IN STX AND TTX BINDING. ((**J.L. Penzotti**, S. Dudley, B. Xu, G. Lipkind, and H. Fozzard)) Cardiac Electrophysiology Labs, University of Chicago, Chicago, IL 60637.

Tetrodotoxin (TTX) and saxitoxin (STX) are marine guanidinium toxins that bind with high affinity to the native rat skeletal muscle sodium channel (μ1) and with lower affinity to the cardiac channel isoform. Satin et al. (Science 256:1202-1205, 1992) determined that Tyr401 in μ1 is partly responsible for TTX and STX sensitivity, since mutation of the corresponding cardiac channel residue, Cys373, to Tyr, resulted in similar increases in STX and TTX sensitivity. This result implied that STX and TTX bind in a similar way to μ1. However, Kirsch et al. (Biophys. J. 67:2305-2315, 1994), found that when STX is bound to the human heart (hH1a) channel isoform, the channel is still sensitive to modification by MTSEA. Conversely, TTX appears to protect the channel from reacting with MTSEA. This implies that TTX is binding closer to the Cys373 residue, and there is more space between STX and the channel at this residue. We examined the effect substituting Asp for Tyr401 in μ1. The native and mutant channels were expressed in *Xenopus* oocytes and analyzed using two-electrode voltage clamp. Our data support Kirsch's conclusion that there are differences in STX and TTX binding:

	Equilibrium K_d (nM)	
channel	**STX**	**TTX**
wildtype μ1	3.07 ± 0.45	35.70 ± 6.28
Y401D	142.20 ± 12.18	150242 ± 28175

The mutation Tyr401Asp renders the μ1 channel relatively insensitive to TTX, while only slightly decreasing STX sensitivity. These results support the model by Lipkind and Fozzard (Biophys. J. 66:1-13, 1994) in which TTX binds with close-range hydrophobic interactions at Tyr401. STX appears to leave a gap between its charged groups and Tyr401 when bound to μ1.
J.L. Penzotti is a Howard Hughes Medical Institute Medical Student Research Training Fellow.

Th-Pos78

USE-DEPENDENCE OF TTX-BLOCK OF NA^+-CHANNELS WITH MUTATED RESIDUES IN THE EXTRACELLULAR PORE REGION. ((A. Boccaccio, P. Ghisellini, **O. Moran**, K. Imoto* and F. Conti)) ICB-CNR, Genova, Italy, and *National Institutes for Physiological Sciences, Okazaki, Japan.

Use-dependent block (UD) of Na^+-channels (NaCh) by tetrodotoxin (TTX) may be attributed to a relief of partial TTX-binding inhibition by extracellular cations when the competing ions escape to the intracellular medium upon channel opening[(1)]. The extent of inhibition depends on the repulsion energy between TTX and the trapped cation, whereas the kinetics of the UD effect are mainly governed by the interaction of TTX with its binding site. UD has been studied in three mutants of the rat brain NaCh-IIA α-subunit that are much less sensitive to TTX because of single amino acid changes in the region forming the outer ion-pore entrance: W386Y, E945Q and D1717Q. The TTX half-blocking concentration, IC50, measured in resting conditions was in the order of 30 nM for the wild-type, 200 nM for W386Y, 10 μM for E945Q, and 5 μM for D1717Q. At relatively high extracellular Ca^{2+}-concentrations (≥ 2 mM) UD effects are dominated by TTX-Ca^{2+} competition and are well fitted in all cases by the trapped-ion model. The parameters of the model are the second-order association rate constant of TTX, and the two dissociation rate constants of the toxin in presence or in absence of a trapped cation. The parameters most affected by the single-point mutations are the dissociation constants, which are both increased roughly proportionally to the IC50. These results are consistent with a constant "on" binding rate and a constant distance between the bound toxin molecule and a calcium ion trapped in the energy well adjacent to the selectivity filter. Apparently, the mutations strongly alter the energy of interaction of TTX with the vestibular pocket of the pore without modifying the structure of the toxin-channel complex.

(1) Conti F., Gheri A., Pusch M. and O. Moran (1996). Biophys. J. 71:1295-1312

Th-Pos79

ISOFORM-SPECIFIC DIFFERENCES IN RECOVERY KINETICS OF ANTHOPLEURA TOXIN-MODIFIED SODIUM CHANNELS. ((**G.R. Benzinger** and D.A. Hanck)) University of Chicago, Chicago IL 60637.

Sodium currents modified by toxin ApB from the sea anemone *Anthopleura xanthogrammica* display a markedly slowed inactivation upon depolarization, probably arising from a selective slowing of the rate constant of inactivation from the open state (O→I). Consistent with this model, toxin produces lengthened mean open times in single-channel recordings, although with a larger effect on cardiac channels than neuronal. Macroscopic current inactivation is partial, leading to a non-inactivating plateau which is larger in neuronal channels than in cardiac (fig). The plateau current comprises bursts of one or more openings, separated by long non-conducting periods. Such current may therefore arise from a substantial rate of recovery from inactivation at depolarized potentials.

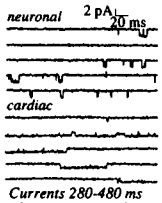

Whole-cell measurements of recovery from inactivation confirm an increased recovery rate in modified channels. The usual delay before onset of recovery is greatly lessened in toxin-modified currents of both isoforms, suggesting that recovery of modified channels does not require transit through multiple inactivated states, but can occur through distal C→O, or perhaps I→O, transitions. In cardiac channels, the enhancement of recovery is independent of recovery potential, while in neuronal channels enhancement is greater and strongly voltage-dependent. This distinction may reflect quantitative differences in the toxin-induced enhancement of recovery rates between channel isoforms.

Th-Pos80

COMPARISON OF Na^+ CHANNELS ON NATIVE SKELETAL MUSCLE FIBERS FROM YOUNG-ADULT AND AGED RATS. ((**J.F. Desaphy**, A. De Luca and D. Conte Camerino)) Unit of Pharmacology, Dept. of Pharmacobiology, Faculty of Pharmacy Univ. of Bari, Bari, Italy.

Ageing induces morphological and electrophysiological changes in mammalian skeletal muscle. Particularly, the global chloride conductance is greatly decreased. As expected from this, the latency from the application of the current pulse to the onset of action potential is increased but the expected tendency to fire is not observed. This suggests a modification of other channels involved in action potential behavior. We used the inside-out patch-clamp method to investigate Na^+ channels in fibers of *flexor digitorum brevis* muscle freshly dissociated from young-adult (4-6 months) and aged (20-24 months) rats. In our conditions, a run-down of Na^+ channel activity is observed which may be due to slow voltage-dependent inactivation. This run-down is accentuated in aged rats resulting from either a shift to more negative potentials of the inactivation voltage-dependence and/or elongation of the time for recovery from inactivation. Unitary conductance is 16.6 ± 0.9 pS (n=9) in young-adult rat while 8.0 ± 0.6 pS (n=5) in aged rat ($p<0.01$). No difference is found in mean open time. Furthermore, we calculated channel density by dividing the number of channels in the patch (estimated by the measure of the peak current amplitude at 0 mV) by the square of pipette conductance (which is assumed to be linearly correlated to the patch area). Hypothesizing a constant open probability over the age, Na^+ channel density appears sixfold greater in fibers from aged rats ($p<0.01$). The difference is still significant if we consider a lower open probability of 30% in aged rats. Nevertheless, lower conductance and pronounced inactivation may account for some of the modifications of electrophysiological properties during ageing.

Supported by the Italian CNR (P.F. Invecchiamento)

Th-Pos81

CHANGES IN SODIUM CHANNEL FUNCTION DURING POSTNATAL BRAIN DEVELOPMENT REFLECT INCREASES IN THE LEVEL OF CHANNEL SIALIDATION ((**Cecilia Castillo**, Mary E. Díaz, Domingo Balbi, Esperanza Recio-Pinto)) Instituto de Estudios Avanzados (IDEA), Caracas 1015A, Venezuela. Department of Anesthesiology, Cornell University Medical College, NY 10021.

Previous studies using acutely dissociated rat brain cortical neurons, have reported that the voltage dependence of activation of Na^+ currents undergo a hyperpolarization shift (Cummins et al., 1994) or no change (Huguenard et al., 1988) during postnatal development. Moreover, when mRNA from young (< P5) and from adult (>P30) rat brains are injected into Xenopus oocytes, the voltage dependence of activation is the same at both ages (Virginio and Cherubini, 1995). We decided to further investigate this question at the single channel level, by using the planar bilayer system and native brain Na^+ channels. The use of native Na^+ channels has the advantage that the channel's posttranslational modifications are preserved. This is important since some of them such as the level of sialidation has been shown to affect the activation properties of various voltage-dependent channels including Na^+ (Recio-Pinto et al., 1990) and K^+ (Thornhill et al., 1996). The use of the bilayer system also eliminates channel functional differences that could reflect differences in the membrane lipid composition or in neuronal survival. We found that the midpoint potential of activation was -64,-75 & -81mV for P0, P15 and adult (P30/P180) channels, respectively. At negative potentials gating state changes were observed in all channels; at positive potentials they were observed in P0 but rarely in older channels. A long nonconductive state was displayed by P0 but rarely by older channels. The apparent MW was 218, 228 and 235kDa for P0, P15 and adult channels, respectively. Upon neuraminidase treatment, these differences in MW were abolished and the behavior of adult channels resembled that of P0 channels. Developmental changes in the function of brain Na^+ channels correlate with changes in the channels' sialidation level.

Th-Pos82

SINGLE CHANNEL CHARACTERIZATION OF A SKELETAL MUSCLE SODIUM CHANNEL LACKING FAST INACTIVATION. ((**J. Kimbrough** and K.Gingrich)) Depts of Anes., Pharm. and Phys., U. of Rochester, Sch. of Med., Rochester, NY14642

Inactivated states of voltage gated Na+ channels underlie action potential refractoriness and likely play a critical role in long-lived block by local anesthetics. The structural underpinnings of fast inactivation involve an IFM motif in the intracellular linker between domains III and IV that when mutated to QQQ eliminates fast inactivation (West *et al.*, 1992). This mutant form has only been studied in neuronal and cardiac isoforms. We wished to explore, at the single channel level, the gating of this mutant in a skeletal muscle isoform. To this end, we mutated the α-subunit (μ1) of rat skeletal muscle (Rskm1) to the QQQ genotype (1303Q, 1304Q, 1305Q). We measured single channel currents (i_{Na}) in membrane patches from *Xenopus* oocytes injected with cRNA.

Shown below are typical i_{Na}'s triggered by 200ms voltage-clamp depolarizations (as indicated, HP=-100mV, bars mark baseline). Both traces are marked by frequent reopenings where greater depolarization appears to increase open probability by enhancing open times (OT) and reducing closed times (CT). Grouped time constants (ms, means±SEM, N≥3) from histogram analysis confirm these observations. OT histograms were monoexponentially distributed (-40mv, 1.06±0.19; 0mV, 3.57±0.84). CT histograms were more complex although dominated by a single exponential (-40mv, 1.02±0.06; 0mV, 0.50±0.06). These results demonstrate that Rskm1-QQQ lacks fast inactivation while exhibiting voltage dependent activation and deactivation characteristic of Na+ channel gating.

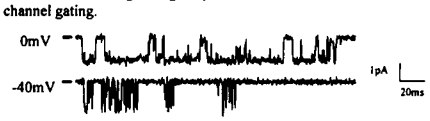

Th-Pos83

ELECTROPHYSIOLOGICAL STUDIES OF SPINAL MOTOR NEURON VOLTAGE-GATED SODIUM CHANNELS. ((Brian Delisle and Jonathan Satin)) Department of Physiology, The University of Kentucky College of Medicine, Lexington, KY 40536-0084

A variety of sodium channel isoforms are expressed in the central nervous system. Phosphorylation of central nervous system Na channels alters channel gating and current amplitude. There are, however, differences among isoforms that are expressed in similar cells. The rat brain 2a channel has four more protein kinase A glycosylation sites than the mouse brain 8a channel. In this respect the brain 8 channel is similar to the adult skeletal muscle isoform (c.f., Smith and Goldin, 1996). Both the brain 2a and 8a channels are expressed in spinal motoneurons. *In situ* hybridization studies confirm the presence of mouse brain 8a in motor neurons. The brain 8a channel is critical for normal motoneuron function. In a transgenic knock-out mouse, mis-expression of brain 8a leads to motor endplate disease. We studied the effect of ß1 subunit coexpression on phosphorylation of central nervous system sodium channels. We expressed channels in *Xenopus* oocytes and measured the effects of protein kinase A and C. Channels were expressed with and without the ß1 subunit. In oocytes, PK-A caused a modest change in current amplitude. Stimulation of PK-C with DOG caused a decrease of current amplitude along with shifts of voltage-gating. We are currently investigating whether there are differential effects of phosphorylation on the isoforms expressed by motor neurons.

Th-Pos84

SODIUM CHANNELS IN PERIPHERAL NEURONS ARE BLOCKED BY HALOTHANE AND PENTOBARBITAL. ((**T.N.Vysotskaya** and D.S.Duch)) Departments of Anesthesiology and Physiology, Cornell University Medical College, New York, NY 10021.

It has been reported recently that mammalian CNS sodium channels are sensitive to both volatile and IV anesthetics, with volatile anesthetics causing significant block at clinical concentrations (*Anesthesiology*, 1996, 84:1223). To examine whether mammalian peripheral neurons had similar responses to these anesthetics, we examined the effects of halothane and pentobarbital on rat sensory neurons. Primary cultures of spinal and trigeminal ganglionic neurons from adult rat were obtained after enzymatic dissociation. Control measurements of the cells elicited normal action potentials and ionic currents. Sodium currents were measured using the whole cell patch clamp configuration; the extra-cellular Hank's balanced salt solution contained additionally 5mM HEPES and 0.1mM $CdCl_2$, pH 7.2,while the internal solution was 140mM CsF,10 mM NaCl, 5 mM HEPES pH 7.4. Sodium currents and anesthetic suppression were measured with depolarizing test potentials from a hyperpolarizing holding potential (-80 mV). Similar to results with CNS channels, halothane (1 mM and less) reversibly decreased sodium current.. Additionally there was an increase in membrane leakage current (non-toxic). Pentobarbital also blocked sodium current in the same concentration range as CNS neurons under these same conditions (1.8 mM and less) and increased leakage current. Halothane suppression was biphasic, pentobarbital suppression was monophasic during 20 min,application.

Th-Pos85

SODIUM CURRENTS ASSOCIATED WITH NERVE-CONTACT OF *XENOPUS* MUSCLE CELLS IN CULTURE. ((M. Fry and **F. Moody-Corbett**)) Division of Basic Medical Sciences, Faculty of Medicine, Memorial University of Newfoundland, St. John's, NF A1B 3V6.

The post-synaptic membrane of the adult neuromuscular junction has both a high density of acetylcholine receptors (AChRs) and sodium channels. The localization of AChRs at sites of nerve-muscle contact occurs very early in development and is well documented in the *Xenopus* nerve-muscle culture preparation. The purpose of the present study was to determine if these sites also had a high density of sodium channels. *Xenopus* embryonic muscle and nerve cells were grown in culture. Macroscopic currents were recorded from patches of muscle membrane close to or distant from sites of nerve-muscle contact using a List patch clamp and large bore patch electrodes. The electrodes were constructed from borosilicate glass, Sylgard-coated, fire polished and filled with extracellular recording solution. We found that >70% of the macropatches which had I_{Na} occurred within 25 μm of the nerve-contact. In addition, these patches contained an inactivating outward potassium current, I_{IK}. Patches of muscle membrane away from the nerve-contact had a low probability of containing I_{Na}. These results suggest that sites of nerve-contact on *Xenopus* muscle cells in culture have a high density of sodium channels compared to other areas of the muscle membrane.

Th-Pos86

PROPERTIES OF VOLTAGE-DEPENDENT SODIUM CHANNELS (I_{Na}) IN ISOLATED HUMAN HIPPOCAMPAL NEURONES

((**G. Reckziegel**[1,2], H. Beck[2], J. Schramm[3], C.E. Elger[2] and B.W. Urban[1])) [1]Dept. of Anesthesiology, [2]Dept. of Epileptology, [3]Dept. of Neurosurgery, Univ. Bonn Med. Ctr., 53105 Bonn, Germany

The properties of I_{Na} were investigated in 25 neurones isolated from the resected hippocampus of 5 patients with therapy-refractory temporal lobe epilepsy using the whole-cell voltage-clamp technique (series resistance ~5MΩ, 40-90% compensation). Sodium currents showed a high current density (0.81 mA/cm^2) and were sensitive to TTX. The current voltage relation of the activation showed a threshold around -30 mV and peaked at -10 mV. At this voltage, the time-dependent activation was rapid with a time to peak around 700 μs. The voltage-dependent steady-state inactivation could be fitted with a Boltzmann function with a half-maximal inactivation $V_{1/2inact}$ at -59.3 mV. The removal of inactivation showed a rapid and a slow component in the order of milliseconds and seconds. This may account for the marked frequency-dependence observed upon repetitively eliciting the current upon stimulation with 2, 5 and 20 Hz. I_{Na} decayed to steady-state values of 81, 67, and 46% of the initial current amplitude, respectively. The properties of I_{Na} were remarkably homogeneous in each individual patient. In comparison to the properties of sodium channels in mouse neuroblastoma cells[1] and human cortical tissue[2], dentate granule cells showed a $V_{1/2inact}$ at more depolarized potentials, consistent with the more positive resting membrane potential of granule cells (~ -60 mV vs. ~ -70 mV)[3,4]. In addition, the frequency-dependent reduction of I_{Na} was markedly stronger in dentate granule cells. Finally, the current density was significantly higher than in mouse neuroblastoma cells. Future studies will address the impact of these differences on neuronal discharge properties.

1: Willow, M., Gonoi, T., and Catterall, W.A., (1985) Molec. Pharmacol. 27: 549-558
2: Cummins, T.R., Xia, Y., and Haddad, G.G., (1994) J. Neurophys. 71:1052-1064
3: Isokawa, M., Levesque, M.F., Babb, T.L., and Engel, J., (1991) Epilepsy Res. 9:242-250
4: Schwartzkorn, P.A. and Knowles, W.D., (1984) Science. 223:709-712

Th-Pos87

MOLECULAR CLONING OF A TERTRODOTOXIN-RESISTANT SODIUM CHANNEL α1 SUBUNIT FROM DOG NODOSE GANGALION NEURONS

((**Jun Chen***, Stephen R. Ikeda[§], Wenhua Lang* and Xiangyang Wei*))
*Inst.for Mol. Med.& Genet., Medical College of Georgia, Augusta, GA30912 and [§]Guthrie Res. Inst., Sayre, PA 18840. (Spon. By X. Wei)

Voltage- gated Tetrodotoxin -resistant sodium current present in sensory neurons might be responsible for the excitability of nociceptors which underlie pain and tenderness asscociated with tissure injury and inflammation. We have cloned a sodium channel α1 subunit (NaNG) from dog nodose gangalia. The full length cDNA predicts an open reading frame of 5,886 nucleotides which encodes a protein of 1,962 amino acids. At the amino acid level, it is 82.3 % identical to the recentl discovered TTX-resistant sodium channel (SNS/PN3). In the putative TTX- binding site, a hydrophilic serine appears instead of Cys (as cardiac Nach) and Tyr/Phe (as in TTX-sensitive Nachs). Coupled transcrition and translation assay resulted a 220 kd protein; Northern blot and RT-PCR showed that it is only expressed in nodose gangalia, but not in cerebral cortex, hippocampus, cerebellum, liver, heart or skeletal muscle. We propose that NaNG is a new member of TTX-resistant sodium channels.
(Supported by AHA Grant-In Aid 93-1202 to X. Wei)

Th-Pos88

SODIUM CURRENT KINETICS ARE MODULATED BY $[Ca^{2+}]_i$ AND PROTEIN KINASE C. ((**C.L. Watson**, M.R. Gold)) University of Maryland, Baltimore, MD

During ischemia $[Ca^{2+}]_i$ accumulates from intracellular organelles and from stimulation of receptor linked phospholipases. This may activate Ca^{2+} dependent signaling pathways, including protein kinase C (PKC). To investigate the modulation of cardiac sodium current (I_{Na}) by $Ca^{2+}{}_i$, we used whole cell patch clamp techniques in neonatal cardiomyocytes and compared the changes in I_{Na} caused by 1)a PKC activator peptide in the pipette solution 2)a buffered 50 nM Ca^{2+} pipette solution 3)a Ca^{2+} chelated pipette solution. The $V_{1/2}$ of steady-state inactivation shifted 8-10 mV in the depolarizing direction during Ca^{2+} and PKC perfusion. Recovery from inactivation was faster during PKC activation and Ca^2 perfusion. The fast τ of recovery was 10.5 ± 1.4, 6.1 ± 1.0 and 4.0 ± 0.5 ms during control, PKC and Ca^{2+}, respectively while the slow τ was 117.6 ± 33.7, 67.1 ± 19.7 and 40.4 ± 6.5 ms. The onset of inactivation from resting states, measured with a step to 0 mV following a conditioning pulse of varying duration to -65 mV, was prolonged 40- 50% by both PKC and Ca^{2+}. The effects of the PKC activator peptide were fully inhibited by PKC inhibitors. However, complete suppression of Ca^{2+} effects on I_{Na} required genistein, a specific inhibitor of tyrosine kinase. We conclude that elevated $[Ca^{2+}]_i$ and PKC have similar modulatory effects on I_{Na} which are part of a complex phosphorylation pathway that includes tyrosine kinase.

Th-Pos89

ENZYMATIC PROPERTIES OF VOLTAGE-GATED CHANNELS AND ANDERSEN'S DEHYDRATION-AND-ASSOCIATION MODEL.

((**H. Richard Leuchtag**)) Department of Biology, Texas Southern University, Houston, TX 77004.

It has been suggested that the four S4 segments of a voltage-gated ion channel make a transition from α helices to an extended structure in which the Na^+ or other cations can bind weakly to the backbone carbonyl oxygens and nitrogens, replacing the H^+ connecting the loops of the helix; this transition would convert the open channel into a metalloprotein [Leuchtag, H. R., Biophys. J. 66:217-224 (1994), 70:A321 (1996); Biophys. Chem. 53:197-205 (1995)]. Thus an arriving sodium ion may shed its hydration shell and attach to the outermost oxygen site of the four-S4 bundle by the ion-exchange reaction: $Na^+\cdot(H_2O)_n + N\text{-}H\cdots O{=}C \longrightarrow N\text{-}Na\cdots O{=}C + nH_2O + H^+$ where n is the number of water molecules in the Na^+ hydration shell. The stripping of the hydration shell from the ion as it becomes chelated in the channel probably would be catalyzed by an enzymatic moiety of the channel, presumably one or more of the external, hydrophilic loops such as the S5-S6 linkers. This appears to be consistent with a model [Andersen, O. S., Ann. Rev. Physiol. 46:531-548 (1984); Andersen, O. S. and Koeppe II, R. E., Physiol. Rev. 72:S89-S158 (1992)], in which ions in an outer aqueous vestibule undergo dehydration and association, followed by translocation through the membrane, then dissociation and hydration in an outer aqueous vestibule. We therefore identify the outer and inner vestibules with the aqueous regions occupied by the hydrophilic linkers.

Th-Pos90

COMPARISON OF A CHANNEL GATING MODEL BASED ON A LIQUID-CRYSTAL ELECTROCLINIC EFFECT IN S4 SEGMENTS WITH BAUMANN'S AGGREGATION MODEL.

((**H. Richard Leuchtag** and Vladimir S. Bystrov[§]))
Dept. of Biology, Texas Southern University, Houston, TX 77004 and [§]Pushchino State University, Pushchino, Moscow Region, 142292, Russia. (Spon. by M. Hillar.)

The ferroelectric liquid crystal model of channel gating [Leuchtag, H. R. 1995. Biophys. Chem. 53:197-205], which describes channel opening as a transition from a ferroelectric smectic C* (tilted chiral) to a paraelectric smectic A* (normal to membrane plane) liquid crystal, appears to be partially consistent with the nonrestricted aggregation reaction system [Baumannn, G. 1979. Math. Biosci. 46:107-115]. In Baumann's model, dipolar channel modules rotate 90° from the bilayer surface to form an aggregated transmembrane structure. In the electroclinic-effect model, the four S4 segments rotate from a tilted orientation to a parallel orientation normal to the membrane plane, where they aggregate to form an ion-conducting configuration. They are held in this configuration by the permeant metal ions, forming a membrane-spanning metalloprotein phase in which the permeant ions move by thermally activated hopping. Despite significant differences (the tilt angle in our model is <= 45° and the dipoles are in the plane of the membrane), Baumann's proof that his model is consistent with the Cole-Moore effect, in which a hyperpolarizing prepulse delays onset of the ion current, appears to be sufficiently general to cover the present model.

Th-Pos91

Optical (polarized) study of Na channel orientation in squid axon ((David Landowne)) University of Miami School of Medicine, Miami, FL 33101

Histologically and functionally nerve cells are polarized with a receptor->effector axis. Many nerve cells conduct action potentials in a preferred direction along this axis. This study suggests that the underlying Na channels have a preferred orientation with respect to this axis.

Axon segments were mounted on a rotating stage with the proximal end near 0°. Each end had a pair of leads and an insulated 0.1 mm Pt ball electrode touched the axon integument near the center of the beam. A calcite polarizer provided -45° plane polarized light from below, a +45 analyzer above filtered out unaffected photons. Changes in light intensity (ΔI) were obtained by signal averaging synchronized with stimulation through one pair of leads. Changes in potential were recorded with the central ball electrode.

In 25 comparisons on 12 axons, the amplitude ΔI following proximal stimulation of the segment was 11±4% (sem) *smaller* than the amplitude following distal stimulation. Previous studies have associated most of ΔI with conformational changes associated with Na channels. Simulations with the Neuron computer program suggest that the amplitude of the action potential following proximal stimulation might be 0.5% *larger* compared to distal stimulation due to axon tapering. The difference in the optical measure suggests the conformational changes of the sodium channels, or some unknown electrically excitable molecule, is sensitive to the direction of impulse propagation. This could occur if the symmetry axes of the channels were tilted away from the membrane normal along the receptor->effector axis.

Supported by NIH Grant NS26651

Th-Pos92

[^{3}H]WIN 17317-3. A HIGH-AFFINITY PROBE FOR NEURONAL NA$^+$ CHANNELS. ((**S.G.Wanner**[1], M.M.Smith[2], K.Rupprecht[2], R. Baker[2], H.Glossmann[1], G.J.Kaczorowski[2], M.L.Garcia[2] and H.G.Knaus[1])) [1]Inst.Bioch.Pharmacology, A-6020 Innsbruck, Austria. [2]Merck Research Laboratories, Rahway, NJ, 07065.

WIN 17317-3 (1-benzyl-7-chloro-4-n-propylimino-1,4-dihydroquinoline HCl) was originally described as a ligand for the voltage-gated K$^+$ channel K_v1.3 (Hill, R.J. et al., *Mol. Pharmacol.* **48**, 98-104 (1995)). To directly investigate the binding properties of this ligand in neuronal and cardiac tissues, we synthesized [^{3}H]WIN 17317-3. In rat brain membranes, [^{3}H]WIN 17317-3 binds reversibly and saturably to a single class of high-affinity sites (K_d 1.9±0.3 nM; B_{max} 5.3±0.2 pmoles/mg of protein), while no binding is observed to cardiac membranes. K$^+$ channel ligands (e.g. the K_v1.3 blockers margatoxin & charybdotoxin; TEA; tolbutamide; minoxidil) have no effect on [^{3}H]WIN 17317-3 binding to rat brain membranes. In contrast, the Na$^+$ channel modulators batrachotoxin, aconitine and veratridine displace [^{3}H]WIN 17317-3 binding with IC_{50} values of 4.8-8.2 μM, while binding is unaffected by tetrodotoxin, sea anaemone toxin 2 and brevetoxin A. Moreover, [^{3}H]WIN 17317-3 binding is inhibited by local anesthetics (cocaine, lidocaine, procaine) and antiarrhythmics (e.g. propafenone, prajmaline, quinidine, ajmaline, mexiletine) with potencies identical as those described for Na$^+$ channel ligand inhibition. The anticonvulsant phenytoin stimulates [^{3}H]WIN 17317-3 binding up to 250% (EC_{50} value 2.9 μM) by slowing radioligand dissociation. The enantiomers of the Na$^+$ channel agonists DPI 201-106 and BDF 8784 are high-affinity inhibitors of [^{3}H]WIN 17317-3 binding (IC_{50} values between 4.2 and 6.4 nM). WIN 17317-3 dose-dependently inhibits agonist-stimulated ^{22}Na influx into CHO cells stably transfected with neuronal Na$^+$ channels (IC_{50} value ≈ 60 nM). These results clearly indicate that WIN 17317-3 is a high-affinity ligand of neuronal Na$^+$ channels and does not appear to interact with voltage-gated K$^+$ channels in this tissue.

ANION CHANNELS

Th-Pos93

HYPOTONICITY ACTIVATES CHLORIDE CHANNELS IN MOUSE CULTURED NEURONS

((A. Carpaneto, A. Accardi, M. Pisciotta and F. Gambale)) CNR-Istituto di Cibernetica e Biofisica, Genova, Italy 16149 (Spon. by F. Gambale)

The whole-cell configuration of the patch-clamp recording technique was used to characterize an osmotically sensitive channel permeable to chloride ions in the neuron cell line N2A. Hyposmotic bath solutions led to a sustained activation of chloride currents that vanished restoring iso-hyperosmotic bath solution. The permeability sequence for these anion channels was: $Br^- > Cl^- > F^- >$ Gluconate≈Glutamate.
In symmetrical solutions, the osmo-regulated channel displayed time independent currents and moderate outward rectifying characteristic, in the voltage range comprised between -100 mV and +100 mV.
Micromolar concentration of DIDS and SITS (added to the bath solution) blocked in a voltage dependent manner and almost reversibly the chloride channel. Other known blockers of anion channels like lanthanum (1 mM), zinc (1 mM) and niflumic acid (500 μM) did not affect the currents. Preliminary noise analysis indicate a single channel conductance of about 1 pS in the presence of 110 mM NaCl in the bath and 50 mM NaCl in the pipette.
These channels show strict biophysical and pharmacological similarities with mini chloride channels which are supposed to play a crucial role in cell volume regulation in lymphocytes (Lewis et al. 1993).

-Lewis R., Ross P. and Cahalan M. 1993 J. Gen. Physiol. 101, 801-826

Th-Pos94

PROBING THE IONIC PORE OF HUMAN CLC-1 WITH IODIDE ((**Ch. Fahlke**, Ch. Dürr, and A. L. George, Jr.)) Vanderbilt University, Nashville, TN 37232

Gating of a recombinant human muscle Cl^- channel (hClC-1) is mediated by two structurally distinct mechanisms: a fast voltage-dependent process mediating transitions between three conducting states, and a slow opening-closing reaction mediated by a cytoplasmic gate (Fahlke, *et al*, **Biophys J**, 71:695-706, 1996). We examined hClC-1 block by iodide (I^-) to probe the conduction pathway during these gating events. Extracellular I^- causes voltage-dependent block of both inward and outward current, shifts the voltage-dependent distribution of the channel in each kinetic state to the hyperpolarizing direction, but has no effect on deactivation time constants. Intracellular Cl^- competes with external I^- for these effects. By contrast, intracellular I^- blocks only inward current, and causes time constants for deactivation to become larger and more voltage-dependent. These different effects of external vs internal I^- on hClC-1 gating help to distinguish two distinct ion binding sites within the pore. By fitting the concentration dependence of deactivation time constants (for internal I^-) and fractional current amplitudes (for external I^-) with Langmuir isotherms, we determined K_D values for I^- in each of the three kinetic states. Channel affinity for external I^- differs significantly between fast deactivating, slow deactivating, and non-deactivating states. K_D values are voltage-dependent only in the slow deactivating and non-deactivating states. These fits provide limiting values for fractional current amplitudes at high external [I^-] showing that I^- locks the channel in the non-deactivating state thus explaining the observed concentration dependence of gating. Affinity for internal I^- also differs between kinetic states with smaller K_D values in the fast deactivating state. These experiments demonstrate that voltage-dependent gating events in hClC-1 are associated with changes in ion binding affinity at two distinct sites within the channel pore.

Th-Pos95

DIFFERENTIAL EXPRESSION OF Cl- CHANNEL TRANSCRIPTS: A POSSIBLE TOOL FOR IDENTIFICATION OF NOVEL CHANNEL ISOFORMS. ((**J.L. Kugler**, C.E.Sedwick, W.Xie, K.Holevinsky, J. LaMendola, L. Man, D.J. Nelson)) The University of Chicago, Chicago, IL 60637.

We have previously characterized an anion conductance expressed in many cells which appears to be upregulated in the presence of CaMK-II. To date, no molecular species has been convincingly shown to underlie this current. We are employing a coupled approach of electrophysiology and PCR to attempt to pair known molecular species, specifically the members of the ClC gene family, with their functional/physiological counterparts. Using isoform-specific PCR detection of ClC genes, we have shown the presence of transcripts coding for ClC-2, -3, -4, -5, and -7, but not ClC-1 or -6 in the murine monocyte-derived cell line J774.1. The epithelial cell line CaCo-2 expresses -3, -4, and -7 (ClC-1 and ClC-5 have not yet been tested for). Both of these cell types exhibit large CaMK-II activated anion conductances. Of particular interest in this study are changes in ion channel expression concomitant with adhesion-dependant differentiation in human peripheral monocyte-derived macrophages. We have shown a time-dependant change in respiratory burst activity which seems to correlate with expression levels of the CaMK-II dependent anion conductance. This increase in expression during monocyte-to-\macrophage differentiation in culture may provide a means of discovering the molecular identity of the CaMK-II dependent anion conductance. Supported by NIH GM 36823.

Th-Pos96

CaM KINASE II REGULATION OF CALCIUM-ACTIVATED CHLORIDE CHANNELS IN EPITHELIAL CELLS. **((J. Arreola[1], J.E. Melvin[2] and T. Begenisich[3])) IF-UASLP, San Luis Potosí, SLP 78290, México[1], and Departments of Dental Research[2] and of Pharmacology and Physiology[3], University of Rochester, Rochester NY 14642.**

The participation of multifunctional Ca^{2+}- and calmodulin-dependent protein kinase type II (CaM kinase II) in the activation of Ca^{2+}-activated Cl^- channels was studied using selective inhibitors of CaM kinase II and calmodulin. Ca^{2+}-dependent Cl^- channels from rat parotid acinar and T84 cells were activated by 4 μM ionomycin or by 0.25 μM free Ca^{2+} and the resulting Cl^- currents were recorded using the whole cell patch clamp technique. Direct inhibition of CaM kinase II by 10 μM KN-62 and by 40 μM of peptide inhibitor 281-302 did not block the Cl^- current in acinar cells. In contrast, KN-62 inhibited Cl^- currents in T84 cells by >50%. We also dialyzed cells with 0.5 μM of the calmodulin binding domain peptide 290-309 to competitively inhibit calmodulin and therefore calmodulin-dependent processes. This peptide did not affect the ionomycin-induced Cl^- current in parotid acinar cells, whereas the peptide reduced the ionomycin-induced Cl^- current in colonic T84 cells by about 70%. We conclude that unlike the channels in T84 cells, the Ca^{2+}-dependent Cl^- channels in rat parotid acinar cells are activated by Ca^{2+} in a manner that is independent of CaM kinase II. (Supported in part by NIH grant DE09692).

Th-Pos97

BLOCKADE OF hClC-1 CURRENTS BY Zn^{2+} AND OTHER THIOL-REACTIVE COMPOUNDS: POTENTIAL SITES OF ACTION

((**L.L. Kürz**, H. Klink, S. Benz, M. Kuchenbecker and R. Rüdel)) Department of General Physiology, University of Ulm, 89069 Ulm, Germany

Treatment of the major skeletal muscle chloride channel hClC-1, stably expressed in HEK-293 cells, with 1 mM externally applied Zn^{2+} led to massive current reduction (Kürz et al., Pflügers Arch, in press). The blockade was not voltage-dependent, the relative open probabilities and the reversal potential remained practically unchanged. Internally applied Zn^{2+} did not substantially reduce the current, indicating that the relevant binding sites are extracellularly located. The sulfhydryl-reactive compound $CH_3SO_2SCH_2CH_2N(CH_3)_3^+$ (MTSET) and the histidyl-reactive diethylpyrocarbonate (DEPC), applied externally, also reduced instantaneous hClC-1 currents. Since Zn^{2+}-binding sites with mixed ligands (e.g. histidine and cysteine side chains) are not uncommon, we explored the possibility that all three compounds share the same target site(s). MTSET and DEPC applied together did not entirely mimic the effect of Zn^{2+}. Application of 5-10 mM H_2O_2 in order to test for potential disulfide bridge formation of sterically close cysteine residues left chloride currents practically unchanged. Blockade by Zn^{2+} was strongly pH-dependent with a pK_a around 6.9, compatible with a histidine side chain. However, at pH 6.0, where no Zn^{2+}-effect was detected, currents were still affected by 1mM DEPC, even in cells pretreated with 1 mM Zn^{2+}. This suggests that DEPC and Zn^{2+} exert their action at different sites of the protein. Candidate cysteine and histidine residues are currently being mutated in order to identify the target sites of the various compounds. (DFG grant Ru 138/20-1).

Th-Pos98

LARGE TEMPERATURE DEPENDENCE OF SLOW GATING OF CLC-0 Cl^- CHANNELS

((**Michael Pusch**, Uwe Ludewig and Thomas J. Jentsch)) ZMNH, UKE. Hamburg University, Martinistr.52, Germany

The chloride channel from the *Torpedo* electric organ, ClC-0, is the best studied member of a large gene-family. We investigate the temperature-dependence of the slow gate of ClC-0 expressed in *Xenopus* oocytes. The slow gate operates simultaneously on both protochannels of the "double-barrelled" ClC-0. Macroscopic measurements of deactivation kinetics at positive voltages revealed a very high Q_{10} of about 40. Steady-state open probability of the slow gate can be described by a Boltzmann distribution with an apparent gating valence of ≈2 and a variable "offset" at positive voltages. We note a positive correlation of this offset (i.e. the fraction of channels that are not closed by the slow gate) with the amount of expression. This offset is also highly temperature-sensitive, being drastically decreased at high temperatures. Paradoxically, also the maximum degree of activation of the slow gate decreases at higher temperatures. Within a Markovian-type description at least two open and two closed states are needed to describe slow gating. The large Q_{10} of kinetics of slow gating, the correlation of the fraction of non-inactivating channels with the amount of expression, and the fact that the slow gate closes both protochannels simultaneously suggests that the slow gate is coupled to subunit interaction of the dimeric ClC-0 channel.

Th-Pos99

ANION PERMEABILITY IN THE CFTR CHLORIDE CHANNEL: LYOTROPIC SELECTIVITY SEQUENCE AND ESTIMATION OF PORE DIAMETER.

((**Paul Linsdell** and John W. Hanrahan)) Department of Physiology, McGill University, Montréal, Québec, Canada.

The selectivity of macroscopic CFTR chloride channel currents to different intracellular anions was examined using inside-out membrane patches excised from BHK cells expressing a high density of CFTR channels. Reversal potential measurements revealed the permeability sequence $SCN>NO_3>Br>Cl>I>$formate $>ClO_4>$acetate$>F$. Permeability was inversely related to energy of hydration, indicating the presence of a lyotropic or weak field strength selectivity site, although the low permeability to the very lyotropic anion ClO_4 suggests factors other than hydration energy also affect ClO_4 permeability. We were unable to accurately measure a reversal potential with intracellular benzoate, another highly lyotropic anion. Low concentrations of benzoate also blocked Cl permeation in a voltage dependent manner, suggesting that it binds relatively tightly within the pore. Macroscopic reversal potentials indicated a slight permeability to several larger anions, which allowed estimation of the functional pore diameter. The pore mutant R347D-CFTR, which has altered conductance and anion-binding properties, had the same relative permeability to intracellular SCN, Br, I, ClO_4, acetate and F as wild type, suggesting that this mutation does not alter overall channel selectivity. However, P_{NO3}/P_{Cl} was reduced from 1.49 to 1.05, indicating that this mutation abolishes the ability of the channel to discriminate between Cl and NO_3. *Supported by the Canadian CF Foundation, MRC (Canada), and NIH(NIDDK).*

Th-Pos100

THE FIFTH PUTATIVE TRANSMEMBRANE HELIX OF CFTR CONTRIBUTES TO THE PORE ARCHITECTURE

((**S.S. Smith**, M. K. Mansoura, J. A. Schaefer, C.R. Cooke, Z. Shariat- Madar, F. Sun, and D. C. Dawson)) Dept. of Physiology, Univ. of Michigan, Ann Arbor, MI.

The Cystic Fibrosis Transmembrane conductance Regulator (CFTR) has twelve membrane spanning segments that presumably are involved in forming the Cl- selective pore. The fifth putative transmembrane helix has been identified as a region homologous to the H5 domain of a broad range of ion channels, a region implicated as 'pore-lining' (Jan, LY and YN Jan, Nature 371:119-123, 1994). In previous studies we analyzed the disease-related glycine to glutamic acid mutation at position 314 (G314E) and showed that there were significant changes in both the conduction and gating properties, suggesting that TM5 may play a role in the formation of the pore. To explore the role of TM5, we assayed the ion channel properties of CFTR variants bearing mutations in the fifth and sixth putative transmembrane segments using *Xenopus* oocytes and two-electrode voltage clamp. Conduction properties were probed by examining the effect of substituting thiocyanate (SCN-) for chloride (Cl-) in the extracellular bath. CFTR gating was assayed by measuring the dose-dependent activation of chloride currents in response to increasing concentrations of 3-isobutyl-1-methylxanthine (IBMX) in the presence of 10 mM forskolin. For wild type CFTR, SCN- in the external bath caused the reversal potential to shift to more negative values, indicating that SCN- gains access to the pore more readily than Cl-, however the conductance was greatly reduced, suggesting that once in the pore SCN- binds tightly so that anion flow is blocked. Substitution of glutamic acid for R347 in TM6, implicated by Tabcharani et al (Nature 366:79-82,1993) in SCN binding, eliminated SCN block, and caused a slight reduction in sensitivity to activation by IBMX. We also examined the effect of substitutions for V317 which is predicted to be one helical turn outward from G314 in TM5, and is the site of a patient mutation (V317A). Substitution with alanine or glutamine slightly reduced the efficacy of SCN block, but significantly reduced the sensitivity to activation by IBMX. Insertion of glutamic acid also compromised activation. SCN block was absent; in fact the conductance of V317E was increased in the presence of SCN. These results are consistent with the notion that TM5 contributes to the architecture of the pore and is important for anion binding, which may be destabilized by placing a negative charge at V317. (Supported by NIH and the CF foundation).

Th-Pos101

LOCATING THE ANION-SELECTIVITY FILTER IN THE CFTR CHANNEL.

((**Myles H. Akabas** and Min Cheung)) Center for Molecular Recognition, Columbia University, New York, NY 10032.

The cystic fibrosis transmembrane conductance regulator (CFTR) forms an anion-selective channel; the site and mechanism of charge selectivity, however, is unknown. We previously reported that cysteines substituted, one at a time, for Ile331, Leu333, Arg334, Lys335, Phe337, Ser341, Ile344, Arg347, Thr351, Arg352 and Gln353, in and flanking the sixth membrane-spanning segment (M6), reacted with charged, hydrophilic, sulfhydryl-specific, methanethiosulfonate (MTS) reagents. We inferred that these residues are on the water-accessible surface of the protein and may line the ion channel. By comparing the reaction rates of the negatively and positively charged MTS reagents with these cysteines, we measured the extent of anion selectivity from the extracellular end of the channel to each of these residues. The relative rate of reaction of the anionic MTS reagent was about 20-fold faster with two residues, T351C and Q353C, near the cytoplasmic end of the M6 segment. At the other positions tested the relative rates were comparable to the relative rates of reaction with sulfhydryls in free solution. We infer that there is little charge selectivity for ion entry into the extracellular end of the channel and that the major site determining anion vs cation selectivity is near the cytoplasmic end of the channel. It appears that the residue Arg352 is an important determinant of anion selectivity. Supported by CFF, New York Heart Association and NIH NS30808.

Th-Pos102

PROTON TRANSFER AT HIS-347 IN THE CFTR PORE REVEALS TWO DISTINCT CONDUCTANCE STATES

((**Joseph F. Cotten** and Michael J. Welsh)) Howard Hughes Medical Institute and the Departments of Internal Medicine and Physiology, University of Iowa College of Medicine, Iowa City, Iowa 52242.

CFTR is an ATP- and phosphorylation-regulated epithelial Cl^- channel. Previous studies have shown that when the pore lining residue Arg-347 is mutated to a histidine (R347H), channel conductance can be modulated by cytoplasmic pH. We hypothesized that CFTR-R347H can reside in two discrete conductance states depending on the protonation state of His-347. We used the patch-clamp technique to study CFTR-R347H expressed in HeLa cells at cytosolic pHs near and flanking the predicted pKa for a histidine. CFTR-R347H alternated between a high (O_B; 8 pS) and low conductance (O_L; 4 pS) state. The lifetimes of both states were pH and voltage-dependent (at pH 6.5 and -120 mV; $\tau_B = 5.6 \pm 0.2$ ms and $\tau_L = 14.5 \pm 0.6$ ms; $n = 6$), and only one population of each was resolved. The apparent pKa for the protonated site was 6.8 (0 mV) and the voltage-dependence suggested the protonation site was 0.15 of the electrical distance from the cytoplasmic solution. Extracellular pH did not affect dwell-times even with hyperpolarizing voltages; this suggests that the pore of CFTR contains a barrier to proton migration at a point that lies extracellular to His-347. Steric or electrostatic hindrance within the pore or intracellular vestibule of CFTR-R347H may explain the observed slow rate of protonation (~100X slower than proton transfer to an imidazole in free solution). Our data suggests a two-state model in which one proton enters the CFTR pore from the cytoplasmic surface and interacts with His347 accounting directly for the OB and OL states. In addition, the data are best fit by models in which CFTR functions as a monomer.

Th-Pos103

NITRIC OXIDE SUPPRESSES CATECHOLAMINE SECRETION IN CULTURED CHROMAFFIN CELLS FROM SPONTANEOUSLY HYPERTENSIVE RATS. ((J. Fan, L. Cleemann, and M. Morad)) Department of Pharmacology. Georgetown University Medical Center. Washington, DC 20007.

Adrenal release of catecholamine exerting vascular control, and possibly contributing to hypertension, is directly controlled by cholinergic nerve endings, but may also be modulated by other factors such as nitric oxide (NO) present in the cell or from capillary endothelial cells. This mechanism was examined using adrenal chromaffin cells from a strain of spontaneously hypertensive rats (SHR), dispersed and maintained in primary cultures up to a week. Voltage clamp- and KCl-induced secretion was measured with a carbon fiber micro-electrode and was quantified in terms frequency, amplitude, duration and charge of current spikes representing individual secretory events using custom written soft-ware as an addition to the pCLAMP programs. Basal rate of secretion and calcium current (I_{Ca}) were larger in SHR than in control (WKY) rats. The possible involvement of NO in control of secretion was tested with L-arginine and SIN-1 (NO donors) and L-NAME (inhibitor of NO-syntase). SIN-1 (0.1 mM) reduced basal and KCl-induced secretion. Arginine (1 mM) suppressed I_{Ca}, generally reduced KCl-induced secretion, and had variable effects on basal secretion often leading to a transient stimulation of spontaneous secretion. L-NAME increased basal and KCl-induced secretion. In these cell secretion, Ca^{2+} influx (Fluo-3 or Fura-2) and I_{Ca} were closely linked since they were all suppressed by Nifedipine, Mibefredil and reduced $[Ca^{2+}]_o$, and were increased by Bay-K and elevated $[Ca^{2+}]_o$. The results indicate that adrenal secretion is modulated by NO, is greater in SHR than in normal rats and that these responses may be mediated, in part, by the Ca^{2+} channel

Supported by NIH RO1 HL 16152.

Th-Pos104

Abstract Withdrawn.

Th-Pos105

EFFECTS OF OUABAIN ON SPONTANEOUS INTRACELLULAR CALCIUM OSCILLATIONS IN RAT CULTURED HIPPOCAMPAL NEURONS. **(G.R. Monteith, T.Y Chaney and M.P Blaustein). U.of Md. Med. Sch., Baltimore, MD.**

The role of the Na^+-pump, which indirectly influences Ca^{2+} metabolism, is not fully understood in neurons undergoing spontaneous oscillations in $[Ca^{2+}]_i$. We have examined the effects of the Na^+-pump inhibitor ouabain, on these spontaneous increases in $[Ca^{2+}]_i$. Three week old astrocyte and neuronal co-cultures derived from rat embryonic hippocampus were loaded with the Ca^{2+}-sensitive indicator, fluo-3. We observed spontaneous and rapid oscillations of $[Ca^{2+}]_i$ in resting neurons. Increases in $[Ca^{2+}]_i$ also occurred in resting astrocytes; however, these were less frequent, and the rates of rise and fall of $[Ca^{2+}]_i$ were slower than in neurons. To confirm assignment of particular $[Ca^{2+}]_i$ signalling events to neurons or astrocytes, cells were fixed, after Ca^{2+} measurements, and were characterized using fluorescence immuno-histochemistry. Astrocytes stained positive for GFAP. Neurons did not stain with GFAP, but stained strongly with an antibody against Ca^{2+}/CaM-dependent protein kinase II. Ouabain either perturbed $[Ca^{2+}]_i$ oscillations or caused a sustained elevation in free Ca^{2+} in the neuron . These effects were dose-dependent and may reflect distinct roles of particular Na^+-pump α-subunit isoforms which, in rat tissues, differ markedly in their affinity for ouabain. Neurons were more sensitive to ouabain than astrocytes: in neurons but not astrocytes ouabain ≥ 10 µM, produced sustained elevations in $[Ca^{2+}]_i$. The effects of ouabain were mimicked by K-free solution, indicating that these effects are the result of Na^+-pump inhibition. The effects of K^+ free solution but not ouabain were readily reversible. Modulation of spontaneous oscillations in $[Ca^{2+}]_i$ may be one of the mechanisms by which an endogenous ouabain-like agent could regulate neuronal activity or by which ouabain produces neurotoxicity.

This work was supported by NIH grant - NS 16106 and an Eleanor Sophia Wood Fellowship.

Th-Pos106

ROLE OF DESENSITIZATION AND BUFFERING IN SHAPING FAST EXCITATORY SYNAPTIC CURRENTS - MONTE CARLO SIMULATION. M.I. Glavinovic[1] and H.R. Rabie[2]. Depts. of Anaesthesia Research[1], Physiology[1] and Chemistry[2], McGill University, Montreal, P.Q. H3G 1Y6, Canada

It is still controversial whether: a) the kinetics of spontaneous fast excitatory synaptic currents (mEPSCs) is amplitude dependent, b) desensitization of AMPA receptors and buffering of glutamate in the cleft play any role in shaping the time course of mEPSCs. In this study fast excitatory synaptic currents are simulated using Monte Carlo methods (Bartol et al., Biophys. J. 59: 1290-1307, 1991; Wahl et al., J. Neurophysiol 75: 597-608, 1996) by following the diffusion of individual neurotransmitter molecules through the synaptic cleft and their interaction with postsynaptic receptors at 37°C. mEPSCs of various sizes are simulated by releasing a different number of neurotransmitter molecules (150-20000) from a point source centered 15 nm above a rectangular grid of 14 x 14 postsynaptic receptors. The time constants of decay ($T_{d\text{-}EPSC}$s) are found to be moderately amplitude dependent in physiological conditions and markedly so when desensitization is abolished. A change occurs because both the occupancy of bound activatable states, and the buffering of glutamate molecules in the synaptic cleft are concentration dependent and are increased when desensitization is abolished. Desensitization (and generally gating mechanism) and buffering in the synaptic cleft are closely linked processes, both highly important in shaping mEPSCs.

Supported by the Medical Research Council (Canada).

Th-Pos107

ROLES OF $[Ca^{2+}]_{in}$-ACTIVATED NON-SELECTIVE CATION CHANNELS IN OSCILLATORY ACTIVITY OF NERVE CELL: MODEL STUDIES. ((A.O.Komendantov[#@] and N.I.Kononenko[#])) [#]Bogomoletz Institute of Physiology and [@]Institute of Physics, Natl.Acad.Sci., GSP 252601, Kiev, Ukraine. (Spon. by T.R.Chay)

It is known that calcium-activated non-selective (CAN) channels play an important role in both physiological functions and pathological processes of the nervous system [1]. We have incorporated this CAN current in a model of pacemaker activity of snail neuron. This updated model allows us to demonstrate different regimes of oscillatory activity (beating, bursting, chaotic), mode transitions [2] and to explore theoretically some interesting phenomena which may be provided by neuronal CAN channels. We have found that in a silent neuron with CAN channels the short activation of the synaptic input can produce the persistent bursting activity. The bifurcation analysis reveals the crisis besides the period-doubling chaos as the chemosensitive neuropeptide-dependent conductance is increased. When this conductance is more than a critical value the size of chaotic attractor changes suddenly and long periods of quiescence are appeared in high firing rates. Such phenomena have a neurobiological relevance. They may be implicated in learning and memory at the neuronal level as well as in epileptogenesis, ischemia and migraine symptoms.

[1] Partridge et al.(1994) Brain Res. Rev., 19: 319.

[2] Komendantov and Kononenko (1995) SAMS,18-19:725; J.theor.Biol.(in press).

Th-Pos108

NEURONAL SHAPE TRANSFORMATION AND NERVE CONDUCTION. ((Darrell L. Tanelian and Vladislav S. Markin)) Departments of Anesthesiology and Pain Management and Biomedical Engineering, University of Texas Southwestern Medical Center, Dallas, Texas 75235-9068.

Mechanical and chemical stimulation of the nervous and subsequent receptor internalization causes neuronal processes to change their shape from homogeneous cylinders to a heterogeneous string of swollen varicosities (beads) connected by thin segments. We propose quantitative mechanisms for dendritic transformation based on the relationship between membrane area and neuronal process volume. Our theory predicts the relationship between the initial dendrite radius and the average radii of the transformed dendritic varicosities and connecting segments, as well as the periodicity of the string of varicosities. The results of our model are in good agreement with experimental observations of this beading phenomenon in the spinal cord and brain.

Beading of the neuronal process can have important consequences for action potential propagation. Analusis reveals three possible outcomes: normal impulse propagation, action potential reflection, and conduction block. When action potential reflection is the prevailing condition, it can lead to both linear and nonlinear filtering of the incoming action potential train. Functionally, this process of dendritic transformation may serve as a mechanism for information processing along fine peripheral and central neuronal terminals.

Supported by the Sid W. Richardson Foundation.

Th-Pos109

KINETIC ANALISYS OF CAFFEINE INDUCED Ca^{2+} RELEASE IN MAMMALIAN SYMPATHETIC NEURONS. ((**A.L.Escobar***, A.Hernandez-Cruz+ and N.Jimenez+))(Spon:G.Whittembury) *CBB-IVIC, Caracas, Venezuela and +IFC-UNAM, Mexico City, D.F., Mexico.

We have analyzed the physiological parameters that determine the dynamics of Caffeine induced Ca^{2+} release in single Fura-2 loaded sympathetic neurons. Two components with different kinetics were observed: an early, transient increase in the free $[Ca^{2+}]_i$ and a delayed component that persists during the Caffeine application. Both components of Ca^{2+} release are sensitive to micromolar concentrations of Ryanodine. The transient component shows refractoriness, depending on the filling status of the stores. In addition, it was abolished by tetracaine and intracellular BAPTA. This effect seems to be due to the interference with the Ca^{2+} mediated positive feedback loop and suggests a Ca^{2+} induced Ca^{2+} release phenomenon. When Ca^{2+} was fully substituted by Sr^{2+} the dynamics of the fluorescence transients were strongly affected. These changes were mostly reflected in the relaxation of the transient component, being the Sr^{2+} transients much more slower than the Ca^{2+} ones. This suggests that Sr^{2+} is much less efficient in inactivating the transient component of the release process. We were able to simulate caffeine responses integrating a compartmentalized linear diffusional mathematical model: When the intracellular stores were completely filled of Ca^{2+}, the rapid initial change in free $[Ca^{2+}]$ induced a fast occupation of the Ryanodine receptor Ca^{2+} -activation site promoting a regenerative release. In contrast, when the stores where partially loaded, the smaller driving force for the Ca^{2+} efflux caused a slower change in the cytosolic free $[Ca^{2+}]$. This allows the inactivating site to be occupied almost as fast as the activating site, suppressing the initial transient release.
Supported by CONICIT grant S1-95000493 (Venezuela) and DGAPA-UNAM IN212194, IN206395 (Mexico) and CONACyT 400346-5-2366PN (Mexico)

Th-Pos110

IN VITRO CALCIUM BINDING KINETICS OF CALCIUM CHELATORS AS REVEALED BY TEMPERATURE-JUMP RELAXATION
((**M. Naraghi**, E. Neher)) Max-Planck-Institute for Biophysical Chemistry, Dept. of Membrane Biophysics, Am Fassberg 11, D-37077 Goettingen, Germany (Spon. by M. Naraghi)

Calcium chelators are used to measure cytosolic free calcium concentration or to buffer calcium to a predefined level. Recent studies (J. Physiol. (1995), 489.3, 825-840) have investigated the kinetic competition between chelators and the secretion apparatus at a fast central synapse. These kinetic studies indicate the importance of a quantitative knowledge of the binding kinetices of the chelators in investigating fast physiological processes on a millisecond timescale. Kao et al. (Biophys. J. (1988), 53, 635-639) were the first to study the kinetics of FURA-2 in vitro.
Using the temperature-jump relaxation method, we have studied the in vitro kinetics of FURA-2, BIS-FURA-2, FURAPTRA, FLUO-3, CALCIUM-GREEN-1, CALCIUM-GREEN-2, CALCIUM-GREEN-5N, CALCIUM-ORANGE, CALCIUM-ORANGE-5N as well as EGTA, BAPTA and HEDTA in conditions which are identical to those implemented in our patch clamp recordings, i.e. 120-140 mM CsCl, 20-40 mM Cs-HEPES, 8 mM NaCl, pH=7.2 at 23° C. The results can be summarized as follows: All fluorescent indicators have on-rates around $5x10^8$ $M^{-1}s^{-1}$. They differ significantly with respect to their off-rates from each other according to their affinities, ranging from 100 s^{-1} up to 26000 s^{-1}. BAPTA is kinetically almost indistinguishable from FURA-2. EGTA and HEDTA have small binding rate constants for calcium in the range of $2.5x10^6$ M^{-1} s^{-1} since, at the pH of 7.2, protons need to be dissociated from the chelator before it can bind a calcium ion.

Th-Pos111

INTRACELLULAR CA^{2+} BINDING AND CA^{2+} CLEARANCE KINETICS STUDIED IN ADRENAL BOVINE CHROMAFFIN CELLS.
((**T. Xu***#, M. Naraghi*, H.G. Kang# and E. Neher*)) * Department of Membrane Biophysics, MPI for Biophysical Chemistry, D-37077, Göttingen, Germany. # Institute of Biophysics and Biochemistry, Huazhong University of Science and Technology, Wuhan 430074, China. (Spon. by E. Neher)

The photolabile Ca^{2+} chelator, DM-nitrophen, has been used extensively to study calcium triggered exocytosis. Since the rate of exocytosis depends steeply on the intracellular free Ca^{2+} concentration ($[Ca^{2+}]_i$), it is important to have better understanding of $[Ca^{2+}]_i$ dynamics generated by photolysis of DM-nitrophen in cells. Thus, the Ca^{2+} binding kinetics of fura-2, DM-nitrophen and endogenous Ca^{2+} buffer, which determine the time course of Ca^{2+} changes after photolysis of DM-nitrophen, were studied in bovine chromaffin cells. The *in vivo* Ca^{2+} association rate constant of fura-2, DM-nitrophen and endogenous Ca^{2+} buffer were measured to be $5.17x10^8$ $M^{-1}s^{-1}$, $3.5x10^7$ $M^{-1}s^{-1}$ and $1.07x10^8$ $M^{-1}s^{-1}$, respectively. The endogenous Ca^{2+} buffer appeared to have a low affinity to Ca^{2+} with a dissociation constant around 100 μM. Also a fast Ca^{2+} clearance mechanism was found to play a dominant role at high $[Ca^{2+}]_i$ in clearance of Ca^{2+} after flashes, causing $[Ca^{2+}]_i$ to decay with a time constant of 0.73 s. This Ca^{2+} clearance was identified as mitochondrial Ca^{2+} uptake; its uptake kinetics was studied by analyzing the Ca^{2+} decay at high level $[Ca^{2+}]_i$ after flash photolysis of DM-nitrophen.

Th-Pos112

R-TYPE Ca^{2+} CHANNELS PREFERENTIALLY REGULATE OXYTOCIN RELEASE FROM NEUROHYPOPHYSIAL TERMINALS. ((**G. Wang**, G. Dayanithi, D. Moorman and J.R. Lemos)) WFBR, Shrewsbury, MA 01545

We have previously shown that, besides "*L*" and "*N*", a "*Q*"-type Ca^{2+} current component exists in isolated nerve terminals of the neurohypophysis (Wang et al., 1994, *Abst. Soc. Neurosci.*20:629). Moreover, when either high (≥300 nM) concentrations of ω-AgaIVA or low (≤100 nM) concentrations of ω-MVIIC were added to the isolated terminals, a dihydropyridine- and ω-GVIA-resistant component of vasopressin (AVP) release was essentially abolished. In contrast, a similar resistant component (35.5 ± 5.1%) of oxytocin (OT) release was essentially unchanged by the same concentrations of *Q*-type channel-blockers. Perforated patch-clamp measurements of Ba^{2+} currents (I_{Ba}) revealed that the terminals fall into two groups: those in which the GVIA- and DHP-resistant component was sensitive to ω-AgaIVA/ω-MVIIC (*1*) and those in which were insensitive (*2*). The resistant I_{Ba} component in this latter group is a high-voltage ($V_{1/2}$ = -4.1 mV) activated, transient (τ_i = 25.6 ms) current which shows moderate steady-state inactivation ($V_{1/2}$ = -44.1 mV). These properties are most consistent with the "*R*"-type Ca^{2+}-channel type. This was confirmed by the low levels (86 μM) of Ni^{2+} which can half-maximally block this component of the current in group *2* terminals. Immunoblot results indicate that group *2* nerve terminals appear to be OT-containing, while group *1* terminals appear to be AVP-containing. These results lead to the conclusion that the *R*-type channels are preferentially localized on OTergic nerve terminals, and thus do not affect intraterminal Ca^{2+}-levels or release in AVPergic nerve terminals.
(Supported by NIH grant NS29470 to J.R.L.)

Th-Pos113

TIMING OF FAST SYNAPTIC TRANSMISSION IN THE MAMMALIAN BRAIN. ((**Bernardo Sabatini** and Wade Regehr)) Department of Neurobiology, Harvard Medical School, Boston, MA 02115.

The synaptic delay from the depolarization of the presynaptic neuron to the opening of ligand gated channels in the postsynaptic neuron limits the communication rate between neurons and constrains the molecular interactions responsible for vesicle fusion. It has been difficult to elucidate the factors controlling the timing of synaptic transmission in the mammalian brain, where presynaptic terminals are typically less than 1 μm in diameter. We have developed an approach which allows us to study the timing of synaptic transmission at the granule cell to stellate cell synapse in rat cerebellar slices. We performed simultaneous optical recordings of presynaptic depolarization and presynaptic calcium influx while monitoring postsynaptic currents with whole cell voltage clamp. At room temperature, similarly to what has been shown previously in squid, vesicle release at this synapse is driven by calcium entering during the repolarization phase of the action potential. However, at physiological temperatures this classical view no longer holds: calcium influx commences only 90 μs after the start of the action potential, allowing significant calcium influx to occur during the action potential upstroke. In addition, at these temperatures, calcium driven vesicle fusion occurs less than 60 μs after the start of calcium influx. The combination of these two factors results in total synaptic delays of less than 150 μs.

Th-Pos114

PRESYNAPTIC CALCIUM AND FACILITATION AT THE GRANULE CELL TO PURKINJE CELL SYNAPSE. ((**Pradeep P. Atluri** and Wade G. Regehr)) Dept. of Neurobiology, Harvard Medical School, Boston, MA 02115.

Presynaptic calcium has long been implicated in short-term facilitation, but its precise role is unclear, particularly at synapses in the mammalian CNS. In rat cerebellar slices, paired-pulse electrical stimulation of granule cell axons produced a 2.5-fold enhancement of EPSC peak amplitude that decayed with a time constant of about 200 ms, as assessed by voltage-clamp recordings from Purkinje cells. Using fluorescent calcium-sensitive indicators, we studied the role of presynaptic residual free calcium ($[Ca]_{res}$) in facilitation. In control conditions, $[Ca]_{res}$ decayed more rapidly than did facilitation. Introducing EGTA into presynaptic terminals sped the decays of $[Ca]_{res}$ and of facilitation in a dose-dependent manner. When $[Ca]_{res}$ was reduced to a brief impulse lasting only a few milliseconds, facilitation was reduced in amplitude and duration. Facilitation decayed with an intrinsic time constant of approximately 40 ms. These results suggest that facilitation at this synapse is produced by a calcium-driven process with a high apparent calcium affinity and a slow effective off-rate. Both $[Ca]_{res}$ dynamics and the properties of a calcium-driven reaction determine the time course of facilitation. We are currently studying the determinants of the amplitude of facilitation.

Th-Pos115

BOTULINUM TOXIN C1 SELECTIVELY CLEAVES SYNTAXIN IN THE CALYX NERVE TERMINAL OF THE CHICK CILARY GANGLION. ((**R.R. Mirotznik** and E.F. Stanley)) Synaptic Mechanisms Section, NINDS, NIH, Bethesda MD 20892. (Spon. D. Gilbert)

Botulinum toxins A-G irreversibly block transmitter release in cholinergic nerve terminals by targeting specific protein elements of the release mechanism. Each toxin variant cleaves one of the proteins that share a common SNARE motif: syntaxin, SNAP-25 or synaptobrevin (VAMP) (Rossetto et al. Nature 372:415). Of these toxins botulinum C1 (BTC1) is unusual in two respects. First, it is the only toxin of the group that has been reported to cleave syntaxin and second, it also targets a second protein SNAP-25, removing a short peptide from the C-terminal region (Williamson J.Biol.Chem. 271:7694; Foran Biochem. 35:2630). We have used computer-enhanced immunofluorescent staining (Scanalytics) of the giant calyx-type presynaptic nerve terminal in the chick ciliary ganglion to test the effect of this toxin on release site-associated proteins. Antibodies against syntaxin stained both the release face and the external face of the nerve terminal but the release face also exhibited patches that probably reflect release sites. BTC1 reduced membrane staining and increased cytoplasmic staining, consistent with cleavage of syntaxin and diffusion of the resulting fragment into the terminal interior. Staining of SNAP-25 with either an antibody directed to the N-terminal or C-terminal regions was very similar, highlighting the membrane of the terminal. BTC1 did not affect the staining pattern of either anti-SNAP-25 antibody. Thus, our results indicate that BTC1 can be used to specifically cleave syntaxin in these nerve terminals.

Th-Pos116

INACTIVATION KINETICS OF CARDIAC L-TYPE Ca^{2+} CHANNELS IS REGULATED BY SR Ca^{2+} CONTENT, STUDIED IN TRANSGENIC MICE. **H. Masaki**, V. J. Kadambi, W. Luo, Y. Sato, E. G. Kranias and A. Yatani. Dep. of Pharmacology and Cell Biophysics, University of Cincinnati, Cincinnati OH 45267.

Ca^{2+} entry through the L-type Ca^{2+} channels (CaCh) is responsible for initiating and maintaining cardiac contraction. Cardiac CaCh show negative feedback regulation, i.e. they decline in response to prior Ca^{2+} entry (Ca^{2+}-dependent inactivation) and this decay of the current provides an important role for intracellular Ca^{2+}-homeostasis. Studies using pharmacological interventions which alter sarcoplasmic reticulum (SR) Ca^{2+} content have suggested that the rate of Ca^{2+}-dependent inactivation is regulated by Ca^{2+} released from the SR. In recent studies, cells from the phospholamban knockout (PLB-KO) mouse showed significantly increased SR Ca^{2+} transport rates, while PLB over-expression (PLB-OEX) mouse hearts showed decreased SR Ca^{2+} transport rates. To test whether corresponding changes in the SR Ca^{2+} content in these models alter CaCh function, we compared the properties of CaCh currents (I_{Ca}) in ventricular myocytes from adult wild-type (WT), PLB-KO and PLB-OEX mice. Current density, gating and sensitivities to dihydropyridine drugs of I_{Ca} were similar to other mammalian species, and these properties were not modulated by alterations in the levels of PLB. I_{Ca} from the three groups revealed two (fast and slow) components of inactivation kinetics. Inactivation of I_{Ca} was significantly faster in PLB-KO cells with an increase in the fast component compared to WT cells, while, inactivation was slower in PLB-OEX cells with a reduced fast component. The application of caffeine or ryanodine abolished the differences between WT and transgenic cells. These results suggest that Ca^{2+} released from the SR regulates CaCh inactivation by altering local Ca^{2+} concentration which modulates Ca^{2+}-dependent inactivation.

Th-Pos117

ASYNCHRONY OF QUANTAL EVENTS IN EVOKED POSTSYNAPTIC RESPONSES ((**M. Bykhovskaia**, J.T. Hackett, and M.K. Worden)) Dept. Molec. Physiol. and Biol. Physics., U. Virginia Health Sciences Ctr. 22908, and Sechenov I.E.Ph.B, S-Petersburg 194223, Russia (Spon. by M.K. Worden)

The assumption that quanta are released in a mutually independent manner in response to presynaptic stimulation underlies many quantal analyses of the neurotransmitter release process. To test this assumption, distributions of quantal latencies obtained from extracellular recordings of postsynaptic responses at the lobster neuromuscular junction at stimulation frequencies between 1-10 Hz were compared with distributions obtained from simulated populations of multiquantal postsynaptic responses generated under the assumption that quanta are released in a mutually independent manner. The results of these comparisons show that these quantal latencies distributions are fundamentally different. At the neuromuscular junction, the proportion of responses exhibiting late quantal events increases as a function of quantal content whereas the proportion of responses exhibiting early quantal events remains constant. In contrast, in computer simulated data sets both the proportion of responses exhibiting early quantal events and the proportion of responses exhibiting late quantal events increase as a function of quantal content. Quantal counts and integration of simulated and experimental current traces show that the observed asynchrony of quantal release at the neuromuscular junction is critical for correct estimation of quantal content. These results suggest that quantal releases are interdependent, such that the simultaneous release of multiple quanta is prevented or suppressed.

Th-Pos118

MEMBRANE POTENTIAL CHANGE IN OUTER HAIR CELLS OF GUINEA PIG COCHLEA. ((**T.Nakagawa**, J.S.Oghalai, M.Saeki, P.Saggau, W.E.Brownell)) Dept. of Oto/Com Sci, Baylor College of Medicine, Houston, TX 77030

Outer hair cells (OHCs) of the mammalian cochlea have electromotility and play a role in the sharp tuning of hearing. Several kinds of ionic channels have been previously reported in OHCs. Moreover, an uneven distribution has been noticed. For example, K^+ channels are mainly distributed at the basal end. Chemical receptors such as for ACh, ATP and substance-P are located at the basal, apical and basolateral walls, respectively. Mechano-electrical transduction channels are located at the cilia of apex. These observations suggest the possibility of temporal and spatial differences in membrane potential. The use of fluorescence to monitor cellular electrical activity is a new technique designed to investigate voltage differences within a single cell. We developed a method to measure the OHC transmembrane potential using a voltage-sensitive dye under voltage clamp conditions. OHCs were isolated from guinea pigs by enzymatic and mechanical procedures. Di-8-ANEPPS was used as the voltage-sensitive dye. Cells were incubated for 10-30 min. The cells were voltage-clamped using a whole cell configuration. Excitation light was guided by fiber optics. By manipulating the location of fiber optics, the size and location of the light spot could be controlled. Emission light was high-pass filtered above 520nm and collected by single photodiode. The dye stained only the cytoplasmic membrane. Membrane potential was stimulated by sine wave voltage stimuli of various frequency ranges. The dye response recorded from both the whole cell and discrete portions of cell could follow the voltage changes in each frequency, indicating the reliable frequency characteristics. Further studies using various stimuli are expected to clarify the electroanatomy in OHC.

Th-Pos119

CURRENT NOISE POWER SPECTRUM OF THE MEMBRANE MOTOR OF THE COCHLEAR OUTER HAIR CELL. ((**David Ehrenstein** and K. H. Iwasa)) NIDCD, NIH, Bethesda, MD 20892-0922.

The outer hair cell (OHC) in the mammalian cochlea is an unusual mechanoreceptor cell that exhibits a membrane potential-dependent motility which is considered to be important for frequency discrimination. The OHC motility mechanism is independent of chemical energy and is thought to be a voltage-gated membrane protein which changes the cell's size by switching between compact and extended conformations. The gating charge of this protein and its rates of conformational fluctuations are observable through the membrane's current noise power spectrum and frequency-dependent capacitance. We have observed these phenomena on large membrane patches using the macro-patch technique. We present our observations of these quantities and compare them to the predictions of a simple two-state theory.

Th-Pos120

Steady-State Currents and Fluctuation Analysis in Proline Transporters. ((**A.Galli***, R.T. Fremeau#, L.J. DeFelice*)) *Dept. of Pharmacology, Vanderbilt University School of Medicine, Nashville TN 37232. #Dept. of Pharm. and Neurobiology, Duke Univ. Medical Center, Durham, NC27710

The high affinity L-proline transporter (PROT) is a member of the Na^+ and Cl^--dependent family of neurotransmitter transporter proteins. Within the rat hippocampal formation, high affinity L-proline uptake is confined to a subset of glutametergic nerve terminals. These findings support a synaptic role for L-proline in specific exitatory pathways in the CNS. Presumably PROTs remove proline from the synaptic cleft utilizing the electrochemical gradient of Na^+ and Cl^-. To study voltage regulation, we stably transfected HEK-293 cells with cloned rat proline transporter (rPROT). In physiological solutions under whole-cell voltage clamp, proline generates an inward current between -160 and 40 mV. Des-Tyr-Leu-enkephalin (GGFL) a competitive inhibitor of PROT, is able to reduce this current to the control level. The maximum steady state proline current was -30 pA at -120 mV. To study the uptake mechanism of PROT, we also have mesuared current fluctuations induced by proline. The control variance was typically 0.4 pA^2 in the absence of substrate at -120 mV. Adding 40 μM proline to the bath increased the variance to 1 pA^2 . The ratio of the change in variance to the change in current was typically -0.04 pA at -120 mV. These data indicates that proline transporter operates in a classical transporter mode. Supported by NIH, NS 34075-01, NS 32501.

Th-Pos121

AXONAL ELECTRICAL FUNCTION CANNOT BE INFERRED FROM EXCLUSION OF EXTRACELLULAR DYE BY SQUID GIANT AXONS.

((C.S. **Eddleman*** , H.M. Fishman* and G.D. Bittner*†)) University of Texas, Medical Branch at Galveston, TX 77555* and Austin, TX 78712†.

Exclusion versus uptake of extracellular dye by a damaged axon (complete transection or a small hole [<50μm]) is often used to assess axonal sealing with the implicit assumption that exclusion implies functionality. We measured the resting potential (RP) of intact, isolated squid giant axons (GAs) in artificial sea water (ASW) containing a hydrophilic dye (HD, 0.1% of either FITC-dextran, Texas Red-dextran or pyrene) and used confocal microscopy to image the longitudinal midsection fluorescence for > 2 hrs. GAs depolarized by ≥ 20 mV from controls (RP ~ -60mV) (due to non-specific damage during dissection) and control GAs both excluded dye completely. However, HDs rapidly (s) move into the desheathed axoplasm of a GA in Ca^{2+}-free ASW and quickly (min) spread into the axoplasm of the attached intact portion of axon indicating that axoplasm does not impede dye diffusion in Ca^{2+}-free ASW. By contrast, when GAs were transected in ASW (with Ca^{2+}) containing HD, the fluorescence intensity indicating uptake could not be distinguished qualitatively from the lack of fluorescence of intact control GAs until 1.5 hrs or more posttransection. After addition of styryl dye (lipid binding, 25μM FM4-64) to the bath of cut GAs, we observed increasingly intense fluorescence with time at the plume of debris extending out of the cut end indicating the formation of a hydrophobic environment. We conclude that (1) dye exclusion is equivocal with respect to axonal electrical function (i.e. a normal RP and an ability to generate action potentials cannot be inferred solely from dye exclusion data) and (2) the plume of axoplasmic debris and the partially collapsed cut end of a GA severed in ASW substantially slows HD entry. Furthermore, from (1) we conclude that holes in injured GAs, which are too small for penetration by HD molecules but are large enough to allow ionic leakage to render the axon inexcitable, make dye assessments of functional recovery uncertain.

Supported by NIH grant NS31256 and a Texas ATP grant.

Th-Pos122

HYDROPHILIC DYE CHARGE AFFECTS DYE UPTAKE AT CUT ENDS OF TRANSECTED AXONS.

((M.E. Smyers, A. Lore, H.M. Fishman, and G.D. Bittner)) University of Texas, Medical Branch at Galveston, TX 78755, and Austin, TX 78712 (Spon. by O. Hamill)

Membrane integrity, as determined by the exclusion of hydrophilic dyes (HDs), is often used to assess cell viability. However after membrane injury, we observe that various HDs behave differently at the onset of the injury and provide an ambiguous indication of plasmalemmal membrane integrity, as indicated by inconsistencies in the dye exclusion literature. We examined fluorescent dye uptake of severed crayfish medial giant axons or rat sciatic axons at various times pre- and post-transection by the extracellular addition of 1% anionic (pyrene, pyranine, Lucifer Yellow), 1% cationic (sulforhodamine B), or 0.1% neutral (FITC-dextran) dyes to physiological salines. Axons were exposed to the dye solution for 20 min before washout and fluorescence imaging with a Zeiss ICM-35. We find that anionic HDs are excluded (i.e. are not taken up) when added prior to transection, but are not excluded if added at 1-3 min posttransection when examined at 20 min posttransection. In contrast, cationic or neutral HDs added prior to transection or after transection are not excluded by the cut axonal ends under these same conditions. The negatively charged pyranine, when applied with its positively charged collisional quencher DPX, is not excluded when added to the bath saline prior to transection. When both cationic and anionic dyes are added prior to transection, both dyes enter the cut end but the cationic dye diffuses much further within the axon. These data suggest that dye uptake at cut axonal ends is strongly affected by the charge on the dye, with anionic HDs being excluded when added alone prior to transection. These data also demonstrate that dye uptake can be a misleading measure of membrane integrity after plasmalemmal damage under certain circumstances.

Supported by NIH grant NS31256 and a Texas ATP grant.

Th-Pos123

ACTIVATION OF PKC BY PHORBOL ESTERS INHIBITS THE CURRENT AND ALTERS THE PERMEABILITY RATIO IN EXPRESSED KAINATE RECEPTORS.

((S. **Kriegler**, J. L. Yakel)) Lab. of Signal Transduction, National Institute of Environmental Health Sciences, Research Triangle Park, NC 27709. USA (Spon. by G. Augustine)

Activation of PKC has been shown to inhibit inward currents of both monovalent and divalent ions through the non-NMDA subtype of glutamate receptor channel expressed in Xenopus oocytes. In this study we expressed the GluR6 subunit and measured the current-voltage relationship in 60 mM barium solution before and after a 30 minute application of PMA, an activator of PKC. Before application of PMA there was a significant inward current carried by barium with a reversal potential of ~ -40 mV. Application of PMA caused a reduction of both the inward and outward currents, however the inward current was inhibited almost completely. We considered the reversal potential to be the most negative potential where an outward current could be detected. In addition to the reduced currents, Erev showed a shift of ~20 mV in the positive direction after PMA treatment. This shift in reversal potential indicates that the permeability ratio of PBa++/Pmonovalent increases upon phosphorylation of non-NMDA receptors by PKC. The difference between relative permeability and conduction of Ba++ can be explained by divalents entering the channel more easily but then blocking the passage of other ions in a voltage dependent manner. This increased block of glutamate receptors by divalents upon phosphorylation is probably partially responsible for the reduced currents seen in physiological solutions.

Th-Pos124

*POTASSIUM INWARD RECTIFIED CHANNELS DISTRIBUTION IN Müller CELLS FROM EMBRYO AND ADULT Rana Catesbeiana. ((**Legier Rojas**[I] and Richard Orkand)).*

Institute of Neurobiology. University of Puerto Rico 201 Blvd. Del Valle San Juan 00901. [I]Present address: Department of Physiology. Universidad Central del Caribe. Call Box 60327. Bayamón, PR. 00960-6032. (Spon. by V. Eterovic)

In adult Müller glial cells from the vertebrate retina, KIR-channels are located preferentially at the end-feet (EF) comparing to the soma (S), in a 30:1 ratio (EF:S). In this work we explored the KIR-channels distribution from dissociated Müller cells of aquatic embryos and the adult *Rana Catesbeiana* retina using the patch clamp technique. The radius of the vitreous ball (450 and 650 μm) was used to have a reference of the tadpole development. We used pipettes (5-6 MΩ), containing (in mM): KCl 120; NaCl 6; $CaCl_2$ 1; $MgCl_2$ 0.8; EGTA 5, and pH 7.1. To the present analysis we rejected experiments where run-down of channels was observed. From 106 Müller cells recorded from tadpoles, the KIR-channels ratio EF:S was 1.91 obtained from the mean values 4.29/2.25, whereas in 102 cells from adult retina the ratio EF:S was 10.56 (19.11/1.81). The minimal and maximal values of active KIR-channels per patch in tadpoles end-feet and soma were 0 to 11 and 0 to 6 respectively, whereas in adult Müller cells were 1 to 360 and 0 to 5 in end-feet and soma respectively. In tadpole, P_{open} increase sigmoidally with the depolarization, reaching a maximum of 0.70 at -80 mV and a minimum of 0.24 at -160 mV. KIR-channels were not the unique channel type expressed, K(ATP)s and a stretch activated channels (SAC) were recorded. In addition a maxi-chloride channel (350 pS) was present in tadpole. The differences in the KIR-channels distribution observed in tadpole and adult Müller cells can be explained as due to the developmental conditions, however they can be related to the condition determined by the habitat.

Th-Pos125

FUNCTIONAL CHARACTERIZATION OF A *C. ELEGANS* OLFACTORY RECEPTOR IN HETEROLOGOUS EXPRESSION SYSTEMS

((**Y. Zhang**, J. Chou[#], J. Li, H.A. Lester, C.I. Bargmann[#†] and K. Zinn)) Division of Biology, California Institute of Technology, Pasadena, CA 91125, [#]Program in Developmental Biology, Dept. Anatomy, UC San Francisco 94143 and [†]Howard Hughes Medical Institute,

The nematode C. elegans can respond to both volatile and non-volatile odorants through 14 types of chemosensory neurons. Each type of neuron detects several different odorants. A gene, *odr-10*, which encodes a predicted seven transmembrane domain receptor was identified. *C. elegans* deficient in *odr-10* have specific defects in chemotaxis to diacetyl, a volatile metabolic product of soil bacteria. It is not known, however, whether *odr-10* can interact with only a small number of odorants or with a broad spectrum of structurally diverse compounds. The signal transduction pathway for *odr-10* is also not clear.

We used two heterologous expression systems, *Xenopus* oocytes and HEK293 cells, to express and characterize functional properties of *odr-10* using conventional two-electrode voltage clamp recording (in *Xenopus* oocytes) or a Fura-2 based Ca^{2+} imaging system (in HEK293 cells). We also studied cell surface expression of *odr-10* with immuofluroscent staining and the fluorescence activated cell sorting (FACs) assays. Our results indicate that *odr-10* expresses better than cloned mammalian olfactory receptors in HEK293 cells with a larger fraction of cells expressing the receptor on their surfaces. When expressed in HEK293 cells, *odr-10* can be activated by diacetyl and also by structurally similar non-volatile compounds, such as citric acid. The activation of *odr-10* causes release of Ca^{2+} from intracellular stores suggesting that this receptor may be coupled to a Gαq like G-protein. Supported by NIDCD and NIMH

Th-Pos126

PERIPHERAL NERVE REGENERATION USING A NEURAL INTERFACE.

((**P Garzella**)) Scuola Superiore Sant'Anna, Via Carducci 40, Pisa 56100, Italy

Peripheral nervous system axons are capable of regeneration following transection. Regenerating processes are affected by various biological factors and influenced by mechanical devices. Much current interest focuses on neural interfaces housed in tubular guidance structures which may become a powerful tool for clinical applications (motor/sensory limb prostheses for amputees, spinal cord injury cases etc.). A neural interface is a planar array of microelectrodes on a substrate perforated by a plurality of *via holes* ("dice"). This device is placed between the ends of a severed peripheral nerve whose axons could regenerate through via holes (Kovacs G.T.A. et al., IEEE Trans. Biomed. Eng., 39, 1992; Dario P. et al. Micro System Technologies, Berlin 1994). We report herein histological and physiological evidences of nerve regeneration through a implantable neural interface housed in ChronoFlex™ guidance channels using a mammalian animal model. Dices (overall dimension : 1510x1510 μm^2, via holes : 50x50 μm^2 , FhG-IBMT, St. Ingbert, Germany) were housed in 10mm long ChronoFlex™ (PolyMedica Industries, Woburn, MA) guidance channels (Spry thermal-heating process, Kontron Instruments, Everett, MA) by means of a Teflon support. New Zealand albino rabbit were anesthetized the right sciatic nerve was exposed and transversely sectioned. Both proximal and distal nerve stumps were introduced into the ends of the nerve guidance channel leaving a small gap (3-6mm) between the nerve stumps. To verify that small groups of physiologically functional axons could regenerate through our neural interface, electrophysiological experiments were carried out, between 60 and 90 days after the implant procedure, on rabbits under sodium pentobarbital anesthesia. Morphological and histological evidence showed that nerves regenerated through the NI and electrophysiological results demonstrated the recovery of electrical functionality. In addition to nerve signals recording the NI allowed the stimulation of the regenerated nerve producing a visible leg/foot contraction. This work has been supported by funding from EU in the framework of the Esprit Project INTER #8897.

Th-Pos127

SUBCELLULAR METABOLIC TRANSIENTS REVEALED BY CONFOCAL IMAGING IN CARDIAC MYOCYTES

((**Dmitry N. Romashko**, Eduardo Marban and Brian O'Rourke)) Johns Hopkins University Dept. of Medicine, Division of Cardiology, Baltimore, MD 21205

Using endogenous fluorophores (NADH or flavoproteins) as probes, we have previously found that cardiomyocytes deprived of exogenous substrate undergo complex oscillations of mitochondrial redox potential that are linked to transient activation of K,ATP channels. We now report that temporal instabilities of the redox state are associated with complex spatio-temporal patterns of both mitochondrial redox state and mitochondrial membrane potential within and among individual cells. Confocal imaging was used to visualize redox potential (by flavoprotein fluorescence; 488ex./530em.) and/or mitochondrial membrane potential in tetramethylrhodamine ethyl ester-loaded (TMRE) cells (543ex./605em.). Time series analysis of images of redox state revealed three major patterns of dynamic behavior, including: 1) global (cell-wide) transient oxidation of the flavoprotein pool, 2) localized increases in oxidation without propagation, and 3) propagation of a redox wave from one part of the cell to another. These patterns could be simultaneously observed in uncoupled cells within the same field of view and were not correlated with cellular Ca overload. Propagation of a redox wave between coupled cells was also observed, suggesting that biochemical messengers may be involved. Visualization of the pattern of mitochondrial membrane potential with TMRE revealed an uneven and time-varying distribution of energized mitochondria which appeared to be synchronized on the scale of functionally coupled mitochondrial clusters. Together with our previous results correlating K,ATP activation with transient mitochondrial oxidation, the present findings support the hypothesis that mitochondrial membrane potential may undergo transient and massive collapse, resulting in a sharp decrease in the cellular ATP/ADP ratio. These metabolic instabilities may play a role in shaping the excitability of the heart during metabolic stress.

Th-Pos128

INVESTIGATION INTO THE MORPHOLOGY OF THE T-TUBULAR SYSTEM IN LIVING CARDIAC MYOCYTES BY TWO PHOTON EXCITATION MICROSCOPY.

((**C. Soeller** and M.B. Cannell)) Dept. Pharmacology & Clinical Pharmacology, St. George's Hospital Medical School, Cranmer Terrace, London SW17 0RE, UK.

Two-photon excitation microscopy was used to visualise the t-tubular system in living rat cardiac myocytes. Cells were immersed in a solution containing fluorescein which was excited by light from a modelocked Ti:Sapphire laser at 850nm via a 63x 1.25Na objective lens. Images recorded using two-photon excitation looked generally "crisper" than their single photon confocal counterparts (recorded with excitation at 488nm), despite the fact that the two photon excitation point spread function (PSF) was larger than the one photon PSF (see fig.1). Reduced internal scattering when using infrared excitation may explain this impression. Stacks of closely spaced (200 nm) optical sections through the cell were acquired and maximum-likelihood 3D deconvolution applied to further enhance sectioning and contrast. From the reconstructed volume data set the three-dimensional organisation of the t-tubular system was refined by computing a topological skeleton using 3D skinning algorithms. It was possible to estimate the variation in t-tubule radii by assuming a circular cross-section and that the recorded signal was the convolution of the PSF and a cylinder.

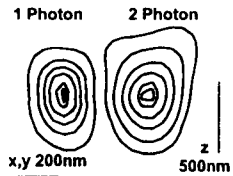

Fig. 1. Measured point spread functions for 1- and 2-photon excitation.

Supported by the Wellcome Trust

Th-Pos129

SPATIO-TEMPORAL EVOLUTION OF SPIRAL WAVE ACTIVITY.

((**N.Davidenko**, J. Beaumont, J.M. Davidenko, J. Jalife)) SUNY, Syracuse NY 13210

An ionic model was used to study the kinetics of activation during spiral wave activity and the formation and maintenance of the center of rotation (core). The simulations indicate that the core remains unexcited but excitable and, once formed, it conveys stability on the activity. We used a geometric procedure (the "ray tracing" method) to study the evolution of the wave front around the core. The method tracks the motion of multiple segments of the activation front. It shows that a spiral wave front can conserve its shape because individual segments of the activation front do not evolve along a circular orbit, as suggested by the circular motion of a rigid excitation pattern. Tracing the trajectories of such segments revealed the following: i) at ~ 1 cm from the core, the evolution of the wave front is rectilinear; ii) in a thin rim at ~ 1 core diameter from the center of rotation (separatrix), the direction of propagation and of the main flow of axial current change rapidly; iii) part of the activation front moves toward the core without reaching it; iv) the null-time derivative of potential crosses the isopotential lines at about 1 core diameter from the center of rotation and reaches it. We have shown also that the maximal curvature of the wave front is located between the separatrix and the junction between the activation front and repolarization tail. At the separatrix, curvature is relatively low. Based on the foregoing, we suggest the following new mechanism whereby spiral wave fronts evolve and the core forms: The change in the direction of propagation at the separatrix is equivalent to applying a local load on it. If the change in direction of propagation is sufficiently rapid, the load is large enough to abort the propagation in the direction where the impulse is curled. Inside that region, decremental propagation must occur.

Th-Pos130

RETROGRADE CONDUCTION IN A 2-D CARDIAC SCAR MODEL.

((**Peter Kohl**, Anthony Varghese and Denis Noble)) University Lab of Physiology, University of Oxford, OX1 3PT, United Kingdom.

Post-ischaemic cardiac scars are known to be an obstacle to impulse transmission and a potential source for ectopic beats. Electrical coupling between cardiomyocytes (C) is reduced in these regions, which furthermore contain high numbers of fibroblasts (F). Here, we examine in a 2-D model the impact of partial uncoupling of C's and local increase in F concentration on conduction of cardiac excitation.

A square lattice of ventricular C (128x128 cells, 0.6 μS C-C coupling) contains a centrally located oval 'scar' (90x60), where C-C coupling is reduced and each C is coupled to one F (by 40 nS). Individual C models are based on the biophysically detailed formulations of Noble *et al.* (1991); F are modelled as electrically passive cells described by a battery (resting membrane potential -20 mV), a membrane conductance (1 nS) and a capacitance (1.3 nF) (Kohl *et al.* 1996).

Straight impulse transmission into the scar is delayed and excitation travels down the surrounding healthy tissue. The distal end of the scar is reached by the wave of excitation with some delay and only when the majority of surrounding healthy C is already depolarized. Due to this increased electrical load at the distal edge, the scar is predominantly being invaded retrogradely, reversing the main direction of impulse transmission. This behaviour could explain uni-directional block of conduction in scars and constitute a novel re-entry mechanism.

Noble D, Noble SJ, Bett GCL *et al.*, *Ann NY Acad Sci* 1991/**639**:334-353.
Kohl P, Varghese A, Dekanski J *et al.*, *Exp Clin Cardiol*, 1996, in press.

Th-Pos131

CHAOTIC BEHAVIOR IN COUPLED CARDIAC CELLS OF ASYMMETRICAL SIZES.

((**M. Landau*** and P. Lorente†)) CNRS/INRIA* and U390 INSERM†, CHU Arnaud de Villeneuve, 34295 Montpellier, France. (Spon. by G. Vassort)

The initiation and propagation of the cardiac impulse depends on intrinsic properties of cells, geometrical arrangements, and intercellular coupling resistances. To address the issue of the interplay between these factors in a simple way, we have used a system, based on the van Capelle and Dürrer model, including a pacemaker and a non pacemaker cell linked by an ohmic coupling resistance. The influence of asymmetrical cell sizes and electrotonic load was investigated by using numerical simulations and continuation-bifurcation techniques. The loading of a small pacemaker cell by a large non pacemaker one (pacemaker : non pacemaker size ratio = 0.3) was expressed as a pronounced early repolarization in the pacemaker cell and a quite long latency for the impulse propagation. Using coupling resistance as the continuation parameter, three behavioral zones were detected from low to high coupling resistance values: a zone of total quiescence (0:0), a zone of effective entrainment (1:1), and a zone of total block (1:0 pattern). At the boundary between 1:1 and 1:0 patterns, for relatively high coupling resistance values, a cascade of period doubling bifurcations emerged, corresponding to discrete changes of propagation patterns leading into irregular dynamics. Another route to irregular dynamics was also observed in the parameter space. The high sensitivity of the detected irregular dynamics to initial conditions and the positive value of the maximum Lyapunov exponent allowed us to identify these dynamics as being chaotic. Since neither intermediate block patterns nor irregular dynamics were observed with larger size ratios, we suggest that the interplay between resting membrane conductance of the non pacemaker cell and intercellular coupling may bring about these rhythmic disturbances.

Th-Pos132

STIMULATION OF L-TYPE CALCIUM CURRENT BY cGMP IN NEWBORN RABBIT VENTRICULAR CELLS IS NOT MEDIATED BY cGMP-INHIBITED PHOSPHODIESTERASES.

((**Takao Namiki**, Rajiv Kumar and Ronald W. Joyner)) Department of Pediatrics, Emory University, Atlanta, GA, 30322)

We studied cGMP mediated regulation of whole cell L-type Ca^{2+} current (I_{Ca}, pA/pF) in isolated newborn (NB, 1-4 day old) heart cells. I_{Ca} was elicited by a pulse to +15 mV from a holding potential of -40 mV. Basal I_{Ca} was increased by intracellular perfusion of 8BrcGMP or 8CPT-cGMP (which stimulate cGMP dependent protein kinase (PKG)) and inhibited by methylene blue and LY-83583 (which decrease cGMP levels by inhibiting G-cyclase). The effect of 8CPT-cGMP was not blocked by cAMP dependent protein kinase inhibitor (PKI). We also used GSNO, a relatively stable NO donor, to increase cGMP levels. Extracellular application of GSNO (10 μM) resulted in an increase of basal I_{Ca} by about 50% (basal I_{Ca} of 2.52±0.29 pA/pF increased to 3.76±0.32 pA/pF by GSNO, $p<0.05$, n=5). PKG inhibitor KT-5823 (0.2 μM) decreased basal I_{Ca} by 40 % (from 2.36±0.27 pA/pF to 1.3±0.17 pA/pF, $p<0.05$, n=5). To investigate possible involvement of cGMP dependent phosphodiesterases (PDEs) in the stimulatory effect of GSNO, we used 50 μM IBMX, which increased basal I_{Ca} by 49±7.2 % (from 2.83±0.23 to 4.2±0.41 pA/pF, $p<0.05$, n=4). GSNO produced an additive increase in I_{Ca} in presence of IBMX and I_{Ca} further increased by 10 μM GSNO by 66 % (from 2.83±0.41 to 6.05±0.66 pA/F, $p<0.05$, n=4) to an overall increase of 115±17 % over control. Isoproterenol (0.1 μM) produced only a 50-70 % increase in basal I_{Ca}, and this effect was enhanced by the presence of 30 μM cGMP or 8BrcGMP. Similarly, GSNO (10 μM) increased I_{Ca} which was already stimulated by 0.1 μM isoproterenol. This shows that the stimulatory effect of cGMP is not mediated by inhibition of cGMP dependent PDEs and that the effect of cGMP is not antagonistic to cAMP on I_{Ca} in NB cells. We conclude that in NB rabbit ventricular cells, PKG plays a crucial role in the maintenance of basal I_{Ca} and the stimulatory effects of cGMP on I_{Ca} are likely to be mediated by PKG.

Th-Pos133

CARDIAC-SPECIFIC OVEREXPRESSION OF ANNEXIN VI ALTERS Ca^{2+} CHANNEL INACTIVATION IN TRANSGENIC MICE. ((*H. Sako, *H. Masaki, +A-M Gunteski-Hamblin,+J. R. Dedman and A. Yatani)) *Dep. of Pharmacol. & Cell Biophysc. and +Dep. of Mol. & Cellular Physiology, Univ. of Cincinnati, Cincinnati, OH 45267.

Annexin VI is a member of a family of Ca^{2+}-dependent, phospholipid-binding proteins that is expressed in the heart. Measurements of the Ca^{2+} transient and shortening of ventricular myocytes from the hearts of transgenic mice, overexpressing annexin VI, have demonstrated significantly reduced contractility and Ca^{2+} transient following depolarization compared to control wild-type (WT) myocytes. These results indicate that annexin VI serves as a regulator of intracellular Ca^{2+}-homeostasis. Cardiac contraction is strongly influenced by both the trigger Ca^{2+} influx via L-type Ca^{2+} channels (CaCh) and SR Ca^{2+} content. However, it was unclear which Ca^{2+}-handling pathways are affected by annexin VI. To test whether annexin VI overexpression was associated with alterations of CaCh function, which may contribute to change in contractile properties, we examined CaCh currents (I_{Ca}) from mouse ventricular myocytes. Basic channel properties including channel density, gating, and sensitivities to CaCh modulator drugs were similar in WT and annexin VI overexpressing myocytes. I_{Ca} from both WT and transgenic cells exhibited two (fast and slow) components of inactivation kinetics, but the faster component was significantly slower in transgenic cells compared to WT. This difference was abolished following depletion of SR Ca^{2+} stores by the application of caffeine or ryanodine. In contrast, the inactivation in Ba^{2+} external solution could be fitted by a single exponential similar to the slower component in Ca^{2+}, and this was not altered in transgenic cells. These results suggest that annexin VI overexpression alters CaCh function by affecting the SR function which controls a Ca^{2+}-mediated inactivation mechanism of CaCh.

Th-Pos134

ANTAGONISM BY EXTRACELLULAR ATP OF L-TYPE CALCIUM CHANNEL CURRENTS PRE-STIMULATED WITH ISOPRENALINE IN GUINEA-PIG SINGLE SINOATRIAL NODAL CELLS. ((Ai-dong Qi and Yiu Wa Kwan)), Department of Pharmacology, Faculty of Medicine, The Chinese University of Hong Kong, Hong Kong.

Our previous studies have shown that extracellular ATP ($[ATP]_o$) caused concentration- and voltage- dependent inhibition of basal L-type Ca^{2+} channel currents in guinea-pig single sinoatrial nodal cells. In this study, we investigated the effect of $[ATP]_o$ on L-type Ca^{2+} channel currents pre-stimulated with isoprenaline, using the whole cell patch-clamp technique (10 mM Ba^{2+} as the charge carrier, 20-22 C) (holding potential = -40 mV, test-pulse potential = +20mV stimulated at 0.2 Hz). 100 nM isoprenaline caused a 5-fold increase of the L-type Ca^{2+} channel currents and application of 100 μM $[ATP]_o$ produced 74.8 ± 6.2 % inhibition of the Ca^{2+} current amplitude. The % inhibition caused by $[ATP]_o$ on the pre-stimulated Ca^{2+} currents was significantly different from the effect of $[ATP]_o$ on basal Ca^{2+} current amplitude (33.4 ± 2.6%). Application of $[ATP]_o$ (0.1 - 100 μM) caused a concentration-dependent inhibition of isoprenaline pre-stimulated Ca^{2+} channel currents. However, application of $[ATP]_o$ with concentrations < 1 μM had no effect on the basal Ca^{2+} current amplitude. Intracellularly applied cAMP (10 μM) also increased the basal Ca^{2+} channel currents and 100 μM $[ATP]_o$ also caused a greater % inhibition of Ca^{2+} current amplitude (42.4 ± 2.8 %). These results suggested that $[ATP]_o$ caused a greater % inhibition on the isoprenaline pre-stimulated than basal Ca^{2+} channel currents and suggested that $[ATP]_o$ plays an important role in the regulation of heart beat by inhibiting the catecholamine stimulatory effect.

Th-Pos135

INVOLVEMENT OF PROTEIN KINASE C IN THE INHIBITION BY EXTRACELLULAR ATP OF L-TYPE CALCIUM CHANNEL CURRENTS IN GUINEA-PIG SINGLE SINOATRIAL NODAL CELL. ((Ai-dong Qi and Yiu Wa Kwan)), Department of Pharmacology, Faculty of Medicine, The Chinese University of Hong Kong, Hong Kong.

Previously, we have shown that application of extracellular ATP ($[ATP]_o$) inhibited the L-type Ca^{2+} channel currents of guinea-pig single sinoatrial nodal cells. In this study, we investigated the role(s) of protein kinase C in the $[ATP]_o$-mediated inhibition of L-type Ca^{2+} channel current amplitude (holding potential = -40 mV, test-pulse potential = +20mV stimulated at 0.2 Hz), using the whole cell patch-clamp technique (20 mM Ba^{2+} as the charge carrier, temperature = 20-22 ℃). 100 μM $[ATP]_o$ caused a 33.4 ± 2.6 % inhibition of Ca^{2+} channel currents. Internal dialysis of the cell by adding the protein kinase C inhibitors (staurosporin, 70nM; calphostin C, 500nM) inside the patch pipette, for 5 min, abolished the $[ATP]_o$-induced inhibition of L-type Ca^{2+} channel currents. Staurosporin (70 nM) and calphostin C (500 nM) abolished the protein kinase C activator TPA (100 nM)-mediated effect on Ca^{2+} channel currents. However, the protein kinase G inhibitors KT 5823 (500 nM), GTPγS (250 μM) GDPβS (250 μM) and activated PTX (4 μg/ml) had no effect on the $[ATP]_o$-mediated inhibition of L-type Ca^{2+} channel currents. We concluded that the inhibitory effect of $[ATP]_o$ on guinea-pig sinoatrial node Ca^{2+} channel currents involved the activation of protein kinase C and is independent of G proteins.

Th-Pos136

DISTINCTIVE EFFECTS OF FENDILINE ON L-TYPE CALCIUM CHANNELS IN VENTRICULAR MYOCYTES FROM RAT HEARTS.
((H. Nawrath and J. Rupp)) Department of Pharmacology, University of Mainz, D-55101 Mainz, Federal Republic of Germany.

Fendiline blocks cardiac L-type calcium channels in rat ventricular myocytes at about hundred times higher concentrations than nifedipine. Surprisingly, the increase in the calcium current (I_{Ca}) by Bay K 8644 is nearly unaffected by nifedipine but almost completely abolished by fendiline. How can this disparity be explained? The effect of fendiline on I_{Ca} in single myocytes was characterized by an acceleration of the inactivation of I_{Ca}. The analysis of fractional current changes revealed a development of block (τ = 80ms) during depolarizing voltage clamp pulses to 10 mV with Ba^{2+} as the charge carrier. This suggests that fendiline may bind preferably to open channels, in contrast to other calcium channel blockers which preferentially bind to the inactivated state of the channel. In single channel experiments (with Ba^{2+} as charge carrier, in the presence of Bay K 8644 1μM) fendiline 10 μM mainly reduced the availability and open probability of the calcium channel, whereas open and shut times were only marginally affected by the drug. In conclusion, fendiline seems to require open calcium channels to become effective, leading to changes in slow gating and a reduction of the mean calcium current. Therefore, the effects of fendiline are enhanced when calcium channels are being kept open by Bay K 8644. Reversely, the effects of calcium antagonists which require, for effectiveness, the inactivated channel state, are reduced in the presence of Bay K 8644.

Th-Pos137

EFFECTS OF THE VENOM OF THE CHILLI ROSE TARANTULA *GRAMMOSTOLA SPATULATA* ON THE CA^{2+} HOMEOSTASIS OF SINGLE GUINEA PIG VENTRICULAR MYOCYTES (Spon. by J.A. Argibay)
((C. Pascarel, O. Cazorla, J-Y Le Guennec, C. Orchard* & E. White*)) Laboratoire de Physiologie des Cellules Cardiaques et Vasculaires, CNRS EP21, Faculté des Sciences 37200 Tours, France. *Department of Physiology, University of Leeds, Leeds LS2 9NQ, U.K.

A major challenge in the study of stretch-activated events is the discovery of a specific strech-activated channel (SAC) blocker. The venom of *G. spatulata* has recently been shown to inhibit SACs in GH_3 cells without blocking Ca^{2+} channels (Chen et al, *Am. J. Physiol*, 270 : C1790-1798). We have investigated the effects of this on the Ca^{2+} homeostasis of single guinea pig ventricular myocytes, by observing its effects upon intracellular Ca^{2+} transients (measured with Indo-1) and L-type Ca^{2+} currents (I_{Ca}). The venom (1/1000), significantly reduced the Ca^{2+} transient by 64 ± 11 % (P>0.01, student t-test, n = 7 cells stimulated at 1 Hz). To test if this reduction in the Ca^{2+} transient might be explained by a blockade of I_{Ca}, cells were whole cell voltage clamped to evoke I_{Ca}. In these experiments intracellular Ca^{2+} was buffered with 10 mM EGTA and K^+ and Na^+ currents were inhibited by ion removal and pharmacological inhibition. The holding membrane potential was -80 mV which was stepped to test potentials between -70 and +70 mV for 300 ms at 0.125 Hz. We observed a dose-dependent inhibition of I_{Ca} with an EC_{50} of 1/10000 (n = 22 cells). Our data suggest that the venom of G. *spatulata*, like other SAC blockers, inhibits I_{Ca} in adult cardiac myocytes.
Supported by the Wellcome Trust and the University of Tours.

Th-Pos138

OVEREXPRESSION OF CARDIAC CALSEQUESTRIN IN TRANSGENIC MYOCYTES ALTERS THE cAMP SENSITIVITY OF Ca^{2+} CURRENT. ((J. Zhang, Y.J. Suzuki, L.R. Jones and M. Morad)) Dept. of Pharmacology, Georgetown Univ. Medical Center, Washington DC 20007. (Spon. by G.D. Ford)

Cardiac calsequestrin (CSQ) is localized to junctional SR and buffers the intra-SR Ca^{2+}. The present study examines the level of expression of I_{Ca} and its regulation in transgenic mice overexpressing CSQ. Transgenic myocytes show an 18-fold increase in cardiac CSQ content using Western blot analysis. Freshly isolated ventricular myocytes from CSQ transgenic mice had no clear striation and had larger cell capacitance compared to their non-transgenic littermates (230±36.65pF, n=9 vs 167.6±62pF, n=8). In whole cell-clamped CSQ transgenic myocytes dialyzed with 110mM Cs^+, 20mM TEA^+, 5mM MgATP, 14mM EGTA and 10mM HEPES, I_{Ca} was activated by a depolarizing pulse from -50 to 0mV at 5sec interval in Na^+ and K^+ free external solutions. I_{Ca} density in cell dialyzed with 200μM cAMP was 10.5±4.1pA/pF (n=9) in CSQ transgenic myocytes, and 18.8±7pA/pF (n=8) in control myocytes, suggesting that in CSQ myocytes I_{Ca} was either down-expressed or not fully phosphorylated. Surprisingly, 5 μM of isoproterenol (ISO) increased I_{Ca} to 16.3±6.2pA/pF (n=9) in CSQ transgenic myocytes and shifted its voltage dependence by 5-10mV, but as expected, had no effect on control myocytes (18.1±7pA/pF, n=7). Note that ISO increased the current density of the transgenic myocytes to values similar to those of control myocytes. Even though ISO markedly increased I_{Ca}, Ca^{2+}-transients increased only slightly in the transgenic myocytes. Membrane-permeable cAMP analogue (8-bromo-cAMP, 500μM) failed to have any effect on I_{Ca} of the transgenic or control myocytes dialyzed with 200μM cAMP. Our results show that in transgenic myocytes overexpressing CSQ, even though the sensitivity of L-type Ca^{2+} channel to cAMP is significantly suppressed, ISO continues to enhance I_{Ca}, suggesting activation of an alternative β-agonist signaling pathway not mediated by cAMP. (Supported by NIH HL16152)

Th-Pos139

Recovery of Inactivated Sodium and Calcium Channels by Strong Depolarizations in Rat Ventricular Myocytes - An Example for Gating Mode Shifts in Whole Cell Recordings? ((**B.C. Knollmann**, M. MacCormack, M. Morad)) Institute for Cardiovascular Sciences and Department of Pharmacology, Georgetown University Medical Center, Washington, DC 20007. (Spon. by W.B. Weglicki)

Sodium and calcium channels are responsible for almost all of the inward membrane current during the cardiac action potential. Once inactivated, they require repolarization to negative membrane potentials for recovery. In this report we examined whether these inward currents can be recovered by strong depolarizations to positive membrane potentials without repolarization to resting potential. In whole cell patch-clamped rat or mouse ventricular myocytes dialyzed with 14mM EGTA, 2mM BAPTA, 20mM TEA, 100mM Cs and 0.2mM cAMP, both sodium and calcium channels were inactivated by a 400 ms depolarization step to zero mV from a holding potential of -60mV. In potassium free external Tyrode's solution containing 137mM Na^+, 2mM Ca^{2+} and 0.2mM Ba^{2+}, very little inward current remained at the end of the inactivation step (-0.30±0.26 pA/pF, n=15). Progressively longer depolarizations at +80mV, following the 400ms inactivation step to zero mV, produced progressively larger inward currents upon returning the membrane to zero mV (e.g. -6.1±2.7 pA/pF after 600ms at +80mV). The magnitude of reactivated current at zero mV increased with more positive conditioning potentials. Independent of duration of the conditioning pulse, the reactivated current decayed monoexponentially with a time constant of 46±12 ms. 10μM Nifedipine, 100μM Cadmium or 1μM TTX each reduced the current between 30% to 70%. When Na^+ was replaced with TEA in external solutions, the reactivated current diminished by 60% without significant changes in its kinetics, and was completely abolished by Nifedipine. Similar results were obtained when Ba^{2+} was the charge carrier through the Ca^{2+}-channel. These findings are consistent with the hypothesis, that strong membrane depolarizations can recover inactivated sodium and calcium channels. The reactivated current may represent a voltage-dependent switch to a different gating mode. Supported by NIH HL16152

Th-Pos140

PROPAFENONE BLOCKS L-TYPE CALCIUM CURRENT IN ATRIOVENTRICULAR NODAL CELLS ISOLATED FROM THE RABBIT HEART. ((**J.S. Mitcheson** and J.C.Hancox)) Department of Physiology, University of Bristol, Bristol, BS8 1TD, United Kingdom.

The class 1 antiarrhythmic drug propafenone is effective in treating a variety of cardiac arrhythmias, including those involving the atrioventricular node (AVN). We have investigated the effects of propafenone on membrane currents in single rabbit AVN cells. With a standard K-based pipette solution, 5μM propafenone reduced L-type calcium current ($I_{Ca,L}$) amplitude and also blocked the delayed rectifier K current (I_K). Using a Cs-based pipette solution to record $I_{Ca,L}$ selectively, propafenone concentrations between 50nM and 0.5mM reduced current amplitude in a dose dependent fashion (IC_{50} 1.7μM) without significantly affecting the voltage dependence of activation. However, in the presence of propafenone, the voltage dependence of inactivation of $I_{Ca,L}$ was shifted in the hyperpolarising direction and the recovery of $I_{Ca,L}$ from inactivation was slowed by propafenone. The $I_{Ca,L}$ blocking properties of propafenone may mediate some of the antiarrhythmic properties of this agent, particularly in regions of the heart such as the AVN in which $I_{Ca,L}$ contributes significantly to the action potential upstroke.
Supported by the British Heart Foundation and Wellcome Trust.

Th-Pos141

SLOW INWARD TAIL CURRENTS OF FROG CARDIAC MYOCYTES STUDIED WITH PERFORATED PATCH CLAMP TECHNIQUE.
((**T.D. Parsons** & H.C. Hartzell)) University of Pennsylvania & Emory University

Regulation of intracellular calcium ($[Ca]_i$) by contractile cells such cardiac myocytes is quintessential. Both transmembrane and cytoplasmic mechanisms interplay in the control of $[Ca]_i$. Calcium currents of the frog ventricular cardiomyocytes were studied with perforated patch clamp technique in an effort to minimize cytoplasmic disturbances and maintain the physiological balance between these different mechanisms. Cells exhibited inward calcium currents (I_{Ca}) following depolarization that were essentially identical to I_{Ca} previously reported using whole cell recording (Fischmeister & Hartzell, 1986). However upon repolarization to a holding potential of -80 mV from a test potential of 0 mV or greater, a slowly decaying inward current was activated that was not observed in the whole cell patch clamp configuration. This current appeared to be generated by the Na-Ca exchanger since it did not reverse near the K-equilibrium, was not blocked by K-channel blockers or TTX and was relatively insensitive to DHP Ca channel blockers, but was inhibited by external Ni or removal of external Ca. The magnitude of the slow tail current increased as the duration and amplitude of the depolarizing test potential increased, suggesting that calcium was able to enter the cell via the exchanger working in the reverse mode. Potentiation of the tail current, however, did not occur over a physiological range of stimuli expected to be achieved during an action potential. Thus, we conclude that the primary role of the Na-Ca exchanger in amphibian cardiac myocytes is to extrude Ca entering via voltage-gated Ca-channels.
Supported by NIH grant HL21195 to HCH.

Th-Pos142

EFFECT OF PROPOFOL ON INTRACELLULAR Ca^{2+} TRANSIENTS IN SINGLE RAT VENTRICULAR MYOCYTES ((**I.A. Kudryashova** and T.J.J. Blanck)) Department of Anesthesiology, The Hospital for Special Surgery, New York, 10021.

The mechanisms of propofol-induced negative inotropy of the heart are still poorly understood. Because of the importance of intracellular Ca^{2+} mobilization in cardiac contraction, sarcolemmal Ca^{2+} influx and sarcoplasmic reticulum Ca^{2+} load can be potential sites at which propofol exerts its cardiac depressant effect. Intracellular $[Ca^{2+}]_i$ transients, elicited by electrical stimulation, by 10 mM caffeine, or by KCl-induced membrane depolarization, were monitored in single rat ventricular myocytes by the fluoresecent Ca^{2+} indicators, indo-1 or fura-2, respectively, with a fluorescent microscope/photometer. When the cell is stimulated at 0.2 Hz after rest, there was a negative staircase, indo-1 fluorescence (IF) transient is large in beat 1 and than decreases in magnitude with beat number until a steady state is reached. After 3 min. of rest and exposure to propofol (100 μM), the electrically stimulated indo-1 transients are smaller in both beats 1 and 10 by 32% and 20% of control, respectively. The peak of caffeine-induced Ca^{2+} release in resting myocytes was decreased by 35.9%, 45.3%, 59.2% after 5 min. exposure to propofol at 50, 70, 100 μM respectively ($P< 0.05$). Propofol at 30 μM did not effect the SR Ca^{2+} content during the application of caffeine. The acute addition of propofol in a concentration range 30-100 μM to perfusion solution caused no transient change in resting $[Ca^{2+}]_i$. On the other hand, we found that the peak of fura-2 fluorescence transient due to 30 mM KCl activated membrane depolarization was reduced upon exposure to propofol at 50, 70, 100 μM by 16.3%, 21%, 37.2%, respectively. We suggest that the cardiac effect of propofol, the intravenous anesthetic, related to modification of SR Ca^{2+} load and sarcolemmal L-type Ca^{2+} influx.

Th-Pos143

THE EFFECT OF TETRACAINE ON ELECTRICALLY STIMULATED CONTRACTIONS IN RAT VENTRICULAR MYOCYTES ((C.L. Overend, S.C. O'Neill & D.A. Eisner)) Vet. Preclinical Sciences, University of Liverpool, P.O. Box 147, Liverpool L69 3BX. U.K.

We have previously shown that the local anaesthetic tetracaine inhibits spontaneous oscillations of rat ventricular myocytes in a manner consistent with an increase of the sarcoplasmic reticulum (s.r.) calcium content. Here we report the effects of tetracaine on electrically stimulated calcium release from the s.r. In field stimulated (0.3 Hz) rat ventricular myocytes, application of 100μM tetracaine produces a transient decrease in contraction, which over a period of 1-2 minutes recovers to the control level. On removing tetracaine there is a large, transient increase of contraction which recovers to the control level over 30 sec.
A likely explanation is that the effects of tetracaine are due to decreased calcium-induced calcium release (CICR). However tetracaine may also be acting on sodium (I_{Na}) and/or calcium (I_{Ca}) transmembrane currents. We have tested this by measuring the effects of tetracaine on contraction and I_{Ca}. At a holding potential of -40 mV, stepping to 0 mV, tetracaine has similar effects on contraction as in field stimulated cells. Tetracaine also reduces the peak I_{Ca}. This reduction is small and although it will contribute to the early reduction in contraction amplitude in tetracaine it is maintained throughout tetracaine application and so plays no role in the subsequent recovery of contraction. Nor can changes in I_{Ca} explain the transient increase of contraction post-tetracaine as there is no transient increase of I_{Ca} only a return to control amplitude. The contribution of changes in I_{Ca} to the early tetracaine-induced reduction of contraction must be small as depolarising to -10mV from -40mV reduces I_{Ca} to 50% of its control level but reduces contraction by only about 20%.
In conclusion we find that the effects of tetracaine are consistent with its major effect being on s.r. calcium release. By inhibiting s.r. calcium release contraction is reduced. The inhibition of release allows greater s.r. accumulation of calcium, allowing contraction to recover. This illustrates how modulation of CICR can have only a transient effect on contraction.

Th-Pos144

PARADOXICAL SENSITIVITY OF FELINE VENTRICULAR I_{TO} TO FLECAINIDE DESPITE AN APPARENT LACK OF SHAL-RELATED TRANSCRIPTS BUT WITH PARALLEL CHANGES IN I_{TO} AND KV1.4 EXPRESSION
((Christopher E. Hansen, Robert S. Decker and Robert E. Ten Eick))
Depts. of MPBC & CMB, Northwestern University, Chicago, IL 60611

The density of the transient outward current (I_{to}) is affected by cardiac hypertrophy, failure, and ischemia, conditions associated with an increased risk of sudden-death. Both increases and decreases have been reported. These findings suggest that an understanding of the regulation of I_{to} expression might be important for an improved understanding of the mechanism(s) of sudden death associated with these conditions. We have previously reported that, 1) mRNA for Kv1.4 decreased in feline ventricular myocytes maintained in primary culture coincident with the loss of I_{to} density, 2) mRNA for Kv1.2 did not significantly decrease in primary culture, and 3) mRNA for Irk1 decreased about 40% coincident with the decrease in Ik1 density. Since that report, we have determined that feline I_{to} is sensitive to flecainide (K_D= 19μM), a compound which has been shown to have selective sensitivity to Shal-related proteins (EC_{50}=10μM) when expressed in vitro. Despite this pharmacological data suggesting a role for Shal in feline ventricular I_{to}, we have been unable to detect any Shal-related transcripts (Kv4.2 or Kv4.3) in feline ventricular tissue using RT-PCR. Our results suggest at least three possibilities: 1) feline I_{to} expression is related to Kv1.4 expression and the sensitivity of Kv1.4 to flecainide is increased when expressed in vivo; 2) that feline I_{to} expression is due to the expression of Shal-related transcripts as yet undetected and that the coincident loss of Kv1.4 and I_{to} in cell culture are epiphenomena; 3) that Kv1.4 and Kv4.3 as heteromultimers and/or other subunits are involved in the expression of I_{to} and that the loss of either might explain the loss of I_{to} in culture.

Th-Pos145

4 AMINOPYRIDINE AND E4031 SENSITIVE CURRENTS IN NORMAL PURKINJE MYOCYTES OF THE CANINE HEART. ((J.M.B.Pinto, S.Chen. and P.A. Boyden)) Dept of Pharmacology, Columbia University, NY, NY 10032. (Spon. by P.Boyden)

We have previously shown that both transient and sustained 4aminopyridine (4AP) sensitive currents exist in normal Purkinje myocytes (PCs). A portion of the sustained 4AP sensitive current is rate independent and does not inactivate with prepulse potential (V_p).To investigate outward currents responsible for repolarization at test voltages <-50mV, PCs were studied under normal clamp conditions ($EGTA_i$=10mM, K^+-containing internal solution) in the absence and presence of the Class III methanesulfonanilide, E4031 (5uM). E4031 was chosen since it specifically blocks rapidly activating, strongly rectifying I_{Kr}, a component of I_K in canine ventricular myocytes. For E4031 sensitive currents, activation threshold is -30mV and noninactivating currents increase with step depolarization (V_h=-40mV to V_t=+50mV). E4031 sensitive currents show time dependence at positive steps (between V_t=-25 and+40mV) that depend on conditioning potential (V_c=-90 to +20mV) and duration of V_c (250ms and 2sec). At depolarized V_c, E4031 currents are sustained (I_{sus}) showing no time dependence. Recovery from block is slow at depolarized potentials. Furthermore, there is no rectification of E4031 sensitive currents at the most positive steps. The average density at +40mV is 2.9+/-0.6pA/pF, n=13. E-4031 sensitive I_{sus} is also blocked by dofetilide(100nM) and 4AP (2mM), and still remains in 0mM K_o. Thus, in PCs, E4031 and 4AP block a large I_{sus} that differs from E4031 sensitive I_{Kr} of the ventricular myocyte. Furthermore, while I_{sus} has a phenotype similar to human atrial I_{Kur}, it shows E4031 sensitivity in PCs. E4031 effects on this PC current may underlie its unwanted arrhythmogenic effects.

Th-Pos146

ACIDOSIS INCREASES TRANSIENT OUTWARD CURRENT (I_{to}) IN RAT VENTRICULAR MYOCYTES. ((J.T. Hulme, M.R. Boyett and C.H. Orchard)) Dept. of Physiology, University of Leeds, LS2 9NQ, U.K.

The effects of acidosis (pH_o 6.5) on I_{to} have been investigated in rat ventricular myocytes. I_{to} was monitored using the perforated patch clamp technique, in the presence of 10 μM nifedipine to abolish the L-type Ca^{2+} current. At control pH_o (7.4), a large I_{to} was activated from a holding potential of -80 mV (I_{to} at +60 mV was 1.79 ± 0.35 nA; mean ± SEM, n=5), whereas at a holding potential of -40 mV, little I_{to} was detected. After 5 min exposure to acidosis, I_{to} activated from -80 mV was not significantly different from that at control pH_o, but that activated from -40 mV was markedly increased (to 1.3 ± 0.16 nA at +60 mV, n=5). Acidosis also caused a +8.5 mV shift in the voltage dependence of inactivation of I_{to}, which could explain the observed effects of acidosis on I_{to}. To investigate the possible role of intracellular $[Ca^{2+}]$ in I_{to} during acidosis, the effect of buffering cytoplasmic Ca^{2+} was investigated. The amplitude of I_{to} evoked from a holding potential of -40 mV in the presence of acidosis was not altered by 10 min application of 5 μM BAPTA-AM (n=5). This suggests that an increase in cytoplasmic $[Ca^{2+}]$ does not underlie the increase in the amplitude of I_{to} that occurs during acidosis. However the time course of inactivation of I_{to} was increased and the current remaining at the end of the voltage clamp pulse was reduced after application of BAPTA-AM. The BAPTA-sensitive current had a time and voltage dependence similar to those reported for the sustained component of I_{to} (J. Gen. Physiol., 97, 973, 1991). *Supported by the British Heart Foundation and The University of Leeds.*

Th-Pos147

PHARMACOLOGICAL CHARACTERIZATION OF FAST INWARD SODIUM CURRENTS IN RABBIT SINO-ATRIAL NODE AND ATRIAL MYOCYTES. ((M. Baruscotti and R.B. Robinson)) Department of Pharmacology, Columbia University, New York, NY 10032

We recently demonstrated the presence of a TTX-sensitive inward sodium current (I_{Na}) in single myocytes isolated from the newborn but not adult rabbit sino-atrial node (SAN). One surprising finding was the effectiveness of TTX in this cardiac tissue, with 3 μM causing 95 % block. We therefore investigated the pharmacologic profile of I_{Na} in the newborn SAN, and compared it to that from other regions and ages of the rabbit heart. The EC_{50} of TTX on the newborn SAN I_{Na} was 26±5 nM (n=6-9), markedly lower than for typical cardiac tissues, and in fact similar to values reported in nerve cells. However, the SAN also was sensitive to Cd^{2+}, a relatively selective blocker of the cardiac I_{Na}, with 200 μM causing 53±7 % block (n=5). Thus, the newborn SAN I_{Na} exhibits an unusual pharmacologic profile, being highly sensitive to both TTX and Cd^{2+}. Unexpectedly, newborn rabbit atrial myocytes show a similar profile (TTX EC_{50}=64±7 nM, n=3-7; 59±12 % block by 200 μM Cd^{2+}, n=5). When adult tissues were examined for TTX sensitivity it was found that adult atrium also had high TTX sensitivity (10 nM caused 41±4 % block; 300 nM caused 74±4 % block; n=6). However, adult ventricular myocytes showed the typical myocardial low TTX sensitivity (10 nM caused 3±1 % block; 300 nM caused 42±10 % block; n=4). Therefore, the newborn rabbit expresses Na currents with novel pharmacologic sensitivity in both SAN and atrial, but not ventricular, myocytes. The expression in the SAN is lost developmentally, but persists in atrial tissue. It remains to be determined if this represents differential regulation of the same channel isoform in the two tissues, or differential expression of distinct but pharmacologically similar isoforms.

Th-Pos148

SINGLE HERG K^+ CHANNELS EXPRESSED IN *XENOPUS* OOCYTES. ((A. Zou, M E. Curran, M.T. Keating and M.C. Sanguinetti)) Departments of Medicine and Human Genetics University of Utah, Salt Lake City, UT 84132

HERG is a K^+ channel with properties similar to I_{Kr}, a delayed rectifier K^+ current important for repolarization of human cardiac myocytes. We characterized the single channel properties of HERG expressed in *Xenopus* oocytes. Currents were measured in cell-attached patches with an extracellular $[K^+]$ of 120 mM. The single HERG channel conductance determined at test potentials between -50 and -110 mV was 12.1 ± 0.6 pS. At positive test potentials (+40 to +80 mV), the probability of channel opening was low and the slope conductance was 5.1 ± 0.6 pS. The mean channel open times at -90 mV were 2.9 ± 0.5 and 11.8 ± 1.0 ms, and the mean channel closed times were 0.54 ± 0.02 and 14.5 ± 5.3 ms. Single HERG channels were blocked by MK-499, a class III antiarrhythmic agent that blocks I_{Kr} in cardiac myocytes. The development of block was more rapid in inside-out patches than in cell-attached patches or in whole-cell recordings, indicating that block occurs from the cytoplasmic side of the membrane. The single channel properties of HERG are similar to I_{Kr} channels of isolated cardiac myocytes, providing further evidence that HERG proteins coassemble to form I_{Kr} channels.

Th-Pos149

INTRAMEMBRANE CHARGE MOVEMENTS (ICM) IN HEART CELLS ARE MORE COMPLEX THAN PREVIOUSLY THOUGHT: PROPERTIES AND PHARMACOLOGY. **((C.O. Malécot, P. Bolaños* and J.A. Argibay)). Lab. Physiologie des Cellules Cardiaques & Vasculaires, CNRS EP 21, Fac. Sciences, F-37200 Tours, France and *CBB.Biofisica del Musculo.IVIC, Caracas, Venezuela.**

ICM properties were re-investigated in guinea-pig ventricular myocytes (22-25°C) with the whole-cell patch-clamp technique. Ionic currents were blocked with (mM): TEACl 140, $CaCl_2$ 1, $MgCl_2$ 2, $CdCl_2$ 2, $GdCl_3$ 0.1, TTX 0.001, Hepes 10, glucose 11, pH 7.3. The pipette contained (mM): TEACl 30, CsCl 110, ATP-Mg 5, EGTA 10, Hepes 10, pH 7.3. From a holding potential (HP) of -110mV, the mean (n=51) maximum Q_{ON} component (cpnt) of ICM was 12.9nC/μF at ≈ +40mV. Its voltage (V_m) dependence was described by two Boltzman functions (BF) with half-activation potential ($V_{1/2}$) of -26 and -1.3 mV (cpnts 1 and 2). Following a 100 ms prepulse (PP) to -50 mV to inactivate ICM originating from Na channels, the mean maximum Q_{ON} in the same cells was 7.8nC/μF. However, two BF were still required to describe its V_m dependence ($V_{1/2}$ of -27 and 2.7mV, P<0.001; cpnts 1' and 2'). The 100ms PP-sensitive ICM consisted of two distinct cpnts (1" and 2", $V_{1/2}$ of -27 and -14mV, P<0.001). Immobilization of ICM (two pulses protocol with a 1ms return to the HP of -100mV, n=16) was complete between +10 and +20mV and two BF were required to describe the V_m dependence ($V_{1/2}$ of -73 and -21.6mV). However, cpnt 2 inactivated only for V_m above -50mV. Studies of I_{Na}, I_{Ca} and of ICM using lidocaine, tetracaine, D600 and nifedipine strongly suggest that (i) from HP=-110mV, cpnt 1 originates from Na and from Ca channels and cpnt 2 presumably from Ca channels; (ii) cpnts 1' and 2' originate from Na and Ca channels; (iii) PP-sensitive cpnts 1" and 2" originate from Na channels; and (iv) the 2 inactivating cpnts originate from Na ($V_{1/2}$ of -73mV) and from Ca channels ($V_{1/2}$ of -21.6mV). Thus, Na like Ca channels might present 2 cpnts of ICM activation and 1 cpnt of ICM inactivation.

Th-Pos150

A POSSIBLE ROLE OF TYROSINE KINASES IN THE REGULATION OF I_f IN RABBIT SA NODE MYOCYTES. ((J.Y. Wu and I.S. Cohen)) Physiology & Biophysics, HSC, Stony Brook, NY 11794-8661.

The hyperpolarization activated current i_f is modulated by the autonomic nervous system. In part this modulation is mediated by direct cAMP gating (DiFrancesco & Tortora, Nature. 351,145-147, 1991) and in part by PKA indirect phosphorylation (Chang *et al.* J. Physiol. 440, 367-384. 1991). Studies of kinase and phosphatase inhibition in SA node and Purkinje fibers and myocytes suggest an important role for phosphorylation in regulating i_f even in the absence of autonomic stimulation. Recently, tyrosine phosphorylation has been reported to regulate ion channel in several systems (Siegelbaum. Current Biology 4(3): 242-245, 1994). We therefore undertook our study on rabbit SA node myocytes to examine whether tyrosine kinases play a role in i_f regulation.
Genistein (50 μM), one of the broad spectrum tyrosine kinase inhibitors, reversibly reduced i_f in all 8 SA node myocytes tested. The reduction of i_f at -75 mV was 23.7%±1.5% (Mean±SEM). In addition to genistein, 35 μM herbimycin A, another tyrosine kinase inhibitor, reversibly decreased i_f by an average of 32.1%±4.3%, n=3, at -75 mV in SA node cells. We employed a two step pulse protocol to determine if the effects of genistein on i_f were caused predominantly by a change of the pacemaker conductance or a shift in voltage dependence. Our results demonstrated that maximal conductance is reduced by genistein, but do not rule out a concomitant negative shift in i_f activation. We next examined the action of an inactive analogue of genistein, daidzein, on i_f in rabbit SA node cells. 50 μM daidzein had no effect on i_f. These results suggest that tyrosine kinases may play an important role in basal regulation of i_f. The factors controlling the activity of these kinases remain to be examined. Supported by NHLBI HL20558, HL28958

Th-Pos151

NPPB activates ATP-sensitive K^+ current in cat isolated ventricular myocytes. ((**B. Jow**, R. Numann and T. Colatsky)) Wyeth-Ayerst Research, Princeton, NJ 08543. (Spon. by R. Numann)

NPPB (5-nitro-2-(3-phenylpropylamino) benzoic acid) is reported to be a potent blocker of Cl^- channels in a variety of cell types. We now report that, in isolated cat ventricular myocytes, NPPB (100μM) reversibly shortens the cardiac action potential by evoking a large outward current. The magnitude of outward current was increased 9.02 ± 3.30 fold (n=9) at a test potential of +50mV by acute superfusion with NPPB. The NPPB activated current reversed at -80mV and was sensitive to glyburide (10μM - 30μM, n = 6). Lower concentrations of NPPB (10μM - 30μM) were much weaker in eliciting this current (1.11 ± 0.10 fold increase, n=4). These results suggest that NPPB can reversibly activate a cardiac ATP-sensitive K^+ current in a dose dependent manner.

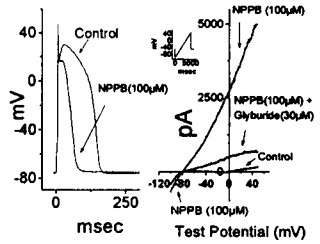

Th-Pos152

REST EFFECTS IN RABBIT VENTRICULAR MYOCYTES CURRENT CLAMPED USING THE PERFORATED PATCH TECHNIQUE. ((J.P. Chanmugam, S.J. Cook, M.K. Lancaster & S.C. O'Neill)) Veterinary Preclinical Sciences, The University of Liverpool, P.O. Box 147, Liverpool, L69 3BX, U.K.

It has been shown that the pores formed in cellular membranes by the antibiotic amphotericin B are permeable to monovalent ions. In certain experimental circumstances it would prove useful to be able to gain control of the intracellular sodium concentration ($[Na^+]_i$). In the present set of experiments we have tried to demonstrate that this is possible using the perforated patch clamp technique in myocytes isolated from rabbit ventricle.

We have several lines of evidence indicating that $[Na^+]_i$ is unable to change when the cell is under perforated patch clamp. When rested rabbit cardiac myocytes undergo rest decay. However, in cells rested while measuring membrane potential using the perforated patch technique (pipettes contained 12mM Na^+) no rest decay occurred. At the end of a 10 minute rest the first post-rest contraction in patched cells (n=12) is 0.79 ± 0.13 of control, in unclamped cells (n=18) 0.26 ± 0.05 ($p < 0.0001$). Indeed it can even be shown that under these circumstances these cells can produce spontaneous oscillations, a phenomenon normally only seen in species (e.g. rat) which demonstrate rest potentiation. The frequency of spontaneous oscillations remains constant throughout the rest period. In rat ventricular myocytes the frequency of oscillations decreases during prolonged rest, due to a fall of $[Na^+]_i$ during the rest.

In patched cells rested for 10 min the first post-rest contraction is potentiated. The subsequent contractions are smaller than control which then recover over the next 2 minutes to control levels. This pattern of recovery is similar to that following a 30 second rest but much slower. This may be because rest, although not able to deplete the sarcoplasmic reticulum as $[Na^+]_i$ does not fall, is having an influence on myofilament sensitivity. The perforated patch technique allows this change to take place independent of changes in $[Na^+]_i$.

PROTEINS OF E-C COUPLING: RyR, FABP, DHPR

Th-Pos153

Mg^{2+} BLOCK REFLECTS DIFFERENTIAL BEHAVIOR OF RYANODINE RECEPTORS FROM SKELETAL MUSCLE (RYR1) VS CARDIAC MUSCLE (RYR2). ((**Julio A. Copello***, Sebastian Barg*, Alois Sonnleitner†, Hansgeorg Schindler† and Sidney Fleischer*)). *Department of Molecular Biology, Vanderbilt University, Nashville, TN, and †Institute for Biophysics, University of Linz, Austria.

Few differences have thusfar been discerned regarding the behavior of skeletal muscle RyR1 vs heart RyR2. In this study, differences can be discerned regarding Mg^{2+} block of channel activity. Skeletal muscle RyR1 and cardiac RyR2 channels were incorporated into planar lipid bilayers. At 5 μM cytosolic $[Ca^{2+}]$, there was wide variation in the mean open probability (P_o) of RyR1 channels (from 0.02 to 0.95) whereas most dog heart RyR2's had high Po (>0.6). Both channels were inhibited by 1 mM Mg^{2+}. A portion of the channels were fully inhibited by Mg^{2+}. For the other portion, the P_o was decreased by only a factor of two. Most RyR1 channels recover from Mg^{2+} block when [ATP] is increased to 4 mM (at constant free $[Mg^{2+}]$ ~ 1 mM). By contrast with RyR1, cardiac RyR2 did not recover when [ATP] is increased to 4 mM. Both HA RyR1 and all RyR2 channels recover from inhibitory effects of Mg^{2+} by increasing $[Ca^{2+}]$ from 5 to 100 μM. Skeletal muscle (but not heart) contain RyRs with very low activity (30% of the channels) that do not recover from Mg^{2+} block by increasing [ATP] or $[Ca^{2+}]$. We have previously reported that block of RyR1 and RyR2 channels by Mg^{2+} (1 to 2.5 mM) can be overcome by phosphorylation with protein kinases. Hence, the phosphorylation state of the RyRs contribute at least in part to the observed differences in sensitivity to Mg^{2}. The more heterogeneous behavior of RyR1 and the differences between RyR1 and RyR2 observed with ATP may reflect the endogenous steady-state of the RyR channels required for EC coupling in heart vs skeletal muscle (Supported by NIH HL32711, HL 46681, and Austrian Research Fond, project S06613).

Th-Pos154

RELIEF OF INACTIVATION OF THE SKELETAL CALCIUM RELEASE CHANNEL BY MEMBRANE POTENTIAL CHANGES. - *A. Zahradníková[1] and L.G. Mészáros[2]*, [1]UMFG SAV, Bratislava, Slovak Republic, [2]Dept. Physiol. & Endocrinol., Medical College of Georgia, Augusta, GA, USA

Using the planar lipid bilayer method to study single-channel activity of the ryanodine receptor (RyR) of rabbit skeletal muscle, we have observed that the application of -50 mV voltage prepulses resulted in a transient but dramatic increase in subsequent RyR channel activity at +30 mV, which stemmed from a simultaneous increase in average open time and frequency of channel openings. The transient P_o increase paralleled the re-distribution of channel activity modes: the rapid appearance of the high (H) and the low (L) activity modes and the disappearance of the inactivated (I) mode after progressively longer prepulses, which was followed by a subsequent slower relaxation of the modes to their steady-state values after the prepulse. The changes in mode distribution suggest that a membrane voltage change induces the relief of channel inactivation, a process that might mimic some electrical event of E-C coupling, such as a possible dipole-dipole interaction between the DHP receptor and the RyR. (Support: AHA, HHMI).

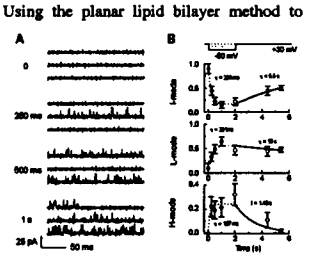

RyR activity at +30 mV after variable length prepulses to -50 mV.
A - representative traces; B - time course of prepulse-induced modal changes.

Th-Pos155

INHIBITION OF THE CARDIAC MUSCLE RYANODINE RECEPTOR CALCIUM RELEASE CHANNEL BY NITRIC OXIDE. A. *Zahradníková[1,2], I. Minarovic[1,2], and L.G. Mészáros[1]*, [1]Dept. Physiol. & Endocrinol., Med. Coll. of Georgia, Augusta, GA 30912, [2]UMFG SAV, 833 34 Bratislava, Slovak Republic.

We have recently reported (*Mészáros et al. Febs Lett. 380: 49, 1996*) that nitric oxide (NO) inhibits (i.e. accelerates the inactivation of) the skeletal muscle ryanodine receptor Ca^{2+} release channel (RyRC) and proposed that this effect of NO on the release channel might represent an important feedback mechanism which involves Ca-dependent activation of NO production and NO-evoked reduction of Ca^{2+} release from intracellular Ca^{2+} stores. Thus, we tested if NO also exerts similar effects on the cardiac release channel.

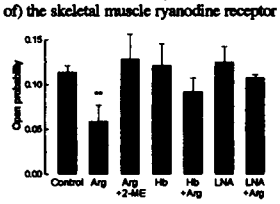

Fig. 1: The effect of L-Arg on P_o of single cardiac RyRCs in lipid bilayers. (** - $p < 0.01$).

We found that both NO donors (SNAP, not shown) and NO that was generated in situ *via* the NOS reaction from L-Arg reduced the rate of Ca^{2+} release from cardiac sarcoplasmic reticulum (not shown) and decreased the activity (i.e. the open probability, P_o) of single cardiac RyRCs fused into planar lipid bilayers (Fig.1). The effect NO generated in the bilayer chamber from L-Arg was reversed by mercaptoethanol (2-ME) and prevented by hemoglobin (Hb) and the NOS inhibitor L-NA, while that of SNAP (not shown) was reversed by 2-ME and prevented by Hb. These results might explain, at least partially, the previously observed negative inotropic effect of NO on cardiac contractility.

Th-Pos156

INHIBITION OF THE CARDIAC SARCOPLASMIC RETICULUM ADP-RIBOSYL CYCLASE BY RYANODINE. László G. Mészáros; Department of Physiology and Endocrinology, Medical College of Georgia, Augusta, GA.

Cyclic ADP-ribose (cADPR) activates the (non-skeletal muscle type) ryanodine receptor channel (RyRC) and, as recent results (*Rakovic et al. Curr. Biol. 6:989, 1996*) suggest, it is likely to be involved in cardiac E-C coupling. We have previously shown that heart muscle possesses two types of ADP-ribosyl cyclase (ADPRC): a plasma membrane- (SLM-) and a sarcoplasmic reticulum- (SR-) associated form.

Here we report that ryanodine (50 μM) inhibits ADPRC activity in SR (Fig. 1) (but not in SLM, not shown), as assessed by using NGD as substrate, which yields the fluorescent product cGDPR. The ryanodine-effect required the presence of micromolar Ca^{2+}, was slightly attenuated by a RYRC antibody MA3-916 (Affinity Bioreagents, Inc.), but was still detectable (although somewhat reduced) in 0.6% CHAPS-solubilized fraction of SR that contained several SR proteins including the RyRC. These findings suggest that the SR ADPRC enzyme, that is mainly responsible for the production of cADPR in cardiac muscle, might be associated with the release channel, the effector protein of the second messenger enzyme ADPRC. (Supported by the Howard Hughes Medical Institute.)

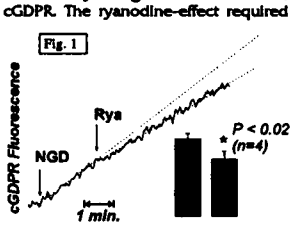

Th-Pos157

DIVALENT CATION SENSITIVITY OF RYANODINE RECEPTOR (RyR) ACTIVATION AND ADAPTATION ((P. Vélez, A. Escobar*, M.E. Zhogbi*, S.R. Caenepeel, B. Suárez-Isla**, and M. Fill)) *Inst. Venezolano de Investigaciones Científicas, Caracas, Venezuela, **Univ. de Chile, Santiago, Chile and Loyola University Chicago, Maywood, IL 60153.

To demonstrate the existence of multiple Ca^{2+} regulatory sites on RyR, we studied the action of different divalent cations on channel function when added to the myoplasmic side of RyR channels incorporated in planar lipid bilayers. The RyR channels were isolated from canine ventricular muscle. Solutions contained 200 mM symmetrical $CsCH_3SO_3$, 20 CsHEPES (pH 7.4). The Ca^{2+}, Sr^{2+} & Ba^{2+} sensitivity of the channel was defined using complex solutions containing a mixture of divalent cation buffers (EGTA, EDTA & NTA). The free divalent concentration was confirmed using ion selective electrodes. Under steady-state conditions, Ca^{2+} and Sr^{2+} activated with a half maximal open probability (Po) occurring at about 1 and 0.1 μM, respectively. The RyR channel was not activated by Ba^{2+}. The maximal Po reached after channel activation by Ca^{2+} and Sr^{2+} was 67 and 92%, respectively. Assuming Ca^{2+} and Sr^{2+} activate by binding to the same site, these data suggest that multiple calcium binding sites or sets of sites regulate the channel. The ability of Sr^{2+} to regulate the RyR was further explored under nonstationary conditions. The response of single RyR channels to a fast Ca^{2+} and Sr^{2+} stimuli applied by laser flash photolysis of DM-nitrophen (3 mM), caged-Sr^{2+} or caged-Ca^{2+}, was defined. The affinity of DM-nitrophen for Sr^{2+} was measured and found to be ≈0.01 μM. Single RyR channels activated rapidly in response to the fast photolytic Sr^{2+} or Ca^{2+} stimuli ($\tau \approx 1$ ms). After reaching peak activity, channel activity spontaneously decayed when Ca^{2+} was the stimulating ion ($\tau \approx 1.3$ s). When Sr^{2+} was the stimulating ion, showed no indication of decay over several seconds. The lack of a spontaneous decay suggests that Sr^{2+} activates but does not support the adaptation process. These data experimentally demonstrate that there are multiple Ca^{2+} binding sites regulating the RyR channel and that adaptation involves at least one Ca^{2+} binding step. AHA & NIH (MF).

Th-Pos158

THE δ ISOMER OF HEXACHLORO-CYCLOHEXANE ALTERS FUNCTION OF VENTRICULAR CARDIOMYOCYTES, RYANODINE RECEPTORS, AND PHYSICAL PROPERTIES OF ARTIFICIAL LIPID MEMBRANES. ((E.D. Buck*, W.G. Lachnit† and I.N. Pessah*.)) *Department of Molecular Biosciences, School of Veterinary Medicine, University of California, Davis, CA and †Roche Bioscience, Palo Alto, CA

Delta-hexachlorocyclohexane (δ-HCH) has been shown to modulate ryanodine-sensitive Ca^{2+} channels of sarcoplasmic reticulum (SR) and contractility of rat atrial strips (Pessah, *et. al., J. Pharmacol. Exp. Therap.* **262:** 661-9, 1992). In the study presented here, we further examine the mechanism of action of δ-HCH by measuring changes in the rate of cell shortening and intracellular Ca^{2+} transients in electrically stimulated single cardiomyocytes isolated from guinea pig. δ-HCH (10μM) is observed to dose-dependently inhibit cell shortening and force of contraction by ~60%, to reduced the peak amplitude by 28%, and to increase the duration of Ca^{2+} transients by 20%. Measurements using cardiac SR Ca^{2+} channels reconstituted in the planar lipid bilayer were used to demonstrate and characterize the direct actions of δ-HCH on channel function. Measurements of gating kinetics show that δ-HCH dramatically increases open probability and mean open time without altering unitary channel conductance. The actions of δ-HCH at the cellular and single channel levels appear to be isoform-selective since γ-HCH (lindane) is significantly less potent in inducing these effects. Interestingly, δ-HCH is shown to dose dependently increase the relaxation time constant of a step potential across the lipid bilayer, possibly by altering the dielectric constant of the membrane. Nevertheless, this novel effect is independent of δ-HCH's action on RyR since changes in channel kinetics occur at concentrations too small to measurably affect the relaxation times of the membranes. These results confirm a novel mechanism by which δ-HCH alters Ca^{2+} signaling in the heart. Supported by the American Heart Association, California Affiliate.

Th-Pos159

RAPID ACTIVATION AND DEACTIVATION OF THE CARDIAC RYANODINE RECEPTOR BY Ca^{2+} SPIKES INDUCED BY PHOTOLYSIS OF CAGED Ca^{2+}. *((A. Zahradníková and S. Györke))* [1]UMFG SAV, Bratislava, Slovak Republic, [2]Dept. Physiology, Texas Tech University HSC, Lubbock, TX, USA (Spon. by R. Nathan)

The local control concept of Ca^{2+}-induced Ca^{2+} release in heart postulates that the activity of the sarcoplasmic reticulum ryanodine receptor channels (RyR) is controlled by Ca^{2+} entry through adjoining single sarcolemmal dihydropyridine receptor (DHPR) channels. One premise of this hypothesis is that the RyR must be fast enough to track the rapid Ca^{2+} changes (<1 ms) associated with single DHPR channel openings. To define the kinetic limits of effective trigger Ca^{2+} signals, we analyzed the activity of cardiac RyRs during rapid and transient increases in $[Ca^{2+}]$, generated by release and subsequent rebinding of Ca^{2+}, upon laser flash photolysis of DM-nitrophen. Single channel activity was recorded using the planar lipid bilayer technique. The magnitude and time course of photolytic Ca^{2+} changes at different resting free $[Ca^{2+}]$s and flash energies were determined according to Ellis-Davies et al. (*Biophys. J.* 70: 1006, 1996). Application of a Ca^{2+} trigger signal with an amplitude of ≈17 μM and duration of ≈0.8 ms (at half-maximal amplitude) from a resting level of 100 nM activated the RyRs in about 20% of the time. RyR activation closely followed the rising phase of the spike ($\tau = 0.28 \pm 0.07$ ms, $\tau_a^{spike} = 0.07$ ms). The activity consisted mostly of single openings and the time constant of deactivation was $\tau_d = 2.8 \pm 0.5$ ms ($\tau_d^{spike} = 0.61$ ms). These results show that brief (< 1 ms) trigger Ca^{2+} signals are adequate to activate the RyR and consistent with the possibility that RyR channels are governed by single DHPR channel events. Support: NIH (HL 52620, SG), Fullbright Scholarship (AZ).

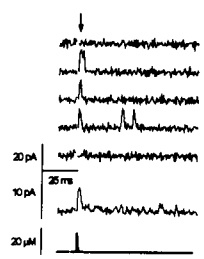

Response of the RyR to Ca spikes. *Top:* Representative traces; *middle:* average response; *bottom:* Ca^{2+} spike

Th-Pos160

GATING OF RYANODINE RECEPTOR 1,2 AND 3 (RyR1, RyR2, RyR3) BY ATP IN THE ABSENCE OF CALCIUM ION. **Alois Sonnleitner***, J. Copello+, S. Fleischer+, V. Sorrentino#, H. Schindler*)) *Institute for Biophysics, University of Linz, Austria; +Department of Molecular Biology, Vanderbilt University, Nashville, TN; #DIBIT-Instuto Scientifico H. San Raffaele, Milan, Italy.

Skeletal muscle terminal cisternae vesicles of sarcoplasmic reticulum were incorporated into planar lipid bilayers. Activation of the calcium release channel (CRC) by ATP was studied in the presence or absence of Mg^{2+} (1 mM free) at the cytoplasmic side. In contrast to the cardiac CRC, which could not be activated by ATP in the absence of Ca^{2+}, the skeletal muscle CRC activated in the presence of 100 μM free ATP (sum of ATP^{4-}, $ATP^{3-}H$, $H^{+}ATP^{3-}H$). The activation occurred in a cooperative fashion with a Hill coefficient of 3.1. The presence of 1 mM free Mg^{2+} had no significant effect on channel gating by free ATP. The mode of activation applied to about 50% of observed channels, while the other channels showed minor activity (p_o<0.01) or did not activate at all. These properties of RyR1 and RyR2 will be complemented by a first account on gating properties of mammalian RyR3 at comparable conditions. Supported by NIH HL32711, Austrian Research Fond project S06613 and EU project PL 960592.

Th-Pos161

REGULATION OF CARDIAC CALCIUM RELEASE CHANNEL (RYANODINE RECEPTOR) BY LUMENAL CA^{2+} ((Le Xu and Gerhard Meissner)) Department of Biochemistry and Biophysics, University of North Carolina, Chapel Hill, NC 27599-7260

Recently, our laboratory has shown that lumenal Ca^{2+} can activate and inactivate the ATP-activated rabbit skeletal muscle Ca^{2+} release channel (ryanodine receptor) (CRC) by having access to the channels cytosolic Ca^{2+} activation and inactivation sites (Biophys. J. 70:2600-2615, 1996). The effect of lumenal Ca^{2+} on the purified canine cardiac muscle Ca^{2+} release channel (ryanodine receptor) (CRC) was examined in planar lipid bilayer single channel measurements in the presence of mM cytosolic caffeine and nM cytosolic Ca^{2+}. An increase in lumenal to cytosolic Ca^{2+} fluxes from 0 to ~1 pA activated the channel, whereas higher Ca^{2+} fluxes caused a decline in channel activity. Kinetic analysis showed that lumenal Ca^{2+} fluxes increased channel activity by increasing the number of events and mean open time. Addition of the fast Ca^{2+} - complexing buffer BAPTA to the cytosolic side of the bilayer further increased channel activity by increasing mean open time. An activation and inactivation of channel activity by lumenal Ca^{2+} could be also observed in the absence of caffeine. We suggest that lumenal Ca^{2+} can regulate cardiac Ca^{2+} release channel activity by passing through the channel and binding to the channel's cytosolic Ca^{2+} activation and inactivation sites. Supported by NIH.

Th-Pos162

S-NITROSYLATION ACTIVATES THE CARDIAC CA^{2+} RELEASE CHANNEL (RYANODINE RECEPTOR) ((L. Xu*, G. Meissner*, P. Eu#, J.S. Stamler#)) * University of North Carolina, Chapel Hill NC 27599, and #Duke University, Durham NC 27710.

S-nitrosylation of specific sites in proteins can alter their allosteric properties and function. Nitrosothiols are one class of endogenous compounds capable of S-nitrosylation. The effects of nitrosothiols (SNO) on cardiac Ca^{2+} release channels (ryanodine receptors) (CRC) were examined in single channel measurements and by determining the CRC-SNO content of purified and reconstituted receptors. Nitrosoglutathione (GSNO) and nitrosocysteine (CysNO) increased several fold the activity of channels reconstituted into planar lipid bilayers and recorded in the presence of a suboptimally activating concentration of 1-2 μM Ca^{2+}. Under conditions resulting in maximal channel activation, several sites on the CRC were S-nitrosylated. Addition of 10 mM DTT resulted in loss of NO binding and returned GSNO- but not CysNO-activated channel activities close to control levels, suggesting that the two compounds may have reacted with different channel sites. DTT by itself was without a noticeable effect on channel activity. SIN-1, which produces peroxynitrite, activated the cardiac Ca^{2+} release channel, but this was not associated with channel S-nitrosylation. Furthermore, channel activation by SIN-1 was not reversed by DTT. Our results suggest that cardiac Ca^{2+} release channel activity may be regulated by direct covalent modification involving the nitrosylation of several classes of sulfhydryls. Supported by NIH.

Th-Pos163

INHIBITION OF CALCIUM RELEASE BY AZUMOLENE IN C2C12 CELLS

((**S.S. Palnitkar**[1] and J. Parness[1,2])) Depts. Anesthesia[1], Pharmacology[2], & Pediatrics[2], UMDNJ-Robert Wood Johnson Medical School, New Brunswick, N.J. 08901

Dantrolene sodium acts by inhibiting Ca^{2+} release from sarcoplasmic reticulum (SR) in skeletal muscle. Dantrolene and its equipotent congener azumolene inhibit this Ca^{2+} release by an unknown mechanism. Recent evidence suggests that dantrolene can both activate (low nM) and inhibit (μM) the Ca^{2+} channel activity of the ryanodine receptor, the primary Ca^{2+} release channel of SR, in a concentration dependent manner. However, we have found only one class of dantrolene binding sites in porcine skeletal muscle SR microsomes. In order to examine the action of dantrolene/azumolene on cellular Ca^{2+} release, we directly determined the effects of azumolene on intracellular Ca^{2+} fluxes. Two millimolar caffeine was used to induce Ca^{2+} waves in differentiated C2C12 cells (mouse skeletal muscle) as determined by changes in Fura-2 fluorescence (frequency ~ 3 per min). Addition of 10 nM azumolene (in the presence of 2 mM caffeine) resulted in a 60-90% decrease in the frequency of oscillations, indicating an inhibition of Ca^{2+} release. Similar results were also obtained when the azumolene concentration was increased to 50 μM. Removal of azumolene from the caffeine containing medium resulted in an increase in the frequency of oscillations to control values, indicating reversibility of azumolene inhibition. Ca^{2+} oscillations were only detected in differentiated cells. Differentiated C2C12 cells can be used as a model to study the mechanism of Ca^{2+} fluxes in skeletal muscle. Azumolene, at low (nM) as well as high (μM) concentrations, inhibits the frequency of Ca^{2+} oscillations induced by caffeine, suggesting a single site of action. (Supported by FAER and Dept. of Anesthesia)

Th-Pos164

DIFFERENT FUNCTIONAL INTERACTIONS OF SKELETAL AND HEART MUSCLE RYANODINE RECEPTORS WITH FK506 BINDING PROTEIN ISOFORMS.

((Sebastian Barg, Julio A. Copello, and Sidney Fleischer)). Department of Molecular Biology, Vanderbilt University, Nashville, TN 37235.

The ryanodine receptor (RyR1) as isolated from skeletal muscle sarcoplasmic reticulum is tightly associated with the immunophilin FKBP12 in a stoichiometric complex, (RyR protomer)$_4$ (FKBP)$_4$. Recently, cardiac RyR2 was found to consist of a similar complex, albeit with a novel FKBP12 isoform termed FKBP12.6. In the present study, we compare functional consequences of dissociation and reconstitution of FKBP12 and FKBP12.6 with RyRs from cardiac and skeletal muscle. The skeletal muscle RyR1 channel becomes activated (the sensitivity to Ca^{2+} and caffeine increases) upon removal of endogenously bound FKBP, consistent with previous reports. Both FKBP12 and FKBP12.6 rebind to FKBP depleted RyR1 and restore its quiescent channel behaviour by altering ligand sensitivity, as studied by single channel recordings in planar bilayers, and macroscopic behaviour of the channels (ryanodine binding and net energized Ca^{2+} uptake). By contrast, removal of FKBP12.6 from the cardiac RyR2 did not modulate the function of the channel using the same types of assays as for RyR1. Addition of FKBP12 or 12.6 to FKBP12.6 depleted cardiac RyR2 was also without effect on channel activity even though FKBP12.6 rebinds. Our studies reveal important differences between the two ryanodine receptor isoforms with respect to their functional interaction with FKBP12 and FKBP12.6. Such differences may reflect their respective involvement in excitation-contraction coupling, i.e., depolarization induced Ca^{2+} release in skeletal muscle vs calcium induced calcium release in heart (Supported in part by NIH HL32711 and HL46681 and Muscular Dystrophy Association of America).

Th-Pos165

THE FKBP12.6 ISOFORM IS SELECTIVELY ASSOCIATED WITH CARDIAC CALCIUM RELEASE CHANNEL (CRC) FROM DIVERSE ANIMALS.

((**Ying Qi**, Katherine Murray*, and Sidney Fleischer)) Department of Molecular Biology, Pharmacology and Medicine*, Vanderbilt University, Nashville, TN 37235.

The skeletal muscle CRC/ryanodine receptor (RyR1) of terminal cisternae of sarcoplasmic reticulum (SR) from rabbit fast twitch skeletal muscle is associated with FK binding protein (FKBP12).The stoichiometry is four FKBP/ryanodine receptor. The structural formula of RyR1 can be written as (RyR1 protomer)$_4$(FKBP12)$_4$. In vitro studies show that FKBP modulates the activity of the RyR channel (Timerman et al. J. Biol. Chem. 268 1993). RyR1 from diverse animal species of vertebrates is likewise associated with the FKBP12 isoform (Freund et al. Biophys. J. 66 1994). The cardiac ryanodine receptor (RyR2) from dog heart SR was found to be associated with a novel isoform of FKBP, designated FKBP12.6 (Lam et al. J. Biol. Chem. 270 1996). The structural formula of dog RyR2 can be written as (RyR2 protomer)$_4$ (FKBP12.6)$_4$. We now report that cardiac ryanodine receptor (RyR2) from several diverse vertebrate animals is selectively associated with the FKBP12.6 isoform. The studies include animal species from mammals (dog and human), reptile (turtle) and bird (chicken). The studies are consistent with the association of FKBP with both RyR1 and RyR2, albeit RyR1 with FKBP12 and RyR2 with FKBP12.6. Supported in part by NIH HL32711 and HL46681.

Th-Pos166

EXCHANGE OF FKBP12 AND FKBP12.6 WITH RYANODINE RECEPTORS (RYR1) OF SKELETAL MUSCLE SARCOPLASMIC RETICULUM (SR) FROM DIVERSE ANIMALS.

((**Ying Qi**, Eunice Ogunbunmi, Loice Jeyakumar, Yuqi Qiao, Julio Copello and Sidney Fleischer)) Dept. of Mol. Biology, Vanderbilt Univ., Nashville, TN 37235.

FK binding protein12 (FKBP12) is specifically associated with rabbit (Rb) skeletal muscle SR (RyR1), and the FKBP12.6 isoform was found to be selectively associated with dog heart (DH) RyR2 (Lam et al., J. Biol. Chem. 270 1995, and Timerman et al., J. Biol. Chem. 271 1996). In vitro, FKBP12.6 binds to and exchanges with Rb and DH SR, whereas the FKBP12 isoform binds to and exchanges only with skeletal muscle RyR1. We studied the exchange of ^{35}S-FKBP12 and ^{35}S-FKBP12.6 with skeletal muscle terminal cisternae of animals representing different classes of vertebrates, i.e. rabbit (mammal), chicken (bird), turtle (reptile), rainbow trout (fish). The stoichiometry of FKBP/RyR obtained from the exchange studies for FKBP12 and FKBP12.6, resp., were: rabbit (3.48 and 3.64); chicken (1.7 and 1.7); turtle (0.62 and 2.26); and rainbow trout (1.6 and 5.4) The dog heart control was 0.31 and 2.9. These studies suggest that the binding and exchange specificity of the ryanodine receptors differ in these different animals. The basis for the different specificity is not clear. Relevant may be that skeletal muscle from bird, reptile and fish consist of both RyR1 and RyR3 isoforms, whereas mammalian skeletal muscle contains mainly RyR1. NIH HL32711 and Muscular Dystrophy Assoc.

Th-Pos167

DETERMINATION OF THE AMINO ACIDS OF FKBP12.6 INVOLVED IN ASSOCIATION WITH CARDIAC RYANODINE RECEPTOR BY SITE-DIRECTED MUTAGENESIS

((**Hong-Bo Xin**, Takashi Kanematsu, Gregory Wiederrecht* and Sidney Fleischer)) Dept. Mol. Biology, Vanderbilt Univ., Nashville, TN 37235 and *Dept. Immun., Merck Research Laboratories, Rahway, NJ 07065-0090

Although the newly described FKBP12.6 differs from FKBP12 by only 18 of 107 amino acids(Lam et. al. (1995), J. Biol. Chem. 270: 26511-26522), FKBP12.6 specifically binds to cardiac ryanodine receptor (RyR-2), whereas both FKBP isoforms exchange with bound FKBP of skeletal muscle RyR (RyR-1) (Timerman et. al. (1996), J. Biol. Chem. 271:20385-20391). Site-directed mutagenesis is being used to define which amino acids of FKBP12.6 are critical for binding to cardiac RyR. Thus far, eight mutants of FKBP12.6 were made. For each mutant, one or two amino acids were changed to the FKBP12 sequence. We find that two mutants (Q31E/N32D and F59W) significantly decreased the EC_{50} for exchange of ^{35}S-FKBP12.6, preexchanged with cardiac sarcoplasmic reticulum (CSR). The decrease in EC_{50} was used as index of amino acids of FKBP12.6 involved in association with cardiac RyR. The EC_{50} (μM) for the various FKBPs and mutants were as follows: 0.021 (FKBP12.6), 0.025 (E3Q), 0.053 (C76I), 0.053 (V80Y), 0.065 (N105K), 0.067 (N94H), 0.096 (R49M), 0.77 (Q31E/N32D), 0.81 (F59W) and 18.3 (FKBP12), respectively. These results suggest that Glutamine (31), Asparagine (32) and Phenylalanine (59) serve a role in binding of FKBP12.6 to cardiac RyR. We would suggest that comparable positions of the amino acids of FKBP12 are involved in binding surface to skeletal muscle RyR (RyR-1). (NIH HL32711, HL46681 and Muscular Dystrophy Association)

Th-Pos168

EXTENDED JUNCTIONAL SARCOPLASMIC RETICULUM OF CARDIAC MUSCLE MAY CONTAIN DISTINCT CA^{2+} RELEASE CHANNELS.

((**D.G. Ferguson**, S.A. Lewis Carl, E.A. Accili*)) Dept. of Anatomy, Case Western Reserve University, Cleveland, OH 44106, *Rammelkamp Research Center, MetroHealth Hospital, Cleveland, OH 44109

The cardiac dyad, the presumed site of excitation contraction (EC) coupling, is a specialized junction formed between an element of the sarcoplasmic reticulum (SR) and the sarcolemma (or T-tubule). The junctional SR (jSR) of the dyad contains ryanodine receptors (RyR), the SR Ca^{2+} release channel. Extended junctional SR (ejSR), one form of which is called corbular SR, is jSR that contains RyR but exists free in the cytoplasm and does not participate in formation of the dyad junction. In cardiac myocytes that lack a T-tubule network, ejSR comprises a relatively major fraction of the junctional SR surface, however, the role of this component in EC coupling is not well-understood. In immunoblot and indirect immunolocalization studies we observed that a previously undescribed putative RyR was apparently preferentially associated with the ejSR. In addition, we used a peptide-specific antibody raised against a conserved sequence found in IP3 receptors I, II & III to immunolocalize the cardiac IP3 receptor (IP3R). Using indirect immunofluorescence combined with confocal laser scanning microscopy, we observed that this antibody did not stain the subsarcolemmal dyadic jSR but preferentially stained cytoplasmic ejSR in neonatal rat atrium and ventricle, and adult rat sinoatrial node. These data suggest that the ejSR are a unique compartment and that Ca^{2+} release from the ejSR may be regulated by different mechanisms than Ca^{2+} release from the dyadic jSR.

Th-Pos169

IDENTIFICATION OF A 68 KDA TRIADIN BINDING PROTEIN IN SKELETAL MUSCLE TRIADS. ((Neil Brandt & **Anthony H. Caswell**)), Dept. Molecular & Cellular Pharmacology, Univ. Miami School of Medicine.

A 68 kDa protein extracted from skeletal muscle triads in 250 mM sucrose, 20 mM TrisCl, 2 mM EDTA, 2 mM DTT, pH 8.3 (TDE) and purified by DEAE Sepharose chromatography overlays triadin and $pGST_{tag}$ triadin fusion protein constructs on Western blots. $pGST_{tag}$ triadin fusion proteins immobilized on Glutathione Sepharose selectively bind the 68 kDa protein from TDE triad extracts. The binding reaction is enhanced by mM Ca^{2+} in 200 mM NaCl. Calsequestrin bound to triadin fusion proteins and GST alone in 200 mM NaCl, 2 mM EGTA; calsequestrin precipitated in Sepharose 4B in media containing mM Ca^{2+}. The 68 kDa protein is found in both T-tubule and terminal cisternae but not longitudinal reticulum fractions and does not co-electrophorese with rabbit serum albumin (Sigma) in non-reducing SDS-PAGE. The 68 kDa protein binds to both cytoplasmic and luminal fusion protein constructs of triadin, suggesting that it recognizes a common or repeated region on triadin. (supported by NIH RO1 AR43355)

Th-Pos170

INTERACTION OF THE Ca2+ BINDING PROTEIN S100A1 WITH THE RYANODINE RECEPTOR OF SKELETAL MUSCLE.

((**S. Treves**, E.Scutari, S. Groh*, M. Robert*, M. Ronjat*, and F. Zorzato)) Istituto di Patologia Generale, Universita di Ferrara Via Borsari 46, 44100 Ferrara Italy. * Lab BMC/DBMS-CEA Grenoble 17 rue des Martyrs 38054 Grenoble, France.

S100A1 is a member of the large family of EF hand Ca2+ binding proteins and was found specifically in cytoplasm from neurons, kidney, heart and skeletal muscle. In skeletal muscle sarcoplasmic reticulum (SR) preparations, S100A1 and S100B have been shown to stimulate Ca2+ induced Ca2+ release as well as ryanodine binding. In this work we show that S100A1 activates ryanodine binding (40 +/-7%) on SR vesicles only in presence of low Ca2+ concentrations (10 nM). Half maximal concentration for stimulatory effect of S100A1 is 70nM. Using surface plasmon resonance measurement and overlay technique, we demonstrate that S100A1 interacts with the purified ryanodine receptor (RYR). We then mapped three RYR domains involved in the interaction with S100A1: two are localized in the central portion of the protein (S100A1#1 and S100A1#2) and one (S100A1#3) in the COOH terminal region of the protein. Binding of S100A1 to domain S100A1#1 was observed in 1mM or 10nM Ca2+. For S100A1#2, the binding of S100A1 was maximal in presence of 1mM Ca2+. S100A1#3 domain exhibits a weak binding in presence of 1mM Ca2+ and a strong binding in presence of 10nM Ca2+. Interestingly S100A1#3 domain overlaps with the Ca2+ dependent calmodulin binding domain. The role of S100A1 in ryanodine receptor regulation is discussed. *Supported by Association Francaise contre les Myopathies (AFM).*

Th-Pos171

THE ROLE OF THE α_1 AND THE β_1 SUBUNITS OF THE DIHYDROPYRIDINE RECEPTOR (DHPR) IN EXPRESSION OF THE OTHER PROTEINS OF THE TRIAD ((**J.A. Powell**, S. Haynes, M. Suhkareva*, P.A., C. Strube*, R. Coronado*, P.A. Powers# and R.G. Gregg#)) Dept. Bio. Sci., Smith College, Northampton, MA; *Dept. Physiology and # Waisman Center, University of Wisconsin, Madison, WI.

Excitation-contraction coupling in skeletal muscle is dependent on the interactions of the voltage sensor of the dihydropyridine receptor (DHPR) located in the T-tubules and the ryanodine receptor (RyR-1) located in the terminal cisternae of the SR. The DHPR is a voltage gated slow calcium channel consisting of α_1, α_2/δ, β_1 and γ subunits. We assessed the role of the α_1 and β_1 subunits in the targeting of DHPR subunits and RyR-1 to the triads. We used fluorescence immunocytology to examine the expression pattern of the α_1 and β_1 subunits and RyR-1 in cultured muscle cells from normal, dysgenic (*mdg*) and β_1-null mice. Dysgenic muscle which lacks the α_1 subunit and in which α_2 is mistargeted, expresses the β_1 subunit in a punctate pattern, reminiscent of T-tubule labeling in normal cells. The α_1 subunit is undetectable in the β_1-null cells while the RyR-1 is expressed in a normal pattern in both dysgenic and β_1-null muscle. In chimeras of dysgenic and β_1-null muscle, both α_1 and β_1 proteins are expressed as in wild type cells and skeletal type E-C coupling is restored as demonstrated by the presence of Ca^{2+} transients obtained by video imaging and single cell photometry of Fluo-3. L-type Ca^{2+} currents were nearly identical in amplitude and kinetics to those of control cells. These results demonstrate that α_1 is not necessary for β_1 targeting. They also support the biochemical and physiological evidence that the β_1-subunit is necessary for normal membrane localization of the α1-subunit and that neither is required for the localization of RyR-1 to the SR. (Supported by the Blakeslee Endowment Fund and MDA (J.P.), NSF (RGG & PAP) and NIH (RC).

Th-Pos172

AGE-RELATED CHANGES IN L-TYPE Ca^{2+} CHANNEL AND RYANODINE RECEPTOR GENE EXPRESSION IN SINGLE MUSCLE FIBERS. (María Laura Messi*, Elena Grigorenko* and Osvaldo Delbono*+) Bowman Gray School of Medicine of The Wake Forest University, Dept. of Physiology and Pharmacology* and Internal Medicine (Gerontology)+, Winston-Salem, NC 27157

Alterations in the L-type Ca^{2+} channel/Ryanodine receptor (RYR1) ratio contributes to a decline in Ca^{2+} supply for contractile proteins in aging skeletal muscle (Delbono et al., 1995; Renganathan et al., 1997). In this work, the level of mRNA encoding both channels was determined in single muscle fibers at different ages. The antisense RNA synthesis, representing the pool of cellular mRNA, is based on two rounds of T7 RNA polymerase amplification (Eberwine et al. 1992). The antisense RNA method circumvents the errors of Taq polymerase and allows for a relative linear L-type Ca^{2+} and RYR1 mRNAs amplification. The amplified ^{32}P-radiolabeled mRNA was used as a probe with the cDNAs encoding the L-type Ca^{2+} channel and the RYR1 (reverse Northern blots). Levels of mRNAs in young and old single muscle fibers were quantitated using a beta scanner blot analyzer. Saturating concentrations of DNAs in the nylon filters were determined using capillary transfer and dot blotting methods. The ratio of L-type Ca^{2+} channel mRNA/RYR1 mRNA ranged from 3 to 4 in 7 month old mice. Absolute decreases in the levels of both mRNAs and alterations in their ratio were found in older muscles fibers. (Supported by NIH).

Th-Pos173

RECOVERY OF EXCITATION-CONTRACTION COUPLING AND L-TYPE CALCIUM CURRENT IN β1-NULL MYOTUBES TRANSFECTED WITH β_1 DIHYDROPYRIDINE RECEPTOR SUBUNIT cDNA. (M. Beurg, M. Sukhareva, P.A. Powers*, R.G. Gregg*, R. Coronado) Department of Physiology and Waisman Center*, University of Wisconsin, Madison, WI 53706, USA.

Skeletal muscle cells from mice homozygous for a null mutation in the cchb1 gene encoding the β_1 subunit of the DHP receptor lack EC coupling (Gregg et al., 1996 ; Strube et al., 1996). Cultured β_1-null myotubes fail to contract spontaneously or in response to electrical stimulation at all stages. The L-type current of β_1-null cultured cells has a ~7 fold lower density than that of similar cultures of normal cells, faster activation kinetics (τ activation at +40 mV is 28.4 ± 7.1 ms vs 57.3 ± 7.7 ms in normal), slower inactivation, and a 3.8 fold higher than normal sensitivity to BayK-8644. 4 to 13 days after lipofection of cultures with β_1 cDNA spontaneous and evoked contractions were observed in 20 to 50% of β_1-null myotubes (n=570 total cells). L-type Ca^{2+} currents and intracellular Ca^{2+} transients were measured simultaneously in rescued cells. Recovery of L-type Ca^{2+} currents was complete (4 ± 0.87 pA/pF vs 4.49 ± 0.75 pA/pF in normal). Activation and inactivation kinetics and sensitivity to BayK-8644 were restored to normal values. Ca^{2+} transients had the same voltage dependence as in normal myotubes. Peak Ca^{2+} remained at a maximum at all positive potentials in the range of +20 to +60 mV. Recovery of skeletal-type EC coupling was further confirmed by removal on external Ca^{2+} and by using of blockers of the L-type Ca^{2+} current. The expression of the β_1 subunit in β_1-null cells is sufficient to restore a skeletal-type EC coupling and L-type current with normal properties.
Supported by AHA, Philippe Foundation, NIH and NSF

Th-Pos174

RYANODINE RECEPTOR TYPE III (Ry_3R) IDENTIFICATION IN MOUSE PAROTID ACINI ((**Dennis. H. DiJulio**[1], Edmond D. Buck[3], Eileen L. Watson[1,2] and Isaac N. Pessah[3])) Departments of Oral Biology[1] and Pharmacology[2], University of Washington, Seattle, WA 98195; Department of Molecular Biosciences[3], University of California, Davis, CA 95616

[^{3}H]Ryanodine binding, immunoblot analysis, and single channel measurements using the planar lipid bilayer were used to characterize a ryanodine receptor expressed in mouse parotid acini. [^{3}H]Ryanodine binding to microsomal fractions in the presence of 500 mM KCl and 100 μM Ca^{2+} reveal a saturable and specific high affinity (K_d=6 nM) binding site and with a maximum binding capacity (B_{max}) of 275 fmol/mg protein. Results obtained using Western blot analysis reveal that the ryanodine receptor type III (Ry_3) is the only detectable ryanodine receptor isoform in these preparations. [^{3}H]Ryanodine binding at 23°C is observed to be dependent on Ca^{2+}, to be stimulated by ATP, and to be inhibited by Mg^{2+} and ruthenium red. Bastadins, which have been shown to modulate RyR through an interaction with the immunophilin FKBP-12, dramatically increases [^{3}H]ryanodine binding in the acinar preparations 3-4 fold. The immunosuppressant FK506 enhances [^{3}H]ryanodine receptor occupancy at >100 μM and antagonizes the actions of bastadin, suggesting that an immunophilin also modulates RyR function in parotid acini. Single channel measurements using the planar lipid bilayer in the presence of CsCl reveal a Ca^{2+} dependent channel with lower conductance than either Ry_1 or Ry_2. These results suggest that Ry_3R may play an important role in Ca^{2+} homeostasis in mouse parotid acini.

Th-Pos175

ALTERED EXPRESSION OF JUNCTIONAL SKELETAL SARCOPLASMIC RETICULUM PROTEINS ASSOCIATED WITH AGE.

((**T.E. Jones** and D.J. Bigelow)) Department of Biochemistry, University of Kansas, Lawrence, KS 66045-0021.

In order to address the role of calcium homeostasis as a contributor to decreased function of aged skeletal muscle, we have examined the expression of junctional sarcoplasmic reticulum proteins that are involved in translating the action potential of skeletal muscle to calcium release from intracellular stores. We have purified a heavy sarcoplasmic reticulum (HSR) fraction from the hind limb skeletal muscle of the aging model, Fischer 344 x Brown Norway rat. Immunoblots of these preparations confirm enrichment of the ryanodine receptor (RyR) and of other junctional proteins, e.g., triadin and the dihydropyridine receptor (DHPR). Densitometry of SDS-PAGE indicates that the protein content of the RyR in HSR, identified by Western blot, is 60%, 55%, and 61% isolated from 14, 22, and 30 mo old animals, respectively, relative to that from 5 mo old young adults and suggests decreased expression of the RyR with late maturation. Densitometry of Western immunoblots demonstrates a progressive decrease with age of triadin protein, i.e., triadin expression is 81%, 77%, and 68% of 14, 22, and 30 mo old animals, respectively, relative to 5 mo old young adults. On the other hand expression of the DHPR remains constant throughout the lifespan. These alterations in relative proportions of DHPR, RyR, and triadin may have implications for functional coupling between these junctional proteins.

Th-Pos176

FISH EXPRESS A SLOW TWITCH MUSCLE-SPECIFIC RYANODINE RECEPTOR 1 ISOFORM ((J.P.C. Franck, J.E. Keen, J. Morrissette and B.A. Block)) Stanford University, Hopkins Marine Station, Pacific Grove, CA, 93950.

Fish are often used as a model system for examining the properties of different muscle fiber types due to the discrete anatomical separation of the slow and fast-twitch muscles. We have cloned the complete cDNA sequence that codes for the skeletal ryanodine receptor isoform (RyR1) of fish. This sequence encodes a protein of 5081 amino acids with a calculated molecular mass of 576 KDa The deduced amino acid sequence shows strong sequence identity to RyR1 isoforms and phylogenetic analyses of the protein clusters it with confidence with the RyR1 isoforms of frog and mammals. Antisera raised against a fusion protein of a RyR 1 specific region of the cDNA sequence reacted to a single polypeptide of approximately 576 KDa in fish skeletal muscles. We have also isolated a single clone, λBMRR1a, that partially codes for a RyR1 isoform distinct from the full length RyR1 cDNA. The deduced amino acid sequence for this clone is approximately 80% identical to the corresponding region of the full length RyR1 sequence from fish, mammals, and frog, and phylogenetic analyses cluster λBMRR1a with the RyR1 isoforms. Hybridization of synthetic RNA probes derived from the full length cDNA and λBMRR1a demonstrate different tissue distributions for the two messages. The probe derived from the full length RyR1 isoform hybridized to messages in slow-twitch and extraocular muscle (the latter has a mosaic of fiber types) but not to fast-twitch muscle RNA preparations, whereas the probe synthesized from λBMRR1a hybridized to messages in fast-twitch and extraocular muscle but not the slow-twitch muscle preparation. Neither of the isoforms could be detected by the RNase protection assays in cardiac RNA preparations. [^{3}H]ryanodine binding studies revealed a left shift in the bell-shaped Ca^{2+} dependence curve of fish slow-twitch muscle sarcoplasmic reticulum (SR) when compared to fast-twitch muscle SR. Western blot analyses with several antisera revealed a single high molecular weight RyR in fish slow-twitch muscle (RyR1) and two polypeptides in the fast-twitch muscle (RyR1 and RyR3). This latter result combined with the observation of a specific RyR1 message distinct from fast twitch muscle and the difference in binding characteristics suggest that fish possess a RyR1 isoform that is unique to slow twitch muscle fiber types.

Th-Pos177

THE CONTROL OF TRIAD-ASSOCIATED PROTEIN EXPRESSION BY THE α_1 SUBUNIT OF THE DIHYDROPYRIDINE RECEPTOR (DHPR) IN SKELETAL MUSCLE IN CULTURE

((C. Lei* , A. C. Hall# and **J.A. Powell***)) Departments of Biological Sciences* and Psychology#, Smith College, Northampton, MA 01063. (Spon. by S.P. Scordilis)

Proteins involved in excitation-contraction coupling at the triad are: the DHPR located in the T-tubules, the ryanodine receptor (RyR) located in the membrane of the SR, calsequestrin in the SR, and triadin bound to DHPR, RyR and calsequestrin. The DHPR consists of α_1, β, α_2/δ and γ subunits. To assess how the α_1 subunit might influence the expression of the other triad proteins, a vector containing cDNA of the skeletal DHPR α_1 and a neomycin resistant gene was transfected into α_1 null (dysgenic) mouse myoblasts. With selection, all myotubes died in the sham transfected plates. The α_1 transfected, selected cultures, were stimulated with electric pulses and the contracting myotubes were circled and recorded either by still photography or video. The expression of α_1 was detected by whole-cell patch clamp recordings as the presence of a voltage-gated slow calcium current which was absent in the dysgenic cells. The slow currents were similar to those recorded from normal myotubes and both were reversibly blocked by 10 μM nifedipine. The expression of α_1 protein and related muscle-specific proteins, such as RyR, triadin, α-actinin and troponin-T were detected by immunofluorescence. α_1 expression was not uniform. In some myotubes very high levels of α_1 protein were very clearly detected in nuclear domains concordant with very strong calcium release (as indicated by calcium imaging) and contraction domains. The RyR and triadin proteins, however, were overexpressed and usually evenly distributed in transfected myotubes. There was no apparent over expression of non-triad proteins such as α-actinin and troponin-T in α_1 transfected dysgenic myotubes. (Supported by the Sally Wilens and Blakeslee Endowment Funds to Smith College and the Muscular Dystrophy Assoc. of America).

Th-Pos178

IMMUNOCYTOLOGICAL LOCALIZATION OF SARCOPLASMIC RETICULUM (SR) PROTEINS IN PORCINE AND MURINE MYOTUBES.

((S. Li, J. Snover, J.R. Mickelson, E.M. Gallant, and **J.A. Powell**)) Biology Department, Smith College, Northampton, MA 01063 and Department of Veterinary PathoBiology, University of Minnesota, St. Paul, MN 55108.

We used antibodies to SR Ca^{2+}ATPase, skeletal and brain Ca^{2+} release channel/ryanodine receptor (RyR) isoforms, RyR1 and RyR3 respectively, and a triadin/SR marker (t/SR) in conjunction with fluorescence immunocytochemistry to describe SR development in porcine and murine myotubes. Early and late myotube stages were differentiated by striated α-actinin immuno-staining patterns. In early murine myotubes, Ca^{2+}ATPase exhibited regular banding reflecting triad organization, whereas early porcine myotubes had only diffuse staining, especially around the nuclei. Punctate RyR1 and RyR3 staining was strong throughout early mouse and pig myotubes. RyR3 staining was prominent around nuclei and became less intense in late myotubes while RyR1 staining remained strong. RT PCR of mRNA from porcine myotubes confirmed the expression of both RyR1 and RyR3. Both early and late murine myotubes had punctate t/SR staining aligned in longitudinal arrays. t/SR labeling in early porcine myotubes, however, was both punctate and vesicular, often surrounding nuclei; t/SR vesicles were absent from all mouse myotubes and late porcine myotubes. t/SR vesicles in early porcine myotubes may represent early stages in the formation of triad SR. Our results demonstrate that both porcine and murine myotubes express both RyR1 and RyR3. Further, the SR terminal cisternae appear to develop more slowly in porcine than in murine myotubes, and early porcine myotubes have a unique vesicular form of SR. (Funded by Sally Wilens & Blakeslee Funds of Smith College, NIH AR41270, and MDA of America..)

Th-Pos179

SUBCELLULAR DISTRIBUTION OF CALSEQUESTRIN (CSQ) BINDING PROTEINS IN CARDIAC SARCOPLASMIC RETICULUM (SR).

((C. **Thompson***, W. Arnold*, A.C.-Y. Shen*, L. Jones+ and A.O. Jorgensen*)) *Dept. Of Anat. and Cell Biology, U. of Toronto, Toronto M5S 1A8 Canada and +Krannert Inst. of Cardiology, Indiana U. School of Medicine, Indianapolis Indiana 46202.

It has been proposed that the CSQ binding proteins junctin and triadin anchor CSQ to the Ca^{2+} release domains of the SR in cardiac and skeletal muscle. This proposal predicts that junctin and triadin should colocalize with CSQ and the ryanodine receptor (RyR), which have previously been shown to localize to junctional (j) SR and corbular (c) SR. While a previous immunofluorescence labeling study suggested that triadin is localized to both jSR and cSR (Lewis-Carl et. al., J. Cell Biol. 129, 673 (1995)), our study suggested that junctin is densely distributed in jSR but not detected in cSR (Jorgensen et. al., Biophysical J. 70, A163 (`1996)). To test this possibility we have determined the subcellular distribution of junctin by immunoelectron microscopical (IEM), labeling. The results show directly that junctin is densely distributed in jSR and not detecetd in cSR. Furthermore, immunoblotting of cardiac microsomes show that junctin is expressed in ventricular microsomes at 3.5 times the level found in atrial microsomes. At the same time the levels of CSQ and the RyR, which are both present in cSR and jSR, were only 1.3-1.5 times higher in ventricular microsomes than in atrial microsomes. The unique localization of junctin to jSR is the first evidence to suggest that the protein composition and thus presumably the function/regulation of jSR as a Ca^{2+} storage/release site is distinct form that of cSR. The apparent absence of junctin from cSR also suggests that junctin is not essential for anchoring CSQ to the RyR containing domain of cSR. This function may be carried out by triadin, since immunofluorescence studies suggested that it is present in both jSR and cSR. We are trying to determine the subcellular distribution of triadin in cardiac muscle by IEM labeling.
Supported by grants from MRC of Canada (AOJ), HSFO (AOJ) and NIH (LRJ).

Th-Pos179a

IGF1-INDUCED PHOSPHORYLATION OF THE SKELETAL MUSCLE L-TYPE CALCIUM CHANNEL IMPAIRMENT WITH AGING.

(Muthukrishnan Renganathan and Osvaldo Delbono) Bowman Gray School of Medicine of The Wake Forest University, Dept. of Physiology and Pharmacology and Internal Medicine (Gerontology), Winston-Salem, NC 27157

The insulin-like growth factor-1 (IGF1) promotes skeletal muscle differentiation and growth. We postulated that the L-type Ca^{2+} channel is involved in muscle fiber IGF1 signalling at different stages of post-natal development (Delbono et al., Biophys. J. A388, 1996). In this work, we examined the hypothesis that the decline in muscle trophism and function associated with aging results from an impairment in IGF1R mediated L-type Ca^{2+} channel α_1 - subunit phosphorylation. To test this hypothesis [γ-^{32}P]ATP phosphorylation of the Ca^{2+} channel was induced by IGF1 in monolayers of fast-twitch skeletal muscles from 4, 7, 14 and 28 month old C57BL/6 mice. Phosphorylation was quantitated and results were expressed as integral of the optical density of scanned autoradiographs. IGF1- induced Ca^{2+} current potentiation and Ca^{2+} channel phosphorylation showed similar time-dependence. The effect of various Ca^{2+} concentrations, and PKC, PKA and tyrosine-kinase specific inhibitors on IGF1-dependent L-type Ca^{2+} phosphorylation was explored. The ratio of IGF1-dependent phosphorylation in the presence and absence of the PKC inhibitor peptide [19-36] was 4.2 (7 month old), 4.9 (14) and 2.8 (28). In summary, decreases in IGF1-dependent Ca^{2+} current enhancement with aging is associated with a decrease in channel phosphorylation. (Supported by NIH).

Th-Pos180

THE CAPACITY OF INCREASED HYDROGEN ION CONCENTRATION (DECREASED pH) TO DECREASE FORCE GENERATION OF SKELETAL MUSCLE IS NOT DUE TO PROTEIN DESTABILIZATION. ((R.H. Jadick and **M.A. Andrews**)) Department of PCME - Physiology, NY College of Osteopathic Medicine, Old Westbury, NY 11568.

It has been shown that the methylamine compound trimethylamine *N*-oxide (TMAO) has the capacity to ameliorate the capacity of inorganic phosphate, a fatigue metabolite, to decrease maximal Ca^{2+}-activated force generation (F_{max}) of skinned skeletal muscle fibers (Andrews 1993 *Biophys. J. 64*:A361). This capacity of TMAO is due to its putative capacity to thermodynamically stabilize the muscle proteins, thus protecting them against binding of, and denaturation by, inorganic phosphate ions. The present experiments were run to determine whether hydrogen ions, another fatigue metabolite, may also be working via a similar binding and destabilization mechanism. To determine this, we used single Triton X-100 skinned rat extensor digitorum longus fibers with experiments run at 22° C, with pH 7 being used as control. All solutions were formulated according to a program which solves the set of simultaneous equations describing the multiple equilibria of ions in solution. Solutions contained (mM): 5 EGTA, 20 Imidazole, 2 Mg^{2+}, 5 MgATP, 15 phosphocreatine, and 100 u/ml CPK. Total ionic strength was maintained at 200 mM ($KMeSO_3$ added). Fibers were activated at pCa = 4, in solutions of pH 6.6, 6.8 or 7.0, relaxed, then reactivated in a set of solutions at the same pH level, but containing TMAO at 50, 100, 200, or 300 mM concentrations. Results show that addition of TMAO increases force generation under all condition (as expected), however, unlike its effect in the presence of inorganic phosphate, there is no significant capacity of TMAO to ameliorate the decreased F_{max} caused by an increased hydrogen ion concentration (lower pH) in skeletal muscle. These results indicate that the effect of increased hydrogen ion concentration on force generation are not, to any significant degree, due to a capacity of hydrogen ions to destabilize the muscle proteins (Support: NYCOMRI).

Th-Pos181

FAILURE IN THE REGULATORY MECHANISM OF MUSCLE AT LOW IONIC STRENGTH IS RESPONSIBLE FOR GENERATION OF NON-CALCIUM-DEPENDENT FORCE GENERATION. ((**M.A. Andrews** and C. Goltz)) Department of PCME - Physiology, NY College of Osteopathic Medicine, Old Westbury, NY 11568.

An observation noted by many investigators is the generation of non-Ca^{2+}-dependent (NCaD) force by muscle fibers bathed low ionic strength (LIS) solutions. Recent results using birefringence interference microscopy also indicate a possible change in the myosin crossbridge orientation at LIS (Folkes, et al. 1996, *Biophys. J. 70*: A17). Such NCaD force and changes in orientation could possibly be due to destabilization of muscle proteins. To determine whether or not such is the case, we introduced trimethylamine *N*-oxide (TMAO), a protein stabilizer, into LIS solutions in which single demembranated rat extensor digitorum longus fibers were bathed (pH = 7 and 22°C). LIS solutions contained (in mM): 5 EGTA, 20 imidazole, 1 Mg^{2+}, 2 MgATP, 15 PCr, with a total ionic strength (IS) of 90 mM. At pCa < 8.5 average NCaD force was 3.4% of the control maximal Ca^{2+}-activated force generation (F_{max}) at physiological ionic strength. As 100, 300, or 500 mM TMAO was introduced into the LIS solution the average NCaD force was noted to decrease to 2.5%, 1.2%, and 0.5% of F_{max}, respectively. Additionally, in LIS solutions of pCa = 4, force generation reached 144% of F_{max} (such increases are expected), however there was no significant change in force as up to 500 mM TMAO was added. Fibers bathed in a second set of LIS solutions containing (in mM): 2 EGTA, 5 imidazole, 1 Mg^{2+}, 2 MgATP, 5 PCr, with an IS of 42.5 mM, generated similar results. Such amelioration of NCaD force by TMAO indicates NCaD force is related to destabilization / malfunction of the contractile apparatus. Specifically, results indicate that the regulatory proteins loose some of their capacity to inhibit actomyosin complexation, and force is generated. In the presence of Ca^{2+} all regulation by troponin and tropomyosin is already inhibited, and force generation should not be decreased in the presence of TMAO (Support: NYCOMRI).

Th-Pos182

INHIBITION OF CONTRACTION BY BERYLLIUM FLUORIDE IN SKINNED FIBERS FROM RABBIT PSOAS MUSCLE ((**M. Regnier**, D.A. Martyn, C.J. Freitag and P.B. Chase)) Center for Bioengineering, Depts. of Radiology and Physiology & Biophysics, University of Washington, Seattle, WA 98195. (Spon. by R.W. Wiseman)

Recent evidence suggests that truncated, recombinant *Dictyostelium* motor domain complexed with MgADP and slowly dissociating analogs of Pi may crystallize into two main structural states (S1-MgADP plus BeF_x vs. AlF_4^- or Vi) associated with force generation by actomyosin (Fisher *et al* 1995. *Biophys J* 68:19s; *Biochem* 34:8960; Smith & Rayment 1995. *Biochem* 35:5404). We have reported extensively on the effects of Vi and particularly AlF_4^- on skinned fiber mechanics (Chase *et al* 1994. *J Muscle Res Cell Motil* 15:119; 1993. *J Physiol* 460:231), thus a comparison with BeF_x was undertaken. At pCa 5 (12°C), we measured (i) steady-state isometric force (f_{iso}), (ii) stiffness (K_S; 1 kHz sinusoids), and (iii) unloaded shortening velocity (V_{US}; slack test). With 3 mM total fluoride (added as NaF), 3 μM Be inhibited both f_{iso} and K_S by ~50% (>10-fold higher Al is needed for this extent of inhibition, although the exact concentrations of inhibitory complexes depend on binding equilibria); increasing Be to 10 μM further reduced f_{iso} to ~15% P_0 but had little further effect on K_S. In contrast, both f_{iso} and K_S can be reduced to low levels with AlF_4^-. Like AlF_4^-, V_{US} decreased in proportion to force inhibition by BeF_x (f_{iso} >50%). However, inhibition by BeF_x was more rapidly reversed than inhibition by AlF_4^- (Chase *et al* 1994). Our results suggest that BeF_x may induce a different crossbridge state in fibers than do AlF_4^- or Vi, but all three analogs of Pi form complexes which correspond to crossbridge states early in the crossbridge cycle. (Supported by NIH grants HL52558 and HL51277)

Th-Pos183

CALCIUM REGULATION OF TENSION REDEVELOPMENT KINETICS WITH 2-DEOXY-ATP OR LOW [ATP] SUBSTRATE IN SKINNED FIBERS FROM RABBIT PSOAS MUSCLE ((**M. Regnier**, P.B. Chase and D.A. Martyn)) Center for Bioengineering, Depts. of Radiology and Physiology & Biophysics, University of Washington, Seattle, WA 98195. (Spon. by B. Hille)

We have shown that altering the kinetics of thin filament Ca^{2+} dissociation with a Ca^{2+} sensitizer (calmidazolium; CDZ) causes tension redevelopment kinetics (k_{TR}) to be elevated to a greater extent than expected from CDZ effects on force alone (Regnier *et al.* 1996 *Biophys J* Nov., in press). This indicates a modulatory role for thin filament regulatory units on k_{TR} at submaximum Ca^{2+}-activation. To determine the extent to which the rate of crossbridge cycling also affects the activation dependence of k_{TR}, we examined substrate conditions in which cycling rate (determined by unloaded shortening velocity--see next abstract) increased by ~30% (5 mM 2-deoxy-ATP; dATP) or decreased by ~30% (0.5 mM ATP; low ATP) relative to control (5 mM ATP). At pCa 4.5, force (f_{iso}) was unchanged in dATP while k_{TR} increased ~10% (also see Regnier *et al Biophys J*, 1993, 64:A250; 1996, 70:A290); f_{iso} increased by ~8% and k_{TR} decreased ~10% at pCa 4.5 in low ATP. The force-pCa relation was similar for low ATP but was shifted ~0.1 pCa unit leftward by dATP. At submaximal Ca^{2+}-activation (<75% f_{iso}), k_{TR} with dATP was unchanged from control while k_{TR} with low ATP was slightly faster than control (data compared at similar force levels). This suggests that crossbridge cycling rate is not the sole determinant of tension redevelopment rate in skeletal muscle at submaximum Ca^{2+}-activation. (Supported by NIH grants HL52558 and HL51277)

Th-Pos184

EFFECTS OF 2-DEOXY ATP (dATP) AND LOW [ATP] ON THE CALCIUM SENSITIVITY OF UNLOADED SHORTENING VELOCITY IN SKINNED RABBIT PSOAS FIBERS. ((**M. Regnier**)) Dept. of Bioengineering, University of Washington, Seattle, WA 98195.

Under conditions of submaximal thin filament activation (ie. low [Ca^{2+}]), slack-test plots of unloaded shortening velocity (V_u) are biphasic, with an initial high velocity phase (V_{uH}) followed by a low velocity phase (V_{uL}) of muscle fiber shortening (Moss 1988, *J. Physiol.* 398:165). It has been proposed that, at low Ca^{2+}, a buildup of highly (negative) strained crossbridges at the end of the power stroke is responsible for the transition from V_{uH} to V_{uL}. An increase in ATP hydrolysis products has been shown to influence this transition (Metzger 1996, *Biophys. J.* 70:409). To further test this hypothesis we chose conditions that either speed up the overall crossbridge cycling rate in skinned rabbit psoas fibers by replacing ATP (5mM) with dATP (5mM) or slowed the cycling rate by reducing [ATP] to 0.5mM. At pCa 4.5 (12°C) V_u was elevated ~30% by dATP and reduced ~30% with low ATP, as reported earlier by Regnier *et al.* (*Biophys. J.* 1993, 64:A250; 1996, 70:A290). Vu, V_{uH}, V_{uL} and isometric force all increase with increasing [Ca^{2+}]. For all submaximal [Ca^{2+}] that produced isometric force >25% P_o, V_u was faster with dATP and slower with low ATP (we were unable to distinguish differences in V_u at Ca^{2+} concentrations that produced <25% P_o). Comparison of the two velocity phases at submaximal [Ca^{2+}] showed that both V_{uH} and V_{uL} were increased with dATP and slowed with low ATP at submaximal Ca^{2+} concentrations, but the effect on V_{uH} was more pronounced than the effect on V_{uL}. These results suggest the transition from V_{uH} to V_{uL} can occur by buildup of negatively strained crossbridges which occur via the intrinsic crossbridge cycling rate alone, rather than by a Ca^{2+} regulatory mechanism. Supported by NIH HL52558 and HL51277.

Th-Pos185

EFFECT OF NATIVE AND A TRUNCATED C-TERMINAL MUTANT OF CARDIAC TROPONIN I ON MYOFILAMENT FORCE. ((**R.S. Keller**, H.M. Rarick, A.F. Martin, R.J. Solaro)) Dept. of Physiology and Biophysics, Univ of IL, Chicago, IL 60612.

Activation of cross-bridge cycling and force production is mediated through release of cardiac troponin I (cTnI) inhibition. Previously, we have demonstrated that residues C-terminal to the inhibitory region of cTnI are essential for full inhibitory activity of myofibrillar ATPase and for recovery of Ca^{2+}-sensitivity (*Rarick et al J Mol Cell Cardiol 28(6):A139, 1996*). To determine the role of the C-terminal domain in force production, cTnI and cardiac troponin C (cTnC) were extracted from detergent skinned fiber bundles and reconstituted with either native (N) cTnI or a cTnI lacking 60 C-terminal amino acid residues ($cTnI_{1-151}$) and wild type (WT) cTnC. Triton X-100 skinned fiber bundles were extracted with vanadate (10 mM, pH 6.7) and routinely developed 70-80% force after extraction and had less than 15% Ca^{2+}-sensitivity. Force measured after extraction was inhibited 100% following reconstitution with either N-cTnI (n=4) (75 min) or $cTnI_{1-151}$ (n=5) in the presence of ATP. Approximately 60% of Ca^{2+}-sensitive force was recovered after reconstitution with N-cTnI/WT-cTnC whereas only 20% of Ca^{2+}-sensitive force was recovered after reconstitution with $cTnI_{1-151}$/WT-cTnC. These data suggest that the residues C-terminal to the inhibitory region of cTnI are important in recovery of Ca^{2+}-sensitive force, but may not be essential for inhibition of force. We repeated the above experiments in the absence of ATP to evaluate rigor conditions on the reconstitution process. In rigor condition, the $cTnI_{1-151}$ mutant only inhibited 75% of the extracted force (n=4). Recovery of the Ca^{2+}-sensitivity of force development was not affected by rigor conditions. Our data suggest that the level of crossbridge connections may affect reconstitution of extracted fibers with cTnI/cTnC.

Th-Pos186

AMP-PNP: AN ANALOG FOR WEAK-BINDING CROSS-BRIDGE STATES.

((S. Heizmann, Th. Kraft, B. Brenner)) Medical School, 30625 Hannover, Germany.

The nucleotide analog AMP-PNP has been used in several earlier studies as an anlog to characterize properties of strong-binding cross-bridge states (Greene J. Biol. Chem. 257, 1982; Schoenberg, BJ.56, 1987). However, based on the observation that at saturating [AMP-PNP] without Ca^{++} the intensity ratio of the equatorial 1,0 and 1,1 reflections approached the value of relaxed fibers (Frisbie et al., BJ.68, A141) the question was raised whether AMP-PNP may actually represent a weak binding analog. Since weak binding states, in contrast to strong binding states, are characterized by their inability to activate the contractile system we examined whether cross-bridges with AMP-PNP can activate thin filaments or not. We found that fibers that start to become activated by lowering the [ATP] relax completely when AMP-PNP is added on top of the low [ATP], while they become even more activated upon addition of PP_i. This indicates that AMP-PNP cross-bridges, different from PP_i-cross-bridges, cannot activate the contractile system. Stiffness-speed relations and TnI-fluorescence recorded at saturating [AMP-PNP] (40mM; with hexokinase and glucose to rule out ATP-contamination) without Ca^{++} are very similar to stiffness and fluorescence with ATP under the same ionic strength conditions. However, at lower [AMP-PNP] without Ca^{++} stiffness increases and the stiffness-speed relation shifts to the left due to an increasing number of nucleotide-free cross-bridges. In the presence of Ca^{++}, even at 40mM AMP-PNP stiffness is still very high (80% of rigor) and nucleotide saturation cannot be reached similar to the previously observed effect of Ca^{++} on ATPγS-saturation (Kraft et al., PNAS 1992). Therefore, activation of thin filaments in the presence of AMP-PNP (Greene, J. Biol. Chem.257, 1982) and the PP_i-like stiffness-speed relation at 4mM AMP-PNP (Schoenberg, BJ.56, 1989) apparently are due to nucleotide-free cross-bridges under these conditions. Our data, however, indicate that cross-bridges with AMP-PNP are unable to activate the thin filament and thus represent weak-binding cross-bridge states.

Th-Pos187

THE EFFECT OF STRONG BINDING CROSS-BRIDGES ON THE RATE OF TENSION RELAXATION INDUCED BY PHOTOLYSIS OF DIAZO-2 IN SKELETAL MUSCLE FIBERS.

((G.M. Diffee, **J.R. Patel** and R.L. Moss)) Dept. of Physiology, University of Wisconsin, Madison, WI 53706.

We examined regulation of the rate of relaxation from isometric tension in bundles of rabbit skinned psoas fibers at 15 °C. Relaxation was initiated during steady state tension as a result of rapid chelation of Ca^{2+} by photolysis of the caged Ca^{2+} chelator, diazo-2. At steady tensions of less than 0.6 P_o, the relaxation transient was triphasic consisting of a linear phase (relative amplitude = 0.4) followed by fast (amplitude = 0.5) and slow (amplitude = 0.1) exponential phases, while at tensions greater than 0.6 P_o the linear phase was not observed. In control experiments, the slope of the linear phase, the rate constant, k_1, of the fast exponential phase and the rate constant, k_2, of the slow exponential phase all showed a steep force dependence with the rates decreasing with increasing levels of activation. In order to examine the effect of strongly bound cross bridges in modulating the rate of relaxation, we used the strong-binding cross-bridge analog N-ethylmaleimide modified myosin S-1 (NEM-S1). In the presence of NEM-S1 the rate of relaxation in each of the three phases was slowed at low forces such that the force dependence of relaxation rates was diminished. NEM-S1 had no significant effect on the relative amplitudes of the phases of relaxation. We also examined the effect of myosin regulatory light chain (RLC) phosphorylation and found that RLC phosphorylation had similar effects to those observed with NEM-S1, i.e. elimination of the activation dependence of the slope of the linear phase as well as k_1 and k_2. Based on these results, we conclude that at low forces the presence of strong-binding cross bridges maintains the thin filament in an activated state, thus slowing the relaxation from isometric tension induced by flash photolysis of diazo-2. Supported by NIH AR08226 and HL47053

Th-Pos188

CROSSBRIDGE KINETICS IN SKINNED FIBRES OF PHENOTYPICALLY TRANSFORMED SKELETAL MUSCLE

((*#**G.J. Wilson**, *#S. Harroothunian, *D.T.A. Hardman, *S.N. Hunyor and *#G.H. Rossmanith)) *Cooperative Research Centre for Cardiac Technology, Royal North Shore Hospital, St Leonards, NSW 2065, and School of Mathematics, Physics, Computing and Electronics, Macquarie University, North Ryde, NSW 2113, Australia.

Chronic electrical burst pacing of skeletal muscle can be manipulated to obtain different repertoires of contractile protein isoforms which impart specific mechanical properties. Latissimus dorsi muscles (LDM) of 6 sheep were paced *in vivo* for 4 or 8 weeks (Telectronics Model 7220 Myostimulators). Experimental and contralateral control LDMs were excised and fibres were chemically skinned using glycerol. Ca^{2+}-activated myosin cross-bridge kinetics of single fibres were assessed by mechanical perturbation analysis using pseudo-random-binary-noise to determine stiffness minimum frequency (f_{min}). Fibres from controls mostly displayed fast mechanics (f_{min}=6.13±0.98 Hz (mean±SD), n=54). Few slow (f_{min}=1.48±0.41 Hz, n=5) or intermediate (f_{min}=4.70±0.14 Hz, n=2) fibres were present. Pacing induced a large, time-dependent increase in the proportion of slow fibres. However, slow f_{min} was not dependent upon duration of pacing (pooled f_{min}=0.89±0.25 Hz, n=54). The proportion of intermediate fibres was unaltered, indicating that transformation from fast to slow crossbridge kinetics depended upon a sudden, discrete step in contractile protein gene expression. However, f_{min} of LDM control slow and paced slow fibres were not equivalent ($p<0.05$), suggesting that f_{min} is dependent upon more than one contractile protein.

Th-Pos189

EFFECT OF TEMPERATURE ON THE KINETICS OF PHOSPHATE RELEASE IN CARDIAC MUSCLE STUDIED BY PHOTOLYSIS OF CAGED-PHOSPHATE.

((Hunter Martin and R.J.Barsotti)) Bockus Research Institute, The Graduate Hospital, Philadelphia, Pennsylvania 19146

Martin and Barsotti (*Biophys.J.* 70:A47) reported the initial rate of tension decline (k_R) following photolysis of caged-phosphate (1-(2-nitro)phenylethyl phosphate) in fully activated (pCa 4.5, I=200mM, 21° C) triton skinned Guinea-pig trabeculae saturates at higher concentrations of inorganic phosphate ([P_i]), consistent with a two step mechanism of phosphate release in which a force bearing state containing the products of ATP hydrolysis isomerizes to release phosphate and generate a second force bearing state. To understand more completely the relation between these states and the non-force bearing state preceding them, we have determined k_R at lower temperatures (n = 9). Under these conditions an extended lag precedes force decline (see Figure, approximately 800μM P_i released in each trace). k_R increases at $7.9 \times 10^2\ M^{-1}\ sec^{-1}$ extrapolating to $1.8\ sec^{-1}$ at $[P_i] = 0$ and does not saturate in the range of phosphate concentrations attainable (300μM - 3mM). These results demonstrate the lag in force decline predicted by a two step mechanism and show the transition to the initial force bearing state ($AM{\cdot}ADP{\cdot}P_i$) is highly temperature sensitive ($Q_{10} \cong 9$). Supported by NIH HL40953

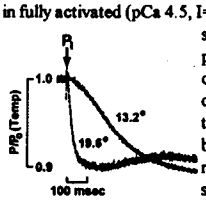

Th-Pos190

THE EFFECT OF POLYETHELENE GLYCOL ON THE MECHANICS AND ATPASE ACTIVITY OF ACTIVE MUSCLE FIBERS

((**K. Myburgh,** M. Chen, T. Pham and R. Cooke)) Dept. of Biochemistry, & Biophysics, Cardiovascular Research Institute, University of California, San Francisco, CA 94143.

Addition of polyethelene glycol (PEG) is known to potentiate protein-protein interactions. Previous work by ourselves (Highsmith et al, Biophys. J., 70:2830, 1996) and by H.White (White et al, Biophys J. 68:A17, 1995) has shown that addition of PEG potentiates the apparent affinity of myosin for actin in the presence of ATP by a factor of 10-25. To determine the effect of an increase in the apparent affinity of myosin for actin in active muscle fibers we added 0-5% PEG (MW: 300 or 4000). Addition of PEG (5%) to active fibers increased isometric tension by 30%, decreased velocity by 30% and decreased the isometric ATPase activity by 40%. To determine which transitions are altered by PEG we measured the effect of two ligands, ADP and BDM ± PEG. PEG had no effect on the perturbation of added ADP, suggesting that PEG has not changed the affinity of ADP for myosin at the end of the powerstroke. In the presence of BDM (a molecule that stabilizes a prepowerstroke state) tension was inhibited to 13% of control, while stiffness remained high at 71% of control. This suggests that PEG enhances binding of this prepowerstroke state to actin, further suggesting that a large protein-protein interface is formed in this complex. Addition of PEG would be useful for enhancing the fraction of myosin heads attached to actin for structural studies. Supported by the NIH, MDA (Supported by HL32145 and a grant from the MDA)

Th-Pos191

REGULATION OF TENSION REDEVELOPMENT KINETICS BY $[Ca^{2+}]$ IN INTACT CARDIAC MUSCLE.

((**A.J. Baker,** E.C. Keung, V.M. Figueredo, S.A. Camacho)). Depts. Radiology & Cardiology, Univ. Calif. San Francisco. CA 94143.

In skinned skeletal muscle, Ca^{2+} has been suggested to regulate tension development by affecting cross-bridge attachment kinetics. However, in skinned cardiac muscle, there is uncertainty on whether cross-bridge attachment kinetics are also regulated by Ca^{2+}; and there have been no studies of intact cardiac muscle. Therefore, the **goal** of this study was to determine if Ca^{2+} regulates cross-bridge attachment kinetics in intact cardiac muscle. **Methods.** In intact rat RV trabeculae, graded steady state levels of tension and cytosolic $[Ca^{2+}]$ were produced by tetanization with different superfusate $[Ca^{2+}]$. During tetani, cross-bridges were forcibly detached by a rapid muscle stretch. Tension redeveloped exponentially and cross-bridge attachment kinetics were reflected in the rate constant for tension redevelopment (*ktr*). **Results.** The figure shows *ktr* versus tension for tetani at different superfusate $[Ca^{2+}]$ (values normalized to maximum). The figure shows there was a close relationship between *ktr* and tension when tetanic tension was increased by increasing superfusate $[Ca^{2+}]$ ($r = 0.906$; $p < 0.001$). **Conclusion:** These findings suggest that in cardiac muscle, Ca^{2+} regulates tension development via an effect on cross-bridge attachment kinetics.

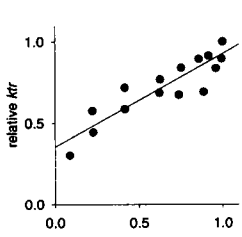

Th-Pos192

CROSS-BRIDGE KINETICS OF SKELETAL MUSCLE FIBRES UNDER RIGOR CONDITIONS STUDIED WITH EDC CROSS-LINKING

((**M. Ketelaars**[1,2], U.A. van der Heide[1,2], B.W. Treijtel[1], E.L. de Beer[2], T. Blangé[1])) [1]Dep. of Physiology, UvA, [2]Dep. of Med. Physiology, UU (NL). (Spon. by T. Blangé)

Stretch and release experiments on skeletal muscle fibres under rigor conditions suggest that the tension response on a length change is governed by a wide range of reaction constants. In earlier studies this was attributed to transitions between distinct strongly bound states in rigor. The nature of these transitions is unknown, but could be connected to slip of myosin heads along the thin filament (Biophys.J., submitted).

In this study skinned skeletal muscle fibres of the frog were cross-linked with EDC in order to covalently bind myosin cross bridges to the thin filament. Stepwise length changes were applied to determine the frequency dependence of the Young's modulus. The effectiveness of the cross-linking with respect to the actin-myosin linking was tested in two ways. First a comparison of the Young's modulus was made in rigor and in a high-salt relaxing solution and secondly the amount of stress relaxation was determined by measuring the tension decay after stepwise stretching of the fibre up to its active isometric tension.

The results show that after half an hour of EDC incubation the frequency dependence of the Young's modulus in high salt relaxing solution resembles that in rigor with a magnitude of about 80%. However, stress relaxation was not significantly changed. It can not be excluded that a mechanism other than cross-linking actin to myosin, is responsible for the increased Young's modulus in high-salt relaxing solution and that the properties of the actin-myosin link are not greatly affected.

Th-Pos193

Muscle Fiber ATP Consumption Rate Depends on Myosin Heavy Chain (MHC) Isoform Expression and Power Output ((Young S. Han, Gary C. Sieck)) Dept. of Anesthesiology and Physiology & Biophysics, Mayo Foundation, Rochester, MN 55902. (Spon. by P. Fischer)

In 1923, Fenn was the first to demonstrate that energy utilization by muscle fibers increases as work increases (J. Physiol. (Lond) 58:175-203, 1923). Subsequently, a number of studies have verified the Fenn Effect at the level of whole muscles. The purpose of the present study was to compare the ATP consumption rates of different fiber types in the rat diaphragm during isometric and isovelocity conditions. Single triton-X permeabilized fibers were mounted between force and displacement transducers in a Scientific Instruments Muscle Research System. Fibers were maximally activated at a pCa 4.0, and ATP consumption rate was measured using an NADH-linked fluorescence technique. Fiber type was determined *post hoc* by immunoreactivity to specific myosin heavy chain (MHC) antibodies and by electrophoretic analysis. The ATP consumption rate of type IIx/b fibers was found to be highest during both isometric activation and isovelocity conditions, followed by type IIa and type I fibers (1.54 ± 0.21, 0.81 ± 0.12 and 0.52 ± 0.06 nmol mm^{-3} s^{-1}, respectively). In all fibers, ATP consumption rate was found to be highest during isovelocity shortening corresponding to maximum power output (~33% of maximum shortening velocity for each fiber). Compared to isometric conditions, ATP consumption rate increased by ~80-110% during maximum power output. These results confirm the Fenn effect at the level of individual muscle fibers and verify the importance of MHC isoform expression in muscle fiber energetics. Supported by NIH grants HL34817 and HL37680.

Th-Pos194

EFFECTS OF CTP ON POWER OUTPUT OF FAST AND SLOW SINGLE SKINNED SKELETAL MUSCLE FIBERS

((Philip A. Wahr and Joseph M. Metzger)) Dept. of Physiology, Univ. of Michigan, Ann Arbor, MI 48109

The effect of the ATP analog CTP on the power output of Ca^{2+}-activated (pCa 4.5) single skinned skeletal muscle fibers from rabbit psoas and rat soleus at 15°C was investigated. Experiments were performed with either 4 mM ATP or 4 mM CTP in the bathing solutions. Additional experiments performed with 10 mM CTP to ensure sufficient nucleotide saturation of the fibers gave qualitatively similar results. V_{max} was determined by fitting Hill's equation to plots of force per cross sectional area (CSA) vs. shortening velocity per fiber length (l_f). Similarly, power curves were determined from the product of normalized force and shortening velocity. At 4 mM ATP, psoas fibers produced a V_{max} of 3.26 ± 0.50 l_f/s and a peak power of 36.6 ± 2.3 kW/m^3 (n = 4). Soleus fibers displayed a slower V_{max} of 1.94 ± 0.24 l_f/s and a lower peak power of 13.5 ± 0.8 kW/m^3 (n = 13). Substitution of 4 mM CTP for 4 mM ATP significantly reduced V_{max} to 1.02 ± 0.03 l_f/s (n = 4) in psoas and to 0.99 ± 0.10 l_f/s (n = 9) in soleus, thus eliminating the fiber type difference in V_{max}. Also, peak force was decreased in soleus fibers to 0.75 ± 0.01 Po under these conditions. Since CTP produced decreases in both V_{max} and Po, we expected CTP to produce less peak power in these fibers than ATP. Surprisingly, the peak power in soleus fibers was unaffected by the change in nucleotide, and only slightly reduced in psoas fibers. This unexpected result is explained by a 3-5 fold decrease in the curvature of the force-velocity fit, as measured by a/Po, in both psoas and soleus fibers. These results are indicative of a relationship between the strain dependent rate of crossbridge detachment and the nucleotide.

Th-Pos195

CORRELATIONS BETWEEN MAXIMUM SHORTENING VELOCITY AND ISOMETRIC ATPASE ACTIVITY IN SINGLE MUSCLE FIBRES: BARANY'S PLOT REVISITED.

((Roberto Bottinelli, °Carlo Reggiani°, Ger J.M. Stienen°)) °Institute of Human Physiology, University of Pavia, Italy, and °Laboratory for Physiology, Free University, Amsterdam, The Netherlands.

Our previous studies have shown that whereas maximum shortening velocity (Vo) is modulated by both myosin heavy chain (MHC) and myosin light chain (MLC) isoforms composition of muscle fibres, isometric ATPase activity (Ao) is determined only by MHC isoforms. If Vo and Ao are controlled by two at least partially independent mechanisms, their relation might be less strict than generally believed. Single muscle fibres from rat (n=63) and from human (n=93) muscles were chemically skinned and maximally activated at 12°C. Ao was determined photometrically from NADH absorbance. Vo was determined with the slack test method. On the basis of MHC isoform composition determined by polyacrylamide gel electrophoresis, rat fibres were classified as slow (type 1), 2A, 2X and 2B and human fibres as type 1, 2A and 2B. A significant positive correlation was found between the mean values of Vo and the mean values of Ao of the different fibre types. In each species the higher Vo the greater Ao. Comparing homologous isoforms, rat fibres had higher Vo and Ao than human fibres. A closer inspection, however, revealed that the coupling between Ao and Vo was not so tight. The ratio between Vo and Ao varied up to 3 times between fibre groups. For example, slow fibres of the rat and type 2A human fibres had very similar Vo (1.13 and 1.12 L/s respectively) but 2 times different Ao values (0.045 and 0.103 mM/s respectively). Vo was 3 times higher in rat than in human slow fibres (1.13 versus 0.28 L/s), but their Ao values were very similar (0.045 versus 0.044 mM/s). Furthermore, when Vo was plotted versus Ao within sets of fibres containing the same MHC, no significant relation was found. The present results show that in single fibres Ao and Vo are not so closely coupled as expected on the basis of whole muscle studies (Barany, J. Gen. Physiol. 50:197-218, 1967). This is consistent with the evidence that two distinct sites of the myosin molecule and two different steps of the acto-myosin cycle control enzymatic activity and motile activity.

Th-Pos196

HIGH TIME-RESOLUTION MEASUREMENTS OF ATPASE ACTIVITY DURING CONTRACTION AND RELAXATION IN RAT CARDIAC MUSCLE.

((Z.H. He, R. K. Chillingworth, M. Brune, M.R. Webb and M. A. Ferenczi)) National Institute for Medical Research, The Ridgeway, Mill Hill, London NW7 1AA, UK

ATPase rates in rat right ventricular trabeculae were measured after permeabilization with Triton X-100 by monitoring phosphate release from ATP hydrolysis using the MDCC-PBP assay(1). The trabeculae were incubated in rigor with 0.6-1.2 mM MDCC-PBP, 10 mM NPE-caged ATP in the presence or absence of calcium at 12 °C, pH 7.1. Following photolytic release of ATP in the absence of calcium, the relaxation from rigor was accompanied with a slow and linear increase in fluorescence corresponding to an ATPase rate of 0.23 ± 0.02 s^{-1} (n=8, assuming [S1]=157 μM)(2). In the presence of calcium, photorelease of ATP caused tension to rise with $t_{1/2}$ = 66±7 ms (n=6) and fluorescence to increase bi-exponentially with an initial rate of 5.7 ± 0.9 s^{-1}(n=6) and amplitude of 176±9 μM. During the second and third turnover, the ATPase rate reduced to 3.0 ± 0.3 s^{-1} and 2.0 ± 0.2 s^{-1}, respectively.

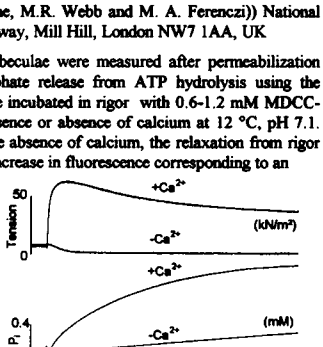

Tension and P_i traces (average of 6 expts.)

(1) Ferenczi, M.A., He, Z.-H., Chillingworth, R. S., Brune, M.., Corrie, J.E.T. Trentham, D. R. & Webb, M.R.(1995) *Biophys.J.* **68**, 191s-193s

(2) Barsotti, R.J. & Ferenczi, M.A. (1988) *J. Biol. Chem* **263** 16750-16756.

Th-Pos197

PLATEAU IN SHORTENING-INDUCED REDUCTION OF FORCE REDEVELOPMENT RATE IN FROG SKELETAL MUSCLE FIBERS.

((**R. Vandenboom**, D.R. Claflin, and F.J. Julian)). Department of Anesthesia Research Laboratories, Brigham and Women's Hospital, Harvard Medical School, Boston MA 02115.

We examined the effect of length step size on force redevelopment rates after shortening in frog skeletal muscle fibers. Single fibers were dissected from tibialis anterior muscles of *R. temporaria* and maintained at 3.0° C. Fibers (n=4) were stimulated at 30 s^{-1} to contract isometrically at initial sarcomere lengths ranging from 2.35 to 2.05 μm. During the plateau of the tetanus, step length changes of 0.05 to 0.35 μm per sarcomere were applied to drop active force to 0. After various periods of unloaded shortening (range: 1.5 ±0.2 to 52.0 ±1.7ms) force redeveloped at a fixed sarcomere length of 2.00 μm. The amplitude of the force redevelopment following each length step was similar for all step sizes. The effect of length step size on force redevelopment rate is shown in the figure. Data are normalized to the force redevelopment rate measured after the shortest step. For length steps up to 0.20 μm, increasing step sizes reduced force redevelopment rate. Length steps in excess of 0.20 μm had little additional effect on reducing force redevelopment rate. We hypothesize that the observed reductions in force redevelopment rates are mediated by shortening-induced reductions in Ca^{2+} binding to the thin filament. This effect may be saturated for shortening in excess of 0.20 μm. Supported by N.I.H. grant HL 35032.

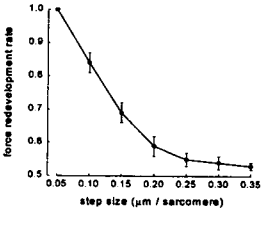

Th-Pos198

TENSION INCREASE WITH STRETCH IN ACTIVATED MYOFIBRILS NOT DUE TO INHOMOGENEITY. ((**Dwayne L. Dunaway,** Rocco Hüneke, Gerald H. Pollack)) University of Wash., Seattle, WA 98195

Experiments examining the relation between active tension and filament overlap have consistently yielded anomalous results: when activated specimens are ramp-stretched to less overlap, tension is increased. This unexpected result -- higher tension with less overlap -- conflicts with the accepted length-tension relation. It has been suggested that this behavior might arise fortuitously out of "undetected" sarcomeres whose dynamics may have differed from the bulk of the population; one hypothesis is that upon stretch a few weaker sarcomeres become unstable and elongate uncontrollably to lengths where passive tension can support the increased tension. To follow up, we are carrying out similar experiments on single myofibrils. Any ambiguity that might arise from hidden, or undetected sarcomeres is averted in the single myofibril because all sarcomeres are in series and bear the same tension, and because the length of each sarcomere can be measured. Myofibrils were activated, then stretched by 5 - 10% of initial length. Tension rose steeply during stretch and then declined to a new, steady value. This steady value was always higher than the prestretch value, even though measurements on *single sarcomeres* showed that these sarcomeres were stretched to less filament overlap. The passive tension increase due to sarcomere elongation was negligible in comparision to the tension increase with stretch. Inhomogeneity is present in the activated myofibril; however, essentially all sarcomeres elongate moderately upon stretch, irrespective of sarcomere length prior to stretch. It appears that increased tension with less overlap is a property inherent to the single sarcomere.

Th-Pos199

A MODEL FOR FORCE PRODUCTION DURING STRETCH OF SKELETAL MUSCLE FIBERS. ((E. Burmeister Getz, R. Cooke and S. **Lehman**)) Dept. of Biochem./Biophysics, UCSF, San Francisco, CA 94143, Dept. of Hum. Bio., UCB, Berkeley, CA 94720 and UCSF/UCB Bioengineering Graduate Group, Berkeley, CA 94720

We present data on single glycerinated rabbit psoas fibers stretched at constant velocity under sarcomere length control, showing that: 1. Force rises in two phases: a steep first phase, over an extension of only a few nm per half sarcomere, and a much less steep second phase. 2. Phase I ends after extension beyond a critical strain. 3. For velocities exceeding 1 L/s, the critical strain, the force reached at the critical strain, and stiffness after exceeding the critical strain are nearly independent of velocity of stretch. We propose a cross bridge model to account for these observations. In the isometric fiber, most attached cross bridges are in a strongly-attached state. When the fiber is forcibly stretched, these cross bridges are stretched into a new region of the same attached state, accessed only by stretch. The phase transition (1) corresponds to attached cross bridges leaving the isometric distribution. The critical strain (2) corresponds to the width of the isometric distribution. The velocity independences above 1 L/s of critical strain, force at critical strain and stiffness (3) result from a very rapid on rate for cross bridges once stretched beyond critical strain, and a very rapid off rate beyond a maximum strain.

Supported by UCB Graduate Opportunity Fellowship and HL32145.

Th-Pos200

EFFECTS OF AGE AND GENDER ON CONTRACTILITY AT THE WHOLE MUSCLE AND SINGLE FIBRE LEVEL IN THE RAT SOLEUS AND EXTENSOR DIGITORUM LONGUS MUSCLES

((F.Yu, H. Degens, X. Li, H. Gür and L. Larsson)) Department of Clinical Neurophysiology, Karolinska Hospital, Stockholm, Sweden

Profound impairment of motor function, such as muscle weakness and slowing of movement, is a prominent feature of old age in most mammals, but the mechanisms underlying these impairments are not fully understood. In man, the time course of the age-related decline in maximum voluntary force has been reported to differ between men and women. To investigate the effects of ageing and gender on the fibre type composition, force generating capacity and isometric twitch contraction and half relaxation times in whole muscle, and the maximal unloaded shortening velocity (V_0 in ML/s) and the myosin heavy chain (MyHC) isoform composition in single fibres, we used soleus and extensor digitorum longus (EDL) muscles of young (3-6 months) and old (20-22 months) rats of both sexes. The force generating capacity was not significantly affected by age or gender in either muscle. A significant age-related decrease in V_0 was found in single fibres of the soleus, expressing the ß/slow MyHC isoform (male: 1.15 ± 0.47, $n = 78$ vs. 0.62 ± 0.27 $n = 64$; female: 1.00 ± 0.35 $n = 39$ vs. 0.67 ± 0.52, $n = 48$; young vs. old; $p < 0.0001$), but not in fibres expressing type IIA, IIX, IIB or different combinations of these MyHCs of the EDL. In the rat, there were no clear-cut gender-related differences in physiological, biochemical and morphological properties of the soleus and EDL muscles and muscle cells.

SMOOTH MUSCLE PHYSIOLOGY II

Th-Pos201

INHIBITION OF p44 AND p42 MAP KINASE ACTIVITY DOES NOT ALTER SMOOTH MUSCLE CONTRACTION IN SWINE CAROTID ARTERY

((**Isabelle Gorenne,** Xiaoling Su and Robert S. Moreland)) Bockus Research Institute, Graduate Hospital, Philadelphia PA 19146.

The p44 and p42 mitogen-activated protein kinases (MAPK) are activated during contractile agonist stimulation in differentiated vascular smooth muscle. One potential substrate for activated MAPK is caldesmon. Since caldesmon phosphorylation is associated with enhanced actomyosin ATPase activity, MAPK catalyzed caldesmon phosphorylation has been proposed as a possible regulatory pathway in smooth muscle. MAPK are activated by dual phosphorylation of specific Tyr and Thr residue by a MAPK kinase (MEK). In this study we examined the role of MAPK in vascular contraction by using PD98059, reported to be a specific MEK inhibitor. Quantification of MAPK activity was assessed by measurement of MAPK phosphorylation levels in homogenates from arterial strips using an anti-active MAPK antibody specific for the doubly phosphorylated enzyme and the direct measurement of MAPK catalyzed phosphorylation of MBP_{95-98}. MAPK phosphorylation, stimulated by either histamine or PDBu, was inhibited by PD98059 (100 µM). Concentration-dependent inhibition of p44 and p42 phosphorylation levels by PD98059 was linearly correlated with inhibition of MAPK activity. In contrast, PD98059 at concentrations that inhibited 90% of the MAPK activity did not alter either the sensitivity or the maximal contraction of smooth muscle stimulated by histamine or PDBu. In conclusion, our data suggest that the p44 and p42 isoforms of MAPK are not involved in regulation of vascular smooth muscle contraction. These results do not however preclude a role for other isoforms of the MAPK family. This study was supported, in part, by NIH grants HL37956 and HL46704 and a fellowship from the SEPA affiliate of AHA.

Th-Pos202

RHOA-INDUCED CALCIUM SENSITIZATION OF SMOOTH MUSCLE: ISOLATION OF A 116 kDa RHOA-BINDING PROTEIN ((**L.A. Walker,** R.K. Nakamoto, A.V. Somlyo, and A.P. Somlyo)) University of Virginia,, Dept. Mol. Phys. & Biol. Physics, Charlottesville, VA 22908 (Spon. By G. Marechal)

RhoA Ca^{2+}-sensitizes force and MLC_{20} phosphorylation in smooth muscle, but is not a direct inhibitor of smooth muscle myosin phosphatase [(1)]. The purpose of the current study is to identify the effector proteins involved in RhoA-induced Ca^{2+}-sensitization. We show here that RhoA can be immunoprecipitated in resting rabbit ileum smooth muscle, but not in smooth muscle Ca^{2+}-sensitized with GTPγS, suggesting that the reactive epitope is masked, possibly by an effector protein. Pre-ADP-ribosylation of RhoA by the bacterial exoenzyme C3, known to inhibit activation of RhoA, preserves the immunoprecipitability of RhoA in preparations subsequently treated with GTPγS. Additionally, by using RhoA-GST affinity columns, we have isolated a 116 kDa protein that interacts with GTP-bound Val14-RhoA, but not with GDP-bound wild type RhoA. Sequencing of this putative effector protein is in progress. Supported by NIH grant HL19242, HL07284 and AHA VA 96-F-02.

1. Gong, M.C. et al. (1996) *Proc. Natl. Acad. Sci.* 93:1340-1345

Th-Pos203

POSSIBLE ROLE OF ATYPICAL PROTEIN KINASE C (PKC) ACTIVATED BY ARACHIDONIC ACID (AA) IN Ca^{2+} -SENSITIZATION OF SMOOTH MUSCLE. ((**Ph. Gailly**, M.C. Gong, A.V. Somlyo and A.P. Somlyo)) Department of Molecular Physiology and Biological Physics, University of Virginia, Charlottesville, Virginia 22908

We compared the effects of pseudosubstrate peptide inhibitors of, respectively, conventional ($PKC\alpha_{22-30}$) and atypical PKCs ($PKC\zeta_{116-124}$) on Ca^{2+}-sensitization (Ca^{2+}-S) of force and myosin light chain phosphorylation (MLC_{20}) in femoral artery (FA) and portal vein (PV) permeabilized with β-escin. Ca^{2+}-S induced by the α_1-adrenergic agonist phenylephrine (PE) and by AA was significantly (about 50%) inhibited by $PKC\zeta_{116-124}$, but not by the conventional PKC (cPKC) peptide inhibitor that inhibited diacylglycerol (DAG) -induced Ca^{2+}-S. The effects of the two peptide inhibitors on PE-induced Ca^{2+}-S were not additive, suggesting that cPKCs and aPKCs converge on a common mechanism. A phospholipase A_2, (PLA_2) inhibitor, ONO-RS-082, completely abolished the PE-induced release of AA in FA and decreased by 50% the PE-induced Ca^{2+}-S of force; this effect was not additive to that of the aPKC peptide inhibitor, suggesting that some of the effect of AA is due to activation of aPKC(s) and/or related kinase(s). Our results (see also 1) also indicate that DAG- and phorbol ester-activated PKCs, such as PKCε, have only minor roles in Ca^{2+}-S. The inability of the combination of the two (aPKC and cPKC) inhibitors to completely eliminate Ca^{2+}-sensitization also suggests the presence of a third, still unidentified, pathway of this mechanism.

[1]Jensen et al., *Biochem. J.* 318:469-475.

Supported by NIH grant PO1-HL48807.

Th-Pos204

EFFECTS OF INHIBITED POLYAMINE SYNTHESIS IN TISSUE CULTURE ON CONTRACTION OF INTESTINAL SMOOTH MUSCLE

((**K.H. Swärd**, B.-O. Nilsson and P. Hellstrand)) Dept of Physiology and Neuroscience, University of Lund, S-223 62 Lund, Sweden

To investigate the putative influence of polyamines on excitation-contraction coupling, longitudinal muscle from guinea-pig ileum was cultured in the presence and absence of CGP 48664 and DFMO, specific inhibitors of polyamine and diamine biosynthesis. 10 μM CGP 48664 decreased spermidine and spermine contents to 50 % of control, whereas putrescine was increased 20-fold, consistent with feedback stimulation of ornithine decarboxylase activity. Spontaneous contractile activity was increased, while responsiveness of depolarized strips to cumulative addition of calcium was decreased. The latter effect was not associated with a reduction of intracellular calcium as measured with Fura-2. 1 μM CGP 48664 had similar effects on polyamine contents, but showed less influence on spontaneous activity and on sensitivity of depolarized strips to Ca^{2+}. When 1 μM CGP 48664 was combined with 1 mM DFMO to reduce ornithine decarboxylase activity, putrescine contents decreased below control levels, while spermidine and spermine were still reduced. This was not accompanied by any alteration in the relationship between extracellular calcium and force. Although tissue polyamine contents and physiological parameters depend differently on inhibitor concentration, the results are consistent with previously demonstrated effects of di- and polyamines on membrane activity and excitation-contraction coupling.

Th-Pos205

VERAPAMIL PREVENTS DECLINE IN FORCE DEVELOPMENT OF CULTURED ARTERIAL SMOOTH MUSCLE

((**A. Lindqvist**, B.-O. Nilsson and P. Hellstrand)) Dept of Physiology and Neuroscience, Lund University, S-223 62 Lund, Sweden

The addition of the growth stimulator fetal calf serum (FCS, 10 %) to rings of rat tail artery causes an increase in $[Ca^{2+}]_i$, accompanied by contraction. This response was inhibited by the calcium entry blocker verapamil. To investigate the effect of Ca^{2+}-entry blockade on growth and contractility, rings of rat tail artery were cultured for four days in medium with or without FCS, then mounted for tension registration and stimulated with noradrenaline (NA) or high-K^+ solution. Growth was quantitated by [^{3}H]-thymidine incorporation and increase in protein contents. FCS stimulated DNA synthesis two-fold and increased protein contents by 70 %. The growth-stimulated cultured rings developed less force than freshly prepared rings (2.2 ± 0.3 vs. 8.3 ± 1.0 mN/mm). The addition of 1 μM verapamil during culture increased maximal NA evoked force to 5.0 ± 0.4 mN/mm but did not affect DNA synthesis or protein contents. Growth-arrested rings, cultured without FCS, developed more force than growth-stimulated rings (6.9 ± 0.6 mN/mm). Verapamil did not affect maximal force in these rings. Similar responses were seen when contraction was elicited by high-K^+ solution. Preliminary data suggest that culture with verapamil does not affect force after permeabilization with β-escin. We conclude that verapamil, present during culture, preserves contractility of arterial smooth muscle, and that this effect is not parallel to inhibition of growth.

Th-Pos206

OVEREXPRESSION OF INACTIVE MYOSIN LIGHT CHAIN KINASE IN SMOOTH MUSCLE CELLS. ((R.W. Grange, Z.Jiang, R. Higginbotham, K.E. Kamm)) Dept. Physiol. U.T. Southwestern, Dallas, TX 75235.

Phosphorylation of the regulatory light chain (RLC) of smooth and nonmuscle isoforms of myosin II by myosin light chain kinase (MLCK) activates actomyosin MgATPase. We hypothesized that inhibition of MLCK activity would slow or suspend actomyosin-dependent functions in cells, and in addition, might reveal potential collateral regulatory processes in smooth muscle. An inactive form of MLCK was engineered by mutating the reactive lysine 725 of rabbit smooth muscle MLCK to alanine (K725A). In protein kinases, this invariant reactive lysine is critical to binding ATP for phosphotransfer; thus K725A should bind but not phosphorylate its specific substrate the RLC. To express the dominant-negative phenotype with high efficiency in cells, an adenovirus encoding CMV-K725A MLCK was constructed. For successful packaging, the full length K725A cDNA (3.8 kb) was truncated (T) by ≈700 bases removing the C-terminal "telokin" region of MLCK. T-K725A was sub-cloned into the pACsk.2CMV5 vector and co-transfected into 293 cells with the adenoviral genomic vector pJM17 for homologous recombination (Adv-T-K725A). Compared to wild-type (WT) MLCK, both the full length (FL) and truncated mutants are catalytically inactive when assayed in COS cell lysates (66±5 (WT) vs 1.1± 0.7 (FL) vs 0.5±0.2 (T) vs 0.5 (control) pmol/min/μl). Bovine tracheal (BT) smooth muscle cells (pass 1, serum-free) infected with Adv-T-K725A expressed a 10-fold excess of T-K725A compared to endogenous MLCK (200 pg vs 25 pg/μg total protein) 72 hr after infection with titers yielding 90%. BT cells infected with Adv-T-K725A for 72 hr followed by replating at low density demonstrated ≈5-fold reduction in rates of proliferation compared to control cells. Myosin II is involved in cell shape changes during the cell cycle (cytokinesis, cell spreading). The present results indicate that the strategy of high efficiency expression of inactive MLCK to inhibit endogenous MLCK activity will yield insights into the regulation of actomyosin-dependent cytoskeletal and contractile functions.

Th-Pos207

DIFFERENCES OF ENDOTHELIUM-DEPENDENT VASORELAXATION MEDIATED BY EDHF IN SMALL RESISTANCE CEREBRAL VERSUS PERIPHERAL VESSELS OF GUINEA PIG. ((**H. Dong**, W.C. Cole and C.R. Triggle)), Smooth Muscle Research Group and Department of Pharmacology & Therapeutics, University of Calgary, Calgary, Alberta, Canada, T2N 4N1.

The contribution of nitric oxide (NO) in mediating endothelium-dependent relaxation in vascular smooth muscle is now well established, however, the role of a putative endothelium-derived hyperpolarizing factor (EDHF), which is pharmacologically distinct from NO or prostacyclin, is still unclear. In the present study, the endothelium-dependent vasorelaxations mediated by EDHF in middle cerebral artery (MCA) and mesenteric artery (MA) of guinea pig were compared and the effects of K^+ channel blockers (glibenclamide and charybotoxin (CTX)) and cytochrome P450 inhibitors (17-octadecynoic acid (17-ODYA), clotrimazole and 1-aminobenzotriazole (1-ABT)) were determined. ACh-induced relaxations of histamine preconstricted MCA or of cirazoline preconstricted MA were measured in the presence of 100 μM N^G-nitro-L-arginine (L-NNA) plus 10 μM indomethacin (Ind) to block NO synthase and cyclooxygenase. This L-NNA/Ind resistant relaxation induced by ACh was more obvious in MA than in MCA (maximum relaxation 98% *vs* 76%). In MCA, the EDHF-mediated relaxation was unaffected by 10 μM glibenclamide or 3 μM 17-ODYA, but was abolished by 0.1 μM CTX or 1 μM clotrimazole. However, in MA, the EDHF-mediated relaxation was unaffected by glibenclamide or clotrimazole, but largely inhibited by CTX and 17-ODYA. Interestingly, 1-ABT concentration-dependently augmented the EDHF-mediate relaxation in MA. Our data indicate that EDHF is a major factor mediating endothelium-dependent vasorelaxation in both small resistance cerebral and peripheral vessels of guinea pig. We also suggest that the nature and/or the cellular mechanisms of EDHF are different in cerebral *vs* peripheral vessels. (Supported by the AHFMR and MRC)

Th-Pos208

SUB-CONTRACTILE CONCENTRATIONS OF ANGIOTENSIN II ENHANCE MYOSIN LIGHT CHAIN PHOSPHORYLATION IN RAT TAIL ARTERY SMOOTH MUSCLE CELLS.

S.K.O'Neill, M.P.Walsh, X-F.Li, & **C.R.Triggle**. Smooth Muscle Research Group and Departments of Pharmacology & Therapeutics and Medical Biochemistry, The University of Calgary, 3330 Hospital Drive NW, Calgary, Alberta,Canada T2N 4N1.

A number of vasoactive factors have been shown to amplify adrenergic mediated vasoconstriction in vascular tissue, however, the molecular mechanisms involved remain unknown. We have previously shown that angiotensin II (AII), at concentrations too low to initiate a direct contractile response in rat tail artery or increase intracellular $[Ca^{2+}]$ as measured with fura 2, enhances responses mediated by alpha 1 and alpha 2 adrenoceptor activation. In the present study we have measured the effects of AII on myosin light chain (LC_{20}) phosphorylation in rat tail artery ring preparations. 10nM AII increased phosphorylation levels from 0.18+0.002 to 0.31+0.03 mol P_i/mol LC_{20} but did not elicit contraction of the tissue. Furthermore this same concentration of AII enhanced the alpha 2 mediated increase in both contraction and LC_{20} phosphorylation. Pretreatment with PKC inhibitors, such as chelerythrine, inhibited both the AII-induced increase in LC_{20} phosphorylation and the enhanced response to an alpha 2 agonist. These data indicate that contractile "subthreshold" concentrations of AII enhance the responsiveness of vascular smooth muscle by a mechanism(s) involving LC_{20} phosphorylation and the activation of PKC. (Supported by MRC and AHFMR.)

Th-Pos209

THE RELATIONSHIP BETWEEN REGULATORY MYOSIN LIGHT CHAIN (rMLC) PHOSPHORYLATION AND ATP UTILIZATION IN DETERGENT-SKINNED CANINE TRACHEAL SMOOTH MUSCLE (CTSM) ((K.A. Jones, Y.S. Prakash, G.C. Sieck, R.R. Lorenz, and D.O. Warner)) Departments of Anesthesiology and Physiology and Biophysics, Mayo Clinic, Rochester, MN 55905

The Hai and Murphy kinetic model of smooth muscle energetics proposes that two populations of actin-myosin crossbridges contribute to force, one which is phosphorylated and rapidly cycling (high ATP usage), and a second which is nonphosphorylated and slowly cycling (low ATP usage). This model predicts that rMLC phosphorylation is the primary regulator of the crossbridge cycle rate during contraction and that the ATP usage associated with rMLC phosphorylation/dephosphorylation (phos/dephos) is high relative to that used by actin-myosin ATPase. This study tested these predictions in triton X-100-skinned CTSM strips. ATP usage was measured using NADH-linked fluorometry and rMLC phosphorylation was determined by 2-dimensional gel electrophoresis. 10 μM free Ca^{2+} (EC_{100}) caused sustained monophasic increases in isometric force, muscle stiffness (50 Hz frequency), and rMLC phosphorylation (from baseline values of 5±2% to steady-state values of 48±4%). In contrast, there was an initial increase in ATP usage from baseline values of 22±2 nmol cm^{-3} s^{-1} to 65±4 nmol cm^{-3} s^{-1} by 1 min., followed by a decline over 5-6 min. to steady-state levels of 37±4 nmol cm^{-3} s^{-1}. To determine the relative contribution of rMLC-phos/dephos to total ATP usage, a second set of strips was thiophosphorylated (>95%) with 2 mM ATPγS and then contracted with a low Ca^{2+} (<1 nM)/ high ATP (7.5 mM) solution. Whereas ATP caused sustained monophasic increases in isometric force and muscle stiffness, the increase in ATP usage was still biphasic, reaching peak values of 72±6 nmol•cm^{-3}•s^{-1} which declined to steady-state values of 43±4 nmol cm^{-3} s^{-1}. These findings are inconsistent with the Hai and Murphy model and suggest that rMLC phosphorylation is not the primary regulator of crossbridge cycle rate in airway smooth muscle. (Supported by NIH grant HL54757, HL45532, and HL30099).

Th-Pos210

SMOOTH MUSCLE FROM MICE LACKING DESMIN GENERATES LOWER ACTIVE FORCE AND HAVE INCREASED COMPLIANCE.
((R. Sjuve, Z. Li*, D. Paulin*, J.V. Small** and **A. Arner**)) Dept Physiol. and Neuroscience, Lund University, Sweden; *Inst. Pasteur, Paris, France; **Inst. Mol. Biol., Salzburg, Austria.

Mice with a null mutation introduced in the desmin gene (Li *et al.*, 1996; Dev. Biol. 175:362) were used to study the role of the intermediate filaments in transmission of force in smooth muscle cells. Vas deferens (VD) and urinary bladder (UB) were obtained from adult animals lacking desmin (*Des* -/-) and from age- and weight-matched wild-type animals (*Des* +/+). The relation between length and active/passive force was determined in intact preparations. Active force per cross-sectional area was decreased in the *Des* -/- compared with *Des* +/+ (VD to 42%; UB to 34%). This may in part be due to lowered cellular content of myosin (VD to 75%; UB to 84%). The organization of the contractile apparatus appeared unchanged in electron microscopy. Similar reduction in stress of skinned fibers from *Des* -/- exclude that altered activation mechanisms are involved. The results thus suggest that the reduced active force is due to low intrinsic force generation of the contractile filaments or subtle modifications in the coupling between the contractile elements and the cyto-skeleton. The relation between length and passive stress was less steep in the *Des* -/- and a second length force curve after maximal extension revealed a loss of passive stress. The results show that the intermediate filaments in smooth muscle have a role in cellular transmission of both active and passive force.

Th-Pos211

VASCULAR SMOOTH MUSCLE OXIDATIVE METABOLISM DURING VASOSPASM.
((Gail J. Pyne, Thomas Cadoux-Hudson, Zayne Domingo, George K. Radda & Joseph F.Clark)) University of Oxford, UK, Supported by the MRC)

Cerebral Vasospasm is a significant, sometimes fatal, complication after sub-arachnoid haemorrhage (SAH), in patients that survive the initial event. A potential cause of this phenomenon is the formation, from the mixture of blood and Cerebral Spinal Fluid (CSF), of a vasoconstrictive compound. This compound is thought to send the cerebral vessels into a pathological state of vasoconstriction, i.e. vasospasm. Experiments were done using CSF samples from patients that had had an SAH, and were either vasospastic (CSF_v) or asymptomatic (CSF_c). Lengths of porcine carotid artery were incubated and exposed to various agents inside an oxygen electrode chamber. It was found that the CSF_v elicited a >5 fold increase in O_2 consumption, but the CSF_c had no effect. The vessels were exposed to a variety of compounds to determine the mechanism; a PKC inhibitor, a PKA inhibitor, and an endothelin antagonist were not able to prevent the stimulation caused by CSF_v. The increase in O_2 consumption has, so far, proven to be irreversible, however, compounds acting through alpha-1 adrenergic receptors, such as dobutamine and noradrenaline, have been shown to PREVENT the stimulation.

Th-Pos212

DIFFERENTIAL DISTRIBUTION OF MYOSIN ISOFORMS IN PRIMARY CULTURES OF RAT AORTIC SMOOTH MUSCLE CELLS.
((D.G. Ferguson, R.Y-K. Pun and **A.F. Martin***)) Mol. and Cellular Physiology, Pharmacology and Cell Biophysics, Univ. of Cincinnati, Cincinnati, OH 45267

Smooth muscle cells in culture undergo loss of smooth muscle specific proteins and contractile capacity. We have examined the myosin heavy chain composition in cultured rat aortic smooth muscle cells at various times up to 14 days. The myosin heavy chain isoforms were separated by SDS-PAGE into three components, the smooth muscle myosin heavy chain isoforms, SM1 (204 kDa), SM2 (200 kDa) and the nonmuscle myosin heavy chain isoform (NM, 196 kDa). SM1, decreased to approximately 40 % of the total myosin over 14 days in culture whereas SM2 decreased to approximately 15-20% during the same time period. After five days in culture NM comprised 40-45% of the total myosin and remained at this level through 14 days. The distribution of SM1 and SM2 within individual cells was also determined using indirect immunofluorescence. The SM1 and SM2 isoforms were co-localized throughout the cell after 1 day in culture. After 3-4 days in culture the SM2 isoform was absent from the peripheral region of the cell where the SM1 isoform was detectable. After 3-5 days in culture the SM1 isoform remained distributed throughout the cell in stress-fiber-like structures but the SM2 isoform was predominantly localized around the nucleus. This differential response of the two smooth muscle myosin isoforms to cell isolation and culture conditions indicates differential regulation of the two isoforms at the protein level.

Th-Pos213

PURIFICATION, CHARACTERIZATION AND cDNA-CLONING OF CPI-17, A PHOSPHORYLATABLE PROTEIN PHOSPHATASE-1 INHIBITORY PROTEIN.
((**M. Eto**, S. Senba, F. Morita and M. Yazawa)) Division of Chemistry, Graduate School of Science, Hokkaido University, Sapporo 060, Japan

A phosphorylation-dependent inhibitory protein was identified as a novel regulatory factor for smooth muscle myosin LC_{20} phosphatase (MLCP). The isolated inhibitory protein from porcine aorta was phosphorylated by protein kinase C and dephosphorylated by PP2A. The phosphorylated inhibitory protein potently suppressed the MLCP with an IC_{50} of 1.4 nM and also decreased the activity of the catalytic subunit from skeletal muscle protein phosphatase-1 (PP1) (Eto et al., *J. Biochem.* (1995) **118**, 1104-1107). Based on the known, available partial amino acid sequence, cDNA clones of the inhibitory protein were isolated from porcine aorta. The complete amino acid sequence deduced from the nucleotide sequence shows the protein has 147 residues with a calculated molecular weight of 16.7 kDa. The sequence is distinct from that of any known PP1 inhibitory protein or PP1 subunit. Therefore, we have named this 17 kDa PKC-potentiated PP1 inhibitory protein, CPI-17. Northern hybridization analysis revealed that CPI-17 mRNA was predominantly expressed in porcine and rat smooth muscles over other tissues. These results suggest that CPI-17 is involved in the regulation of smooth muscle contraction through modulation of MLCP activity. (See next poster for the effect on smooth muscle contraction)

Th-Pos214

MOLECULAR CLONING AND CHARACTERIZATION OF SMOOTH MUSCLE CALCYCLIN (S100A6). **((C. Sutherland, B.G. Allen* and M.P. Walsh)) Smooth Muscle Research Group, University of Calgary, Calgary, Alberta T2N 4N1, Canada, and *Institut de Cardiologie de Montréal, Montréal, Québec, Canada.**

Full-length cDNA encoding smooth muscle calcylin (S100A6) was cloned from chicken gizzard total RNA using 5'- and 3'-Rapid Amplification of cDNA ends and PCR amplification. The deduced amino acid sequence contains 92 residues with 15 substitutions and a two-amino acid *C*-terminal extension when compared to rabbit lung calcyclin. Calcyclin was purified from chicken gizzard by Ca^{2+}-dependent hydrophobic chromatography, heat treatment and anion-exchange chromatography. *N*-terminal sequencing of two CNBr peptides confirmed its identity as calcyclin. Two isoforms of calcyclin (A and B), which differ with respect to the presence or absence of a *C*-terminal lysine, were identified and the native protein shown to exist as non-covalently associated homo-(AA and BB) and heterodimers (AB). Incubation of purified calcyclin AA with an extract of chicken gizzard did not result in degradation of calcyclin A or appearance of calcylin B suggesting that calcyclin B is a *bona fide* isoform rather than a proteolytic fragment generated during purification. Western blotting of chicken tissues with anti-(gizzard calcyclin) indicated abundant expression of calcyclin in smooth muscle tissues, in particular oesophagus, large intestine and trachea, with lower levels in lung, heart, kidney and brain, and none detectable in liver or skeletal muscle. (Supported by MRC Canada.)

Th-Pos215

SMOOTH MUSCLE MYOSIN PHOSPHORYLATION DETERMINES THE RATE OF FORCE REDEVELOPMENT INDEPENDENT OF THE MYOPLASMIC $[Ca^{2+}]_i$.

((J.D. Strauss, D. Saunders, R.A. Murphy)) Department of Molecular Physiology and Biological Physics, University of Virginia, Charlottesville, VA, 22906-0011

We measured the initial rate of force redevelopment after a quick release as an index of cross-bridge cycle rate in swine carotid medial rings. Force was allowed to redevelop for 2.5 seconds after a 10% step shortening. The time course of force redevelopment, expressed as a percentage of isometric stress just prior to the release, was fit to a double exponential function. The tissues were re-stretched to L_o using a ramp function (10-30 seconds). The slow restretch was followed by a transient decline in force to approximately 95% of original isometric stress, with recovery to stable isometric levels within 10 minutes. In contrast, a step restretch or short ramp (<5 seconds) irreversibly impaired active isometric stress generation. The transient decline in force after slow restretch (transient inactivation?) was a function of restretch rate such that slower ramps (>30 seconds) resulted in greater declines and delayed recovery of isometric stress. Force redevelopment after a quick release was highly reproducible over a series of releases in any given tissue, whether repeated within a single contraction or as measured in multiple contractions. Relative to control (109 mM KCl), lower concentrations of K^+ (40 mM) or a combination of stimuli (109 mM KCl plus 30 μM Histamine) resulted in marked differences in the rate of force redevelopment (71.7 ±3.6% SEM, n=11, p=0.0002 and 124 ±7.9%, n=4, p=0.0219, respectively). The rate of force redevelopment under these conditions was proportional to myosin regulatory light chain phosphorylation (MRLC-P_i). K^+-induced depolarization (109 mM) and histamine alone (30 μM) elicit comparable levels of MRLC-P_i. Histamine elicits a higher calcium sensitivity than K^+-depolarization, and thus achieves similar MRLC-P_i levels at lower concentrations of $Ca^{2+}{}_i$. The rates of force redevelopment under force-matched conditions were not significantly different (30 μM histamine, 95.9 ±4.6% of 109 mM KCl, n=7, p=0.583). These results are consistent with shortening velocity measurements under similar conditions and confirm that cross-bridge cycle rate is a function of MRLC-P_i and not dependent upon $Ca^{2+}{}_i$. This work supported by NIH PO1 HL 19242 (RAM) and AHA-Virginia Affiliate (JDS).

Th-Pos216

DOWNREGULATION OF G-PROTEIN-MEDIATED CALCIUM-SENSITIZATION IN SMOOTH MUSCLE ((M. C. Gong, H. Fujihara, L. A. Walker, A. V. Somlyo and A. P. Somlyo)) Department of Mol. Physiol. & Biol. Physics, UVa, Charlottesville, VA 22908

Prolonged treatment with GTPγS (5-15 h, 50 μM) of smooth muscle permeabilized with *S. aureus* α-toxin "downregulated" (abolished) the acute Ca^{2+}-sensitization of force by GTPγS, AlF_4^-, phenylephrine and endothelin, but not the response to phorbol dibutyrate (PDBu) or a phosphatase inhibitor, tautomycin. It also abolished GTPγS-induced increase in myosin light chain (MLC_{20}) phosphorylation at constant $[Ca^{2+}]$, caused extensive translocation of $p21^{rhoA}$ to the particulate fraction, prevented its immunoprecipitation and inhibited its ADP-ribosylation, but had no effect on the immunodetectable content of G-proteins ($p21^{rhoA}$, $p21^{ras}$, $G_{\alpha q/11}$, $G_{\alpha i3}$, G_β) or protein kinase C (PKC-α, -β_1, -β_2, δ, ε, η, θ, ζ). Our results suggest that 1). downregulation of GTPγS- and agonist-induced Ca^{2+}-sensitization by prolonged treatment with GTPγS may be related to a conformational change in $p21^{rhoA}$ and/or to downregulation of its (yet to be identified) effector(1) and 2). provide novel evidence of the independent pathways of, respectively, G-protein-coupled and phorbol ester-induced Ca^{2+}-sensitization (2).

1. Gong et al, Proc. Natl. Acad. Sci. USA, 93: 1340-1345, 1996; 2. Jensen et al, Biochem. J. 318: 469-475, 1996 (Supported by NIH P01 HL48807)

Th-Pos217

CALCIUM-SENSITIZATION AND TRANSLOCATION OF $P21^{RHOA}$ IN VASCULAR SMOOTH MUSCLE ((M. C. Gong, H. Fujihara, A. V. Somlyo and A. P. Somlyo)) Department of Mol. Physiol. and Biol. Physics, UVa, Charlottesville, VA 22906-0011, USA

In α-toxin-permeabilized rabbit portal vein smooth muscle the particulate, hydrophobic (Triton X-114 partitioned) fraction of $p21^{rhoA}$ was 8 ± 1.5% of total in controls, and was increased ($p<0.05$) by phenylephrine to 18 ± 5.5% at 5 min, by AlF_4^- to 26 ± 8.4% at 20 min, by GTPγS to 73% at 20 min, and by high Ca^{2+} to 31 ± 5.8% at 15 min. GTPγS (50 μM) recruited $p21^{rhoA}$ to the membrane within 1 min, paralleling the initial time course of force, but the "recruited" particulate $p21^{rhoA}$ did not decrease concomitantly with the reversal of sensitization. The small amount of membrane-associated $p21^{rhoA}$ in nonstimulated smooth muscle was a good substrate for *in vitro* ADP ribosylation by *botulinum* exoenzyme C_3, whereas the large amount found after stimulation with GTPγS was not. We conclude that: 1., the time course of translocation of $p21^{rhoA}$ is consistent with its causal role in Ca^{2+}-sensitization(1); 2., membrane-bound $p21^{rhoA}$ can exist in two or more states, as indicated by its availability for ADP ribosylation; and 3., AlF_4^- can interact with $p21^{rhoA}$ in a cellular environment.

1. Gong et al, Proc. Natl. Acad. Sci. USA 93: 1340-1345, 1996
Supported by NIH P01 HL48807

Th-Pos218

A HIGHLY CONSERVED HOMOLOGUE OF BOVINE NEUROCALCIN δ IS EXPRESSED IN SMOOTH MUSCLE. **((B.O. Schönekess, B.G. Allen* and M.P. Walsh)) Smooth Muscle Research Group, University of Calgary, Calgary, Alberta T2N 4N1, Canada, and *Institut de Cardiologie de Montréal, Montréal, Québec, Canada.**

The recoverin subfamily of EF-hand Ca^{2+}-binding proteins includes visinin, hippocalcin, frequenin and neurocalcin. Bovine neurocalcin δ (bNCal), one of multiple neurocalcin isoforms, is a 21 kDa protein characterized by three functional EF-hands and its purported localization to neuronal tissue. We have isolated a protein from chicken gizzard smooth muscle that binds to a phenyl-Sepharose column in a Ca^{2+}-dependent manner, can be purified on a DEAE-Sephacel column, is approximately 21 kDa as measured by SDS-PAGE, binds $^{45}Ca^{2+}$ in a gel overlay assay, and is immunoreactive to antibodies raised against bNCal. Partial amino acid sequencing of the protein yielded a fragment that is identical to bNCal (Y-108 to E-120) with the exception of two conservative substitutions. Using a radiolabelled probe made from the entire bNCal coding sequence, we detected a transcript of 3.8 kb by Northern blot analysis of chicken gizzard smooth muscle total RNA, compared with a 5.0 kb transcript in bovine brain total RNA. Polymerase Chain Reaction techniques yielded a partial nucleotide sequence for chicken gizzard neurocalcin which encodes the region homologous to L-35 to F-193 of bNCal. We conclude that neurocalcin is highly conserved across species and is not restricted to neuronal tissues. (Supported by MRC Canada.)

Th-Pos219

THE RESPONSE OF CEREBRAL RESISTANCE ARTERIES TO STEP CHANGES IN PRESSURE: A ROLE FOR NITRIC OXIDE. ((J.M. Doughty and P.D.Langton)). Dept of Physiology, University of Bristol, Bristol, BS8 1TD, U.K.)

Resistance arteries respond to changes in transmural pressure by contracting to maintain a constant blood flow. This mechanism is termed the myogenic response. A vasodilator, nitric oxide (NO) is synthesized from L-arginine by NO synthase (NOS). A role for NO in the response of cerebral arteries to rapid step changes in pressure was tested.

Methods: Rat cerebral arteries were mounted in a Halpern Pressure Myograph and pressurized to 75mmHg at 21°C. The temperature was raised to 37°C and the artery developed tone, such that it contracted to 78.2%±7.42 of its initial diameter (n=7 ±s.d).The transmural pressure was decreased to 30mmHg, and rapid pressure steps were made to 75mmHg. Pressure steps were repeated in the presence of 20μM L-NAME, an inhibitor of NOS, or 400μM L-arginine.

Results: A typical response to a 30mmHg-75mmHg pressure step is shown in the figure. The artery initially distended to 112%±5.4 of the diameter at 30mmHg (measurement 'b') (n=7±s.d). Several minutes after the step was applied, the artery contracted back to a steady state diameter of 95.8%±7.9 of the diameter at 30mmHg (measurement 'c'). 20μM L-NAME (n=6), reduced the diameter at 30mmHg ('a') to 84.2%±18.5 of the control. The initial distension 'b' was reduced to 105%±4.45, but the steady state diameter 'c' was unaffected (96.4%±6.81). 400μM L-arginine (n=6) had no effect on the diameter at 'a' (98.7%±7.5), but the initial distension, 'b', was increased to 117%±10.8. There may also have been some increase in the steady state diameter 'c' (102%±13.5).

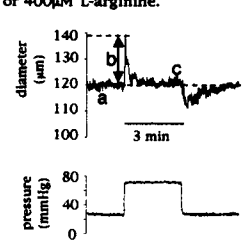

These data suggest that an initial distension of cerebral resistance arteries in response to increases in transmural pressure is NO-mediated, while a steady state sustainable contraction reflects the myogenic response, which is independent of NO. *This work was supported by the British Heart Foundation.*

Th-Pos220

REACTION OF PEROXYNITRITE WITH F-ACTIN

((**L.C. Gershman**[§¶‡], L.A. Selden[§], A. J. Johnson[‡‡], T. J. Ferro[§¶‡], and J.E. Estes[§¶],)) [§]Research and [‡]Medical Services, Department of Veterans Affairs Medical Center, Albany, NY 12208 and Departments of [‡]Medicine and [¶]Physiology and Cell Biology, Albany Medical College, Albany, NY 12208.

The highly reactive oxidant, peroxynitrite (ONOO), results from reaction between nitric oxide and superoxide. At physiologic pH peroxynitrite is converted to peroxynitrous acid which decomposes rapidly (~ 2 s.). Treatment of F-actin with a bolus of 1 mM ONOO results in variable amounts of nitrotyrosine (NT). This ONOO-modified actin exhibits abnormal polymerization characteristics (*Selden et. al., Mol. Biol. Cell 6:20a, 1995).* We have modified the reaction conditions by slowly infusing ONOO into F-actin solutions. This protocol results in reproducible nitration under conditions which are closer to the physiologic scenario of a constant production of low amounts of ONOO over time. We find that infusing 23 μM F-actin with 1.5 μM ONOO/sec for 165, 330, and 660 seconds results in 1,2 and 3 NT/actin respectively. As NT/actin increases, isoelectric focusing gels show additional acidic bands which stain with anti-nitrotyrosine antibody. Measurement of actin intrinsic fluorescence shows no shift in the tryptophan spectrum and no evidence of denaturation. However, a substantial quenching of tryptophan fluorescence which increases with increase in NT/actin is evident. Increasing the pH from 6.4 to 8.4 which shifts the NT absorption spectrum does not affect the quenching, suggesting that fluorescence energy transfer between tryptophan and tyrosine is not responsible for the quenching. This implies that the nitrated tyrosine residues are not in close proximity to tryptophan residues. The tryptophan quenching could be caused by structural changes in F-actin due to nitration of tyrosine residues or oxidation of other residues by ONOO, or to ONOO oxidation of a residue(s) near tryptophan in the structure. These experiments demonstrate that F-actin is a viable target of ONOO *in vivo* with at least 3 readily reactive tyrosines/monomer subunit. (This work was supported by NIH grants GM32007(JEE), HL-48406(AJJ) and by the Department of Veterans Affairs (LCG, TJF).

Th-Pos221

Ca^{2+}-INDUCED CONFORMATIONAL CHANGES IN THE N-TERMINAL HALF OF PLASMA GELSOLIN. ((**L.A. Selden**[§], C. Hurwitz[‡], H.J. Kinosian[¶], J.E. Estes[§¶], and L.C. Gershman[§¶‡])) [§]Research and [‡]Medical Services, Department of Veterans Affairs Medical Center, Albany, NY 12208 and Departments of [‡]Medicine and [¶]Physiology and Cell Biology, Albany Medical College, Albany, NY 12208.

Ca^{2+} activation of F-actin severing by whole gelsolin is thought to be induced by micromolar Ca^{2+} binding to the C-terminal half of the molecule. The N-terminal half of gelsolin (S1-3), while known to bind Ca^{2+}, has been reported to exhibit Ca^{2+} insensitive severing (*Way et. al., J. Cell Biol. 109:593-605, 1989).* Recently, a new binding/severing assay (*Selden et. al., Biophys J. 70:A345, 1996*) has allowed a continuous analysis of the F-actin binding and severing reactions. Using this assay, we observe that addition of EGTA to S1-3 in the absence of $MgCl_2$ slows the F-actin severing activity in a pH dependent manner, suggesting Ca^{2+} regulation. Saturation of S1-3 with Ca^{2+} caused a 20% tryptophan fluorescence intensity increase, indicative of a conformational change. The S1-3 fluorescence intensity increase in the absence of $MgCl_2$ shows a sigmoidal dependency on the Ca^{2+} concentration, indicating cooperative binding of Ca^{2+}. Fits of the Hill equation to these plots results in K_h = 10 μM and Hill coefficients which increase from 3 at pH 7 to 6.5 at pH 8. In the presence of 2 mM $MgCl_2$, however, the S1-3 fluorescence increases in a hyperbolic manner with a K_d = 1-2 μM at pH 7.0 and 7.5. These results suggest that S1-3 contains a class of divalent cation binding sites which can be occupied by either Mg^{2+} or Ca^{2+}. Occupancy of these sites increases the affinity of a second, higher affinity Ca^{2+} site, and increases the F-actin severing activity of S1-3. Occupancy of the higher affinity sites induces a conformational change resulting in the observed tryptophan fluorescence increase. (This work was supported by NIH grant GM32007and by the Department of Veterans Affairs).

Th-Pos222

Ca^{2+} REGULATION OF F-ACTIN SEVERING ACTIVITY BY GELSOLIN. ((B. Lincoln[†], L. Schick[†], H. Kinosian[¶], L. Selden[§], L. Gershman[§¶‡], J. Estes[§¶], and J. Newman[†])) [†]Department of Physics, Union College, Schenectady, NY 12308; [§]Research Service and [‡]Medical Services, Department Of Veterans Affairs Medical Center, Albany NY 12208 and Departments of [‡]Medicine and [¶]Physiology and Cell Biology, Albany Medical College, Albany, NY 12208.

Gelsolin is a Ca^{2+} activated actin binding protein that can bind both monomeric (G-) and polymeric (F-) actin. The rate of phalloidin-stabilized F-actin severing by gelsolin has been investigated by dynamic light scattering (DLS). Diffusion coefficients for phalloidin-stabilized actin filaments were observed to increase over time after the addition of gelsolin in the presence of Ca^{2+}, indicating that actin filaments were being shortened by gelsolin's severing activity. The number concentration of actin filaments was also assayed by determining the rate of polymerization of fluorescently-labeled monomeric actin nucleated by gelsolin-severed filaments. In agreement with the fluorescence experiments, DLS found that the rate of actin length decrease is sharply dependent on the free Ca^{2+} concentration in the range of 1 - 50 μM. In addition, actin labeled with pyrenyl iodoacetamide (pyrene-actin) was used to study to study the interaction of gelsolin and F-actin. Pyrene-actin, in the presence of phalloidin, exhibits a fluorescence intensity decrease upon binding of gelsolin. The apparent rate of binding was found to vary in a Ca^{2+} concentration range similar to that found for the severing rate. Severing can be stopped by chelation of free Ca^{2+} with EGTA as determined by DLS, with severed filaments remaining capped (i.e. unable to anneal) by gelsolin (as determined by pyrene-actin fluorescence measurements). These results suggest that multiple Ca^{2} binding sites act in a cooperative manner to enable gelsolin to bind to and sever F-actin (Supported by NSF grant MCB-9316025 (JN) and NIH grant GM32007 (JE) and by the Department of Veterans Affairs.)

Th-Pos223

FORCE MEASUREMENTS ON SINGLE ACTIN FILAMENTS USING MICROFABRICATED CANTILEVERS.((**Th. Neumann**, M. Fauver, C. Galambos, G. H. Pollack)) Center for Bioeng. 357962, Univ. of Wash, Seattle, WA 98195

We have developed a system to measure the mechanical properties and dynamics of actin filaments. Force is measured by optically tracking the deflection of a miniature cantilever, 400 μm long, 1 μm wide and 300 nm thick. The cantilevers are produced by microfabrication methods. Thus, a silicon wafer is coated first with silicon nitride, then a photoresist, which is exposed to a pattern. After several developing and etching steps, the nitride film is removed and the cantilevers are broken free. The tips of the cantilevers are coated with gold to increase contrast. To calibrate the cantilevers we use a resonance method to obtain elastic modulus and an electron microscope to measure cantilever dimensions. One such calibration is sufficient to give the stiffness of all cantilevers on a wafer. In initial experiments we suspended a single actin filament between a stiff reference beam and the tip of a cantilever. By translating the stiff beam, the actin filament stretches and thereby deflects the compliant cantilever. Cantilever deflection is measured by a spot-position detector. We have obtained initial measurements of the tensile strength of an fluorescent labeled actin filament of rabbit muscle. The force required to break the filament was ~2000 pN. This value is considerably higher than previously measured by others, but preliminary. The cantilevers will be useful to measure actin filament dynamics in the *in vitro* motility assay. To do so, the cantilever is simply attached to the trailing end of a translating actin filament, and the deflection is measured.

Th-Pos224

A FLUORESCENSE ANISOTROPY ASSAY TO MEASURE THE AFFINITY OF ACANTHAMOEBA PROFILIN FOR ACTIN. (V.K. Vinson, E.M. De La Cruz, and T.D. Pollard) Department of Cell Biology and Anatomy, The Johns Hopkins University School of Medicine, Baltimore, MD 21205.

The lack of a direct assay to measure profilin binding to other proteins has hampered research on profilin. We constructed mutants of *Acanthamoeba* profilin II, S38C and N58C, which maintain wild-type function when labeled with rhodamine maleimide. Fluoresence anisotropy provides a convenient, direct method to measure rhodamine profilin binding to actin monomers. Both labeled profilins have the same affinity for actin. Competition with unlabeled profilin-II confirms that the probe does not interfere with actin binding. We measure the following dissociation equilibrium constants with this assay:

Bound nucleotide	Amoeba actin	Muscle actin
Ca-ATP	0.2 μM	0.5 μM
Ca-ATP (Pyrene labeled)		5.0 μM
Mg-ATP	0.1 μM	0.3 μM
Mg-ADP	0.5 μM	3.0 μM

Profilin-II has a higher affinity for amoeba actin than muscle actin, for Mg-ATP actin than Ca-ATP actin or Mg-ADP actin and for unlabeled actin than pyrene-labeled actin. This confirms, in general, previous observations based on indirect polymerization assays and less accurate direct binding assays, although the affinities are higher with this assay. The effect of pyrene labeling explains the weaker binding constants measured by fluorescence enhancement of pyrene actin. This assay also provides an approach to investigate profilin binding to the ends of actin filaments and competition between profilin and other proteins for binding to actin monomers.

Th-Pos225

BOUND NUCLEOTIDE IS NOT REQUIRED FOR ACTIN POLYMERIZATION OR BINDING PROFILIN. ((**E. M. De La Cruz**, Valda K. Vinson, & T. D. Pollard)) Johns Hopkins Medical School, Baltimore, MD 21205.

We have developed an improved method to prepare nucleotide-free actin in high sucrose [De La Cruz and Pollard (1995) *Biochemistry 34*: 5452] where the nucleotide is hydrolyzed enzymatically with apyrase. Quantitative HPLC analysis demonstrates that ~99% of the actin prepared is nucleotide-free. By pyrene fluorescence, viscometry, light scattering and electron microscopy nucleotide-free actin assembles into filaments. The critical concentration for polymerization is close to zero. Filaments assembled from nucleotide-free actin are stable only in the presence of sucrose and depolymerize upon dilution. We have determined the affinity of profilin for Mg^{2+}-ATP-actin and nucleotide-free actin in sucrose from the fluorescence anisotropy of *Acanthamoeba* profilin-II labelled with rhodamine at an engineered cysteine residue (S38C) situated far from the actin binding site. Profilin-II binds nucleotide-free actin with ~7-fold greater affinity ($K_d \approx 0.03$ μM) than Mg^{2+}-ATP-actin ($K_d \approx 0.2$ μM). Bound nucleotide is not required for polymerization or profilin binding, but greatly stabilizes actin from denaturation.

Th-Pos226

TORSIONAL FLEXIBILITY OF ERYTHROSIN-LABELED F-ACTIN IN THE PRESENCE OF DIVALENT CATIONS.

((**Conrad A. Rebello** & Richard D. Ludescher)), Department of Food Science, Rutgers, The State University, New Brunswick, NJ 08903-0231.

We have used phosphorescence emission anisotropy of erythrosin-5-iodoacetamide labeled actin to measure the microsecond rotational flexibility of F-actin. We have confirmed that Mg^{+2}-F-actin has a higher torsional flexibility than 'normal' F-actin (i.e. F-actin made from G-Ca^{+2} & KCl). However, when phalloidin-stabilized F-actin filaments, prepared from either Ca^{+2}-G actin or Mg^{+2}-G-actin and polymerized with the respective divalent cation (Ca^{+2} or Mg^{+2}) and KCl, were compared to phalloidin-stabilized 'normal' actin, it was seen that both F-Ca^{+2} actin and F-Mg^{+2} actin have similar steady-state anisotropies, but lower than that of 'normal' F-actin. Interestingly, addition of 0.6 mM $CaCl_2$ to either F-Mg^{+2}-actin or to phalloidin-stabilized F-Mg^{+2}-actin did not increase the anisotropy of the respective F-actin to that of 'normal' actin. However, addition of 2 mM $MgCl_2$ to a phalloidin-stabilized Ca^{+2}-F-actin increased the anisotropy to that of 'normal'-F-actin. Since Mg^{+2} associates and dissociates more slowly to the high affinity site on actin than Ca^{+2}, we speculate that binding of Mg^{+2} to sites other than the high affinity site modulates the microsecond rotational flexibility of F-actin.
(Research supported by a grant from the MDA.)

Th-Pos227

NEW FLUORESCENT PHALLOTOXIN CONJUGATES WITH HIGH PHOTOSTABILITY AND IMPROVED OPTICAL PROPERTIES.

((H.C. Kang, J. Bishop-Stewart, P. Millard and R.P. Haugland)) Molecular Probes, Inc., P.O. Box 22010, Eugene, OR 97402.

Fluorescent phallotoxin conjugates have been widely used for labeling F-actin in fixed and permeabilized cells due to their high actin specificity and low molecular weight. In fluorescence microscopy, photostability has been a primary concern, especially with green fluorescent phallotoxin derivatives. We have developed several new fluorescent phallotoxin conjugates with improved spectral properties. To improve photostability of the conjugates, Oregon Green 488 and Oregon Green 514 dyes have been used to prepare phalloidin conjugates. Since the excitation and emission spectra of the Oregon Green 488 dye are virtually superimposable with those of fluorescein, standard fluorescein optical filter sets can be employed. Due to the close match of the absorption maximum of the Oregon Green 514 dye to the second spectral line of the argon ion laser, Oregon Green 514 phalloidin conjugate appears to be very useful for confocal laser scanning microscopy. These two Oregon Green phalloidin conjugates proved to be much more photostable than other green-emitting phallotoxin derivatives. In particular, actin labeled with Oregon Green 514 phalloidin, when mounted in an antifade reagent, shows long-lasting, bright fluorescence, making it easy to visualize and photograph. As an alternative to rhodamine-phalloidin, we have prepared Texas Red-X phalloidin, whose fluorescence emission is better separated from that of many green emitting dyes, making it especially suitable for multiple labeling experiments with other conjugates. Furthermore, Texas Red-X phalloidin can be excited by the Kr laser line (568 nm) used in some cofocal laser scanning microscopes, whereas rhodamine-phalloidin is poorly excited by this light source. We also prepared BODIPY R6G phalloidin, whose absorption maximum at 523 nm makes it an excellent candidate for the newly developed, two photon excitation technique (exciting at 1047 nm).

Th-Pos228

Virtual Reality of Phosphate Release: Opening Actin's Back Door by Micromechanical Manipulation.

((W. Wriggers and K. Schulten)) Beckman Institute and Department of Physics, UIUC, Urbana, IL 61801.

We have recently considered the pathways of water diffusion into actin's enzymatic site and suggested, based on computer simulations, that a "back door" diffusion pathway is used in the release of the inorganic phosphate (P_i) after ATP hydrolysis. To substantiate this hypothesis, we have modelled the dissociation of P_i through the proposed back door pathway. After cleaveage from ATP, the phosphate rotates around the Ca^{2+} cation, turning away from the negatively charged ADP. The position of residue His73 and the electrostatic attraction to the divalent cation prevent, however, a fast release of P_i within a feasible simulation time. The unbinding of the phosphate has been studied further by measuring adhesion forces when pulling the substrate out of its binding pocket. A force of 2700 pN was required to pull P_i off the divalent cation. In comparison, only 600 pN were necessary to drag the substrate through the protein matrix once it was cleaved from the ion. The dissociation from the divalent cation, therefore, appears to be the limiting factor in the release of P_i. The position of His73 indicates a control function of this residue in the dissociation process. In the Lorenz F-actin structure [Lorenz et al., *JMB* 234:826 (1993)], His73 is constrained by phalloidin which would sterically block the back door. One would therefore expect a delay of phosphate release in F-actin induced by phalloidin. This effect has been observed experimentally [Danker and Hess, *Biochim. Biophys. Acta*, 1035:197 (1990)].

Th-Pos229

S1-INDUCED CHANGES IN THE MICROSECOND DYNAMICS OF ACTIN ARE MIMICKED BY OTHER MODIFICATIONS OF MYOSIN BINDING SITES

((**E.Prochniewicz**, and D.D.Thomas)) University of Minnesota.

Time-resolved phosphorescence anisotropy (TPA) of erythrosin iodoacetamide (ErIA) labeled actin revealed that rigor binding of myosin heads (S1) significantly increases the normalized residual anisotropy A_∞ at sub-saturating levels of S1, suggesting cooperativity. To explore the mechanism of this effect, we applied two kinds of perturbation of actin. (1) Residues in the N-terminus of actin, proposed to be involved in the weak-binding interaction with myosin, were blocked by an antibody fragment, F_{ab}(1-7). This induced similar but smaller changes in A_∞, compared with the effect of S1, suggesting that the effect of S1 reflects changes in the actomyosin interface. (2) ErIA-labeled actin monomers were copolymerized with monomers treated with EDC. This resulted in cooperative increase in A_∞ similar to the effect of S1, inhibited the effect of S1 on A_∞, and also changed the rotational motion of ErIA-labeled S1. These data show that the effect of rigor-bound S1 can be mimicked by specific and non-specific modifications of the actomyosin interface. Furthermore, since both F_{ab} and copolymerization inhibit activation of myosin ATPase and *in vitro* motility, we conclude that **actin rotational motions are coupled to functional interactions with myosin**.

Th-Pos230

FUNCTIONAL ENHANCEMENT OF YEAST ACTIN VIA MUTATIONS IN LOOP 38-52.

((**P. Cheung**, E. Bobkova, and E. Reisler)) Dept. of Chemistry and Biochemistry and the Molecular Biology Institute; UCLA, Los Angeles, CA 90095.

It has been shown that K50 on actin can be crosslinked to myosin S1 by glutaraldehyde in the absence but not in the presence of tropomyosin (Bonafe et al., Biochem, 33:2594, (1994)) suggesting a possible control by the regulatory protein over the conformation and/or interactions of loop 38-52 on actin. A K50A/D51A yeast actin mutant was used to investigate the role of these residues in actomyosin function. The mutant and wild type actin were polymerized at the same rate and to similar extent both by $MgCl_2$ and S1. The rigor binding of S1 was tenfold stronger to the mutant F-actin than to wild type actin and the actoS1 ATPase was twofold higher with the mutant protein. In vitro motility (25°C) of K50A/D51A actin was faster (3.5μm/s) than that of WT actin (3.0μm/s). In assays carried out in the presence of pPDM-HMM load the mutant showed greater force generation than WT actin. Tropomyosin increased the sliding velocity of K50A/D51A actin by close to 50% and that of WT actin by 10-15%. This mutational enhancement of yeast actin function is discussed in terms of F-actin structure.

Th-Pos231

FILAMENTOUS ACTIN DESTRUCTION PRECEDES ANHYDRORETINOL TRIGGERED CELL DEATH.

((I. **Korichneva**, F. Derguini, R. Chua and U. Hämmerling)) Program of Immunology, MSKCC, New York, NY 10021.

The metabolites of vitamin A (retinol) belong to the family of lipophilic mediators. 14-hydroxy-4,14-*retro*-retinol (14-HRR) is a regulator of cell growth while anhydroretinol (AR) triggers a signal that leads to nonclassical form of apoptosis (J.Exp.Med. 184, 1996). However, the intracellular target(s) for *retro*-retinoids has not been identified. Morphologically, the cells (ERLD, EL-4, 3T3) show striking changes including shrinking followed by dramatic swelling prior cell death. Because the changes in cell volume and morphology are known to be connected to cytoskeleton the state of organization of actin filaments was studied in AR-treated cells. F-actin was labeled with phalloidin-FITC, and relative F-actin concentration was determined by flow cytometry. In addition the structure of filaments was observed by fluorescence microscopy. AR treatment led to loss in intracellular F-actin content up to 39% within 1 hour and 71% in 3 hours (EL-4 cells). The time-course of decrease in mean fluorescent intensity showed that F-actin loss preceded cell death. Microscopy revealed the loss of the organized array of stress fibers seen in control cells (3T3) and the appearance of short, thick, stick-like and punctate flourescent areas along with increasingly diffuse staining pattern. AR stimulated actin destruction could be prevented by the naturally occurring structural analog14-HRR or herbimycin A, a modulator of certain signal transduction pathways. Thus F-actin appears to be an intracellular target of *retro*-retinoid action. The relation of actin destruction to the cause of AR-induced apoptosis remains to be determined.

Th-Pos232

COMPARISON OF THE THERMODYNAMICS OF BINDING OF MYOSIN S1 AND THE N-TERMINUS OF DYSTROPHIN TO F-ACTIN. ((**Jeffrey G. Forbes**, Frederick P. Schwarz, Kurt J. Amann, and James M. Ervasti)) Department of Chemistry and Biochemistry, University of Maryland, College Park, MD 20742-2021; CARB/NIST, 9600 Gudelsky Drive, Rockville, MD 20850; Department of Physiology, University of Wisconsin, Madison, WI 53706

Protein-protein interactions, which occur largely through hydrophobic effects where water is excluded from the interface, are often entropy-driven processes. An entropy-driven process occurs when $|T\Delta S| > |\Delta H|$ and in many cases $\Delta H > 0$. Actin polymerization, myosin assembly and F-actin-myosin binding are all entropy-driven processes. Our titration microcalorimetric measurements of heavy meromyosin binding to F-actin confirm previous measurements on this system. However, measurements on a recombinant fragment of the first 246 amino acids of human dystrophin yielded entirely different results. The titration microcalorimetry measurements on the dystrophin fragment gave a dissociation constant of 16 uM and an enthalpy of binding of -67 kJ/mol. The thermodynamic values for the interaction of the N-terminus of human dystrophin with rabbit muscle F-actin at 25 C are as follows: ΔG = -27.3 kJ/mol; ΔH = -67 kJ/mol; ΔS = -133 J/mol/K. As these values indicate, the interaction between the N-terminus of dystrophin and F-actin is an enthalpy-driven process rather than the entropy-driven process that occurs with myosin binding. Many of the actin residues which have been identified as being involved in myosin binding have also been identified in the interaction of the N-terminus of dystrophin with F-actin. Our microcalorimetric data indicates that even though these two different proteins interact with many of the same amino acids on F-actin, their binding mechanisms are fundamentally different.

Th-Pos233

MUTAGENETIC ANALYSIS OF THE RELATIONSHIP BETWEEN STRUCTURAL AND FUNCTIONAL DOMAINS IN THE C-TERMINUS OF SMOOTH MUSCLE CALDESMON ((Ze Wang, Zhi-Qiong Yang, and Samuel Chacko)) University of Pennsylvania, Philadelphia, PA 19104 (Spon. by Qiang Wang)

We previously reported that multiple functional domains in chicken gizzard caldesmon (CaD) responsible for the binding of calmodulin (CaM) and the inhibition of actomyosin ATPase are present in the region between residues 598-756. A series of purified internal deletion mutants of CaD generated from a baculovirus expression system were analyzed to precisely localize these functional domains and to further elucidate the functional and structural relationships between them. Our present results suggest the presence of two functionally independent functional motifs, responsible for weak actin-binding and weak inhibition of actomyosin ATPase, in the regions between residues 690-699 and 650-666. We also studied the reversal of CaD-induced inhibition of actomyosin ATPase activity by CaM. Our present data provide direct evidence for the involvement of both CaM-binding sites A and B, located in the C-terminus of CaD, in the reversal of the CaD-induced inhibition of actomyosin ATPase activity by CaM. Furthermore, the two CaM-binding sites function independently. The sequences between residues 598-649, upstream of CaM-binding site A, and 700-717, downstream of CaM-binding site B, appear to have no effect either on actin-binding or CaM-binding. The data from this study also suggest that either CaM-binding site A or B structurally overlaps or lies in close proximity to a weak actin-binding site and a weak inhibitory determinant. (Supported by grants from NIH).

Th-Pos234

DYNAMICS AND COOPERATIVITY WITHIN F-ACTIN: DOES ACTIN RETAIN A MEMORY OF MYOSIN BINDING? ((A. Orlova and E.H. Egelman)) Univ. of Minnesota Medical School, Minneapolis, MN 55455.

Many aspects of cooperative behavior within pure F-actin filaments have been described. With Ca^{2+} bound at the high-affinity metal binding site in actin, there is a very large cooperativity in the binding of HMM, but no cooperativity for S1. With Mg^{2+} bound at the high affinity site, or with conditions that stabilize the conformation of subdomain-2 of actin, there is no cooperativity seen with either HMM or S1. These results show that the two heads of HMM can induce structural changes in F-actin that are not observed with the single head of S1. They also support the notion that the binding of myosin to F-actin induces a conformational change in subdomain-2 of actin, and that under certain conditions this conformational change can be cooperatively propagated through an actin filament. An interesting question is whether the structural state of F-actin "relaxes" after myosin binds and is released, and whether this relaxation time is on a short or long time scale. If the relaxation time is very long (e.g., minutes) it is possible that most of the helical disorder that exists within F-actin may be relatively static. To test this, we are using electron microscopy of actin filaments which have been fully decorated with myosin, and then the myosin is removed. Results from both negative stain and cryo-EM will be presented.

Th-Pos235

IDENTIFICATION OF N-RAP AND ITS ACTIN BINDING DOMAINS. ((**G. Luo**, A.H. Herrera and R. Horowits)) NIAMS, NIH, Bethesda, MD 20892.

We previously described the complete cDNA sequence and domain organization of N-RAP, a nebulin-related protein of striated muscle. We have now expressed and purified whole N-RAP, as well as defined fragments of N-RAP, in E. coli. The expressed fragments include the nebulin-like super repeat region (N-RAP-SR), as well as the region of N-RAP in between the N-terminal LIM domain and the C-terminal super repeat region (N-RAP-IB). Preliminary studies with anti-N-RAP-SR, an antibody that detects the super repeat regions of N-RAP and nebulin, suggested that N-RAP is localized at the myotendon junction in skeletal muscle. Using a synthetic peptide corresponding to sequence from N-RAP-IB as an antigen, we have obtained an antibody that detects whole N-RAP and N-RAP-IB on immunoblots, but fails to detect N-RAP-SR. The anti-N-RAP-IB antibody specifically detects a 185 kDa band on immunoblots of mouse skeletal and cardiac muscle proteins. This 185 kDa band, which was also detected by the less specific anti-N-RAP-SR antibody, is therefore identified as N-RAP. Muscle N-RAP is significantly larger than the 133 kDa size predicted from the full length N-RAP cDNA, indicating that N-RAP undergoes post-translational modifications *in vivo*. Immunofluorescent studies with this specific antibody conclusively show that N-RAP is localized at the myotendon junction in skeletal muscle and at the intercalated disk in cardiac muscle. Using a newly developed gel overlay assay to test the ability of purified proteins to bind actin filaments, we observed significant actin binding to N-RAP-SR, as well as a trace amount of binding to N-RAP-IB. The results are consistent with our hypothesis that N-RAP anchors the terminal actin filaments in the myofibril to the membrane and may be important in transmitting tension from the myofibrils to the extracellular matrix.

Th-Pos236

REEXAMINATION OF THE COMPETITION BETWEEN CALDESMON AND S1 BINDING TO ACTIN. ((**A. Sen**, J. Stephens and J. M. Chalovich)) East Carolina University School of Medicine, Greenville, NC 27858.

A key question regarding the mechanism of caldesmon inhibition of actin activation of myosin-S1 ATPase activity is the importance of the ability of caldesmon to displace bound S1 from actin. Although we demonstrated earlier that caldesmon and S1 compete for binding to actin, recent reports have suggested that complete inhibition of ATPase activity can occur without displacement of S1 from actin under some conditions. We have utilized several different approaches to reexamine this issue. **A:** Cosedimentation of S1-ATP and caldesmon with actin under conditions favoring S1-ATP binding in deference to caldesmon namely, low ionic strength and S1 concentration greater than actin. Caldesmon inhibited both the ATPase activity and the binding in all cases where the initial fraction of the actin with bound S1 exceeded ~10%. **B:** Fluorescence changes associated with the binding of fluorescein-S1 are reversed by caldesmon. Changes in fluorescence can distinguish true binding of S1 to actin from tethering by caldesmon. **C :** It has been suggested that caldesmon is similar to troponin in the skeletal muscle system. We have directly compared the effects of caldesmon and troponin on the binding of S1 to actin and actin-tropomyosin. Our data support our earlier model whereby caldesmon regulates by inhibiting the binding of S1 to actin, although we cannot rule out other contributing factors.

Th-Pos237

THE INTERACTIONS OF A SINGLE NEBULIN SUPERREPEAT WITH ACTIN, MYOSIN HEAD AND CALMODULIN ((**Oleg A. Andreev** and Kuan Wang)) Dept. of Chem. and Biochem. Univ.of Texas, Austin, Tx 78712

Nebulin is a giant actin binding protein consisting of nearly 200 tandem repeats of 35 residue sequence modules. These modules are thought to be actin binding domains along the length of nebulin. Recent studies from this lab demonstrated that certain nebulin modules also bind to myosin head(S1) and calmodulin (Biochem.*33*,12581). To explore the interaction of these proteins, crosslinking of a 7-module human nebulin fragment (NA4), localized in the overlap region between thick and thin filaments, with F-actin, S1 and calmodulin was carried out with EDC, a zero-length crosslinker. Analysis of protein composition and sites of crosslinking were facilitated by fluorescence labeling at selected sites on these proteins and by Western blot. At low molar ratio of NA4 to actin, three acto-NA4 complexes containing one NA4 linked to one, two and three actins were produced. In contrast, cross-linking at a molar excess of NA4 produced only the 1:1 complex. Peptide mapping indicated that several sites of NA4 were cross-linked to the N- or C-termini of actin. S1 significantly reduced NA4/actin crosslinking under rigor conditions, presumably resulting from competition for sites on actin subdomain one. Conversely, NA4 inhibited the cross-linking of actin to S1 via the 50 kDa fragment of S1 and A1 light chain, suggesting that NA4 alters acto-myosin interface. Phalloidin at equimolar concentration to actin did not affect the extent of NA4/actin cross-linking. Calmodulin, on the other hand, completely inhibited the cross-linking of NA4 to F-actin in the presence of calcium ion, probably competing with actin for the same site on nebulin or changing the conformation of nebulin. These crosslinking studies are revealing a set of molecular interfaces on myosin motor, actin, nebulin and a calcium regulatory protein that may participate in the regulation of muscle contraction (supported by NIHAR43514 and FFR).

Th-Pos238

A PHYSIOLOGICAL ROLE FOR ACTIN-TITIN INTERACTION IN CARDIAC MYOFIBRILS

((**W.A. Linke**[1], M. Ivemeyer[1], J.C. Rüegg[1] and M. Gautel[2])) [1]Physiology II, Univ. of Heidelberg, INF 326, D-69120 Heidelberg and [2]EMBL, Meyerhofstrasse 1, D-69012 Heidelberg, Germany

The high resting stiffness of cardiac muscle, relative to skeletal muscle, is explainable mainly by the expression of different length variants of titin (connectin), the giant elastic protein of the vertebrate myofibrillar cytoskeleton, in the two muscle types. However, additional molecular features may account for the high stiffness of cardiac myofibrils, such as interaction between titin and actin, which has previously been demonstrated *in vitro*. Therefore, we have investigated the issue of actin-titin interaction in isolated myofibrils from rat heart, to probe a possible physiological significance. Relaxed myofibrils were subjected to selective removal of actin filaments by a calcium-independent gelsolin fragment, and the "passive" stiffness of the specimens was recorded with a sensitive force transducer. We found that upon actin extraction, stiffness decreased by ~50%, and to a similar degree following high-salt extraction of thick filaments. Thus, actin-titin association may indeed be responsible for part of the high resting tension of cardiac myofibrils.

To identify possible sites of association, we employed a combination of different techniques. Immunofluorescence microscopy revealed that actin extraction increased the extensibility of the previously stiff Z-disc-flanking titin region. Actin-titin interaction within this region was confirmed in *in vitro* co-sedimentation assays, in which recombinant titin fragments were tested for their ability to interact with F-actin. By contrast, such assays showed no actin-titin-binding propensity for sarcomeric regions outside the Z-disc segment. The latter finding was supported by the results of mechanical measurements, which demonstrated that competition of native titin by recombinant titin fragments from both I-band and A-band did not interfere with relaxed myofibril stiffness. Finally, we also failed to detect a change in "active" stiffness upon application of recombinant A-band titin fragments to calcium-activated myofibrils. Thus, it remains unresolved, whether actin-titin interaction can perhaps be a factor in the regulation of active muscle contraction. In conclusion, these results indicate that it is actin-titin association near the Z-disc, but not along the remainder of the sarcomere, which helps to maintain a high stiffness of the relaxed cardiac myofibril *in vivo*.

Th-Pos239

***In Situ* Interactions of Dystrophin with Actin Revealed by Immuno-Resonance Energy Transfer.**

(Douglas D. Root) Department of Biological Sciences, University of North Texas, Denton, Texas 76203.

Biochemical evidence shows that purified actin binds to dystrophin *in vitro*; however, some proteins such as DNAse I, which also bind actin with high affinity *in vitro*, do not interact with actin *in situ*. Consequently, it is imperative to determine if interactions between actin and dystrophin occur within the cell. A novel method was developed to detect molecular level co-localization of dystrophin with actin in rat skeletal muscle cryostat sections by combining resonance energy transfer technology with immuno-labeling techniques. Highly luminescent terbium chelates were conjugated to anti-dystrophin mouse monoclonal antibodies and used as resonance energy transfer donors. Tetramethyl-rhodamine phalloidin can accept energy from these terbium chelates if the distance between the probes is within about 10 nm (about the size of an IgG_{2b} antibody molecule). Muscle tissue sections of 20 μm thickness were dual labeled with the conjugated anti-dystrophin antibody and tetramethyl-rhodamine phalloidin on actin. Verification that these two probes were within 10 nm of each other in the muscle section was established by measuring the sensitized emission of tetramethyl-rhodamine by the terbium chelate after a 200 μs delay following a flashlamp pulse. Sensitized emission was detectable only when both anti-dystrophin antibody and tetramethyl-rhodamine phalloidin were present. These results indicate that actin and dystrophin are closely associated within the cell. This method is generally applicable to the investigation of many types of intracellular associations.

TUBULIN AND MICROTUBULES

Th-Pos240

SEDIMENTATION VELOCITY STUDIES ON THE INTERACTION OF DOLASTATIN 10 WITH PC-TUBULIN

((**John J. Correia**§ and Sharon Lobert¶)) §Dept. of Biochemistry and ¶School of Nursing, Univ. of Mississippi Medical Center, Jackson, MS 39216.

Dolastatin 10, a drug isolated from the Pacific mollusk *Dolabella auricularia*, is reported to induce spiral polymers of tubulin similar to those induced by vinca alkaloids. We have conducted a sedimentation velocity study with phosphocellulose purified tubulin and dolastatin 10 at 25°C in 10 mM Pipes, pH 6.9, 1 mM $MgSO_4$, 2 mM EGTA, and 0.06% DMSO in the presence of 50 μM GTP or GDP. While the initial reaction (< 3 μM drug) suggested an indefinite, isodesmic polymerization, sedimentation distribution analysis [g(s)] revealed a stable intermediate of 20S in both GDP and GTP conditions. At higher drug concentrations (> 3-15 μM drug) a shoulder or an additional intermediate evolves, 30-40S, suggesting growth off this intermediate state. Above 15 μM drug, the entire zone gradually condenses into very large sheet-like aggregates that are visible by EM. In the ultracentrifuge at 30 μM drug these aggregates sediment as broad zones centered near 80S and 235S. GDP enhances the second phase of growth over GTP, but the size of the first intermediate is identical in the presence of either nucleotide. Thus, unlike vinca alkaloids, dolastatin 10-induced assembly of tubulin favors a stable intermediate. We estimate the size of this intermediate to correspond to 8-10 subunits, although we currently do not know its quaternary structure. Supported by NR00056 (S.L.).

Th-Pos241

SEDIMENTATION VELOCITY STUDIES OF VINCA ALKALOID INTERACTIONS WITH TUBULIN ISOTYPES

((**Sharon Lobert**¶, Anthony Frankfurter† and John J. Correia§)) ¶School of Nursing and §Dept. of Biochemistry, Univ. of MS Medical Center, Jackson, MS 39216 and †Dept. of Biology, Univ. of Virginia, Charlottesville, VA 22901.

We used sedimentation velocity to obtain thermodynamic parameters for vinca alkaloid interactions with purified tubulin isotypes, αβII and αβIII, as well as combined αβII and III, αβII and I&IV, and αβIII and I&IV. Data were collected at 25°C in 10 mM Pipes pH 6.9, 1 mM $MgSO_4$, and 2 mM EGTA in the presence of 50 μM GTP or GDP and were fit with an isodesmic ligand-mediated or ligand-mediated plus -facilitated model to obtain binding affinities. In the presence of vincristine and GTP, K_1, drug binding to tubulin heterodimers, is larger for purified αβII or αβIII tubulin compared to unfractionated tubulin (mean values $4.7 \times 10^5 \pm 0.8$ vs. $1.1 \times 10^5 \pm 0.1$ M^{-1}). Additionally purified αβII or αβIII tubulin form smaller spirals than unfractionated tubulin as evidenced in K_2 binding of drug to polymers. For example K_2 (M^{-1}) from data fit with the ligand-mediated model for αβIII is $4.5 \times 10^6 \pm 0.8$ vs. $1.8 \times 10^7 \pm 0.5$ for unfractionated tubulin. When αβII and III are combined or mixed with other isotypes, association constants approach the unfractionated tubulin values. These differences are not observed in the presence of vinblastine or vinorelbine or GDP. Thus we conclude that vincristine interacts differentially with individual tubulin isotypes, suggesting that tubulin isotype composition may impact drug efficacy and toxicity. Supported by NR00056 (S.L.) and NS21142 (A.F.).

Th-Pos242

ROLE OF GUANINE NUCLEOTIDES IN THE VINBLASTINE-INDUCED SELF-ASSOCIATION OF TUBULIN: EFFECTS OF GMPCPP AND GMPCP.

((**B. Vulevic**¶, S. Lobert§ and J.J.Correia¶)) ¶Department of Biochemistry and §School of Nursing, University of Mississippi Medical Center, Jackson, MS 39216.

Guanosine 5'-diphosphate (GDP) enhances tubulin self-association in the presence of vinblastine 2-4 fold over GTP [Lobert et al. (1995) *Biochemistry* 35, 6806-6814]. Here we analyze vinblastine-induced tubulin self-association in the presence of non-hydrolyzable guanine analogs, GMPCPP and GMPCP. Sedimentation velocity experiments were done in 10 and 100 mM Pipes, 1 mM $MgSO_4$, 2 mM EGTA, pH 6.9. In 100 mM Pipes, temperature is limited to < 20°C due to competing microtubule assembly induced by GMPCPP. We found that GMPCPP nearly perfectly mimics GTP in its effect on spiral assembly under all ionic strength conditions. In 10 mM Pipes, GMPCP enhances overall spiral formation by 0.59 ± 0.12 kcal/mol over GMPCPP. This is 0.37 kcal/mol less than the GDP vs GTP enhancement. In 100 mM Pipes overall enhancement for GDP/GTP and GMPCP/GMPCPP corresponds to 0.43 ± 0.13 kcal/mol on average and under these conditions it appears that both analogs mimic parental compounds. This reduction in GDP enhancement can also be achieved by adding 150 mM NaCl to 10 mM Pipes buffer, consistent with an electrostatic component to this nucleotide effect. These data suggest that, by the criteria of vinblastine-induced tubulin self-association, GMPCP is not a perfect GDP analog at low ionic conditions, while GMPCPP acts as a GTP analog under all studied conditions. Supported by NR00056 (S.L.).

Th-Pos243

TAXANE RING IS ENGULFED IN MICROTUBULE STRUCTURE DURING THE TUBULIN POLYMERIZATION.

((**R.Nicholov**, W.Y. Lo) IBME, University of Toronto, Toronto, ON, Canada, M5S 1A4

Spin probes TEMPO and TEPYRO were covalently attached either to C2 or C7 position of the taxane ring to produce spin labelled taxol analogues. The analogues compete with taxol for the same or overlapping binding site.

Tubulin-GTP complex in Mes was polymerized into microtubules in presence of spin labelled taxols. The polymerization of tubulin, confirmed by turbidity measurements and sedimentation assay, was monitored in real time by EPR spectroscopy. Molecular mobility of the analogues was studied before, during, and after microtubule assembly. Spin labelled taxol analogues with a TEMPO radical attached at C2 or at C7 position were not restrained in their molecular motion before the mictotubules assembly. With the increase of the sample temperature, which induces the formation of microtubule, the immobilization of the spin labelled molecule increased displayed by the splitting of the outer resonance lines, and broadening of the central line. Our experimental results show that the taxane ring is engulfed into microtubule structure and is not located at the protein/liquid interface. As a result of this study the orientation and mobility of taxol at its binding site will be determined.